Impact of Leucine and HMB on Acute Muscle Damage: Focus on Repair and Regeneration *in vivo* and *in vitro*

Alexander David Brown
BSc (Hons), MSc, AFHEA

A thesis submitted in partial fulfilment of the requirements of
Liverpool John Moores University

for the degree
Doctor of Philosophy
August 2019

Authors Declaration

I declare that the work in this thesis was carried out in accordance with the regulations of Liverpool John Moores University. Apart from the help and advice acknowledged, the work within was solely completed and carried out by the author.

Any views expressed in this thesis are those of the author and in no way represent those of Liverpool John Moores University and the School of Sport and Exercise Science.

This thesis has not been presented to any other University for examination either in the United Kingdom or overseas. No portion of the work referred to in this research project has been submitted in support of an application for another degree or qualification of this or any other university or institute of learning.

Copyright in text of this research project rests with the author. The ownership of any intellectual property rights, which may be described in this research project, is vested in Liverpool John Moores University and may not be made available for use to any third parties without the written permission of the University.

Signed

Date

Thesis Abstract

<u>Introduction:</u> Skeletal muscle is an amalgamation of multiple terminally differentiated myofibers which are capable of regeneration after injury. The satellite cell is the driving factor for muscle regeneration, influenced by their internal and external environment. The majority of these processes and factors are impaired with age, in particular, the function of the satellite cell. Interventions including leucine and HMB supplementation are consumed with the aim of improving muscle mass. Currently, there is a lack of understanding around muscle repair and regeneration from injury and specifically, the influence of cellular ageing. In addition, the impact of leucine of HMB on these processes is limited. Therefore, the aim was to utilise amino acid supplementation as an intervention to reduce damage and/or facilitate growth and repair in skeletal muscle using *in vivo* and *in vitro* models.

<u>Methods:</u> Three models were used to investigate these processes: 1) strenuous eccentric exercise to establish physiological and immune responses in young males and females, in the absence and presence of supplements; 2) replicatively ageing myoblast models to investigate the impact of age on the migration and fusion potential of myoblasts in the absence or presence of leucine or HMB supplementation and finally; 3) dynamic proteome profiling techniques using control and replicatively aged myoblasts and myotubes as models.

<u>Results:</u>

Post eccentric exercise, at 48 h there was a significant (both $P < 0.05$) increase in muscle soreness and CK in young males. In females, there was a significant ($P < 0.05$) increase in muscle soreness, with no effect on CK. Nutritional supplementation was without effect on functional measures. There were, however, significant ($P < 0.05$) increases in IL-7, with non-significant increases in IL-8 in males vs. females, basally. With leucine, female IL-7 was significantly ($P < 0.05$) increased vs. males, with TNFR1-α also non-significantly increased. Replicatively aged myoblasts migrated significantly ($P < 0.05$) faster than control myoblasts, with the inhibition of Akt significantly ($P < 0.05$) blocking migration. Both models responded to supplements through increased rates of

migration, with the control cells attaining rates similar to aged cells post-supplementation. Replicatively aged myoblasts did not fuse, in the absence or presence of leucine or HMB. Akt, mTOR and ERK activities were significantly (all $P < 0.05$) suppressed along with myogenin, IGF-I and IGF-II gene expression. However, aged cells amino acid transporters responded to supplements with increased Akt activation, suggesting that they are not compromised per se, but rather fusion is blunted at the expense of a different cellular response. The proteome of replicatively aged myoblasts contained significantly ($P < 0.01$) less abundant ribosomal proteins in myoblasts, and myofibrillar proteins in myotubes, with significantly ($P < 0.01$) greater metabolic enzymes vs. control. Finally, replicatively aged myoblasts and myotubes had significantly ($P < 0.01$) less fractional synthesis rates compared to control.

<u>Conclusion</u>: Taken together, supplementation was with little effect on functional capability in humans following an eccentric exercise protocol. Replicatively aged cells migrate efficiently, but do not fuse, with multiple mechanisms suppressed. Aged cells do however, respond to leucine and HMB with relevant signalling pathways being activated, however, fusion is not the output measure. Proteomic analyses suggest altered metabolism in the ageing cells with reductions in ribosomal and contractile proteins underpin the differences and warrant further investigation.

Acknowledgements

Firstly, I would like to thank my lead supervisor, Professor Claire Stewart. Thank you for the unrivalled support, knowledge, guidance, passion and mentoring you have provided during my PhD. I look forward to continuing to work together in the future. Thank you to my supervisor Dr Adam Sharples for the sheer passion you instil and the support you have provided throughout. Thank you Professor Jatin Burniston for the guidance and support during my time learning proteomics, it was truly an inspiring experience.

I would like to thank the LSB cohort, for the support and friendship during the last 4 years. Sharing, experiencing and supporting each other through the highs and lows of research has unquestionably helped. Thank you to Emily for joining me for many a coffee and cake (the undoubtable fuel source for a PhD). These 15-minute breaks to chat and share experiences, good or bad, have helped more than you will ever know.

I would like to thank the Doctoral Academy and the amazing group of staff, led by Professor Julie Sheldon. Thank you for the support, guidance, training and opportunities, which you have provided. There are no words to describe how much it has helped. Thank you for also providing me with the opportunity to join the team during the hardest and last year of my PhD.

To my friends and volleyball family for whom there are too many to mention, thank you for everything. Without you all, and my love for volleyball, I would not have been able to complete my PhD.

Lastly, thank you to my family for unparalleled support, guidance and belief in me throughout the last four years, there are no words to ever describe how much everything means to me.

Dedication

To my family, the support, love and belief you have all provided throughout my life, thank you. To my parents, your unparalleled guidance, love, support and dedication has helped me be the person I am. I do hope you are proud of who I have become as person, and what I have achieved. To my brother and Emma, thank you for the support, belief and inspiration you have been to me throughout. You both lead the way on how to be successful in life at such an early age. To my Aunty Sue and Uncle Baz, thank you for being truly inspirational for what you have achieved in life, risks you have taken to get there, and for the unquestionable support and love you have provided throughout my life. I would also like to thank Professor Claire Stewart, for the guidance and support you have provided throughout my Masters and PhD. You are the best supervisor and person a student could ever ask for. I will be happy if I become half the academic you are. And Finally, to my Grandma and my late Grandad, you have and always will provide the moral pillars to our family, which have allowed us to become the people we all are. Grandad, I hope I have made you proud. You all mean more to me more then I will ever be able to put into words, thank you.

Table of Contents

List of Figures

List of Tables

List of Equations

Abbreviations

AA	Amino Acid
ACN	Acetonitrile
ADAM10	A Disintegrin and Metallopeptidase Domain 10
ADH1	Alcohol Dehydrogenase 1
ADP	Adenosine Diphosphate
Akt	Protein Kinase B
AMP	Adenosine Monophosphate
AMPK	Adenosine Monophosphate-activated Protein Kinase
ANOVA	Analysis of Variance
ATP	Adenosine Triphosphate
BCA	Bicinchoninic Acid
BCAA	Branched Chain Amino Acid
BPI	Base Peak Intensity
BSA	Bovine Serum Albumin
Ca^{2+}	Calcium Ions
CBA	Cytometric Bead Array
CCL2	Chemokine ligand 2
CCL3	Chemokine ligand 3
CCL4	Chemokine ligand 4
CCR2	Chemokine receptor 2
CDH1	Cadherin 1
CID	Collision Induced Dissociation
CK	Creatine Kinase
CO_2	Carbon Dioxide
D_2O	Deuterium Oxide
DM	Differentiation Media
DMEM	Dulbecco's Modified Eagle's medium
DMSO	Dimethyl Sulphoxide
DNA	Deoxyribonucleic Acid
DOMS	Delayed Onset of Muscle Soreness
ECM	Extracellular Matrix

EDTA	Ethylenediaminetetraacetic Acid
ERK	Extracellular Signal-regulated Kinase
ESI	Electrospray Ionization
FA	Formic Acid
FAPs	Fibro-adipogenic precursor
FASP	Filter-aided Sample Preparation
FBS	Heat Inactivated Fetal Bovine Serum
FDR	False Discovery Rate
FGF	Fibroblast Growth Factor
FGF2	Fibroblast Growth Factor 2
FGF6	Fibroblast Growth Factor 6
FOXO	Forkhead Box Protein
FOXO1	Forkhead Box Protein O1
FOXO3	Forkhead Box Protein O3
FSC	Forward Scatter
FSR	Fractional Synthesis Rate
FWHM	Full Width at Half Maximum
GM	Growth Media
HCL	Hydrochloric Acid
HGF	Hepatocyte Growth Factor
HMB	Beta-Hydroxy Beta-methylbutyric Acid
HS	Heat Inactivated Horse Serum
ID3	Inhibitor of DNA Binding 3
IGF-I	Insulin Growth Factor-I
IGF-II	Insulin Growth Factor-II
IL-1β	Interleukin-1 beta
IL-10	Interleukin-10
IL-17	Interleukin-17
IL-2	Interleukin-2
IL-3	Interleukin-3
IL-4	Interleukin-4
IL-6	Interleukin-6
IL-7	Interleukin-7

IL-8	Interleukin-8
JAK	Janus Kinase
JNK	Jun N-terminal Kinase
L-G	L-Glutamine
LC-MS	Liquid Chromatography-Mass Spectrometry
LDH	Lactate Dehydrogenase
LN	Liquid Nitrogen
m_0	Monoisotopic Peak 0
M1	Pro-inflammatory
m_1	Monoisotopic Peak 1
M2	Anti-inflammatory
m_2	Monoisotopic Peak 2
m_3	Monoisotopic Peak 3
m_4	Monoisotopic Peak 4
MAPK	Mitogen-activated Protein Kinase
MEF2	Myocyte Enhancer Factor 2
MMPs	Matrix Metalloproteinases
MPB	Muscle Protein Breakdown
MPE	Molar Percent Excess
MPS	Muscle Protein Synthesis
MRF	Myogenic Regulatory Factors
MRF4	Myogenic Regulatory Factor 4
mRNA	Messenger Ribonucleic Acid
mTOR	Mechanistic Target of Rapamycin
MVC	Maximal Voluntary Contraction
Myf5	Myogenic Factor 5
MyoD	Myogenic Differentiation 1
NBCS	Heat Inactivated New Born Calf Serum
NF-kB	Nuclear Factor-kB
NFATc	Nuclear Factor of Activated T-cells Cytoplasmic
NO	Nitric Oxide
PAX3	Paired Box Factor 3
PAX7	Paired Box Factor 7

PBS	Phosphate Buffered Saline
PCP	Planar Cell Polarity
PE	Phycoerythrin
PI3K	Phosphoinositide 3-kinase
PIK3C3	Phosphatidylinositol 3-kinase Catalytic Subunit Type 3
PS	Penicillin Streptomycin
RCT	Randomised Control Trial
RDA	Recommended Daily Allowance
RNA	Ribonucleic Acid
ROCK	Rho-associated, Coiled-coil-containing Protein Kinase
ROM	Range of Motion
RP2β	Polypeptide B
RT	Room Temperature
RT-PCR	Reverse Transcriptase Polymerase Chain Reaction
SC	Satellite Cell
SD	Standard Deviation
SEM	Standard Error of Mean
SERCA	Sarcoendoplasmic Reticulum Calcium ATPase
SETD3	Actin-histidine N-methyltransferase
SILAC	Stable Isotope Labelling by Amino Acids
SLC3A2	Solute Carrier Family 3 Member 2
SLC7A5	Solute Carrier Family 7 Member 5
SSC	Side Scatter
STAT	Signal Transducer and Activator of Transcription
TFA	Trifluoracetic Acid
TGF-β	Transforming Growth Factor Beta
TMT	Tris-/MES Triton
TNF-α	Tumor Necrosis Factor-Alpha
TNFr-1α	Tumor Necrosis Factor Receptor-1 Alpha
ToF	Time of Flight
URB5	E3 Ubiquitin-protein Ligase
VAS	Visual Analogue Scale
VEGF	Vascular Endothelial Growth Factor

Chapter 1: General Introduction and Review of the Literature

1.1 General Introduction

Ageing is associated with progressive declines in muscle function, decreased fertility and increased susceptibility to diseases. However, due to biomedical advancements, public health has improved significantly since the nineteenth century. Thus, life expectancy is rising, and the ageing population is increasing, with the largest increase in North America and Europe (U.N., 2017). According to latest figures provided by the United Nations, in 2017 worldwide, there were 962 million individuals over the age of 60 years. In context, this is double the numbers reported in the 1980's where the figure was reportedly 382 million. By 2050, it is predicted that the numbers in this age bracket will rise to nearly 2.1 billion (U.N., 2017). In addition, of the 962 million aged over 60, 137 million, approximately 14 % are already aged over 80 years. By 2050, this older group is predicted to rise in numbers to 425 million, approximately 20 % of those aged over 60 (U.N., 2017). The potential social and economic implications are profound. For instance, pressure will be placed on pension schemes and a need for older individuals to continue to work into later life. Critically, if older individuals are not ageing well, the largest impact will be on healthcare systems, with increased demand to treat age related health issues. For instance, type 2 diabetes, obesity, cancers, dementia, Alzheimer's disease, muscle and bone injuries (Gong and Muzumdar, 2012; Srikanthan and Karlamangla, 2014). Ultimately, the increased prominence of these issues will impact negatively on independence and underpin declines in quality of life (Clark and Manini, 2010). It is therefore crucial to understand the ageing process, in order to develop appropriate and timely interventions. One such intervention relates to retaining muscle mass, strength and function.

1.1.1 Sarcopenia

The definition of sarcopenia is the age-related loss of muscle function and mass (Rosenberg, 2011). Loss of muscle mass occurs as early as the fifth decade of life at a rate of approximately 0.8 % per annum (Janssen *et al.*, 2002). With each decade of life, the rate of sarcopenia increases to 1-2 % per year (Hughes

et al., 2002), although the rate varies between individuals (Janssen *et al.*, 2002). This is relevant as sarcopenia is strongly associated with increased morbidity and early mortality (Carmeli *et al.*, 2002). Therefore, establishing techniques with the aim of preventing or delaying sarcopenia is of the upmost importance. Achieving this will not only relieve some economic and social burdens, but importantly could improve quality of life for millions of people.

1.1.2 Current Interventions

Physical activity and nutritional interventions are strategies being investigated to combat sarcopenia. It is known that sedentary individuals are susceptible to increased rates of muscle loss (Montero-Fernández and Serra-Rexach, 2013). Resistance exercise alleviates sarcopenia by promoting muscle protein synthesis (MPS), with repetitive bouts of resistance training, increasing muscle mass and strength in older adults (Churchward-Venne *et al.*, 2015; Yarasheski *et al.*, 2017). In addition, combining resistance exercise with protein supplementation further increases these benefits in terms of enhanced muscle mass and function, with protein supplementation reporting additional benefits (Phillips, 2015). The benefits of hyperaminoacidemia via protein ingestion works synergistically with resistance training to enhance MPS (Churchward-Venne *et al.*, 2015). Since many older people are not able to undertake resistance training and may not have the capacity to ingest high protein supplements, a better understanding of the underlying mechanisms may facilitate alternative therapeutic interventions. Although the mechanisms of sarcopenia and related interventions are multifaceted and complex, gaining insight into these processes at the level of the skeletal muscle stem cell (satellite cell; SC), may begin to provide a better understanding of these aetiologies and therefore alternative interventions.

1.1.3 Muscle Regeneration and the Satellite Cell

The SC was first discovered by Alexander Mauro in 1961, who identified small populations of mononuclear cells in the muscles of frogs that he named SCs (Mauro, 1961), due to their peripheral location between the plasma membrane and basement membrane along the myofiber (Mauro, 1961). In 1968, these cells were first identified in human skeletal muscle (Ishikawa *et al.*, 1968). Mauro hypothesised that these cells had the capability to promote regeneration. Over the following decades, studies confirmed that these cells were indeed activated in response to trauma, including exercise, causing them to proliferate, migrate and differentiate, enabling the repair of injury (Dumont *et al.*, 2015). As research has developed around muscle growth, loss and regeneration, the emerging body of knowledge indicates that multiple factors are involved and interact at the level of the SC. Some of the factors include: other cell types, growth factors, cytokines, signalling molecules, epigenetic processes, integrins and mircoRNA's (Hawke and Garry, 2001; Dumont *et al.*, 2015).

Therefore, the aim of this thesis, following damage, was to utilise amino acid supplementation on biomarkers of skeletal muscle damage to facilitate growth, repair and regeneration using *in vivo* (objective 1) and *in vitro* (objectives 2-4) models.

1.2 Literature Review

1.2.1 Skeletal Muscle Development

The majority of skeletal muscles are produced from the somite, and are formed via interactions between progenitor cells and molecular regulators (Asakura *et al.*, 2002). These somites are created from the paraxial mesoderm along the posterior of the embryo (Bentzinger *et al.*, 2012). The specification, determination and differentiation of myogenic cells are regulated by transcription factors. There are two families of transcription factors: the paired box factors (PAX3 and PAX7) and the myogenic regulatory factors (MRFs: Myf5, MyoD, myogenin and MRF4). During the early stages of myogenic specification, PAX3 is upregulated and is critical in the migration of progenitor cells (Williams and Ordahl, 1994; Epstein *et al.*, 1996). Therefore, both PAX3 and PAX7 are involved in embryonic myogenesis and during postnatal myogenesis.

Myogenic determination is regulated initially by Myf5 and later MyoD. The cloning of MyoD was the first study to demonstrate that this MRF gene was the master regulator in myogenic determination (Davis *et al.*, 1987). Further evidence suggests that both MyoD and Myf5 are critical for myogenic cell determination, with double knockout of these genes in mice showing no skeletal muscle formation (Rudnicki *et al.*, 1993). Further research has shown that single knockout of either MyoD or Myf5 has a mild effect on muscle development (Rudnicki *et al.*, 1993), suggesting a level of compensation exists for these two transcription factors, which is required for efficient myogenic determination and muscle formation.

Following myogenic determination, myogenic differentiation occurs which involves the expression of transcription factors myogenin and MRF4. For instance, when myogenin is knocked out in mice, the animals quickly die due to whole body muscle deficiency (Hasty *et al.*, 1993). MRF4 is also suggested to be involved in late myogenic differentiation, as murine knock out of MRF4

results in myogenin over-expression, which partially rescues myotube formation (Rawls *et al.*, 1998). This indicates, that both MRF4 and myogenin are required full myotube formation.

Overall, the expression of the transcription factors PAX3/7 are critical to myogenic specification, with PAX3 expressed before PAX7 and regulating the expression of MyoD and Myf5 in the embryo. MyoD and Myf5 are critical in controlling myogenic determination. Myogenin is essential for myogenic differentiation, with MRF4 only later partially involved (Figure 1.1). Therefore, for optimal skeletal muscle formation, the interaction between these transcription factors is critical.
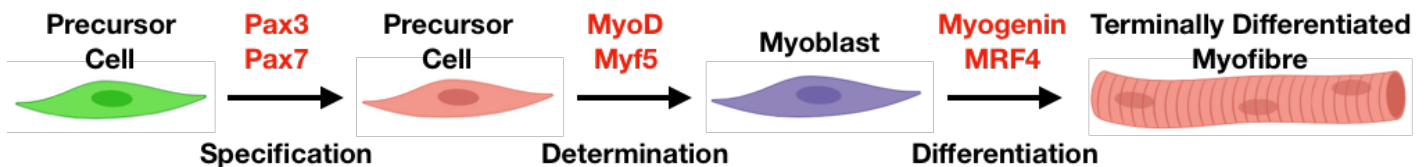
Figure 1.1 Precursor cell development during embryonic development into terminally differentiated myofibre, which can then undergo post-natal myogenesis.

1.2.2 Skeletal Muscle Structure and Function

Skeletal muscle is a remarkable tissue that is essential in maintaining human health and well-being. There are more than 600 different types skeletal muscle in the body that equates to 40 % of total body mass (Lieber, 2002). They all have varying fundamental roles, including: locomotion, postural support, energy metabolism and breathing. The structure and function of skeletal muscle depends on the interactions with nervous, connective and adipose tissue (Lieber, 2002). Surrounding the muscle is the fascia which is comprised of three layers of connective tissue known as the epimysium, perimysium and endomysium (Lieber, 2002). These layers of connective tissue strengthen and support skeletal muscle. The initial layer (epimysium) surrounds the perimysium which is separated by the endomysium (Figure 1.2).
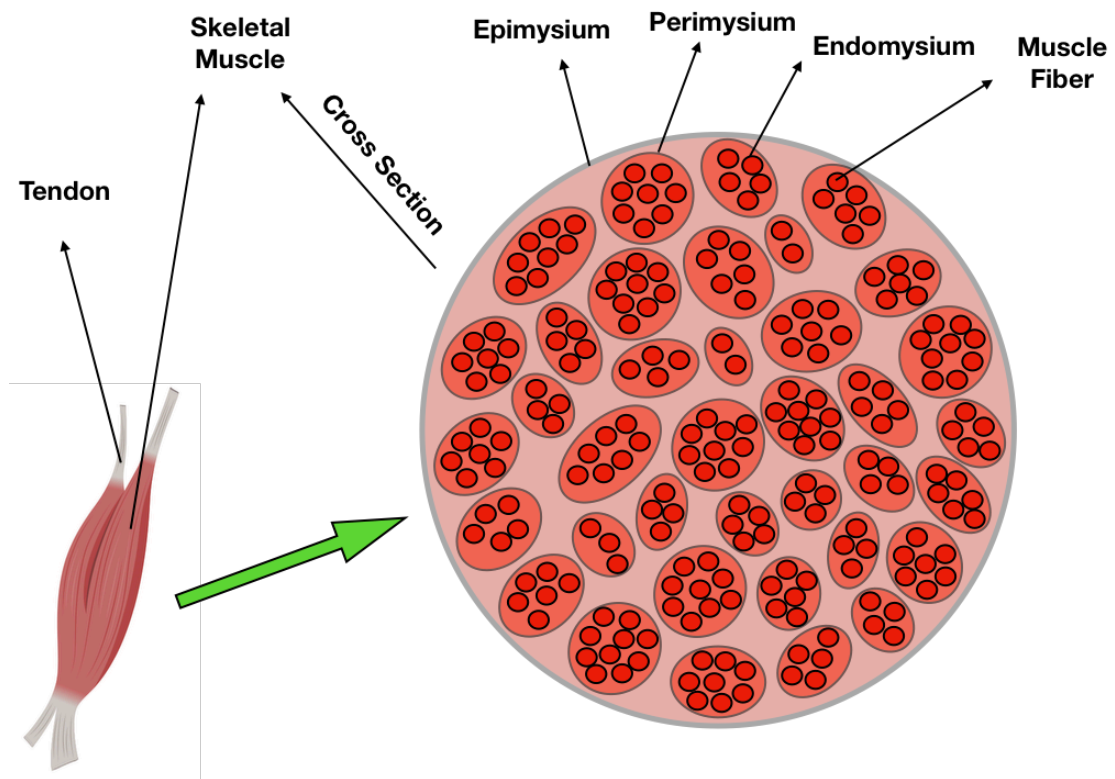
Figure 1.2. Skeletal muscle structure illustrating the components around the muscle fibre.

Skeletal muscle fibres are unique in that they are multinucleated and postmitotic (Sharples *et al.*, 2013). The composition of muscle fibres include: water (75 %), protein (20 %) and other substances such as carbohydrates, fats, minerals and vitamins (5 %) (MacLaren and Morton, 2011). Each myofibre contains specific molecules known as integrins and dystrophin-glycoprotein complex (Ervasti and Campbell, 1993). These complexes connect to the myofilament structure to the extracellular matrix (ECM) via the sarcolemma (Mayer, 2003). The sarcolemma includes the basal lamina and plasma membrane. Within the sarcolemma is the sarcoplasm which contains all the cellular organelles, including stores of vital substrates (muscle glycogen, muscle triglycerides), myoglobin (oxygen) and myofibrils (MacLaren and Morton, 2011).

The myofibrils are described as the contractile apparatus of skeletal muscle fibres (Jones *et al.*, 2017). Surrounding the myofibril is the sarcoplasmic reticulum, which functions in the release of calcium ions via the sarcoendoplasmic reticulum Ca^{2+} ATPase (SERCA) pump (Periasamy and Kalyanasundaram, 2007). This release is critical for muscle contraction. Myofibrils contain the contractile proteins actin (thin filament) and myosin (thick filament) (Huxley, 2004). The thick filament consists of myosin tail and head, with the tail pointing towards the M-line and myosin head towards the thin filament (Huxley, 2004). Whereas, the thin filament contains individual actin molecules that have bonded together in a helix-type structure (Huxley, 2004). Importantly, thin filaments contain the myosin-binding site, which initiate muscle contraction (Huxley, 2004). Furthermore, when observed under a microscope, the sarcomere is divided into dark (A-band) and light (I-band) areas. The I-band includes the actin protein, whereas the A-band consists of myosin, with the H-zone situated in the centre of the A-band, within in this zone there is also the M-line (Figure 1.3).

To summarise, the structure of skeletal muscle is complex and is compiled of multiple components that have specific functions. We are particularly interested in the muscle fibre and the location of the satellite cell, which compliments its specific function in muscle regeneration. Furthermore, muscle contraction, in particular, eccentric contractions activate the SC (Hyldahl *et al.*, 2014). Therefore, the next couple of sections will briefly discuss how muscle and eccentric contraction is initiated and the primary mechanisms involved.

1.2.3 Muscle Contraction

Skeletal muscle is comprised of numerous cells, all integral for its correct function. For example, neurons are essential for the activation of muscle fibres, which subsequently results in muscle contraction. The motor neuron transmits an electrical signal through the neuromuscular junction to the muscle fibre enabling activation (Gandevia, 2001). Interestingly, the two cells do not actually make direct contact. Firstly, the propagation of the action potential occurs,

which involves the transmission of the action potential along the muscle fibre and into the interior of the muscle cell (Sanes and Lichtman, 1992). The next step is the conversion of an electrical signal to chemical signal that initiates the release of calcium from the sarcoplasmic reticulum via the SERCA pump (Periasamy and Kalyanasundaram, 2007). This process demands the presence of the receptors dihydropyridine and ryanodine which open the calcium channels (Periasamy and Kalyanasundaram, 2007). The increase in calcium ions enables contraction, through a mechanism known as the 'sliding filament theory', which was originally proposed by Hanson and Huxley (1953). This process involves the binding of myosin heads to actin filaments, resulting in the actin filaments sliding over one another towards the M-line, shortening the length of the sarcomere, resulting in muscle contraction (Figure 1.3). However, before the sliding filament mechanism can occur, Ca^{2+} is required to release/unwrap tropomyosin from the actin molecule. The process involves four stages, the hydrolysis of adenosine triphosphate (ATP), forming of cross bridges, the shortening of sarcomere (power stroke) and once these stages have concluded, the myosin detaches from actin. Importantly, for these stages to function, there needs to be a constant supply of both ATP and calcium ions (MacLaren and Morton, 2011). During normal muscular contractions, this mechanism works well. However, when stressed, through multiple eccentric contractions, then muscle damage can occur.
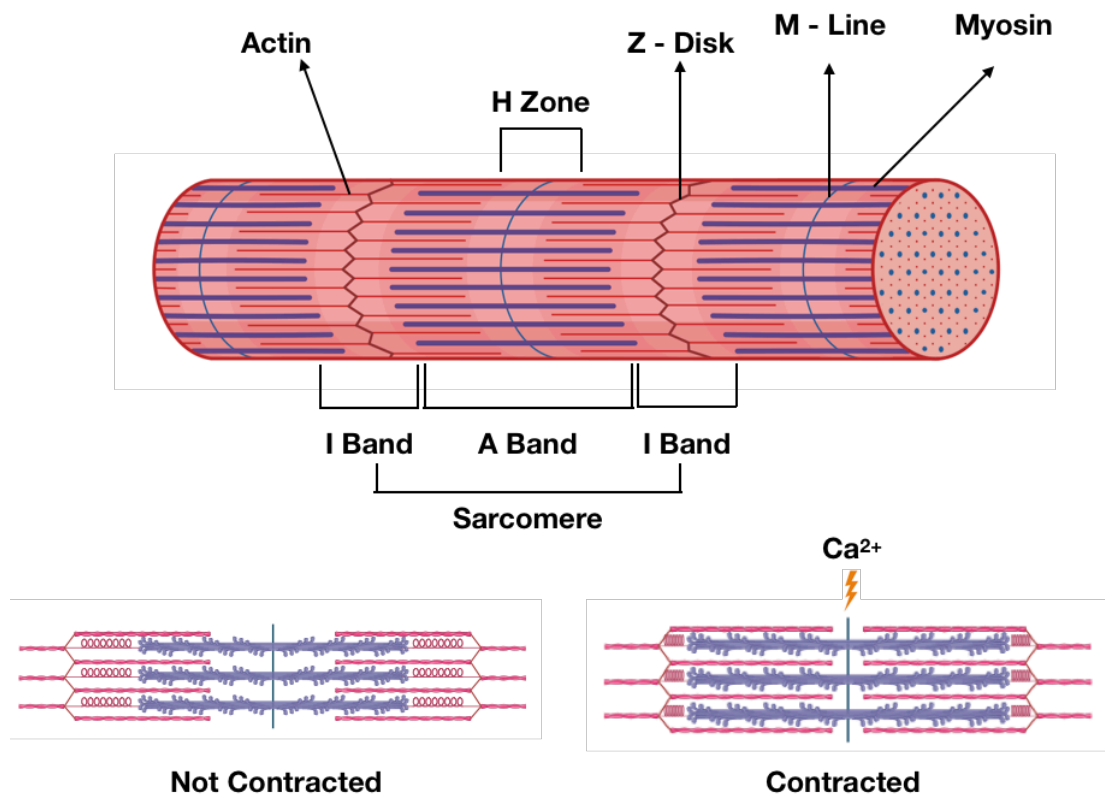
Figure 1.3. Structure of the myofibril and representation of muscle contraction. Created by the author of this thesis using Biorender.

1.2.4 Eccentric Contractions

Many individuals participate in varying sporting activities and exercise regimes. In individuals unaccustomed to sport, this can often result in injury and/or pain. Such muscle damage is caused by excessive unaccustomed eccentric contractions (muscle lengthening under tension) compared to concentric (muscle shortening under tension) or isometric (no change in muscle length under tension) (McCully and Faulkner, 2017). This study inducted injury as a result of eccentric compared isometric and concentric contractions in mice and reported that the eccentric contractions resulted in greater losses in force and an increase in histological damage, acutely, compared to the other two interventions (McCully and Faulkner, 2017). Following muscle injury, two main processes occur 1) repair and; 2) regeneration (Tidball, 2011). The repair stage involves necrosis of the myofibre and the inflammatory response to clean the

injured site. The regeneration. stage which involves the activation of the satellite cell, enabling it to repair the site of damage. These are complex processes involving different cell types and the production of several growth factors and cytokines, all involved in ultimately enabling the damaged muscle to regenerate and to function. Details are provided below (Figure 1.4).
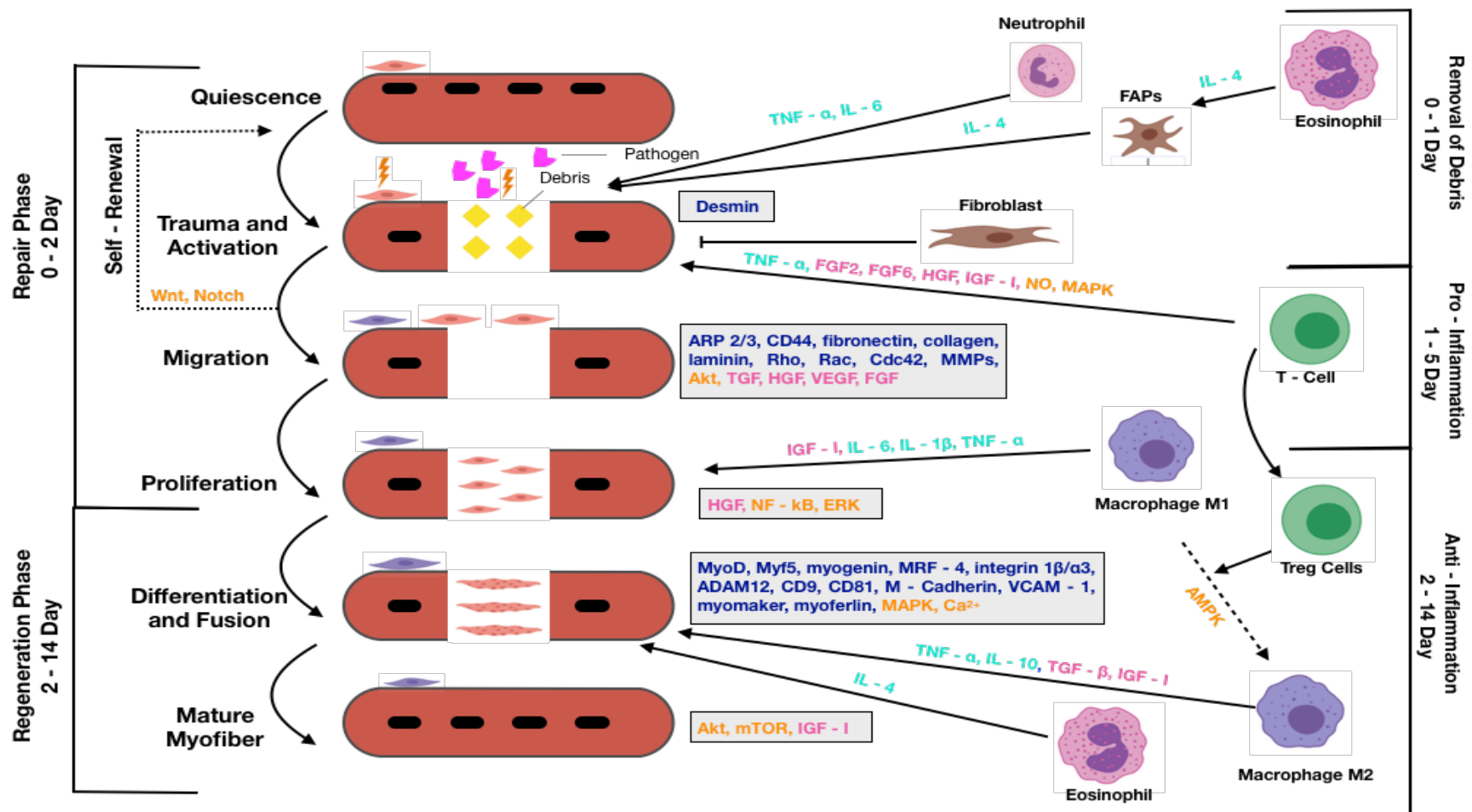
Figure 1.4. Schematic of muscle repair including inflammation and muscle regeneration. Key: light blue = cytokines; pink = growth factors; orange = signalling proteins; dark blue = other proteins.

1.3 The Repair Phase

1.3.1 The Inflammatory Response, Cell to Cell Interactions and Muscle Regeneration

Once muscle injury has occurred, the first response is the activation of mast cells and macrophages from nearby tissue, as well as circulating monocytes in reaction to signals from the damaged muscle (Auffray *et al.*, 2007). Mast cells release cytokines such as Tumor necrosis factor-alpha (TNF-α), tryptase, and interleukin-6 (IL-6) (Dumont *et al.*, 2007). This burst of cytokines consequently results in the stimulation and attraction of blood circulating neutrophils and eosinophils (Figure 1.4). These are the first cells to directly infiltrate the damaged site, and their specific role is to clear the debris, which is achievable due to their high phagocytic capacity (Pizza *et al.*, 2005). Neutrophil stimulation creates a pro-inflammatory cellular environment which enables the recruitment of circulating monocytes. These monocytes can mature into macrophages (Arnold *et al.*, 2007), which are initially determined of a pro-inflammatory phenotype (M1), resulting in higher levels of TNF-α and interleukin-1 beta (IL-1β) at the site of injury. As infiltration and clear up progresses, the macrophages are required to polarize, thus changing phenotype, from pro-inflammatory to anti-inflammatory (M2).

These macrophages, M1 and M2, are distinguished by their markers, function and cytokine profile (Gordon and Martinez, 2010). For instance, M1 macrophages function as pro-inflammatory cells that aid in the initial defence, but further damage tissue. Whereas, M2 macrophages assist in wound healing and tissue repair but have anti-inflammatory properties, which induces the exodus of neutrophils from the damaged tissue (Serhan and Petasis, 2011). In addition, it is suggested that fibroblast activation protein fibro-adipogenic precursor (FAPs) cells also mediate cellular debris clearance (Aurora and Olson, 2014). FAPs are dependent on eosinophil derived interleukin-4 (IL-4), importantly, in the absence of IL-4, FAPs do not clear the debris and muscle degeneration follows (Heredia *et al.*, 2013). Therefore, once injury has occurred in skeletal muscle, both macrophages and FAPs function, initially, to clear the cellular debris (Figure 1.4).

Another important role of immune cells is to control the inflammatory response to injury, allowing for efficient muscle regeneration. In detail, a change in polarisation occurs during the immune response and is driven by M1 and M2 macrophages. Finding a balance between M1 and M2 is critical to control the inflammation. For example, if there are excessive pro-inflammatory hormones, this can result in increased tissue damage and blunting of muscle repair (Aurora and Olson, 2014). On the other hand, if the anti-inflammatory response occurs prematurely then the tissue healing can be negatively affected via incomplete debris removal (Aurora and Olson, 2014). It is suggested that adenosine monophosphate-activated protein kinase (AMPK) is critical in regulating the balance between M1 and M2 macrophages in response to eccentric exercise (Mounier *et al.*, 2013). AMPK primarily senses the energy changes in the ATP, adenosine diphosphate (ADP) and adenosine monophosphate (AMP) ratios. It is therefore possible to conclude that AMPK also changes the polarisation between M1 and M2 phenotypes in the macrophages (Mounier *et al*., 2013). Alternatively, the interactions of macrophages and regulatory T-cells are suggested to be integral in the immune response in skeletal muscle regeneration (Figure 1.4). Regulatory T-cells are involved in the recruitment of both M1 and M2 macrophages to the site of injury (Leavy, 2014) via the CC chemokine ligand 2 (CCL2) and ligand of CC chemokine receptor 2 (CCR2) axis (Burzyn *et al.*, 2013).

Other cell types, including leukocytes, including mast cells, neutrophils, eosinophils and macrophages, interact with satellite cells to allow for muscle regeneration to occur (Figure 1.4) (Chen and Shan, 2019). Firstly, mast cells and neutrophils that are released in the early stages of the inflammatory process release cytokines such as TNF-α and IL-6. It is also suggested that IL-6 assists in the stimulation of satellite cell activation and muscle hypertrophy (Serrano *et al.*, 2008). In addition, TNF-α, as a chemoattractant, is suggested to induce migration of satellite cells through enabling directionality (Terrente *et al.*, 2003). Chemokines, which function to regulate trafficking of leukocytes, are small molecules that are released by immune cells and are also implicated in satellite cell function (Tidball and Villalta, 2010). For instance, the chemokines and their receptors are highly expressed by leukocytes during muscle regeneration. In detail, the chemokines CCL2, chemokine ligand 3 (CCL3) and

chemokine ligand 4 (CCL4) that are secreted by leukocytes can induce the phosphorylation and activation of the extracellular signal-regulated kinase (ERK) 1/2 pathway in C_2C_{12} myoblasts, which is important in satellite cell proliferation (Yahiaoui *et al.*, 2008). Furthermore, monocytes are split into two subtypes, Ly6C+ and Ly6C- (Arnold *et al.*, 2007). Ly6C+ has pro-inflammatory characteristics, with Ly6C- having anti-inflammatory properties. Tidball and Villalta (2010) stated that Ly6C+ secretes factors such as IL-1β and TNF-α, which result in enhanced satellite cell proliferation but inhibits differentiation. In contrast, Ly6C- increase IL-10 and TGF-β that lead to decrements in myoblast proliferation and improved differentiation. These findings correlate to the effects of M1 and M2 on satellite cell function, in that M1 accelerates proliferation through the pro-inflammatory properties, and M2 enhances differentiation and myotube hypertrophy through the anti-inflammatory characteristics.

Extracellular matrix molecules also interact with the satellite cell during various phases of muscle regeneration. For instance, collagen-I, laminin and fibronectin, are in some capacity involved in muscle regeneration. Hauschka and Konigsberg (1966) were the first authors to show that satellite cell proliferation was improved when on a collagen-I substrate. Moreover, satellite cell adhesion, migration and proliferation are increased when cultured on laminin substrates (Silva-Barbosa *et al.*, 2008), suggesting a role for this ECM protein. Fibronectin is implicated in muscle regeneration, through regulating the 'switch' between myoblast proliferation and differentiation through fibronectin absorption through the cell membrane into the cell (Garcia *et al.*, 1999). Other research implies that fibronectin is implicated in myoblast orientation, adhesion and myotube formation (Maley *et al.*, 1994; Altman *et al.*, 2010). Muscle connective tissue fibroblasts are suggested to directly interact with satellite cells within their niche resulting in satellite cell expansion, thus enhancing proliferation and differentiation (Murphy *et al.*, 2011). The ECM contains key regulatory and signalling proteins, including fibronectin, fibroblasts and collagen I which are activated due to trauma, and either directly or indirectly interact with different cells which subsequently influence muscle regenerative (Frantz *et al.*, 2010).

After muscle trauma, growth factors are either released by the muscle or by immune cells, these soluble factors are suggested to exert effects on muscle regeneration. For example, fibroblast growth factor 6 (FGF6), a member of the fibroblast growth factor

(FGF) family, is known to have increased expression and is upregulated during muscle regeneration (Kastner *et al.*, 2000). This growth factor is known to mediate myogenic proliferation and inhibit differentiation (Kastner *et al.*, 2000) via activation of the mitogen-activated protein kinase (MAPK) signalling pathway (Jones *et al.*, 2005). In addition, transforming growth factor beta (TGF-β) which is released by platelets and/or secreted by muscle cells interacts with satellite cells, inhibiting both proliferation and differentiation (McLennan and Koishi, 2002). This unique growth factor also interacts with immune cells, including monocytes, via chemotactic attraction and is dependent chemotactic ligand and cell surface receptors, which indirectly modulates muscle regeneration (Wahl *et al.*, 1987). This in turn, induces angiogenesis (Husmann *et al.*, 1996). Furthermore, hepatocyte growth factor (HGF) is vital for the activation of satellite cells, which subsequently enhances proliferation and inhibits differentiation (Suzuki *et al.*, 2002). Shi and Garry (2006) show that HGF activates either the p38-MAPK, phosphoinositide 3-kinase (PI3K) and ERK (via down regulation of cavelin 1 expression) signalling pathways, which activate the satellite cell from the quiescence state. Finally, insulin growth factor-I (IGF-I) effect both proliferation, differentiation, muscle metabolism, MPS and cell survival (Mourkioti and Rosenthal, 2005) resulting in muscle hypertrophy (Foulstone *et al.*, 2003; Hameed *et al.*, 2004; Sharples and Stewart, 2011; Hughes *et al.*, 2016).

In summary, immune cells are extremely important in the initial response to muscle injury, enabling clearing of damaged tissue, followed by initiation of repair, which contributes to satellite cell regulation. In particular, the macrophage populations M1 and M2 have multiple roles including removal of cellular debris, and control of inflammatory responses. The transition of M1 and M2 macrophages coincides with inhibition of satellite cell proliferation and initiation of differentiation (Chen and Shan, 2019). T-cell regulators control both macrophage recruitment and T-cell numbers, both of which are suggested to have roles in satellite cell differentiation (Aurora and Olson, 2014). In addition, the microenvironment that include other cells, soluble factors and proteins have synergistic roles in activating and/or inhibiting satellite cell processes which are critical for efficient repair and regeneration (Figure 1.5). Following the initial repair of muscle following trauma, the capability of muscle to regeneration will be discussed next, with focus on the pivotal role of the satellite cell (Figure 1.4).
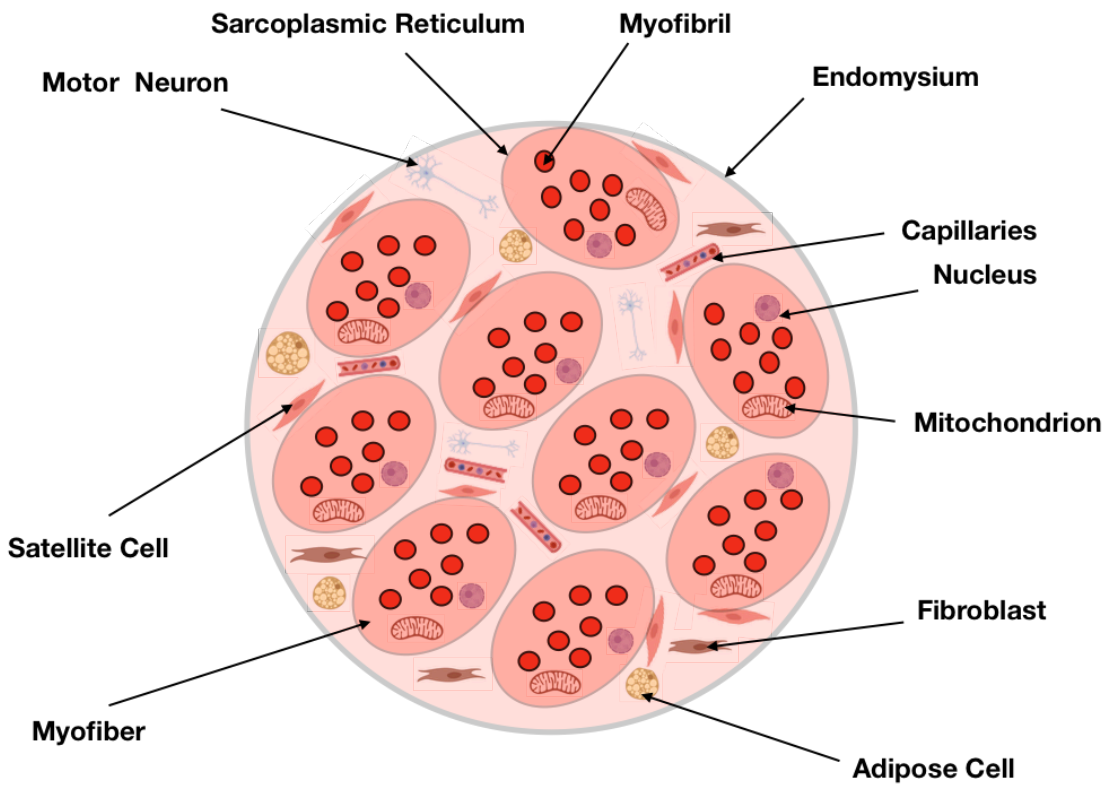
Figure 1.5. The micro environment surrounding muscle fibres including variety of cells types that contribute to muscle contraction.

1.4 The Regeneration Phase

1.4.1 The Role of the Satellite Cell in Muscle Repair and Regeneration

The satellite cells are particular myogenic cells, distinct from other populations, due to their enhanced nucleus-to-cytoplasm ratio. This highly myogenic population of cells are located between the plasma membrane and basement membrane along the myofiber (Mauro, 1961). The role of SCs in muscle generation is divided into the following phases: satellite cell activation (including self-renewal), migration, proliferation, differentiation/fusion and myotube maturation (Dumont *et al*., 2015). Before SCs undergo the regeneration process they are in a quiescent state, until activated by injury, or various other traumas (e.g. burns). Once activated the satellite cells migrate towards the damaged site (Schultz *et al.*, 1985) they re-join the cell cycle and subsequently proliferate prior to differentiating and fusing into myotubes (Hawke and Garry, 2001). Each step is critical and will be discussed in relation to satellite cell function in muscle regeneration.

1.4.2 Activation

Once muscle injury occurs the SCs are activated, by among other things, growth factors originating in the ECM, which are released once trauma has occurred. For example, fibroblast growth factor two (FGF2) and FGF6 two isoforms of FGF, located in the ECM, are suggested to activate satellite cells (Jones *et al.*, 2005; Liu and Schneider, 2014). FGF2 is proposed to increase calcium concentrations leading to Nuclear factor of activated T-cells cytoplasmic (NFATc) translocation into the nucleus resulting in satellite cell activation (Liu & Schneider 2014). Whereas, FGF6 activates the p38 MAPK pathway, which when inhibited prevents satellite cell activation (Jones *et al*., 2005). In addition, Troy *et al*. (2012) isolated mouse primary skeletal muscle cells and these cells were differentiated and transfected. The authors reported that p38 α/β MAPK was initiated in cell activation. In contrast, another growth factor involved in the activation of satellite cells is HGF which is also present in the ECM (Allen *et al.*, 1995). HGF binds to c-met and *in vitro* HGF is suggested to promote satellite cell activation (Allen *et al.*, 1995). Inhibition of nitric oxide (NO) production

impairs SC activation via reduced HGF-cmet binding (Buono *et al.*, 2012), suggesting that NO and HGF are involved in SC activation. Lastly, evidence suggests that IGF-I activate satellite cells (Musarò *et al.*, 2001). The mechanisms behind this are believed to be via the initiation of the protein kinase B (Akt)/mechanistic target of rapamycin (mTOR) pathway that downregulates Forkhead box protein O1 (FOXO1) consequently leading to activation of SCs (Machida *et al.*, 2003). Further, in primary human myoblasts, evidence indicates IGF-I triggers MAPK signalling pathway is involved in primary cell activation (Foulstone *et al.*, 2004). This is supported by Coolican *et al*. (1997) reporting the effect of IGF-I activation of MAPK signalling in L6A1 myoblasts. Indeed, more evidence is required to identify the specific roles that these growth factors play in satellite cell activation and if they work in combination or individually, if relevant interventions are to be developed.

1.4.3 Self-Renewal

Once myoblasts are activated, they then migrate, proliferate and differentiate into myotubes. However, some go through a process of 'self-renewal', the aim of which is to replenish the satellite cell pool for subsequent rounds of muscle regeneration (Figure 1.4). There are two key pathways involved in the satellite cell self-renewal process. Firstly, the planar cell polarity (PCP) pathway is a noncanonical Wnt pathway that is activated by Wnt ligands (Bentzinger *et al.*, 2014). Wnt ligands bind to frizzled receptors, this binding alters the cytoplasmic structure in turn activating the Rac/(Jun N-terminal kinase) JNK and Rho/Rho-associated, coiled-coil-containing protein kinase (ROCK) pathways (Komiya and Habas, 2008). This is suggested to result in symmetrical cell division with the direct interaction between the microenvironment and satellite cells (Kuang *et al.*, 2007), resulting in the initiation of the self-renewal process.

Secondly, the notch signalling pathway is shown to inhibit the differentiation process resulting in self-renewal (Wen *et al.*, 2012). Pisconti *et al*. (2010) suggested that syndecan-3 directly binds and activates notch signalling resulting in the satellite cells returning to their quiescent state. The activation of the notch signalling pathway is driven by forkhead box protein 3 (FOXO3), which is downregulated by the Akt-mTOR pathway. Interestingly, IGF-I concentrations increase during muscle regeneration,

stimulating the Akt-mTOR pathway, this results in the inhibition forkhead box protein (FOXO) pathway consequently reducing notch signalling (Gopinath *et al.*, 2014). Therefore, once the muscle regeneration process has concluded and IGF-I has reduced, the FOXO and notch signalling pathways increase, resulting in satellite self-renewal. Further, the p38 MAPK signalling pathway is suggested to be integral in asymmetric division (Troy *et al.*, 2012). The research regarding satellite cell self-renewal is gaining momentum with many more mechanisms surely to be established. However, thus far it is proposed that the PCP and notch signalling pathways result in satellite cell self-renewal (Figure 1.6).
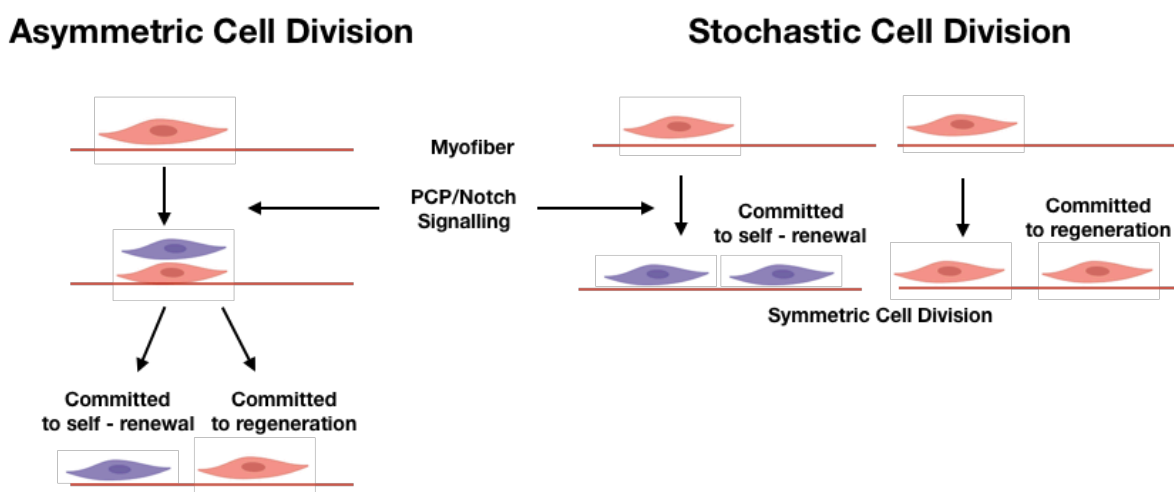
Figure 1.6 Two types of cell division involved in SC self-renewal. Asymmetric division involves the generation of one daughter cell and one myogenic progenitor. Stochastic division generates two daughter SCs or two myogenic progenitor cells.

1.4.4 Migration

The next stage of the muscle regeneration process, following activation and self-renewal, is the migration of cells from their pocket between the basal lamina and sarcolemma membrane to the site of damage, where they undergo mitosis (Schultz *et al.*, 1985). In order for migration to occur, the cell must be polarized, responding to chemoattractant cues and interacting with adhesion molecules to enable appropriate movement. The formation of cell protrusions, cytoskeleton contraction and detachment, prior to reattachment (Charras and Paluch, 2008).

The creation of cell tension is required to provide traction between the cell membrane and the substratum, activating cellular signalling cascades resulting in cell migration (Charras and Paluch, 2008). The adhesion of satellite cells to the ECM is essential for the migration of cells. In particular, fibronectin, collagen and laminin, all ECM components, are involved in inducing migration (Siegel *et al.*, 2009; Vaz *et al.*, 2012). Further, the integrin/adhesion complexes have to detach and dissemble (Palecek *et al.*, 1996). This process is mediated by the proteolytic function of the protein calpain (Glading *et al.*, 2002). For instance, Dedieu *et al.* (2004) reported that inhibition (via over expression of calpastation) of calpain in C_2C_{12} cells prevented cell migration and subsequent myoblast fusion. Leloup *et al.* (2006) conducted similar experiments in C_2C_{12} myoblasts with inhibitors, with similar findings. Additionally, the authors supplemented with IGF-I which further enhanced migration capacity with increases in calpain expression. It is also suggested that calpain enables rear edge detachment of SCs, subsequently fuelling migration through leading edge attachment (Glading *et al.*, 2002).

Furthermore, recent evidence suggests that an alternative mechanism resulting in myoblast migration is through the creation of membrane 'blebs' created by hydrostatic pressure by the sarcoplasm (Charrss and Paluch, 2008). These 'blebs' are often associated with cellular apoptosis and cytokinesis. However, models using three dimensional cultures have shown that migration involves membrane blebbing through contractions of the actomyosin cortex (Charras and Paluch, 2008). Further research is required to quantify the extent in which this process enables myoblast migration.

It is important to consider the role of regulatory molecules and growth factors that are implicated in myoblast migration. The Rho family of GTPases are considered to be the most important regulatory proteins in cell migration, their role involves linking cell surface receptors to intracellular responses including ERK activation within 1 h and 5 h in primary cells (Nobes and Hall, 1999). Rho, Rac and Cdc42 proteins, are a part of the Rho GTPase family, and contain distinct roles in cell migration (Figure 1.4). Rho assembles the contractile filaments while Rac and Cdc42 regulate cell polarisation (Raftopoulou and Hall, 2004). Upstream of the Rho family is PI3K/Akt pathway which when inhibited results in myoblast migration impairment back to control levels in C_2C_{12} myoblasts (Dimchev *et al.*, 2013). Other factors include, the growth factors transforming growth factor (TGF), HGF and FGF all directly increase the migration of SCs (Neuhaus *et al.*, 2003; Siegel *et al.*, 2009). In addition, vascular endothelial growth factor (VEGF) is also suggested to stimulate chemotaxis of satellite cells (Germani *et al.*, 2003). In essence, the migration of satellite cells is mediated by multiple guidance cues, from the site of injury, which give these cells their remarkable capacity to be highly motile during muscle regeneration.

Finally, matrix metalloproteinases (MMPs), which are involved in skeletal muscle maintenance, also play an important role in cell migration. When MMPs are inhibited, impaired migration is observed (Nishimura *et al.*, 2008). Interestingly, Allen *et al*. (2003) demonstrated over expression of MMPs in mouse myoblasts increased migration with supplementation of FGF (1 ng/ml) in combination with fibronectin (25 µl/ml).

1.4.5 Proliferation

After the satellite cells have migrated to the damaged area, they enter the cell cycle where they undergo proliferation to further increase the myogenic pool that is integral for muscle regeneration (Hawke and Garry, 2001). Some research suggests that growth factors (IGF-I, HGF), pro-inflammatory cytokines (IL-6, IL-1β and TNF-α) and some microRNAs (miR-221/222) are critical to satellite cell proliferation (Dumont *et al*., 2015). Studies investigating IGF-I on proliferation have shown that overexpressing

IGF-I, in murine models, resulted in greater satellite cell proliferation (Chakravarthy *et al.*, 2000). On the other hand, low concentrations of HGF promote proliferation, whereas interestingly, high concentrations impair proliferation (Yamada *et al.*, 2010). The pro-inflammatory cytokine IL-6 inhibits satellite cell proliferation when knocked out in mice (Serrano *et al.*, 2008). In contrast, Otis *et al.* (2014) used both C_2C_{12} cells and primary rat myoblasts supplemented with 5-bromo-2′-deoxyuridine to analyse proliferation via flow cytometry. The findings indicated that increases in IL-1β via the nuclear factor-kB (NF-kB) pathway increased IL-6 expression which activated cell proliferation (Otis *et al.*, 2014). Finally, Cardinalli *et al.* (2009) recently demonstrated that microRNAs, particularly mIRs 221/222 are influential in satellite cell proliferation. As expected, there is a very complex set of mechanisms to the proliferation of satellite cells which include growth factors, cytokines and microRNAs, however, it is logical to expect more processes which are involved but yet to be established.

1.4.6 Differentiation

Once the satellite cells have migrated to the damaged area and have undergone proliferation, they differentiate to subsequently fuse and enhance muscle hypertrophy (Owens *et al.*, 2015). The transcription factors Myf5 and MyoD are essential for the progression of satellite cells from the proliferation to the differentiation phase and ultimately enable myotube formation (Hawke and Garry, 2001). Studies using mouse models and primary skeletal cells of MyoD knock out resulted in and absence of myoblast differentiation and thus muscle regeneration (Sabourin *et al.*, 1999; Cornelison *et al.*, 2000). Following the role of MyoD in priming early differentiation, both myogenin and MRF (specifically the isoform MRF-4) are suggested to be integral to late differentiation of satellite cells (Rawls *et al.*, 1998). Molkentin *et al.* (1995) suggested that the myocyte enhancer factor 2 (MEF2) transcription factor family, when co-expressed with both myogenin and MyoD, resulted in increased transcription and therefore resulting in promotion of expression of muscle related genes. This correlated with findings from Liu *et al.* (2014) who suggested that deficiencies in a combination of MEF2 transcription factors A, B and D resulted in decreased muscle regeneration capacity. Indeed, there are critical signalling pathways that regulate this transition phase (proliferation to differentiation), including the MAPK protein p38α and calcium

activated pathways (Perdiguero *et al.,* 2007; Al-Shanti and Stewart, 2008). For instance, roles for p38α include phosphorylating MEF2 transcription factors and reducing the proliferation cycle via inhibition of the JNK pathway (Perdiguero *et al*., 2007). In addition, Al-Shanti and Stewart (2008) treated C2 mouse skeletal muscle myoblasts with 20 μm PD98059, reducing ERK activation and enhancing myoblast fusion through p38 MAPK signalling. However, p38 was shown to be compensatory in the presence of reduced ERK activity although MEF2 abundance was not assessed, whereas myogenin did increase. Foulstone *et al*. (2004) also reported that IGF-I activation of MAPK not only initiates myoblasts activation **(see section 1.4.2)** but also differentiation, along with PI3K/Akt signalling. Additional evidence supports the activation of PI3K/Akt signalling via IGF-I in myoblast differentiation (Coolican *et al.*, 1997). Therefore, IGF-I activation of p38α MAPK and PI3K/Akt signalling is important for activating differentiation.

1.4.7 Myoblast Fusion

Myoblast fusion follows the initial stage of satellite cell differentiation. During the cell-to-cell fusion process repair of damage and/or promotion of hypertrophy can follow. There are two stages involved in the fusion process, one being the contact of two SCs fusing, the other is SC attaching to damaged myotubes and fusing with it to facilitate repair (Chen and Olson, 2005), the former generally occurs during development, the latter generally post-natally. Przewoźniak *et al*. (2013) demonstrated that integrin-α3, integrin-β1, ADAM12, CD9, CD81 and M-Cadherin had increased expression during myoblast to myoblast fusion. Further, Schwander *et al*. (2003) also provided evidence of β1-integrin mediating the fusion between two myoblasts. In addition, Dalkilic *et al*. (2006) reported that filament C (an actin binding protein) was involved in the fusion of myoblasts with each other. Other research has investigated Kirrel proteins on cell to cell fusion (Durcan *et al*., 2013, 2014). In the first paper, the authors reported increases in Kirrel B expression during C_2C_{12} myoblast fusion, and the inverse was reported through chemical inhibition (Durcan *et al*., 2013). Following, the authors completed human damaging protocols (drop jumps and downhill running) and extracted primary human myoblasts (Durcan *et al*., 2014). They reported three splice variants of Kirrel3, however further investigation was required to link with myoblast fusion. Whereas,

during satellite cell fusion to damaged myotubes, it is proposed that calcium activated transcription factors are upregulated, specifically, NFATc2 (Horsley *et al.*, 2003). The same authors concluded that NFATc2 controlled IL-4 expression which was important for the recruitment of additional satellite cells to the site of injury and required for fusion and repair. Lastly, the membrane protein myomaker and the calcium phospholipid protein, myoferlin are suggested to impact myoblast fusion. Millay *et al.* (2013) demonstrated that in the absence of myomaker, myoblast fusion was blocked in murine models. In addition, myofelin null C_2C_{12} cells displayed lack of myoblast fusion (Doherty, 2005). Even though it is generally accepted that are two processes integral for myotube formation, there is a distinct lack of evidence in the mechanisms involved in this stage of muscle regeneration.

1.4.8 Myotube Maturation

The final stage involving muscle regeneration and SCs is myotube maturation. For myotubes to become fully functioning myofibres they must undergo a maturation process. The primary signalling cascade involved in the maturation and hypertrophy of myotubes is the Akt-mTOR pathway (Park and Chen, 2005). The initiation of this pathway via IGF-I stimulation results in a number of other signalling pathways being positively or negatively impacted. For instance, mTOR promotes the activation of the ribosomal protein S6 kinase and the inhibition of the translation of 4E-BP1. In contrast, Akt signalling supports hypertrophy via blocking the FOXO pathway, which is primarily involved in muscle catabolism and promoting mTOR activation which is involved in muscle hypertrophy (Bodine *et al.*, 2001; Sandri *et al.*, 2013).

1.4.9 Wnt Signalling and Myogenesis

The Wnt family includes 19 ligands that bind to Frizzled receptors (of which there are 10) and their lipoprotein receptor-related protein (LRP) 5/6 (Schlessinger *et al.*, 2009; Von Maltzahn *et al.*, 2012). Blocking Wnt disables tissue renewal and muscle regeneration demonstrating the importance of Wnt ligands in myogenesis (Clevers *et al.*, 2014). Specific Wnt ligands activate either canonical or non-canonical pathways based on the involvement of β-catenin (Komiya and Habas, 2008). For instance,

canonical Wnt3A signalling dephosphorylates glycogen synthase 3 (GSK3) increasing β-catenin translocation in the nucleus (Brack *et al.*, 2008), an integral component of SC myogenic linage and commitment to differentiation (Brack *et al.*, 2008). In addition, the activation of Wnt and interaction with Notch signalling via GSK3 was reported to control SC proliferation to differentiation (Brack and Rando, 2007). Evidence suggests that Notch activation controls SC activation and self-renewal, whereas increases in Wnt initiate the exit of SCs from the cell cycle enabling commitment to differentiation (Brack and Rando, 2007). To summarise, therefore, the canonical wnt3a signalling pathway is important for late SC proliferation, early differentiation and myogenic lineage commitment.

In contrast, other Wnt ligands activate non-canonical pathways that also phosphorylate GSK3 (Brack *et al.*, 2008). Lacour *et al.* (2017) demonstrated that R-spondin 1 (RSPO1) activation of non-canonical Wnt signalling was important for efficient myotube formation. Wnt7a binding to frizzled 7 receptor downregulated β-catenin translocation and upregulated Rac1 allowing for increased migration and efficient regeneration (Lacour *et al.*, 2017). In addition, Wnt4 was produced by the muscle fibre and required to maintain SCs in quiescence through activation of non-canonical RhoA and inhibition of Yap (Eliazer *et al.*, 2019). Non-canonical Wnt7a signalling can activate SC self-renewal through the activation of the PCP pathway (Le Grand *et al.*, 2009) but also SC differentiation via activation of PI3K/Akt signalling independent of IGF-I (Von Maltzahn *et al.*, 2012). Therefore, non-canonical Wnt4 signalling maintaining quiescence whereas Wnt7a is involved in self-renewal via PCP and migration and myotube formation via Rho and PI3K Akt. These latter signalling molecules may have importance in ageing muscle cell migration and fusion more generally and warrant further investigation in this thesis.

1.5 Interventions on Muscle Repair and Regeneration

1.5.1 Nutritional Strategies: is Protein the answer?

Overall, once trauma to the muscle has occurred, the reaction of the skeletal muscle is extremely complex, with various cells, matrices, growth factors, cytokines and signalling pathways implicated (Figure 1.4). However, it is the interaction of the satellite cells with the microenvironment which is most important to optimal muscle regeneration. The following section/s discuss the common interventions utilised with the aim of accelerating muscle regeneration.

Individuals that commonly participate in exercise ingest foods afterwards, often containing, protein. For example, athletes who undergo strenuous exercise (e.g. two training sessions per day), use strategies to improve recovery and delayed onset of muscle soreness (DOMS). It known that protein intake post exercise aids recovery and adaptations through promoting a positive muscle protein balance (Hawley *et al.*, 2006). Most of the literature has focused on branched chain amino acid (BCAA) supplementation following eccentric exercise as a useful supplement. The BCAAs contain leucine, which is reported to stimulate MPS (Hawley *et al.*, 2006). The role of leucine's metabolite, beta-Hydroxy beta-methylbutyric acid (HMB), is also of interest and is suggested to increase MPS and attenuate decreases in muscle protein breakdown (MPB), further increasing the net muscle protein balance (Wilson *et al.*, 2013).

Following acute exercise, MPS is increased through elevated hormones and growth factors (Condon and Sabatini, 2019) (Figure 1.7). The ability to further enhance MPS is supported with the addition of protein to the diet and is therefore, reported to promote muscle recovery and hypertrophy following protein supplemented resistance exercise interventions (Atherton *et al.*, 2017). Both the supplements leucine and HMB stimulate MPS through mTOR (Kirby *et al.*, 2012: Wilson *et al.*, 2009). Following ingestion, leucine exits the circulation and enters the cell through the amino acid transporters SLC7A5 and the glycoprotein SLC3A2 (Drummond *et al.*, 2011). Leucine then binds to sestrin deactivating the Gator2 complex via the dissociation of sestrin

(Condon and Sabatini, 2019). Gator1, which is bound to Gator2 on the lysosome is also deactivated (Shen *et al.*, 2018). Gator2 regulates RagA and RagC, which are translocated into the lysosome by Ragulator and this complex activates mTORC1 (Condon and Sabintini, 2019) (Figure 1.7). Unlike leucine, it is unknown how HMB enters the cell and activates mTOR. In the cell cytoplasm, amino acids metabolites bind to the Samtor complex which inhibits Gator1 activation (Gu *et al.*, 2017). The following activation of mTOR is hypothesised to occur. Although, with HMB and other specific amino acid metabolites, more research is required to ascertain the direct mechanisms and the relevance of previously published processes ascribed to e.g. leucine.

Alternatively, it is reported that leucine and HMB both increase insulin and/or IGF-I concentrations, which subsequently activate both the PI3K/Akt and the MAPK/ERK signalling cascades which subsequently stimulate mTOR and subsequently protein synthesis via S6K and 4EBP1 (Kornasio *et al.*, 2009; Sanchez *et al.*, 2012). Anabolic hormones and peptides which activate receptor tyrosine kinases (RTKs), e.g. Insulin and IGFs, subsequently activate insulin receptor substrate (IRS) and growth factor receptor-bound protein 2 (GBR2) enabling PI3K/Akt and MAPK/ERK signalling respectively (Mendoza *et al.*, 2011). In brief, PI3K is activated via IRS and phosphorylates phospha-tidylinositol 4,5 triphosphate (PIP2) into phospha-tidylinositol 3,4,5 triphosphate (PIP3) at the cell membrane, which recruits Akt (Mendoza *et al.*, 2011). As Akt is recruited to the membrane, 3-phosphoinositide-dependent kinase 1 (PDK1) activates Akt which phosphorylates mTORC1 directly, or indirectly through the phosphorylation of tuberous sclerosis complex (TSC) (Fayard *et al.*, 2005). The phosphorylation of TSC releases Ras homolog enriched in brain (RHEB) and consequently activates mTORC1 (Condon and Sabintini, 2019). On the other hand, activation of GRB2 and son of sevenless (SOS) which initiates Ras, then Raf kinases. Following, the mitogen-activated protein kinase (MEF) activates ERK (Bodine *et al.*, 2001). Similar to Akt, TSC is phosphorylated by ERK which activates mTORC1. However, ERK and RSK can translocate directly into the nucleus where they transcribe a number of genes (Zehorai *et al.*, 2010). The Akt and ERK signalling cascades that activate mTOR cause the synthesis of genes that are involved in muscle regeneration including MyoD, Myogenin and IGF-I (Dai *et al.*, 2015, Kornasio *et al.*, 2009).
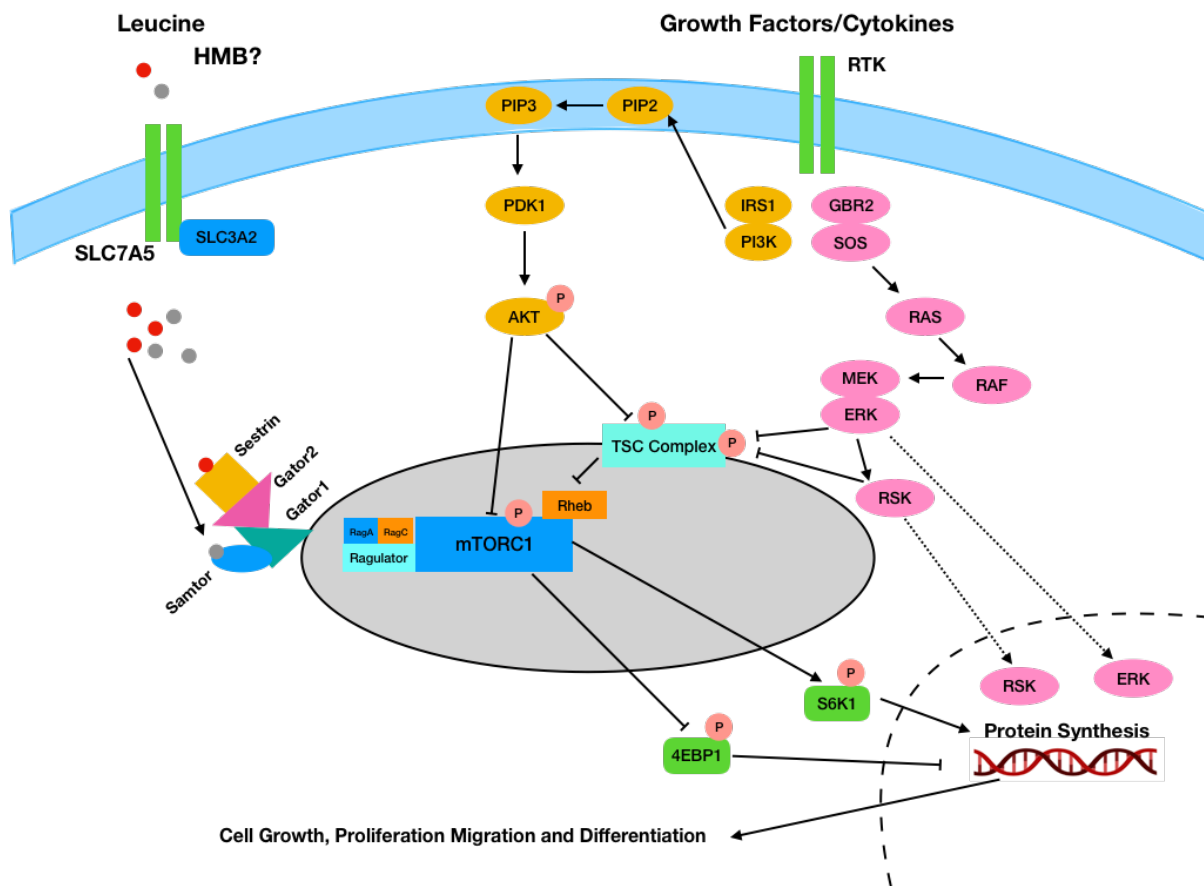
Figure 1.7. Akt, ERK and mTOR signalling by the amino acids leucine, HMB, growth factor IGF-I and hormone insulin.

Although much research has focussed on the potential of protein in muscle hypertrophy regimes, not much research has been conducted investigating the impact of protein supplementation following multiple eccentric contractions and muscle repair and regeneration. Studies have shown following BCAA supplementation following eccentric contractions that markers of damage were attenuated, although markers were different among studies (aldolase, lactate dehydrogenase, granulocyte elastase) (Nosaka *et al.*, 2006; Matsumoto *et al.*, 2009; Shimomura *et al.*, 2010). In addition, research by Howatson *et al.* (2012) demonstrated that BCAA administration (20 g/d for 7-day before and 5-day post exercise) decreased creatine kinase (CK) concentrations and muscle soreness following 100 drop jumps.

While extensive research in the hypertrophic arena has suggested an important role for leucine specifically in protein synthesis, little work has been undertaken investigating its role specifically following dynamic eccentric damaging exercise. Recent work by Kirby *et al.* (2012) recruited 27 healthy males into three groups, control, placebo and leucine with the ratio of participants 8:9:10 respectively. The participants were asked to consume the leucine (250 mg/kg/d) or placebo supplements 30 minutes pre, during and immediately after eccentric exercise. The protocol included five sets of 20 reps of drop jumps, followed by 6 sets of 10 reps of eccentric leg extensions (Kirby *et al.*, 2012). The leucine group attenuated mean peak force compared to placebo, however, the soreness greatly increased immediately post exercise in all groups with no effect of leucine.

Whey supplements contain leucine and other essential amino acids (AA); therefore, the hypothesis is that they improve muscle repair following eccentric contractions, however the research is equivocal or lacking. For example, untrained male volunteers consumed either placebo, whey protein or hydrolysed whey protein after 100 eccentric knee extensions (Buckley *et al.*, 2010). Interestingly, hydrolysed whey attenuated isometric force within 24 h, there was no difference between whey or the placebo, and both were without effect. Etheridge *et al.* (2008) implemented a supplement protocol of a protein rich meal (100 g) immediately following 30 minutes downhill running. The meal had no effect on muscle soreness, or CK activity, but declines in maximal voluntary contraction (MVC) were attenuated.

Indeed, there is some literature investigating the effects of whey protein on satellite cell function, or the muscle regeneration process. Farup *et al.* (2014) recruited 24 healthy males and performed 150 eccentric knee contractions followed by ingestion of 26 g of whey protein which was consumed three times a day. The whey group increased SC number/myonuclei compared to placebo but soreness, MVC and CK levels showed no differences between groups. Alternatively, in a study involving 24 healthy males who followed the same supplement and damaging protocol procedure as that of Farup *et al.* (2015) investigated the response of pericytes (muscle-resident stromal cells which secrete growth factors and cytokines (De Lisio *et al.*, 2014)). The authors concluded that $\alpha7$ and $\beta1A$ integrin content was increased following exercise,

but there was no impact on pericytes of whey supplementation (De Lisio *et al*., 2014). With this study, the question was focused on muscle regeneration and did not include physiological measures.

Finally, with the interest in the impact of leucine containing supplements on MPS/regeneration growing, interest in the impact of HMB has also gained attention (Figure 1.8). Van Someren *et al*. (2005) investigated the effects of HMB and α-ketoisocaproic acid after eccentric exercise. The study conducted 30 bicep curls at 70 % 1 repetition max with 3 g/d of HMB supplementation for 11 days pre exercise and for 3 days post. The authors concluded that CK elevation was fully restored and soreness was reduced with supplementation. The study was a counterbalanced cross over trial, however, the samples size (n = 6) was small and power was not indicated. In contrast, Paddon-Jones *et al*. (2001) indicated no effects of HMB (3 g/d for 10-day) after 24 maximal elbow extensors on any of the authors outcome measures (soreness, CK, arm girth and strength). Interestingly, Wilson *et al*. (2009) conducted a study in 22 untrained men subjected to 55 maximal eccentric contractions and supplemented either pre or post intervention with HMB or placebo. Post HMB showed no differences, however, pre HMB feeding attenuated lactate dehydrogenase (LDH) increase and soreness, although significance was not attained. Recently, Shirato *et al*. (2016) investigated the effects of both HMB and whey protein on symptoms of muscle trauma. They demonstrated that there was no impact of whey combined with HMB, compared to HMB and whey alone. It is important to note that there was no placebo group and the groups sizes were small (n = 6), therefore interpretation of results is limited. The results generally show no impact, however, most of the studies did not control for diet, had relatively small sample sizes and the muscle group damaged differed.
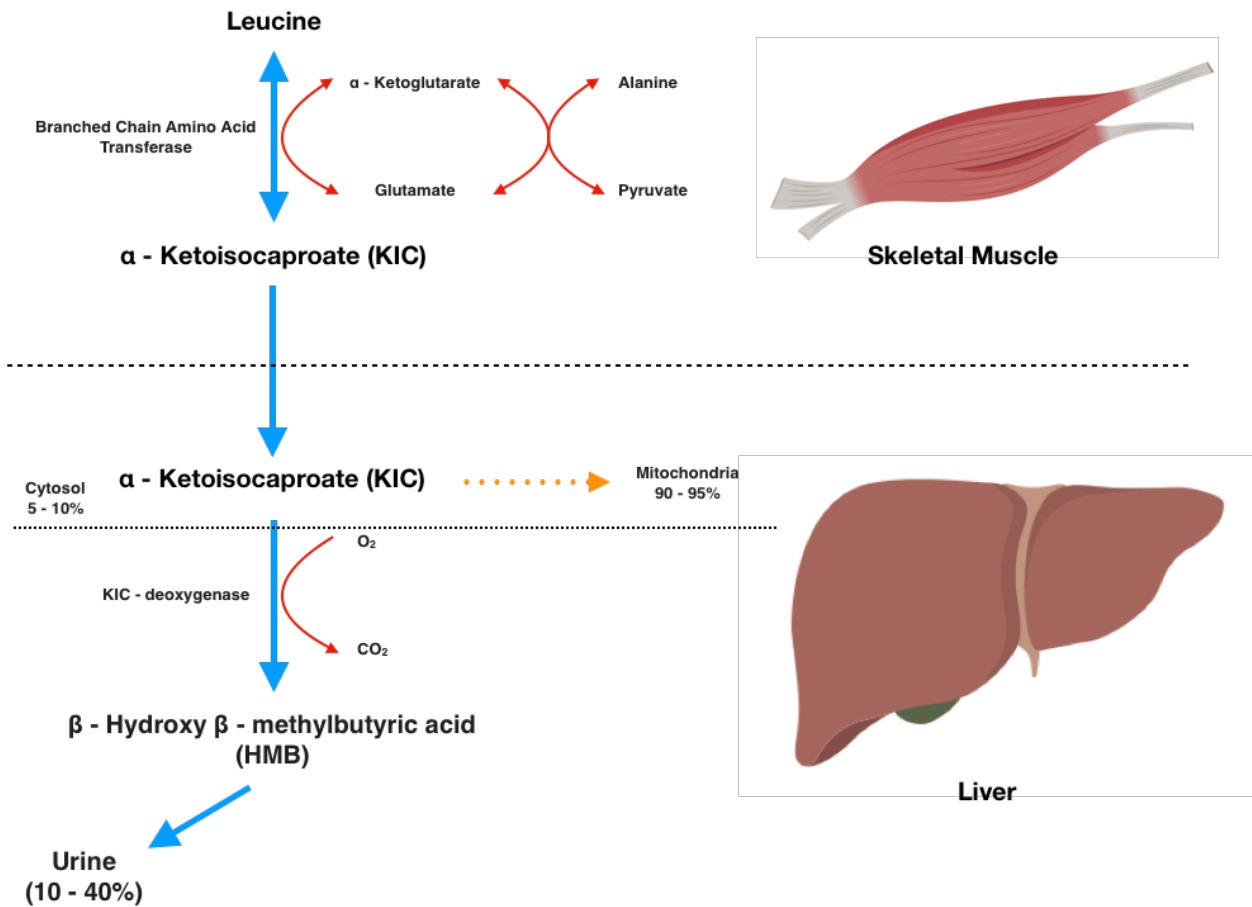
Figure 1.8. Metabolism of leucine into HMB. Created by the author of this thesis using Biorender.

There is less evidence on the impact of leucine and HMB on myogenesis. In cell culture, leucine supplementation (2 mM) increases proliferation in preterm rat myoblasts via increased phosphorylation of mTOR and S6K1 (Dai *et al*., 2015). The authors also reported increased myotube formation following mTOR phosphorylation. Increased mTOR signalling also corresponded to increased MyoD expression. Interestingly, leucine increased myogenin gene expression irrespective of mTOR activation status (Dai *et al*., 2015). How leucine specifically increases myogenin expression requires further investigation. It is not known if either upregulation of Akt or ERK increased mTOR in this study, as they were not measured or manipulated. There is some evidence that HMB stimulates increased myoblast proliferation and differentiation (Kornasio *et al*., 2009). In human myoblasts, 50-100 µg/ml HMB increased both DNA synthesis and myotube formation through increased MAPK/ERK

and PI3K/Akt signalling respectively. However, mTOR signalling, was not measured in this study (Kornasio et al., 2009). Interestingly, HMB supplementation did increase both MyoD and myogenin gene expression, similar to observations with leucine. IGF-I was also increased at both gene expression protein level, providing evidence that increased IGF-I, following HMB supplementation, may have initiated both Akt and ERK signalling – these warrants further investigation with appropriate temporal and inhibitor studies.

Although many athletes and individuals consume a variety of nutritional supplements or foods containing protein with the aim to optimize recovery after eccentric exercise, more research is still required in order to determine whether leucine or HMB supplementation impact on muscle damage, repair and fusion, both *in vivo* and *in vitro* and what the underpinning mechanisms may be.

1.6 Ageing and Impact of Protein Supplementation

1.6.1 Sarcopenia Mechanisms and Impact of Exercise and Protein Intake

Sarcopenia, the progressive loss of muscle mass and strength with age (Rosenberg, 2011) involves many mechanisms, including: increases in intracellular fat and connective tissue accumulation (Kent-Braun et al., 2000; Taaffe et al., 2009), along with decreases in muscle fibre size and number, decreases in type II fibres, decrease in SC number, reduced activation and self-renewal, increased motor neuron death, increases in chronic inflammation and increases in anabolic resistance (Narici and Maffulli, 2010). . The increase of fat infiltration in muscle with ageing supports the increase of macrophage accumulation which culminates in the release of pro-inflammatory cytokines including TNF-α, IL-6 and IL-1 (Neels and Olefsky, 2006). Adipocyte infiltration also releases the adipokines leptin and adiponectin (Neels and Olefsky, 2006). The elevation of macrophages, cytokines and adipocytes increase local inflammation, which is associated with muscle loss and with insulin resistance (Goodpaster et al., 2000).

The loss of muscle mass is a hallmark of sarcopenia and involves the reduction of both muscle fibre size and number, with type II fibres most vulnerable (Larsson and Karlsson, 1978). Evidence indicates that this loss of fast type muscle fibres is due to an increase in motor unit loss (Campbell *et al.*, 1973). Within type II fibres, greater atrophy occurs in the type IIX fibres compared to type IIA (Andersen, 2003), During ageing, type II fibre loss occurs past the seventh decade of life, whereas a loss in type I fibre, to the extent of type II occurs later, during the eighth decade (Andersen, 2003). It appears that sarcopenic individuals are likely to suffer losses in muscle mass in both type I and II fibres past 80 years of life.

Another mechanism of sarcopenia is the blunted response in older individuals to exercise or feeding, termed as anabolic resistance (Cuthbertson *et al.*, 2006). It is reported that in response to amino acid and low glycaemic carbohydrate feeding, the activation of Akt signalling pathway is blunted compared to young individuals (Wilkes *et al.*, 2009), which is important in activating mTOR and thus MPS. Further, muscle protein breakdown (MPB) was reduced by 12% in older individuals vs. by 47% in young individuals, in response to insulin following a low glycaemic feed (Wilkes *et al.*, 2009). In support of this, insulin resistance is reported to culminate in increased protein degradation via activation of the proteasome system (Wang *et al.*, 2006). In this study, the authors reported that the PI3K/Akt reduction increased caspase and proteasome pathway caused an increase in degradation and could result in muscle wasting (Wang *et al.*, 2006). Associations between elevations in protein degradation and chronic inflammation are reported to be a potential cause of sarcopenia (Bowen *et al.*, 2017). Ageing is associated with increased TNF-α (Saini *et al.*, 2006; Schaap *et al.*, 2009) which is linked with increased protein degradation via the NF-κB signalling pathway (Chen and Olson, 2005). However, these increases in protein degradation would need to be greater than the rates of synthesis to result in the overall loss of proteins, and therefore, contribute to sarcopenia.

Furthermore, a complicating contributor to sarcopenia is the underlying incidence of increased sedentary behaviour (Lazarus and Harridge, 2017) and poor nutrition, in particular, inadequate protein intake (Phillips and Martinson, 2019). From an exercise perspective, the model of masters athletes for healthy ageing is reported (Hawkins *et al.*, 2003; Lazarus and Harridge, 2017). With this model, individuals undergo sufficient

exercise regimes for 'optimal' healthspan, although a trajectory of biological ageing (around the 8th decade of life) is still observed (Lazarus and Harridge, 2017). The same authors proposed a 'set point theory' from which master athletes are above this set point, sedentary and inactive individuals are below this set point, and in the latter, healthspan is compromised through declines in physiological function (Seals *et al.*, 2016). The aim is to be above the set point, where health span is optimised and only biological ageing occurs (Lazarus and Harridge, 2017). This demonstrates that sarcopenia is caused by both ageing and inactivity. Different types of exercise exert different physiological responses. For instance, aerobic exercise such as walking, jogging, swimming and cycling can decrease chronic inflammation (Chung *et al.*, 2009), improve mitochondrial function (Konopka and Sreekumaran Nair, 2013) and also enhance sensitivity to protein provision (Fujita *et al.*, 2007b). Whereas, resistance training, such as lifting weights and body weight exercises attenuate sarcopenia through improvements in muscle mass, function and flexibility (Chodzko-Zajko *et al.*, 2009; Liu and Latham, 2009). Therefore, older adults that practice both aerobic and resistance training would improve whole body physiology that would start to mitigate the rate and impact of sarcopenia.

Nutritionally, the main macronutrient that is reported to counteract muscle loss is protein (Phillips, 2015). Worryingly, it is reported that older individuals are consuming insufficient protein based on guidelines such as recommended daily allowances (RDA). In the US and Canada, the RDA is 0.8 g/kg/d, in the UK it is 0.75 g/kg/d (Phillips *et al.*, 2016). Evidence from a number of studies have advocated for increases in RDA to 1.0-1.2 g/kg/d to preserve muscle mass and function (Bauer *et al.*, 2013; Deutz *et al.*, 2014). Due to anabolic resistance of older muscle, it is proposed that 0.40 g/kg/meal is required to maximise MPS (Moore *et al.*, 2015). However, there is a essential amino acid peak for stimulating MPS, which is 10 g for younger individuals and 20 g for the elderly (Cuthbertson *et al.*, 2005). In addition, it is not just the amount of protein that is important, also, the quality of protein. In particular, protein containing foods that contain all 9 essential amino acids, such as meat, fish, eggs, soy and dairy foods are important. Of those 9 EAAs leucine is regarded as the most beneficial, due to its capacity to stimulate MPS (Churchward-Venne *et al.*, 2014). A metanalysis on leucine rich protein supplementation concluded that beneficial effects were observed on body weight, lean body mass but not muscle strength in individuals already prone

to sarcopenia (Komar *et al.*, 2015). There reason for lack increase in muscle strength could be due to the anabolic resistance of elderly skeletal muscle (Cuthbertson *et al*., 2006) It is apparent therefore, that both exercise and protein intake are critical for diminishing the multifaceted causes and effects of sarcopenia.

1.6.2 Impact of Ageing and Protein on Muscle Regeneration

During the human lifespan, there is a gradual, yet progressive loss of skeletal muscle with age, referred to as sarcopenia (Figure 1.9). Sarcopenia is associated with malnutrition, sedentary behaviour, increases in reactive oxygen species and anabolic resistance to AAs (Kim *et al.*, 2010). As sarcopenia progresses, the most obvious response in the muscle is the atrophy (loss of muscle) in type II muscle fibres (Deschenes, 2004). Critically, in addition to the associated loss of mass and strength, declining muscle mass is also accompanied by compromised (insulin resistance) and impaired functional ability. The loss of functional capabilities is associated with increased prevalence of falls, bone fractures and inability to complete daily tasks, influencing an individual's independence (Gault, 2013). Recently, much of the focus to alleviate sarcopenia has resulted in the research community investigating the impact of exercise and nutrition on reducing the "symptoms".

Figure 1.9. Cross sectional area of healthy and sarcopenic muscle fibres. Created by the author of this thesis using Biorender.

The essential role that the immune system has in optimising the muscle regeneration process, is impaired with ageing, thus consequently affecting muscle repair. This primarily affects muscle regeneration through the capacity for immune cells to stimulate SC proliferation and differentiation (Domingues-Faria *et al.*, 2016). Macrophages which in the young population protect satellite cells from apoptosis (Sonnet, 2006), are impaired in ageing animal models resulting in decreased satellite cell activation (Krajnak *et al.*, 2006). In human models, Przybyla *et al*. (2006) reported that older men (aged 70) had fewer macrophages leading to decreased protection against apoptosis in the muscle.

Moreover, the capacity of older individuals to phagocytose debris is also slowed, reducing the subsequent events initiated by immune cells (Dumont *et al.*, 2015). This could lead to a prolonged pro-inflammatory environment, which results in elevations of pro-inflammatory cytokines (TNF-α, IL-6), which coincide with reduced muscle mass and strength in older men and women (Visser *et al.*, 2002). Other stimulators of growth in young individuals include IGF-I, this growth factor is reduced in muscle of older individuals, which is linked with impaired muscle regeneration and sarcopenia (Hameed *et al.*, 2002).

In an ageing individual, the capacity of the muscle to regenerate following muscle trauma is impaired and this is considered to be influential to the onset of sarcopenia (Jang *et al.*, 2011). This is due to, in part, the decreased number of SCs available in the reserve pool (Welle, 2002), potentially as a result of compromised re-quiescence (Bigot *et al.*, 2015), but also the impaired ability of the immune cells to protect SCs from apoptosis (Krajnak *et al.*, 2006). The proportion of SCs committing to myogenesis is higher in aged (95 %) compared to young (80 %), subsequently depleting the reserve pool (Bigot *et al.*, 2015). This decline in self-renewal is in-part caused by a reduction in FGF receptor and elevation in p38 MAPK signalling in mouse myoblasts (Bernet *et al.*, 2014). Further, Cosgrove *et al*. (2014) reported aged mice were overexpressing p38 MAPK which resulted in declines in myoblast self-renewal. Therefore, the authors transiently inhibited the active p38 MAPK signalling restoring SC numbers (Cosgrove *et al.*, 2014). The lower SC numbers have a consequential effect on the subsequent muscle regeneration processes (Shefer *et al.*, 2006; Day *et*

al., 2010). In addition, the majority of evidence in aged cells, either from animals or humans suggests that differentiation capacity is reduced (Sharples and Stewart, 2011; Sharples *et al.*, 2012, 2013), with very few studies showing no difference (Shefer *et al.*, 2006; Alsharidah *et al.*, 2013). The notch and wnt signalling pathways are suggested to be responsible for the impairments in satellite cell function (Conboy *et al.*, 2003; Carlson *et al.*, 2009; Arthur and Cooley, 2012). The notch signalling pathway initiates SC activation, self-renewal and proliferation. In contrast, the wnt pathways is increased, resulting in enhanced conversion of SCs to fibrogenic cells (Brack and Rando, 2007). Recently, it has been proposed that the janus kinase (JAK)/signal transducer and activator of transcription (STAT) signalling pathway is upregulated in aged SCs (Price *et al.*, 2014), through in part, elevated levels of IL-6 (Tierney *et al.*, 2014). This upregulation can inhibit SC self-renewal and asymmetrical division (Dumont *et al.*, 2015). Overall, it is logical to suggest that in an aged individual, there are multifactorial impairments leading to reduced muscle regeneration, and possibly underpinning the progression of sarcopenia.

Although limited, research has been conducted in attempts to alleviate sarcopenia through the use of nutritional aids, mainly protein and in particular leucine. It is well known that inadequate protein intake in the aging population accelerates sarcopenia (Volpi *et al.*, 2001; Wolfe *et al.*, 2008; Moore *et al.*, 2015). In addition, inadequate protein intake has been associated with decline of gene expression related to satellite cell proliferation and differentiation (Welle *et al.*, 2003). For these reasons, the supplementation of protein (e.g. BCAA: leucine) may reduce the catabolism associated with sarcopenia (Han *et al.*, 2008). A study from our group investigated the effect of L-glutamine on stress induced (TNF-α transduction) skeletal muscle atrophy, using C_2C_{12} murine myoblasts as the model. A positive impact on muscle atrophy was reported through maintained differentiation and myotube size when supplemented with L-glutamine reducing the increase in p38 MAPK observed in the presence of a wasting dose of TNF-α (Girven *et al.*, 2016). Similar studies remain to be performed in aged cells. Han *et al.* (2008) treated satellite cells with leucine, demonstrating beneficial responses to phosphorylation of mTOR, p70SK6 and 4EBP1. As previously suggested, the positive effect of leucine on the protein degradation pathways could be in part, due to its conversion to HMB. For instance, Baier *et al.* (2009) recruited older

men and women (average 76 years old) and supplemented with HMB (3 g/d) over a year and reported an increase in MPS and decrease in MPB. In such interventions can be substantiated, they have potential to benefit both older individuals but also patients with muscle cachexia (Smith *et al.,* 2005).

1.7 Recovery Following Acute Unaccustomed Eccentric Exercise in Young and Old

Following an acute bout of unaccustomed eccentric exercise, reductions in muscle function and increases in DOMS occur (Lavender and Nosaka, 2006). Most exercise regimes or sporting movements involve eccentric contractions (Proske and Allen, 2005). In both young and elderly individuals, the sensations of DOMS can result in lack of motivation to exercise for prolonged periods of time. In addition, for elderly individuals, the incidence of DOMS can adversely affect daily function, including increasing the risk of falls (Lavender and Nosaka, 2006). Multiple exercise sessions result in beneficial muscle adaptation in young and attenuate sarcopenia in elderly individuals (Welle, 2002). It is important to alleviate DOMS and improve muscle function as a means of helping individuals commit to prolonged exercise sessions. Therefore exploring interventions to minimise DOMS is warranted and may include: nutraceuticals, pharmaceuticals, ice baths and massage among others (Howatson and Van Someren, 2008). In this thesis, there is a focus on the supplements leucine and HMB, which stimulate MPS following unaccustomed eccentric exercise. However, their role in the repair and regeneration of skeletal muscle following eccentric exercise and therefore their role in reducing DOMS or the impact of DOMS has not been determined and warrants further investigation.

1.8 Summary and Conclusion

This chapter expresses some the underpinning mechanisms on how skeletal muscle is formed during embryonic development and how it adapts across the life course. Following eccentric contractions, the muscle must repair and regenerate to enable normal function and following multiple bouts, provide stimulus for muscle adaptation. Firstly, in a proinflammatory environment, the integration of immune cells, cytokines and growth factors stimulate the removal of debris. This coincides with the activation, migration and proliferation of the muscle stem cell. Secondly, after approximately 48 h, an anti-inflammatory state is evoked and the muscle enters the regenerative phase, that primarily enables the resident and infiltrating SCs to differentiate and to fuse to form fully mature myofibers. Optimising these post exercise processes are of great interest and have implications for aiding repair and recovery in inactive, active and highly trained individuals across the ages. Given the literature on the role of protein supplementation in hypertrophy, a gap existed relating to the role that these supplements may play in injury repair. A need was identified to focus on the impact and mechanisms of leucine and HMB in skeletal muscle behaviour. In particular, the positive impact on muscle regeneration and intracellular signalling cascades including IGF/Akt/mTOR were deemed to be of importance. These mechanistic investigations were tied to physiological measures, following damage, including force production, muscle soreness and indirect damage markers in younger individuals *in vivo*. Given ethical constraints of knowingly inducing muscle damage in older individuals, and thereby increasing the risk of injury related falls, an in vitro model of muscle injury was also adopted to determine whether any impairments are observed in repair and regeneration in a murine muscle cell model of replicative ageing. As an intervention, protein supplementation was investigated. Given the paucity of focusing on muscle cell function with age, this was also identified as an important area for research.

1.9 Perspective and Thesis Aims

Exercise and subsequent muscle repair and regeneration are highly orchestrated processes that involve interactions from extracellular and intracellular stimuli. Exercising optimise these processes and the following adaptations, such as muscle hypertrophy, occur. However, over the lifespan, the muscles contractile and regenerative capacity is reduced. Although the mechanisms are complex and multifaceted. Researching interventions to combat these declines in repair and regeneration is required. Protein supplementation is reported to stimulate muscle hypertrophy in young and also alleviate in aged individuals. However, there is little evidence on the effect of protein supplementation on muscle repair and regeneration in both young and elderly individuals. Therefore, the overarching aim of this thesis is:

To utilise amino acid supplementation as an intervention to reduce damage and/or facilitate growth and repair in skeletal muscle using *in vivo* (objective 1) and *in vitro* (objectives 2-4) models.

With subsequent study objectives including:

1: To reduce the sensation of DOMS and improve skeletal muscle repair and recovery with leucine and HMB supplementation following dynamic eccentric exercise.

2: To investigate the impact of leucine and HMB on control and replicatively aged skeletal muscle cell repair.

3: To determine the impact of nutritional supplements on myotube formation in control and replicatively aged murine myoblasts.

4: To investigate the dynamic protein profiling on replicatively aged and control myoblasts and myotubes.

Chapter 2: Materials and Methods Pertaining to Cell Culture Studies

2.1 Materials, Equipment and Specialised Software

2.1.1 Chemicals, Solvents and Reagents

The chemicals and solvents were purchased from Sigma Aldrich (Poole, UK) and Fisher Scientific (Loughborough, UK). The four anti-bodies used for flow cytometry were: 1) anti-human/mouse phosphor-AKT (S473; APC; 675/25 nm), 2) anti-human/mouse phosphor-ERK1/2 (T202/Y204; Alex-afluor 488; 533/30 nm), 3) anti-human/mouse phosphor-mTOR (S2448; PerCP; 670/LP nm) and 4) anti-human/mouse phosphor-p38 MAPK (T180/Y182; PE; 585/40 nm). They were purchased from Thermo Fisher Scientific (Waltham, USA).

2.1.2 Cell Culture

All cell culture experiments were conducted under a Kojair Biowizard Silverline class II hood (Kojair, Vippula, Finland). All cells were incubated in a HERAcell 150i carbon dioxide (CO_2) Incubator (Thermo Scientific Inc, Chesire, UK). An extraction pump (Charles Austen Pumps Ltd, Surrey, UK), was used to remove waste media and supernatant. Cell culture solutions were prepared using distilled water that was purified through a MilliQ water system (Merck, Darmstadt, Germany). Cell images were performed using a Leica DMI 6000B inverted microscope (Leica Biosystems GmbH, Nussloch, Germany). This microscope has a recording ability for live cell imaging (Leica DCF365 FX). Fluorescent images were taken using the same microscope with a fitted FITC-fluorescence L5 filter cube (excitation wavelength = 480/40 nm).

2.1.3 Cell Culture Reagents

Dulbecco's modified Eagle's medium (DMEM) was purchased from Gibco (Life Technologies, California, US) and was used for murine C_2C_{12} cells. All sera were purchased from Gibco (Life Technologies, California, US) and include: heat inactivated horse serum (HS), heat inactivated new born calf serum (NBCS) and heat inactivated fetal bovine serum (FBS). L-Glutamine (L-G), was added to all media, at a dose of 2 mM. The antibiotic penicillin streptomycin (PS) was also added to all media (1 %: 50 units penicillin/50 µg streptomycin). To clean and wash the cells phosphate buffered saline (PBS) was used. The PBS was purchased from Sigma-Aldrich (Poole, UK) in tablet form and reconstituted to a working concentration of 0.01 M phosphate buffer, 0.0027 M KCl, 0.137 M NaCl at a pH of 7.4 in dH_2O. For cell adherence, gelatin type A from porcine skin was used and purchased from Sigma-Aldrich (Poole, UK) and reconstituted to create a working stock of 0.2 % gelatin. The trypsin was composed of 0.05 % trypsin and 0.02 % Ethylenediaminetetraacetic acid (EDTA) and purchased from Sigma-Aldrich (Poole, UK). For murine C_2C_{12} cells, growth media (GM) included: DMEM, 10 % FBS, 10 % NBCS, 1 % PS and 2 mM L-G. Differentiation media (DM) included: DMEM, 2 % HS, 1 % PS and 2 mM L-G. GM were used to promote cell proliferation and DM was used to promote cell differentiation.

The AAs leucine and HMB were purchased in powder form from MyProtein (Cheshire, UK). Both supplements were reconstituted as 0.5 M stocks in 37 % (12 M) hydrochloric acid (HCl). The mixture was vortexed thoroughly until the amino acid powder was fully dissolved. Prior to supplementation, the stock was filtered with 0.22 µM syringe filter. Doses of both leucine and HMB were prepared via dilution in PBS to final concentrations of: 0 (DM; control dose), 0.625, 1.25, 2.5, 5 and 10 mM. Signalling pathways were manipulated with doses of: LY294002 (10 µM), inhibitor of PI3K signalling, PD98059 (5 µm), inhibitor of ERK signalling or rapamycin (0.5 µM) inhibitor of mTOR (Dimchev *et al.*, 2013; Hatfield *et al.*, 2015).

2.1.4 Plasticware

Tissue culture flasks (T25, T75, 6 well and 12 well plates) were purchased from Nunc Life Sciences, Thermo Fisher Scientific (Rosklide, Denmark). For LDH and bicinchoninic acid (BCA) protein assays, 96 well plates were purchased from Nunc Life Sciences, Thermo Fisher Scientific (Rosklide, Denmark). For CK assays, BD Falcon 96 well clear UV plates were purchased from BD Biosciences (San Jose, CA, USA). All tubes (0.5, 1, 1.5 and 2 ml) were purchased from Eppendorf (Hamburg, Germany). For RNA extraction, RNase Free Microfuge tubes were purchased from Applied Biosystems (Ambion-The RNA Company, Cheshire, UK). Pipette tips used for cell culture, biochemistry and flow cytometry were purchased from Fisher Scientific UK (Loughborough, UK). Pipette tips used for RNA extraction, isolation and reverse transcriptase polymerase chain reaction (RT-PCR) (aerosol resistant tips) were purchased from Molecular Bioproducts Incorporation (San Diego, CA, USA). Other plasticware including: 2 ml cyrogenic vials, cell scrapers, 15 ml and 50 ml sterile tubes, 5 ml, 10 ml, and 25 ml stripettes were all purchased from Fisher Scientific UK (Loughborough, UK). Syringes were from Terumo (Leuven, Belgium). Bottle top (500 ml) 0.22 µM filters and 0.22 µM syringe filters were purchased from Corning (Lowell, MA, USA).

2.1.5 Live Cell Imaging

Live cell imaging was captured using a Leica DMI 6000B inverted microscope (Leica Biosystems GmbH, Nussloch, Germany) with recording ability (Leica DCF365 FX). The environment chamber was programmed to match incubator conditions (37 °C, 5 % CO_2). The microscope was equipped with a heat controller, Pecon incubator and CO_2 controller (PeCon GmbH, Erbach, Germany). Images were captured with a 10x objective and 0.5x magnification c-mount fitted to a camera (Figure 2.1). Videos were generated and exported using the Leica Application Suite software (Wetzlar, Germany). Images (TIFF) were exported into Image J software (IBIDI, Munich, Germany) for analyses.
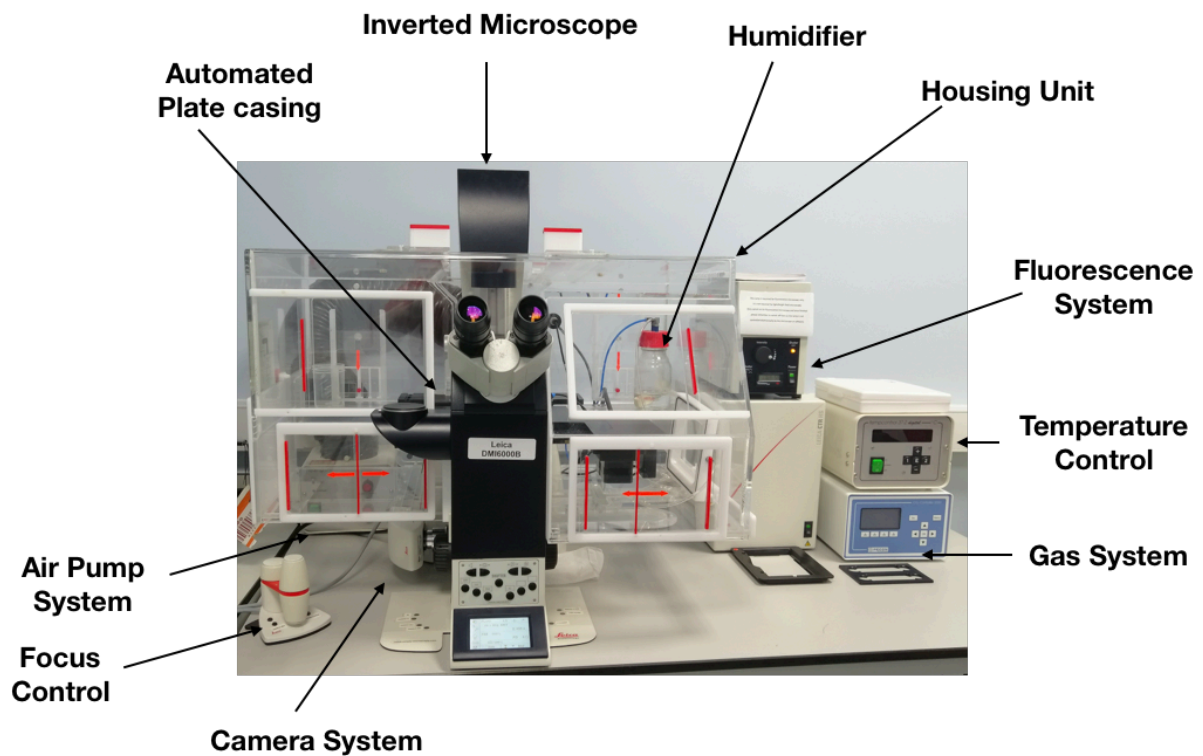
Figure 2.5. Annotated diagram to show the live imaging equipment and compartments.

2.1.6 Biochemical Assays

The Clariostar plate reader was purchased from BMG LABTECH (Ortenberg, Germany) and was utilised for analyses of: 1) LDH, 2) BCA™ protein and 3) CK. The reagents for the LDH assay were purchased from Thermo-Fisher Scientific (Waltham, MA, USA). For the BCA protein assay, the reagents were purchased from Pierce (Rosklide, Denmark). Finally, for CK, the assay reagents were purchased from Catachem incorporation (Connecticut, NE, USA).

2.1.7 Reverse Transcriptase Polymerase Chain Reaction

UV Spectroscopy was used for the assessment of RNA purity and concentration using a Nanodrop UV spectrophotometer (Thermo-Fisher Scientific, Waltham, MA, USA). For amplification of RNA, a Qiagen rotor-gene Q (Qiagen, Manchester, UK) PCR machine was used. To gather amplification curves and Ct values, the rotor-gene Q software (Qiagen, Manchester, UK) was used. All of the reagents used in RT-PCR were purchased from Applied Biosystems (Carlsbad, CA, USA).

2.1.8 Flow Cytometry

The BD Accuri C6 flow cytometer with BD CFlow® Software (BD Biosciences, Wokingham, UK) was used for flow cytometry analysis. Reagents for flow cytometry were purchased from either BD (BD Biosciences, San Jose, CA, USA) or from Thermo-Fisher Scientific (Waltham, MA, USA).

2.2 Cell Types and Culture

Cell culture experiments were performed using the murine C_2C_{12} cell line. The C_2C_{12} cells were purchased from the American Tissue Culture Collection (ATCC, Rockville, MD, USA). The C_2C_{12} cell line was a subclone of the C_2 cell line (Blau *et al.*, 1985), which is no longer commercially available.

2.2.1 C2C12 Muscle Cell Line vs. Primary Cell line

The C_2 cell line was obtained by Yaffe and Saxel (1977) by establishing primary cultures from the thigh of two-month-old mouse, 70 hours post crush injury. Afterwards, the C_2C_{12} cell line, which was established from the C_2 myoblast cell line, involves isolation of myoblasts from adult mouse leg muscle (Blau *et al*., 1985). The C_2C_{12} cell line is commercially available and is commonly used as a model for studying muscle growth, apoptosis, differentiation and hypertrophy.

The other advantages of using the C_2C_{12} Murine Cell line include: cost effectiveness, bypass ethical concerns, are easy to use and are a 'pure' population of cells that improve reproducibility (Kaur and Dufour, 2012). Their extensive use in the literature provides a sound foundation for furthering knowledge and they enable compliance with the remit of the NC3Rs. Biochemically, it is easy to extract high concentrations of protein, RNA and DNA from this cell line, allowing, for example, more genes to be analysed (Carter *et al.*, 2015). On the other hand, a disadvantage is that these cells are of murine origin and are originally derived from a single young animal. Although the C_2C_{12} cell line is generated from one mouse and this may be viewed as a limitation, a potential benefit is that biological variation is minimal (Blau *et al.*, 1985).

Primary cell lines involve tissues isolated directly from a living animal. Therefore, the major advantage is that isolation of muscle cells provides relevance to the physiology of that muscle and animal providing improved potential for translation (Kaur and Dufour, 2012). Although, it is preferred to have improved translation of findings, it is often a trade-off between models, depending on the question and access to models. For instance, not all research institutions have access to isolate cells, particularly from humans. Also, ethical requirements need to be met for the isolation of primary cells, which can take time and requires staff with the expertise to undertake the biopsies and willing participants in the first place. Given the biological repeats, larger numbers of samples, at high cost, may then be required to address individual questions (Carter & Shieh 2010). The use of the C2C12 cells to identify relevant questions for translation to human muscle cell models is therefore of benefit.

2.2.2 Cell Culture of C_2C_{12} Skeletal Muscle Cells

C_2C_{12} myoblasts were resuscitated from liquid nitrogen (LN) in 2 ml cryovials at a cell density of 1×10^6 cells. The cryovials were rapidly warmed and once thawed, were plated onto T75 flasks. The T75 flasks were pre-gelatinised with 5 ml, 0.2 % gelatin. The gelatin was incubated on the flasks at room temperature (RT) for 20 minutes, before the excess gelatin was aspirated. GM was added (15 ml) to the pre-gelatinised T75s, prior to addition of 1×10^6 resuscitated cells. The flasks were agitated front-back and side-side to spread the cells evenly over the plate. For the cells to grow, the flasks

were incubated in a humidified 5 % CO_2 atmosphere at 37 °C. The cells were incubated for up to 72 h, until 80 % confluent (Figure 2.2).

Once the cells were 80 % confluent, they were washed twice with PBS, to remove any excess serum, which is an inhibitor of trypsin. Once washed, 1 ml trypsin/T75 was added to the cells and incubated for 5 minutes at 37 °C to enable cell dissociation. Following confirmation of dissociation, by microscopy, trypsin was neutralised by adding 4 ml GM (5 ml total) to the dish. To prevent cell clumping, the cells were homogenised, by slowly drawing the cell solution up and down using a syringe and 21-gauge needle. The cell suspension was prepared for cell counting in a 1:1 dilution in 0.4 % trypan blue stain (Bio Whittaker, Wokingham, UK). The cell suspension/trypan blue mix was dispensed onto a Neubauer haemocytometer (Assistent, Sondheim, Germany). For cell counting see section **2.2.2.** Once cells were counted, they were seeded onto either 6 or 12 well pre-gelatinised plates, depending on the experiment. Excess cells were frozen in LN for further experiments, see section **2.2.3**. The cells attached within 24 h and were incubated until 80 % confluency was attained. Once confluent, cells were washed twice with PBS and experiments were initiated. Cell culture experiments were started (timepoint 0 h) by transitioning cells from proliferating to differentiating, via adding low serum DM.
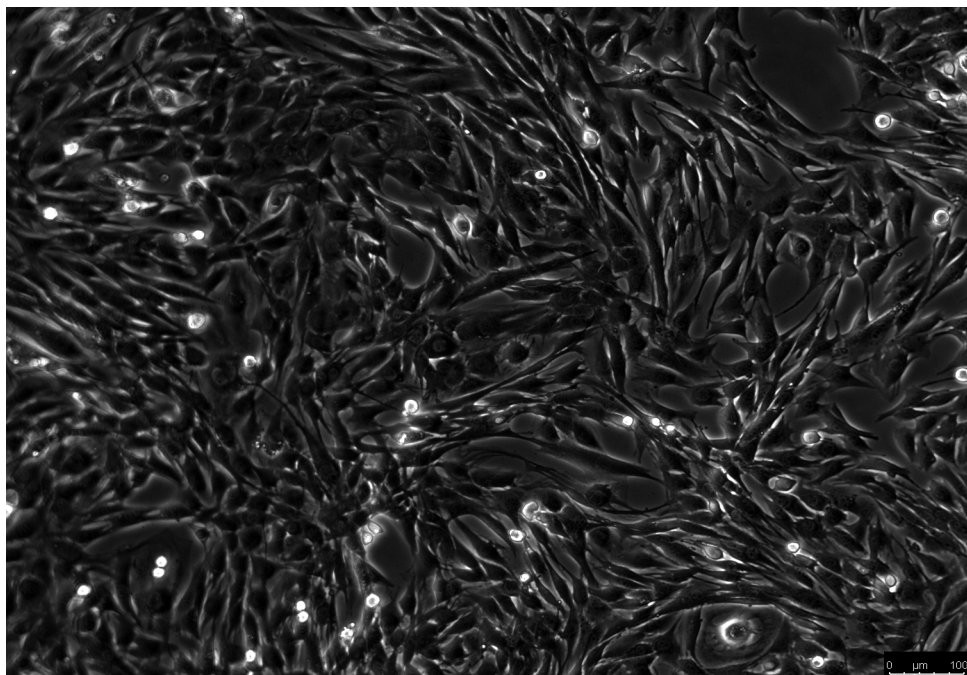
Figure 2.6. Image to show cells at 80 % confluency. Scale 100 µm.

2.2.3 Cell Counting

Ten μl cell suspension and 0.4 % trypan blue mix were pipetted onto a Neubauer Haemocytometer (Figure 2.3A). A glass coverslip was placed onto the counting chamber to evenly spread the liquid. Under the microscope (10x magnification) the two grids were observed, which contained 9 sections. For counting, only the 4 corner sections of each grid were counted (Figure 2.3B). Viable cells were identified as clear, small and round. Non-viable cells contained trypan blue, having lost membrane integrity, and were generally misshapen. Only viable cells were counted. Cells that were on the edge of the corner section were included in the count (black dotted line; Figure 2.3B).

A

B

1 mm
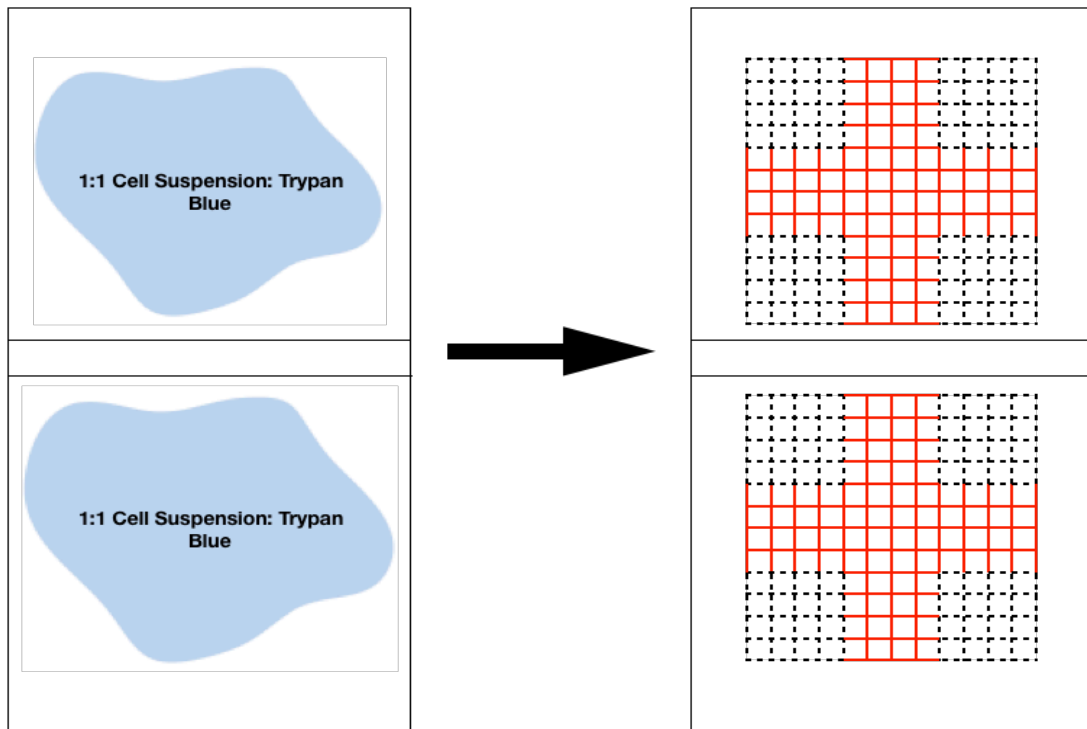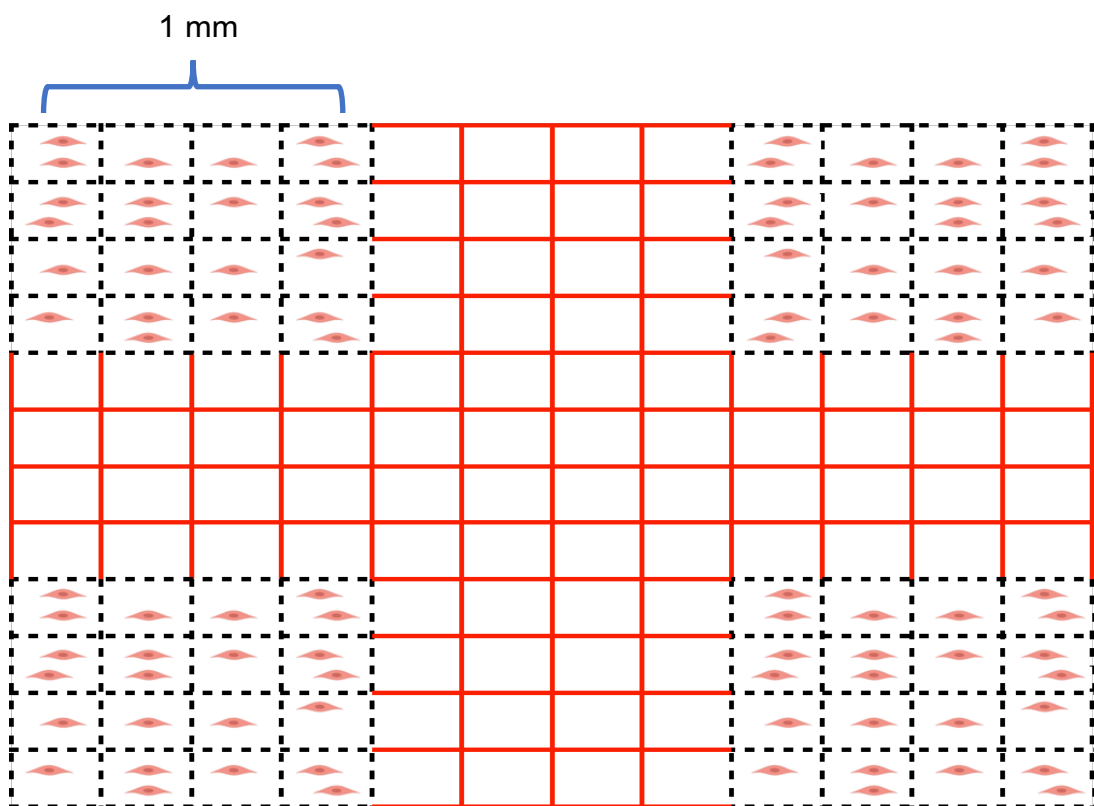
Figure 2.7. A: Illustration to indicate the cell suspension/trypan blue placed on the Haemocytometer grids. B: Zoomed in image of one of the grids with the cells on.

Counts were acquired from each section of both grids (8 replicates in total). The average of the 8 numbers represent the number of cells occupying in 0.1 mm^3. To account for the dilution factor (via trypan blue; 1:1) the average is multiplied by 2. This amount was multiplied by 10,000 (10^4) equating the number of cells from 0.1 mm^3 to 1 cm^3, which would be equivalent to 1 ml of cell suspension. This cell concentration/ml, when multiplied by the original volume of cell suspension equates to the total number of cells/plate or per well. A seeding density of 100,000 cells/ml was selected for plating. In a 6 well plate, 2 ml/well and in a 12 well plate 1 ml/well were the seeding volumes. To calculate if enough cells were present for an experiment, see equations below (Equation 2.1):

1) **Cells/ml = average 8 sections x dilution factor x 10,000**

2) **Total Cells = cells/ml x volume of cell suspension**

3) **Cell Suspension Volume Required (ml) = (100,000 cells/ml ÷ cells/ml) x seeding volume (ml)**

For example:
1) **20 cells x 2 x 10,000 = 400,000 cells/ml**
2) **400,000 cells/ml x 5 ml = 2,000,000 cells**
3) **(100,000 cells/ml ÷ 400,000 cells/ml) x 13 ml = 3.25 ml of cell suspension required (1.75 ml excess).**

Equation 2.1 Calculations of Cell suspensions required for experimental design

2.2.4 Freezing Cells for storage

Once the cells were counted, if there was an excess, for instance in the example above, this was either frozen immediately or alternatively, cell stocks could be expanded. The cells were stored at a density of 1 x 10^6 per ml. After counting, GM was added to the cell suspension to dilute to equal the required cell density. If the cell

concentration was low, in a high volume, the cell suspension was centrifuged for 5 minutes at 450 g and resuspended with the correct amount of GM to equal 1×10^6 cells/ml. To protect the cell against sudden temperature reductions (from room temperature to -80 °C). Ten percent of dimethyl sulphoxide (DMSO) was added to the GM. DMSO reduces ice crystal formation that damages the cells by penetrating the cell membrane and replacing parts of the cell that contain water (Fleming and Hubel, 2006). The cells were stored in 2 ml cyrovials which were labelled with cell type, passage number, cell density, name and date. Before the cells were stored at -80 °C for 24 h, they were put in a Mr. Frosty (Sigma-Aldrich, Poole, UK) with 100 ml of isopropanol. This slows the freezing further. The cyrovials were then transferred to LN for long term storage.

2.2.5 Replicatively Aged C_2C_{12} Myoblasts

Given a global drive to reduce/refine animal research, relevant cell models are required to inform future *in vivo* studies. To this end, we have developed a myoblast model, with an application to ageing muscle cell behaviour (Sharples *et al*., 2011). C_2C_{12} myoblasts underwent multiple population doublings (130-150) to passages 44-50. This was achieved by repeatedly passaging cells. This model is used throughout the thesis and these cells are referred to as 'replicatively aged'.

2.3 Cell Culture Experiment 1: Wound Healing and Cell Migration

The capacity of myoblasts to migrate across a wound was utilised to understand how skeletal muscle repairs in response to damage, which could be evoked by e.g. strenuous exercise. The wound healing assay was established by creating a 'scratch' in the monolayer, using a sterile pipette tip. The response of the cells to this 'scratch' was captured over time (0-48 h) using live cell imaging. This method was easy to perform, and the number, velocity, direction and distance of cell migration was analysed.

2.3.1 Wound Healing Method

Once cells were seeded onto either 6 or 12 well plates (section **2.2.2**) and reached 80 % confluency, they were washed twice with PBS. During the first wash, the cells were wounded, down the centre of the well, using a sterile 1 ml pipette tip. The cells were washed again post 'scratch' to remove excess debris. Then, 2 ml/well low serum DM was added to and live cell imaging was performed over 48 h, using a Leica DMI600B microscope. The microscope was fitted with an autoflow incubator which maintained optimal culture conditions (37 °C and 5 % CO_2). Two hours before the experiment was scheduled to start, the CO_2, temperature controller and heating unit were turned on. Following scratch injury, plates were transferred to the live imaging incubator and the wounds located. Using the mark and find function, at least two independent locations along the wound were identified and saved, such that each image was captured at the same location throughout the experiment. To assess migration, images were captured from these sites, every 30 minutes for 48 h at 10x magnification, enabling the development of real time movies of migration.

2.3.2 Cell Migration Analysis

Once the wound healing experiment was completed, images were exported in TIFF format. These images were imported as stacks into the image J software. The plug ins chemotaxis, cell counter and manual tracking were downloaded (IBIDI, Munich, Germany). Two methods were used to analyse cell migration. Firstly, the number of cells that migrated into three segments of the wound (Figure 2.4) was calculated by using the cell counter plug in. Secondly, using the chemotaxis and manual tracking plug in, individual cell velocity, direction and distance were measured.
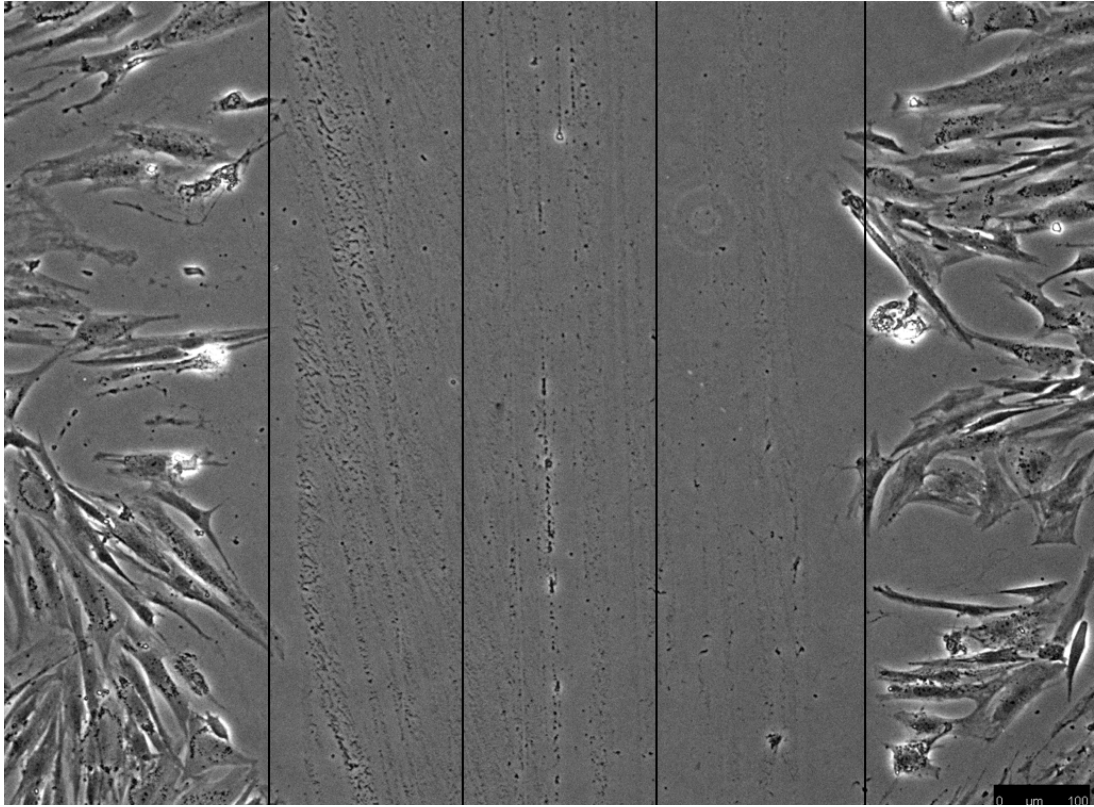
Figure 2.4. Image that represents wound 'scratch' using 1 ml tip. The total wound was 900 µm, that was split into three segments each 300 µm. Scale 100 µm.

2.4 Cell Culture Experiment 2: Myotube Formation

Once cells were transferred from GM to DM at 0 h (Figure 2.5A), they were left to fuse into fully formed myotubes at 96 h (Figure 2.5B). Myotube formation was used as the later stages of muscle regeneration and myofiber hypertrophy. At the last timepoint of the experiment, the myotubes were fixed and the diameter, length and area were analysed.
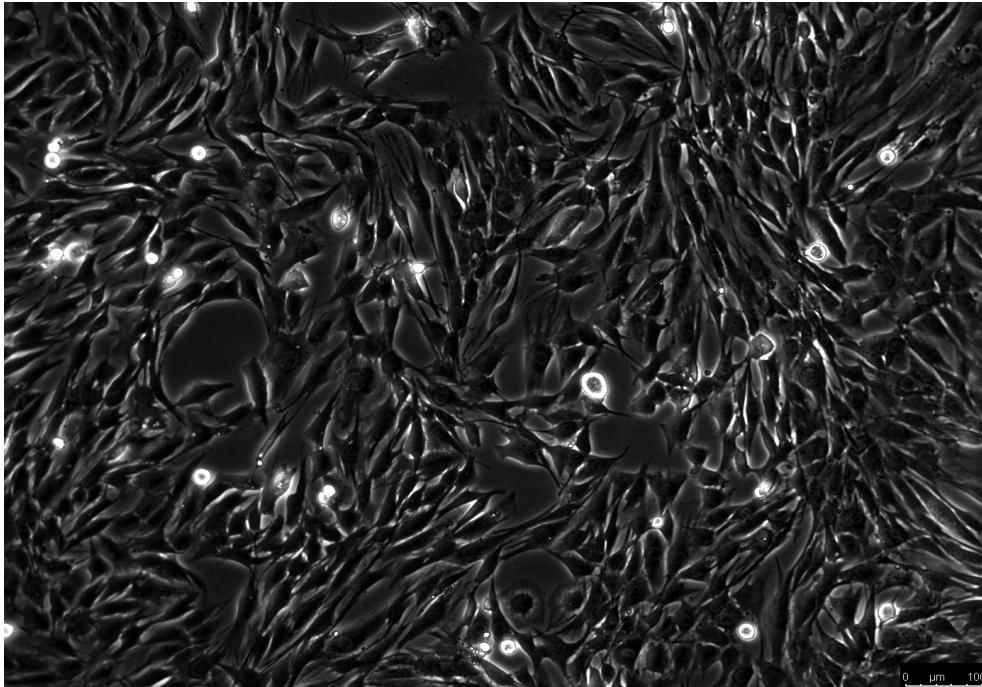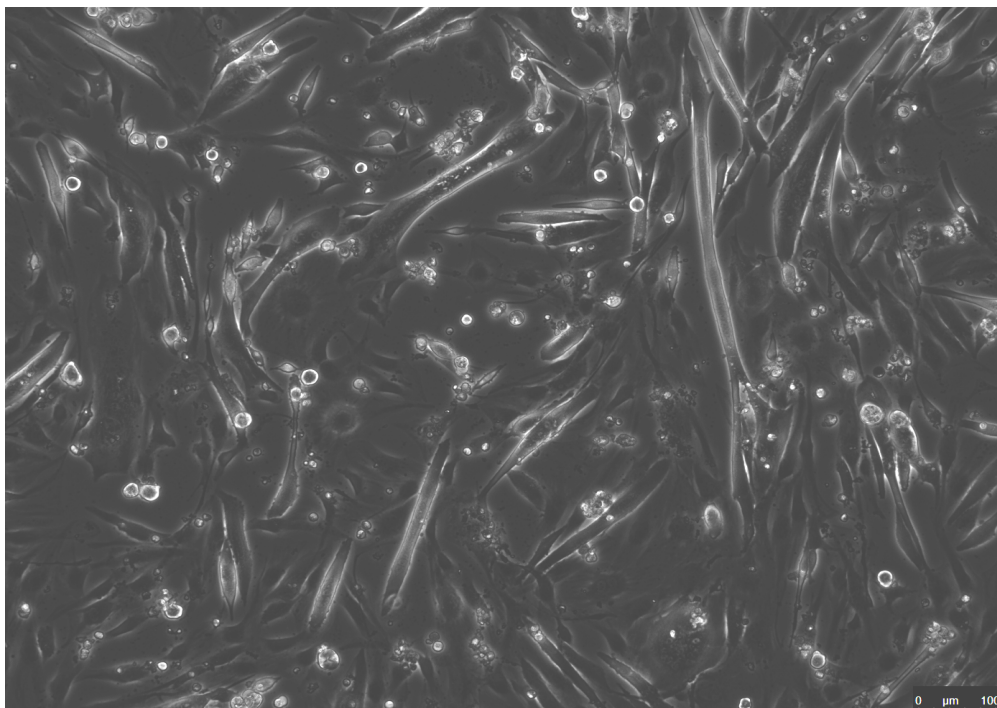
Figure 2.5. A: Images at 0 h when changed from GM to DM. B: Differentiated cells at 96 h. Scale 100 µm.

2.4.1 Myotube Fixation and Analysis

At the last time point, the cells were washed twice with PBS, prior to addition of 1 ml 100 % ethanol. The cells were incubated for 5 minutes and the ethanol was aspirated. To keep the cells hydrated during storage, 1 ml PBS was added. The plates were covered in parafilm and stored at 4 °C. Images were captured at 10x magnification using a Leica DMI600B microscope.

2.5 Cell Extraction Protocols

2.5.1 Creatine Kinase, Total Protein and Lactate Dehydrogenase

At the specific experimental timepoint, all monolayers were washed twice with either 1 ml or 500 µl per well of PBS depending on the plate (6 or 12 well respectively). Following the PBS washes, the cells were lysed with 250 µl or 125 µl per well of 0.05 M Tris/MES Triton Buffer (TMT; 50 mM Tris MES, 1 % Triton X-100). The cells were lysed for 5 minutes at RT. Subsequently, the cells were scraped and collected into 1.5 ml Eppendorf tubes. The samples were stored at -80 °C until further processing.

2.5.2 Cell Extraction for Gene Expression Quantification

The media was aspirated, and cells washed twice with PBS. TRIzol reagent was added to each well, 250 µl and 125 µl for 6/12 well plate respectively. The cells were lysed for a period of 5 minutes at RT. The lysates were collected in 1.5 ml RNase free tubes and stored at -80 °C until further analyses.

2.5.3 Cell Extraction and Fixation for Intracellular Phosphorylation

At each specific timepoint, the media was aspirated and cells washed twice with PBS, followed by trypsinisation. For 6 well plates, 200 µl and for 12 well plates 100 µl was added. The trypsin coated cells were incubated at 37 °C for 5 minutes. Once the cells had detached (via observation under microscope), the trypsin was neutralised by adding GM. For each well, either 800 µl or 400 µl was added into 6/12 well plates respectively at a 4:1 ratio. The supernatant (containing cells) was pipetted into 2 ml Eppendorf tubes. The samples were centrifuged at 775 g for 5 minutes at 4 °C. The supernatant was removed leaving a white cell pellet. The cells were fixed by adding 100 µl 2 % paraformaldehyde. The cells were left to incubate for 60 minutes at RT in the dark. After 60 minutes, 100 % methanol was added to the paraformaldehyde and the samples were stored at -20 °C until further analyses.

2.5.4 Cell Extraction for Proteomic Quantification

The media was aspirated and cells washed twice with cold PBS. During the extraction the cells were kept cold. Therefore, the plates were kept on ice throughout. RIPA buffer (1x) was applied to each well (250 µl) of a 6 well plate. The monolayers were left for 5 minutes. The lysates were scraped and collected into 1.5 ml Eppendorf tubes for protein quantification, digestion and mass spectra analysis.

2.5.5 Supernatant Extraction for Lactate Dehydrogenase

At the specific timepoints, supernatant from each well was collected into 1 ml Eppendorf tubes. The volumes collected were 100 µl and 50 µl in a 6/12 well plate respectively. The samples were labelled and stored at -80 °C until further analyses.

2.6 Protein Assay

2.6.1 Principle

BCA™ assay was used to quantify total protein. In an alkaline environment, protein reduces Cu^{+2} to Cu^{+1} (the biuret reaction). The reagent is then mixed with sample, two molecules of BCA join Cu^{+1} causing the reaction to turn purple. This is due to the macromolecular structure of the protein, the presence of four amino acid residues (tryptophan, cysteine, tyrosine and cystine) and the number of protein bonds (Smith *et al.*, 1985). The absorbance was measured at 593 nM. The darker purple the sample, the more total protein, see equations below (Equation 2.2):
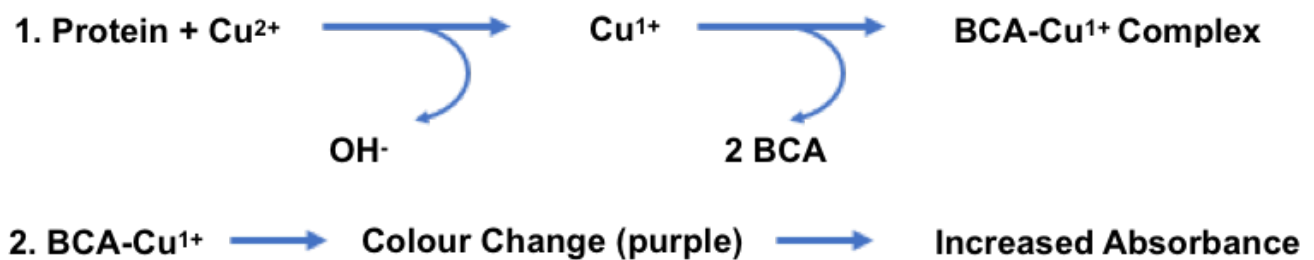
Equation 2.2. Chemical reactions underpinning the BCA protein assay.

2.6.2 Procedure

The determination of protein concentration (mg/ml) was plotted against a standard curve. Standards were made with bovine serum albumin (BSA) at concentrations of 2, 1, 0.5, 0.25, 0.125, 0.0625, 0.03125 and 0 mg/ml. They were prepared by diluting 200 mg BSA (in 0.9 % sodium chloride and sodium azide) with 4.8 ml TMT (50 mM Tris-MES, pH 7.8, 1 % Triton X-100) providing stock solution of 40 mg/ml. To create the standards, 1.9 ml of TMT with 100 µl of stock solution was top standard of 2 mg/ml. Subsequent serial dilution of 1 ml of previous standard with 1 ml of TMT. Only TMT alone (0 mg/ml) was not diluted. For the assay, the Pierce BCA™ protein kit (Rockford, IL, USA) containing two reagents was used. Reagent A (sodium carbonate, sodium

biocarbonate, BCA and sodium tartrate in 0.1 M sodium hydroxide) was mixed using a multipipette channel in a mixing trough with reagent B (4 % cupric acid sulphate) at a ratio of 50:1. In a 96 well plate, 10 µl of sample and standard were pipetted in each well. Using a multipipette channel, 200 µl BCA™ buffer was added to each well. The plate was incubated for 60 minutes at 37 °C. The Clariostar plate reader analysed the samples at 595 nM.

2.7 Creatine Kinase

2.7.1 Principle

The enzyme activity of CK was determined as a marker of myogenic differentiation. Research suggests that CK increases correlate with increases in myoblast fusion (Foulstone *et al.*, 2001; Al-Shanti and Stewart, 2008; Sharples *et al.*, 2013). The mechanisms involve the conversion of PCr and ADP to creatine and ATP (Equation 2.3, step 1). The product, ATP was determined by coupling a hexokinase and G-6-P reaction (Equation 2.3, step 2) to 6-phosphogluconic acid and the concomitant reduction of NAD to NADH (Equation 2.3, step 3). The decline in NAD results in an increased absorbency of NADH at 340 nM. This is directionally proportionate to CK enzyme activity (Equation 2.3).

$$1. \text{ PCr + ADP} \xrightarrow{\text{CK}} \text{Cr + ATP}$$

$$2. \text{ ATP + Glucose} \xrightarrow{\text{HK}} \text{ADP + G-6-P}$$

$$3. \text{ G-6-P + NAD} \xrightarrow{\text{6-PG + NADH}} \text{6-PG + NADH} \rightarrow \text{Increased Absorbance}$$
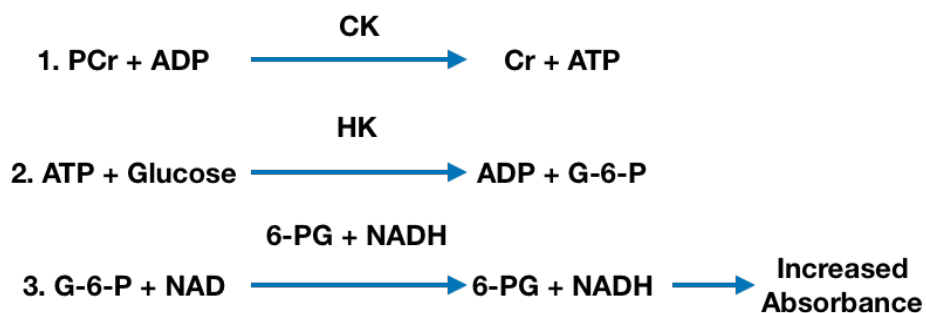
Equation 2.3. Reactions involved in the CK assay. PCr: Phosphocreatine; ADP: Adenosine Diphosphate; CK: Creatine Kinase Cr: Creatine; ATP: Adenosine Triphosphate; HK; Hexokinase; G-6-P; Glucose-6-phosphate; NAD; Nicotinamide Adenine Dinucleotide; 6-PG: 6-Phosphogluconate; NADH; Reduced NAD.

2.7.2 Procedure

For analysis of cell lysates, TMT was loaded in duplicate in a 96 well plate as the negative control. In 96 well plate, 20 µl of sample was loaded in duplicate. The CK reagents were prepared following the manufacturer's instructions (Catachem Inc, Connecticut, US). In detail, 5 ml of reagent A was mixed with 0.0118 g of reagent B. In total, 200 µl of reagent was added to 20 µl of sample/well (Equation 2.4). The combined working reagent contained the following active ingredients: 30 mmol/l creatine phosphate, 2 mmol/l ADP, 5 mmol/l AMP, 2 mmol/l NAD, 20 mmol/l N-acetyl-L-cystine, 3000 U/l HK (yeast), 2000 U/l G-6-PDH, 10 mmol/l magnesium ions, 20 mmol/l D-glucose, 10 µmol/l Di (adenosine 5') pentaphosphate and 2 mmol/l ETDA. Additionally, it was buffered at pH 6.7 and contains 0.05 % sodium azide as a preservative.

1) **Amount of Reagent Bottle A (µl) = Total Reagent (µl) x Number of Samples.**
2) **Amount of powder per ml = 0.118 g ÷ 5 ml = 0.0236 g**
3) **Amount of Powder from Reagent B (g) = Amount of Reagent from Bottle A (ml) x 0.0236 g.**

For 100 Samples:
1) **200 µl x 100 samples = 20,000 µl Bottle A (or 20 ml).**
2) **20 ml x 0.0236 g = 0.472 g Powder from Reagent B.**

Equation 2.4. Equation to determine the amount of Reagent A and B needed for 100 samples for the CK assay.

The plate was protected from light and incubated for 5 minutes at 37 °C. The samples were measured using Clariostar plate reader at an absorbance of 340 nM every minute for 20 minutes. The CK enzyme activity was calculated via the following equation (Equation 2.5).

$$\Delta \text{ A.min}^{-1} = \frac{\text{(Final A - Initial A)}}{\text{(Final Reading Time (mins))} - \text{(Initial Reading Time (mins))}}$$

$$\text{CK (U.L}^{-1}) = \frac{\Delta\text{A.min}^{-1} \times 0.22 \text{ ml} \times 1000}{6.22 \times 0.02 \text{ ml}}$$

- ΔA.min^{-1} = change in absorbance per minute
- 0.22 ml = total reaction volume in ml
- 1000 = conversion of U/ml to U/L
- 6.22 = extinction coefficient
- 0.02 ml = sample volume

Equation 2.5. CK concentration calculation.

2.8 Lactate Dehydrogenase

2.8.1 Principle

LDH is a cytosolic enzyme that is released upon cellular damage (Decker and Lohmann-Matthes, 1988). Once damage has occurred, the plasma membrane becomes leaky, resulting in the release of LDH into the culture media. The extracellular LDH in the supernatant was quantified by measuring the level of formazan formation, which is directly proportional to the amount of LDH released. The LDH released catalyses the conversion between lactate and pyruvate via NAD$^+$ reduction to NADH (Equation 2.6). Then diaphorase uses NADH to reduce tetrazolium salt into the product formazan (red). This product can be measured at 490 nm.
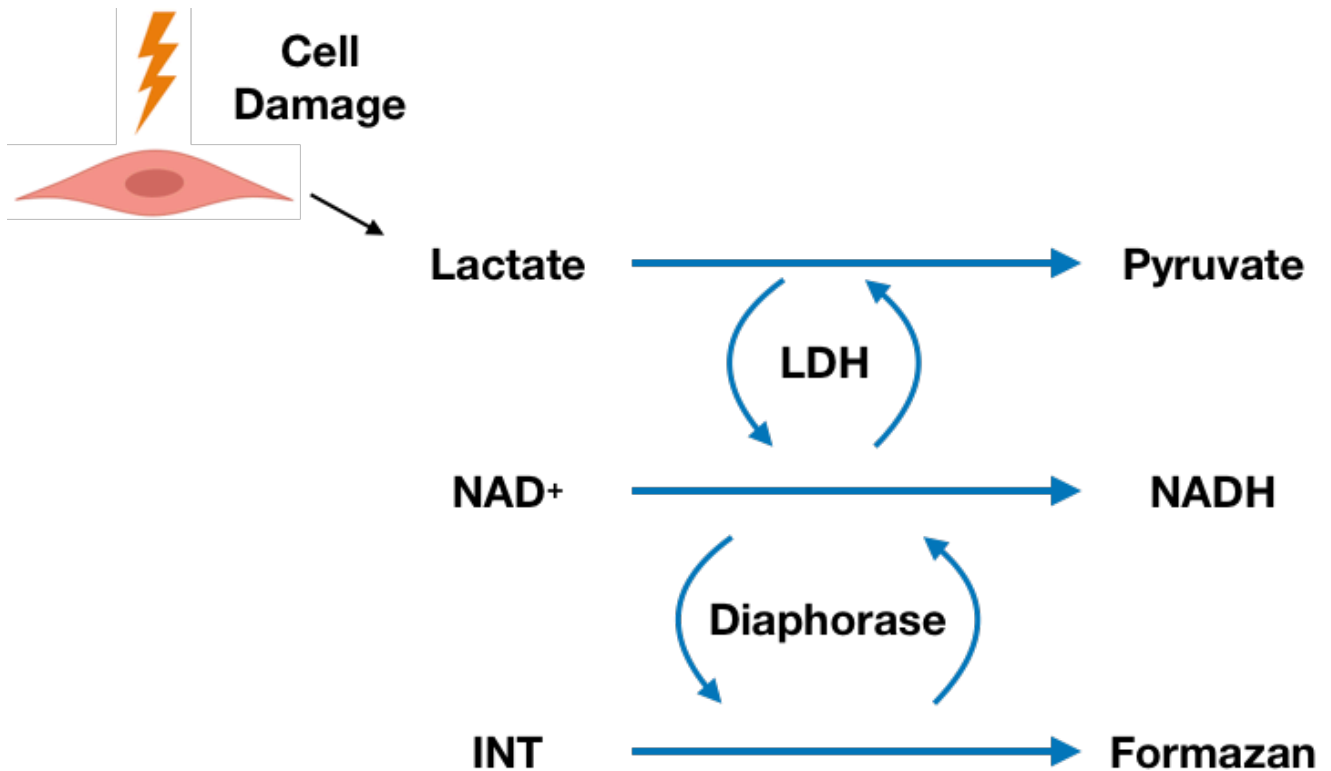
Equation 2.6. Enzyme reactions involved in LDH assay. INT: Tetrazolium Salt

2.8.2 Procedure

Fifty μl sample (cell supernatant) and DM (negative control) were pipetted into 96 well plate. To create the substrate reagent, for 100 samples, 125 μl catalyst was mixed with 5.625 ml of dye, both provided in the kit. Following addition of samples to the 96 well plate, 50 μl substrate solution was added to each well, using a multi-channel pipette. Plates were incubated for 30 minutes in the dark at RT and immediately analysed using the Clariostar plate reader at an absorbance of 490 nM.

2.9 Flow Cytometry

2.9.1 Principle

Flow cytometry measures cells and particles in liquid suspension simultaneously as they pass through a beam of light. The process includes three subsystems: a) fluidics, b) optics and c) electronics. The fluidic system transports cells to a laser beam (or interrogation point) where light and fluorescence are emitted. The hydrodynamic focussing allows sample cores to be aligned in the centre of sheath fluid. In the optic system, the cells pass through the sheath fluid and meet the interrogation point (Cram, 2002), where the laser beam hits each cell (Figure 2.6). The forward scatter (FSC) is emitted into the FSC photo diode. The side scatter (SSC) and fluorescent light are emitted through lenses and octagon detectors (Cram, 2002). All emitted light is filtered through specific filters that allow certain wave lengths to pass through them. Once through the filters, the light signals are converted into numerical data in the electronic system. In detail, photons are collected by a detector which converts the photons into an electrical current. This current is amplified into electrical voltage where signal processing calculates numerical values based on curve height, width and area.
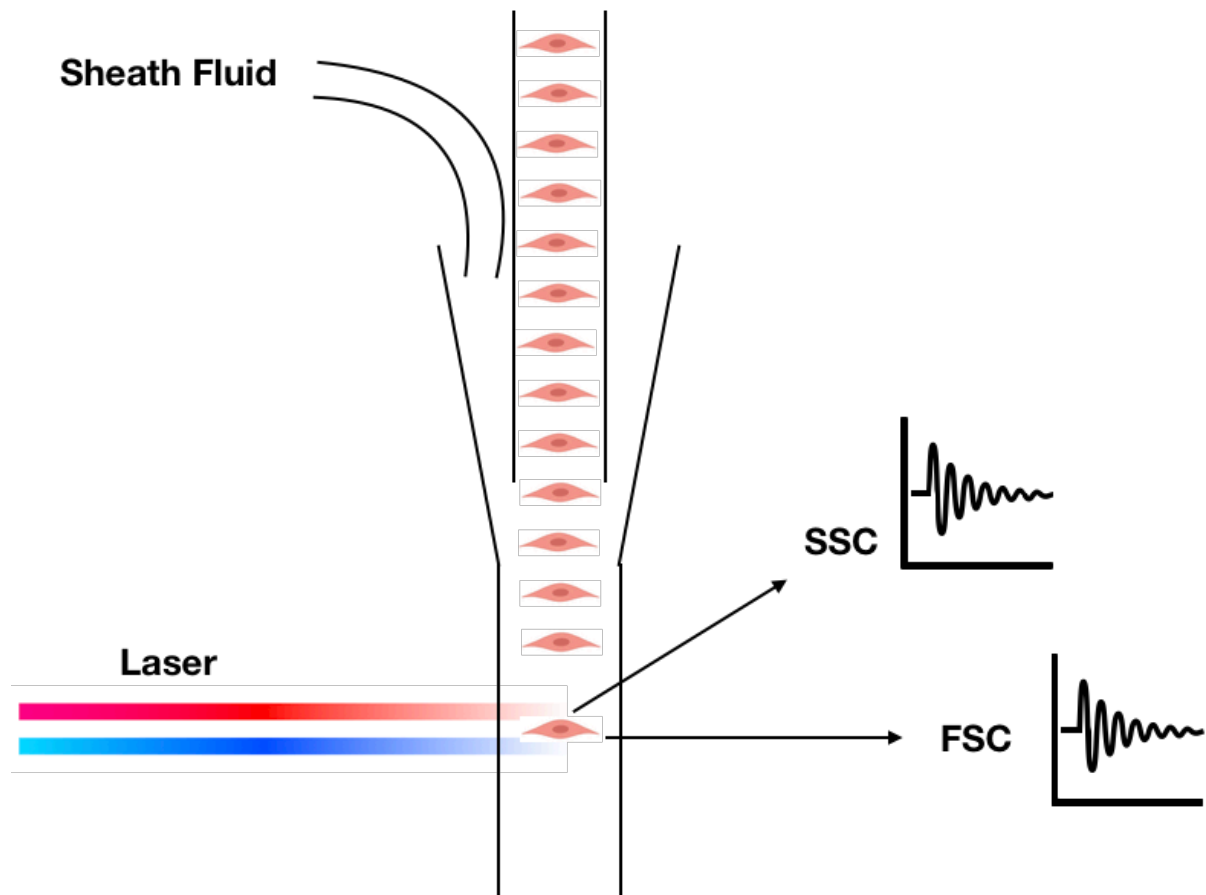
Figure 2.6 Schematic to illustrate the process of flow cytometry

Light scattering occurs when the particle passes through the laser beam. FSC is the signal detected just off the axis of the laser beam in the forward direction and SSC is the signal collected at 90 ° to the laser beam (Figure 2.7). The FSC is an indicator of the cell size and difference between the cell and surrounding sheath fluid (Weaver, 2000). Whereas, SSC is an indicator of cell granularity and structural complexity. The signals detected from FSC and SSC are plotted on a histogram and provide an indication of the type of cell analysed (Weaver, 2000).
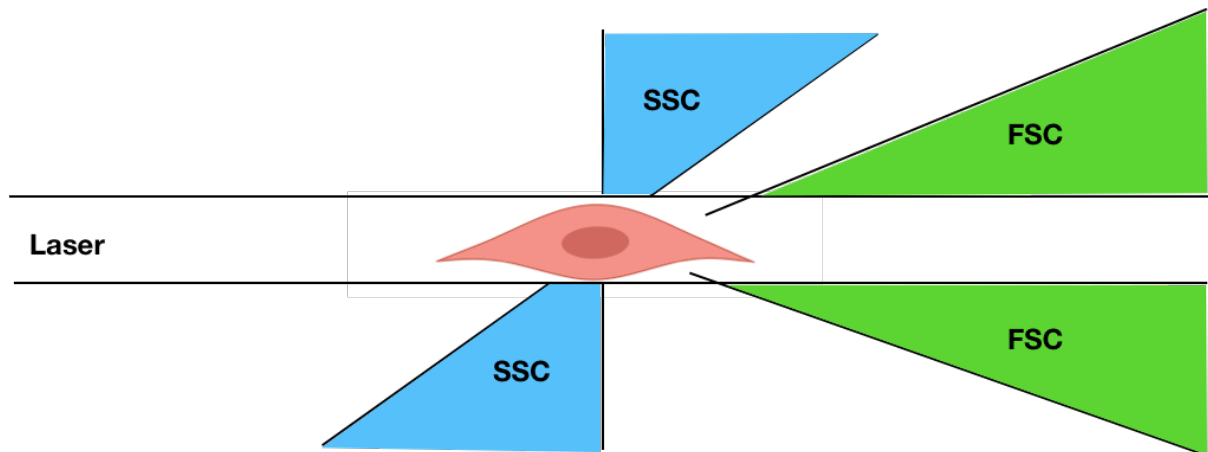
Figure 2.7. Visual representation of how the laser affects SSC and FSC.

2.9.2 Procedure: Intracellular Phosphorylation

For this thesis, fluorophores and beads were used to measure intracellular phosphorylation of cells and specific cytokines in the serum of human participants. The myoblasts were fixed on ice to prevent changes in phosphorylation, which would not be achieved with live cells. The use of fluorophore labelled anti-phospho antibodies determined whether the signalling molecules Akt, ERK, mTOR and p38 were phosphorylated. Fluorophores were excited producing high energy state which subsequently reduced to a baseline state where the fluorophore emits light. Each fluorophore was designed to emit a specific level of energy, which produces a specific light wavelength and colour. Once bound to an antibody and passed through the flow cytometer, the light emitted was then analysed, as described above.

Following removal from storage at -20 °C **(section 2.5.3)**, the cells were washed in flow cytometry buffer (PBS + 0.5 % FBS) and centrifuged at 500 g for 5 minutes at 4 °C and re-suspended in cytometry buffer. The four antibodies for the signalling molecules: Akt, ERK, mTOR and p38 **(see section 2.1.1 for further details)** were added to each sample and incubated at RT in the dark for 60 minutes. The cells were washed a further three times and re-suspended in 200 µl cytometry buffer. The samples were analysed using flow cytometry on a BD Accuri C6 flow cytometer with

BD CFlow® Software, collecting 2000 events per sample. Compensation of individual fluorescent antibodies in multiple detectors was performed to reduce spectral overlap. FSC and SSC gating was performed to ensure single populations of cells. Together these processes reduce data skew and improve accuracy.

2.9.3 Procedure: CBA Cytokine Concentration

Flow cytometry was also used to determine the concentration of cytokines in human serum. The application that measures multiple cytokines simultaneously was BD Cytometric Bead Array (CBA). The procedure combines antibody coated capture beads and fluorophores that detect specific cytokines. To measure the cytokines simultaneously, each bead contains a specific florescence intensity matching its bead size. Different sizes of capture beads detecting different cytokines were mixed in test tubes and analysed concurrently. The cytokines measured and protein sizes were displayed in Table 2.1. All detection anti-bodies were labelled with phycoerythrin (PE).

Table 2.1. Names and Assay Range of all cytokines tested.

Cytokine	Abbreviation	Assay Range (pg/ml)
Interleukin-1β	IL-1β	10-2500
Interleukin-2	IL-2	10-2500
Interleukin-3	IL-3	10-2500
Interleukin-4	IL-4	10-2500
Interleukin-6	IL-6	10-2500
Interleukin-7	IL-7	10-2500
Interleukin-8	IL-8	10-2500
Interleukin-10	IL-10	10-2500
Interleukin-17	IL-17	10-2500
Tumor necrosis factor receptor-1 alpha	TNFr1-α	40-10,000

In 2 ml Eppendorf tubes, 50 µl of premixed beads (supplied within the kits, see Table 2.1) were added to 50 µl of either standards or samples. The samples were incubated for 1 h at RT. Following the 1 h incubation, 50 µl PE conjugated anti-bodies to the 10 analytes (Table 2.1) were added to each sample/standard. This final mixture was incubated for 2 h at RT and protected from light. The beads were washed in a wash buffer provided with the CBA kit. The addition of 500 µl wash buffer to each sample was followed by centrifugation at 200 g for 5 minutes. The samples were resuspended

in wash buffer, vortexed and analysed using a BD Accuri C6 flow cytometer with BD CFlow® Software, collecting 300 events per analyte (3000 events per sample). The flow cytometer was equipped with four filters to analyse the samples (FL1: 533/30 nm, FL2: 585/40 nm, FL3: 780/60 nm, FL4: 675/25 nm). Calibration curves were plotted using 12 standards obtained through serial dilution (top standard of 10,000 pg/mL). The data were filtered and processed using FCS Filter and analysed using FCAP array software (Hungary Software Ltd., for BD Biosciences).

2.10 Gene Expression Quantification

2.10.1 Principle

Proteins are produced by transcribing mRNA molecule from the DNA sequence located in the nucleus. Measuring mRNA can provide an indication of gene expression of a protein of interest. To quantify gene expression, the RNA is extracted, isolated (Figure 2.8A) and quantified via RT-PCR. The first step is to convert mRNA into complementary DNA (cDNA) via reverse transcriptase (Figure 2.8B). This is amplified by RT-PCR (Figure 2.8C). During this step, a fluorescent molecule binds to DNA, which proportionally increases at the same rate DNA synthesis increases. The fluorescent dye utilised in all RT-PCR experiments was SYBR Green. This dye binds to double stranded DNA and emits light when excitation occurs. Simply, as the PCR product increases, the fluorescence also increases in a parallel manner. To identify a gene of interest, specific primers are designed. The primers designed are displayed in Table 2.2. Within these primers was RP2β (housekeeping gene or reference gene) which was used in all experiments to quantify relative gene expression.
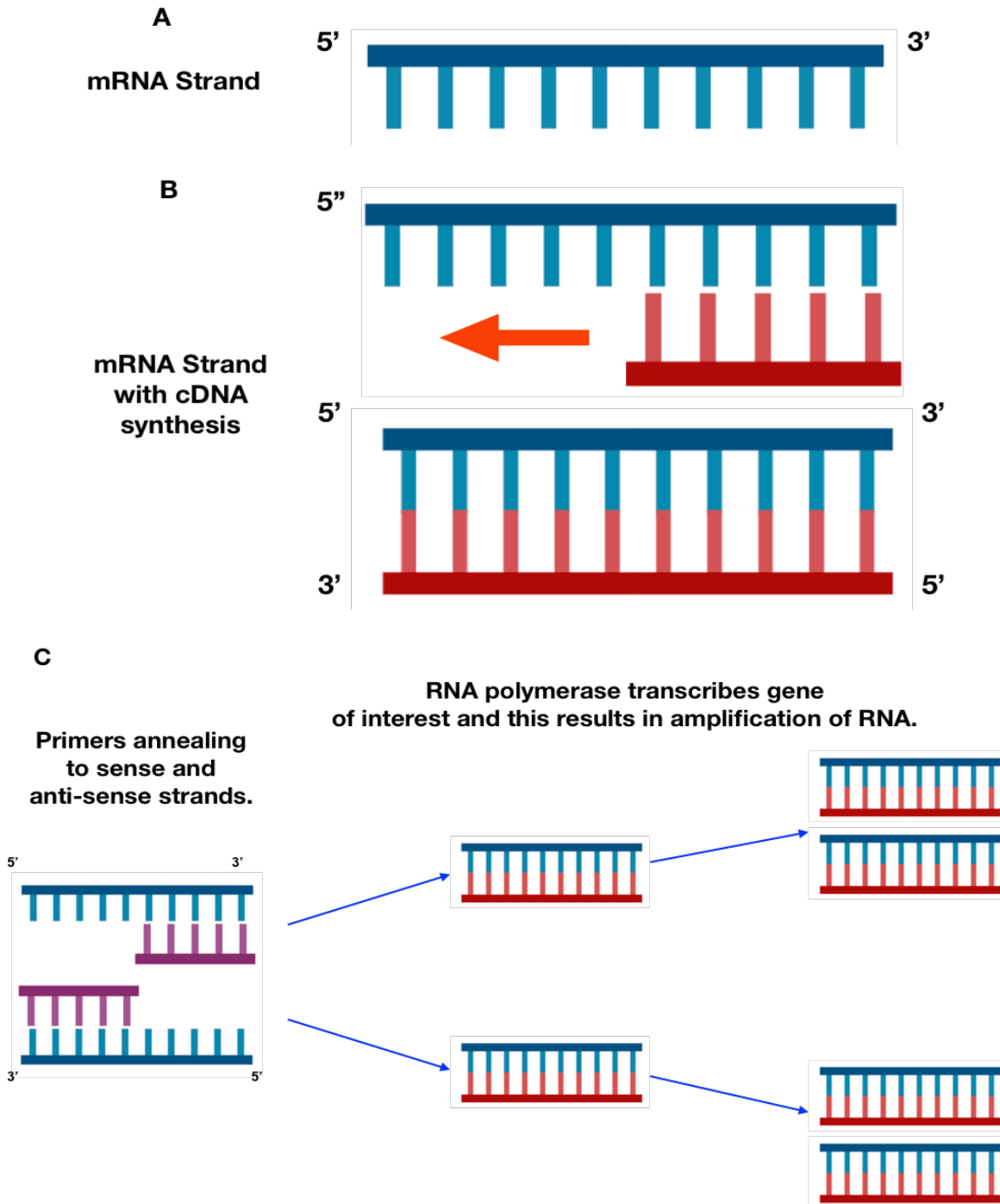
Figure 2.8. Diagram to illustrate the main processes in real time polymerase chain reaction. A: Strand of mRNA isolated from sample. B: Reverse transcription or cDNA synthesis of the same mRNA stand. C: Primers specific to gene of interest anneal at both of the 3' end of the sense (top) and anti-sense (bottom) strand. The PCR reaction then amplifies the amount of RNA by going through 40 cycles.

Table 2.2. Primer sequences for mus musculus with product length. All primers were used under same cycling conditions.

Gene	Accession	Sequence (Forward/Reverse)	Product Length (bp)
RP2β (aka polr2b)	NM_153798.2	F: GATCCGTATCAGGTTCATGTCTGTA R: CGGCATTCGCACCAAGGAA	123
Myogenin	NM_031189	F: CAACCCAGGAGATCATTTGCT R: TGACAGACAATCTCAGTTGGG739	145
Myostatin	NM_010834	F: GACCCGTCAAGACTCCTACA R: CTTCACATCAATACTCTGCCAAATA	146
IGF-I	NM_010512	F: CATCGTCTTTAGGAGTGTTTGTTT R: TAGAATGTTATTGATAAAGGACCAAC	98
IGF-II	NM_010514.3	F: CTCCTGGAGACATACTGTGCC R: AGGTGTCATATTGGAAGAACTTGC	121
ID3	NM_008321.2	F: CGGAACTTGTGATCTCCAAGGA R: CAGAGTCCCAGGGTCCCAA	112
SETD3	NM_028262.3	F: GGTGACCTTGGCTCTGATTCC R: CTCCAGCCTGAAAGTCCTGC	125
PIK3C3	NM_181414	F: CAAGGCTCATCGGCAAGGA R: TCGTTTCTCACTCTCATTTATCATTTC	112
FOXO3	NM_019740.2	F: CCAGGCTGAAGGATCACTGAG R: ACGGATCACTGTCCACTTGC	119
URB5	NM_00108135	F: CGGTGGTTCTGGTCAATAGTAGA R: GCTGGCAATGATGGGCTAGA	89
ADAM10	NM_007399	F: AAACCACTTCCAGGCACTTTAA R: TGTGTCCCATTTGATAACTCTCTC	97
CDH1	NM_009864	F: ACTCTTCTCCTGGTCCTGTTAG R: GGCTGTGGGTTCCTCTGG	89
SLC7A5	NM_011404.3	F: CCTTCTGTCCTCTCCATGATCC R: AGGCGTACATCAGCGTCATG	88
SLC3A2	NM_00116141	F: AGTCCAGCATCTTTCACATCCC R: CGCCGGAACTGGGTAAGGA	97

Specific gene expression was calculated by counting the number of PCR cycles required to reach the fluorescence threshold. Therefore, the lower the number of cycles required for the gene to achieve the fluorescent threshold, the higher the expression and vis versa. Mathematically, this was defined by the number of cycles reaching the fluorescent threshold (C_T value) which was inversely proportionate to the log of the target gene number. To calculate relative quantities of the gene of interest in a sample, the C_T value of the reference gene and the zero-hour control were used.

To establish that only the intended gene was amplified and not contaminated, melt curve analysis was performed. Melt curve analysis distinguishes the melting temperature (Tm) of the product. The melt curve was generated by plotting the fluorescence against the increasing sample temperature. When the product was amplified, a sharp increase in fluorescence was observed, followed by a sharp decrease (Figure 2.9A). However, if multiple peaks are observed, this could indicate contamination, unspecific amplification or primers not annealing to the specific gene (Figure 2.9B). In these cases, the samples were not used for analysis.
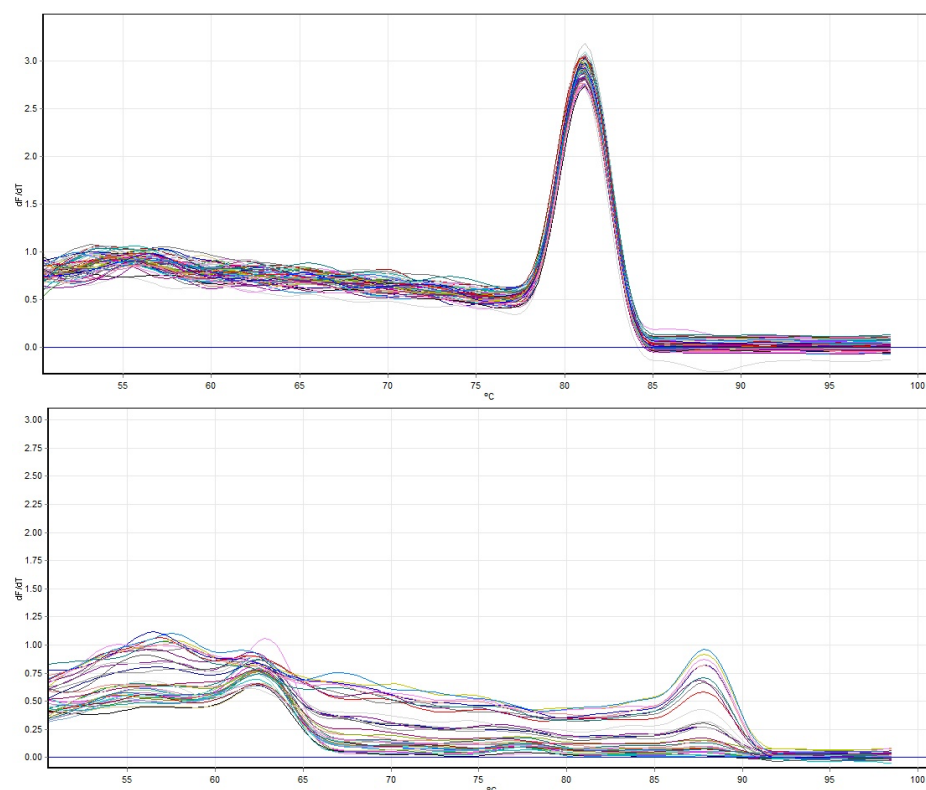
Figure 2.9. Images to show different primer melt curves. A: No issue with melt curve. B: Amplification issues, as no definitive peak.

2.10.2 Procedure

Once the cells were lysed in TRIzol (section **2.5.2),** 0.1 ml of chloroform per 0.5 ml of TRIzol reagent were added to the homogenates, followed by vigorous shaking for 15 seconds. Samples were incubated at RT for 10 minutes, before centrifuged at 12000 g for 15 minutes at 4 °C. The aqueous layer (containing RNA and chloroform) was carefully transferred into a new tube, prior to addition of isopropanol (ratio 1:2), in order to precipitate the RNA. Following 5 minutes incubation at RT, the samples were centrifuged at 12,000 g for 10 minutes at 4 °C. The supernatant was removed, and 1 ml 75 % ethanol was added to the pellet. The samples were centrifuged 7500 g for 5 minutes at 4 °C and the supernatant decanted. The pellet was left to air dry prior to addition of and vortexing in in 20 µl RNA storage solution (Ambion-The RNA Company, Chesire, UK). Importantly, all plasticware used in this procedure was RNA free and laboratory space was cleaned with RNase ZAP (Ambion-The RNA Company, Chesire, UK).

The Nanodrop UV spectrophotometer (Thermo Fisher Scientific, Waltham, USA) was used to assess the RNA quality and quantity. The absorbance was measured at 260/280 nm and 260/230 nm. These are commonly known as the RNA purity ratios. For 260/280: a ratio of 2 was accepted. Whereas, for 260/230 of 1.8-2.2 was accepted. The surface of the spectrophotometer was cleaned with RNA free water. A blank sample was recorded using 1 µl RNA storage solution. The samples were then recorded and Figure 2.10 illustrates an example of nucleic acid spectral that was used to assess RNA quality.
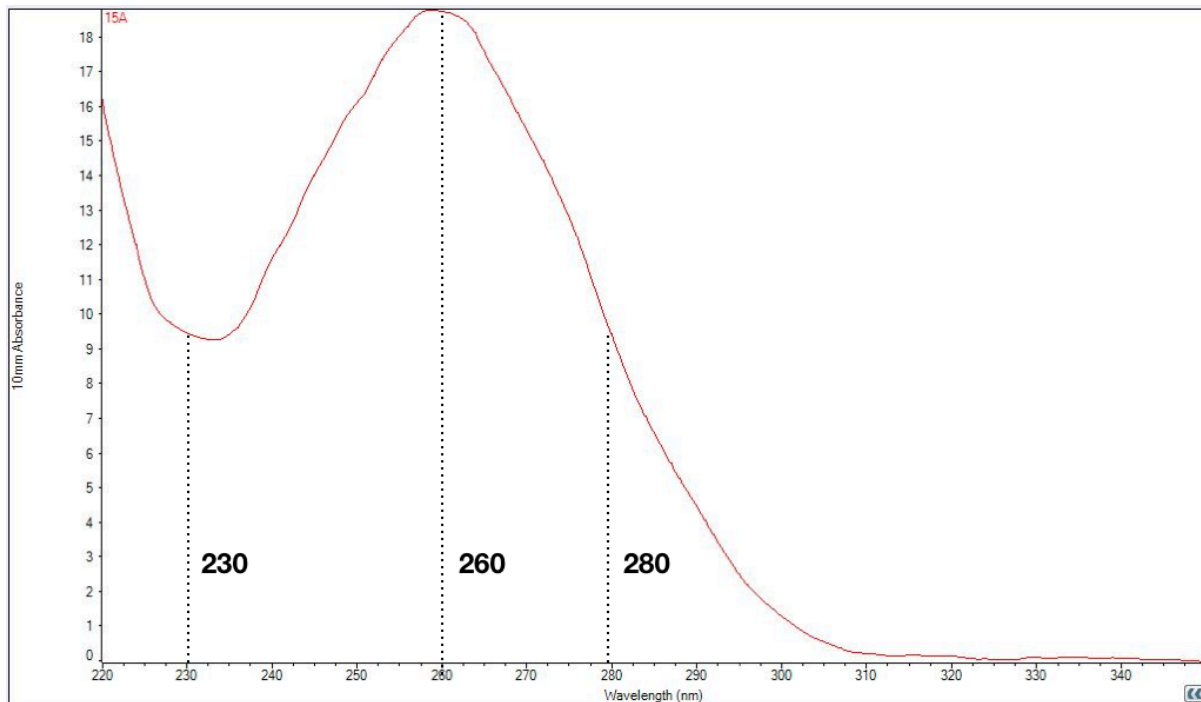
Figure 2.10. Nucleic Acid example used to assess RNA quality.

The data derived from the Nanodrop UV spectrophotometer was also used to calculate RNA quantity based on the absorbance at 260 nm. In detail, it is known that a reading of 260 nm of 1 is equivalent to 40 µg.ml^{-1} of RNA. The following Beer-Lambert equation was used by the Nanodrop software (Equation 2.7).

$$C = \frac{(A \times \varepsilon)}{b}$$

- C is nucleic acid concentration (µg.ml^{-1})
- A is absorbance in AU
- ε is extinction coefficient (ng-cm.µl^{-1}), for RNA it is 40 ng-cm.µl^{-1}
- b is the path length in cm

Equation 2.7. Beer-Lambert equation was used to quantify RNA using the Nanodrop Software.

Finally, if the RNA samples contained high concentrations of mRNA, they were diluted for further storage. For RT-PCR reactions, a final reaction concentration of 70 ng mRNA per gene was used for a one-step protocol. Total reaction volume equaled 20 µl per sample, which contained 11.2 µl of master mix (10 µl quantifast SybrGreen, 1 µl primer, 0.2 µl reverse transcriptase) and 8.8 µl RNA (8 ng/µl) sample. All primers were synthesized by primer design. Samples were added to reaction tubes and analysed on rotor-gene Q (Qiagen, Manchester, UK) PCR machine. The amplification protocols were as follows: reverse transcription (10 minutes at 55 °C), enzyme activation (2 minutes at 95 °C), denaturation (10 seconds at 95 °C) and data collection (60 seconds at 60 °C) which involved 40 cycles and followed by melt curve detection (Figure 2.11). For analysis, melt curves were assessed to see only one peak and uniformity across samples, this was checked with primer design. For C_T values, a threshold was set at 0.1 for all genes. The amplification efficiencies were also analysed, with values 80-100 % proposed as efficient. To relativise C_T values to 0 h control and reference gene the delta delta C_T equation was used (Livak and Schmittgen, 2001).
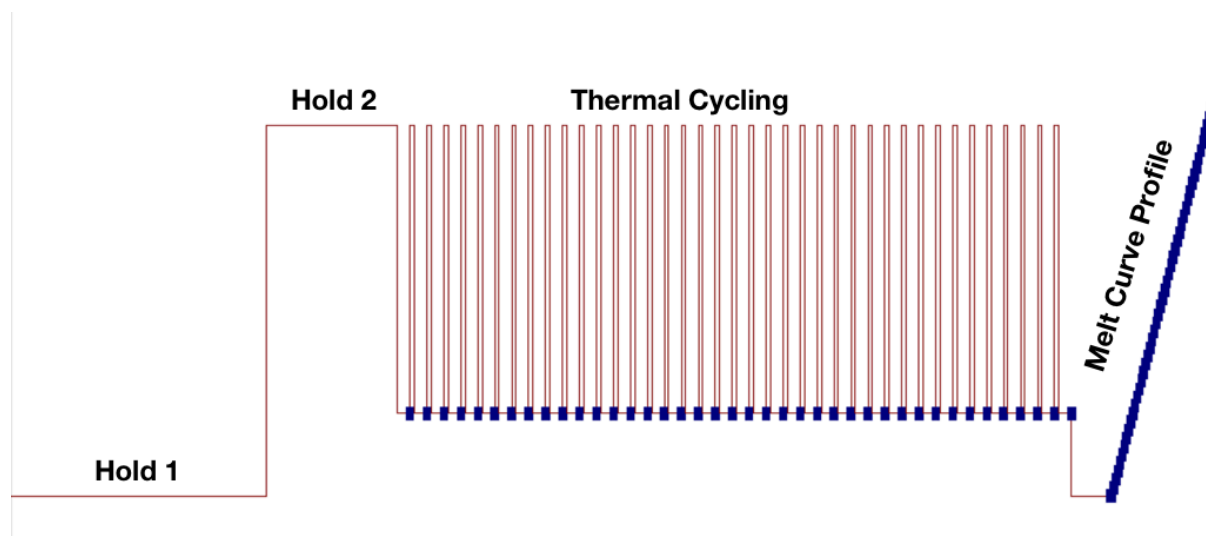
Figure 2.11. Amplification Profile for all RT-PCR reactions.

2.11 Dynamic Proteomic Profiling

2.11.1 Principle

Proteomics involves non-targeted analysis of large numbers of proteins in a cell, tissue or organism. The majority of proteomic research has provided insights into protein function, abundance and post-translational modifications. More recently, protein synthesis and degradation have also been investigated by combining stable isotope (deuterium oxide; D_2O) labelling with liquid chromatography-mass spectrometry (LC-MS). In this thesis, C_2C_{12} myoblasts and myotubes were labelled with D_2O, then lysed and protein content quantified **(sections 2.5.4 and 2.6.2)**. The proteins were digested into peptides and desalted before being analysed by LC-MS (Figure 2.12).

Deuterium oxide, also known as heavy water, is commonly used to investigate protein turnover in humans (Previs *et al.* 2004). The labelling of D_2O occurs intracellularly and labels onto ^2H of the C-H bond of the majority of amino acids. Therefore, D_2O incorporation is not confounded by amino acid metabolism or the transport rates of amino acids across the cell membrane. After a ^2H-labelled amino acid is incorporated in to a polypeptide chain the deuterium label is irreversible (Busch, 2006). When the level of precursor enrichment is known or can be set, i.e. in the current work cell were grown in media containing 4 % D_2O, the incorporation of D_2O into protein can be used to calculate the rate of synthesis by comparing the isotopomer distribution of peptides against the natural distribution of that peptide in the unlabelled sample (Xiao *et al.*, 2008). The subtraction of the unlabelled isotopomer distribution of a peptide against the labelled peptide provides a measure of molar percent excess (MPE). The incorporation of D_2O was calculated from the ratio of unlabelled (m_0) relative to the sum of the labelled (m_1, m_2, m_3, m_4 etc) isotopomers (Figure 2.12). This provides a proportionally greater magnitude of change for a given amount of D_2O incorporation. The monoisotopic (m_0) cannot contain any heavy isotopes, therefore, the molar fraction declines as a function of D_2O incorporation into a peptide. Therefore, data calculations were based on reciprocal decline of the m0 fraction, following an exponential decay pattern.
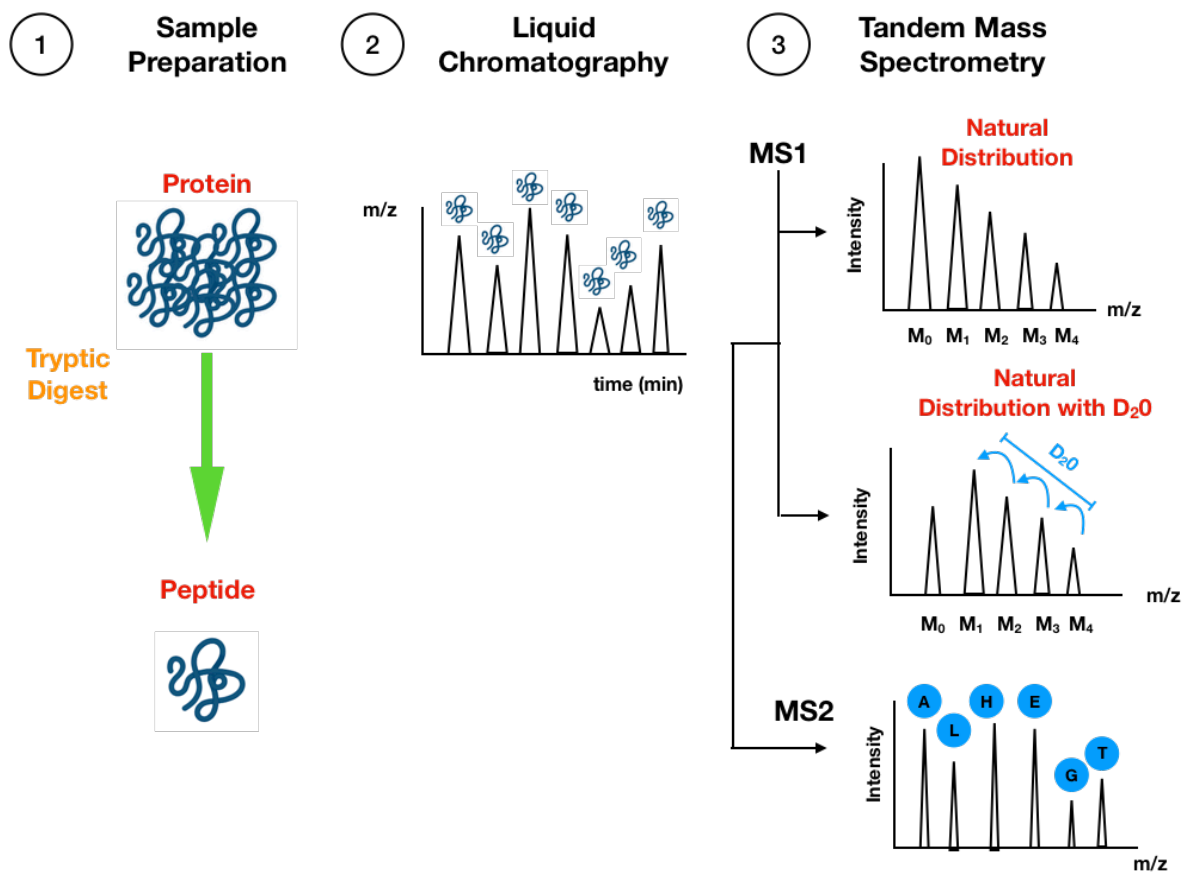
Figure 2.12. Visual representation process performed following cell digestion and protein quantification.

Proteins isolated from C_2C_{12} muscle cells with and without D_2O incorporation. 1: The proteins were digested into peptides via overnight trypsin digest. 2: Peptides were separated in time by reverse-phase liquid chromatography. The peptides were then eluted based on their relative hydrophobicity and transported to the mass spectrometer. 3: Tandem mass spectrometry includes two phases (MS1 and MS2). MS1 records the peptide mass spectra and was used to measure relative abundance and D_2O incorporation based on relative distribution of mass isotopomers. The D_2O labelled amino acids during protein synthesis cause a shift in distribution of m_1, m_2, m_3, m_4… Isotopomers. The m_0 declines as a function of D_2O incorporation/protein synthesis. MS2 the mass spectra of each peptide following fragmentation and used to record amino acid sequences that were matched against protein databases.

Peptide digests from labelled and unlabelled cells were separated by nanoscale reversed-phase ultra-performance liquid chromatography (nanoACQUITY, Waters, Milford, MA). Time-resolved peptides eluting from the LC column were sprayed directly into the integrated electrospray ionization (ESI) quadrupole-time of flight mass spectrometry (Q-TOF Premier, Waters, Manchester, UK). Figure 2.13 illustrates the components of the mass spectrometer that was used. In detail, the sample is sprayed into the lockmass structure, where there is also a reference sprayer. This reference sprayer enables accurate mass measurement in both MS and MS/MS modes. The ESI enables the sample to go from liquid to gas, and the charged particles are transferred through the lockmass compartment. The lockmass compartment also contains a built-in camera so the sprayers were observed for any blockages or irregularities in spraying of either the analyte or reference solution. Once the sample passes through the Lockmass structure it goes through the T-wave Ion guide, which removes non-charged ions and so enhances sensitivity, of the instrument.

The analyte then passes through a quadrupole mass analyser that is used to select ions based on their mass to charge ratio (m/z). The quadrupole mass selector determines whether all peptides (i.e. MS scan) or a select peptide (i.e. fragment ion scan) are passed through the instrument. The next major component of the instrument is the T-wave collision cell. The mass spectrometer has two modes for the analysis of peptides which include: MS1 (MS) and MS2 (MS/MS). In the MS1 mode, the peptides pass through the quadrupole and through the T-wave collision cell, which is not active (no peptides fragmented: 5 v). The peptides are detected in time of flight (ToF) compartment, which selects a parent ion spectrum. The quadrupole filters remove any peptides not within this range. In the second mode MS2 (MS/MS) the T-wave collision cell is activated (40 v) which fragments the peptides into smaller polypeptides and amino acids. Once detected in the ToF analyser another spectrum is produced. The MS1 and MS2 spectrum can be used to work out AA sequences in a peptide. This compartment maintains the ion sensitivity before it passes through the first detector and then onto the ToF analyser. The first detector is called the photomultiplier tube. The analytes have now entered the ToF analyser, where high voltage pulses accelerate the ions down the flight tube and onto the reflectron. The reflectron design increases the length of the flight tube and thus enables higher mass resolution. The ions are reflected the analytes onto the detectors (V optics). This last detector, time-

to-digital converter, records the arrival time after they have travelled from the first detector through the ToF compartment. Ions with different times and therefore different mass spectrum can be created in a resolution < 10,000 full width at half maximum (FWHM).

For example, if the MS1 spectrum detects a parent ion spectrum of 750 m/z, then peptides below 748 m/z and above 752 m/z would be filtered out. Then the MS2 spectrum can be used to analyse amino acid sequences from peptides with 748-752 m/z.
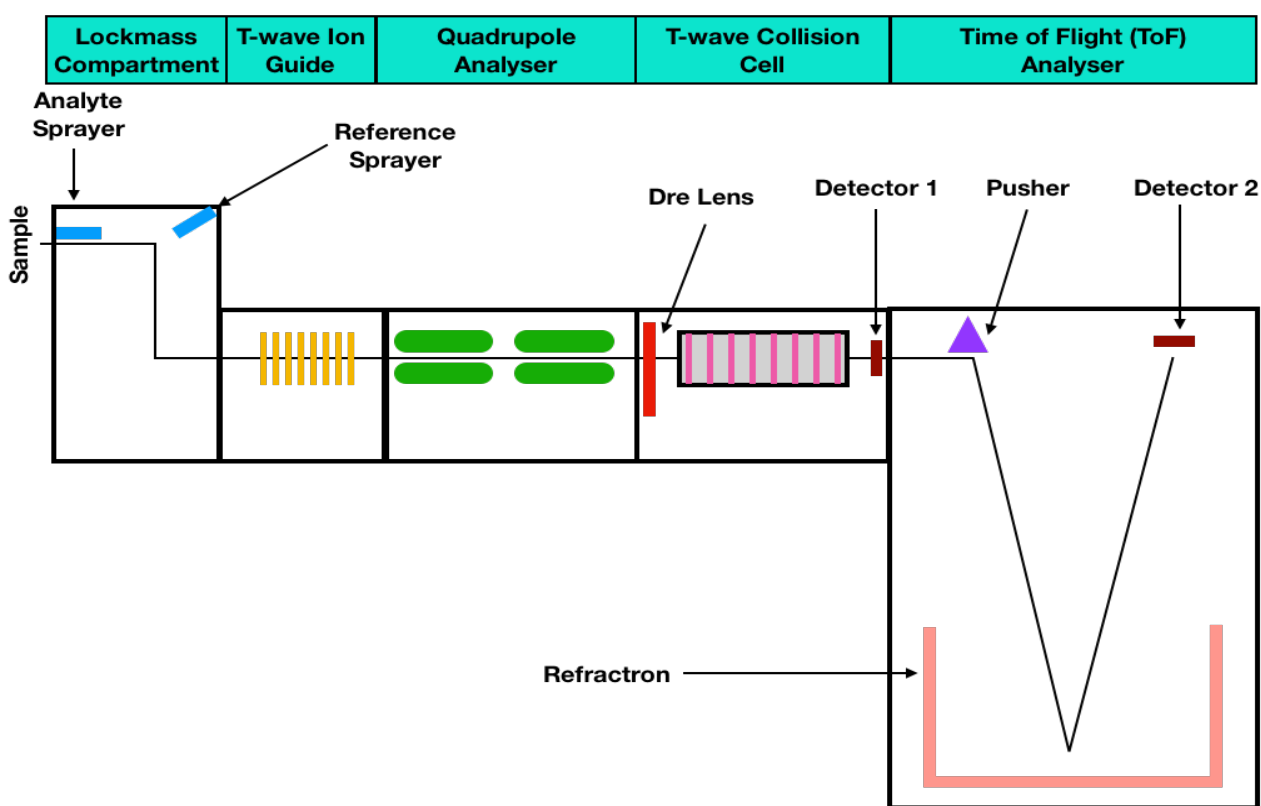
Figure 2.13. Diagram that represents the Mass Spectrometry compartments and how the peptides were detected.

2.11.2 Procedure

2.11.2.1 Muscle Cell Digestion and Dilution

Cell proteins were extracted as described in sections **2.5.4** and **2.6.2**. Extracts containing 100 ug of protein were digested using the filter-aided sample preparation (FASP) method (Wisniewski, 2009). Proteins were precipitated in 5 volumes of acetone for 60 minutes at -20 °C. The samples were centrifuged at 5000 g for 5 minutes at RT, the supernatant was decanted and the pellet was air-dried for 5 minutes. Protein pellets were resuspended in 200 µl of UA buffer (8 M urea, 100 mM Tris, pH 8.5). Samples were placed into sample cups with 30 kDa MWCO filters (Sigma-Aldrich, Dorset, UK) and centrifuged at 14,000 g for 15 minutes at RT to remove excess UA buffer. Samples were incubated at 37 °C for 15 minutes in UA buffer containing 100 mM dithiothreitol and then centrifuged at 14,000 g for 15 minutes at RT. Then, the samples were incubated for 20 minutes at 4 °C and protected from light in UA buffer containing 50 mM iodoacetamide. Samples were centrifuged at 14,000 g for 10 minutes at RT. The samples were washed twice with 100 µl UA buffer. Between washes the samples were centrifuged at 14,000 g for 10 minutes at RT. Ambic (50 mM ammonium hydrogen bicarbonate) was added to samples and mixed on MTP shaker for 2 minutes before centrifugation at 14,000 g for 10 minutes at RT. Sequencing grade trypsin (Promega; Madison, WI, USA) was added at an enzyme: protein ratio of 1:50. The samples were left overnight at 37 °C to fully digest. To terminate digestion, trifluoracetic acid (TFA) was added at a final concentration of 0.2 % (v/v). The final volume was of peptide solution was 100 µl. The samples, containing 4 µg peptides, were desalted using C_{18} Zip-tips (Millipore, Billercia, MA, USA) and the peptide solution was eluted in 50 % acetonitrile (ACN) and 0.1 % TFA to give final concentration of 0.2 µg/ul. To reduce ACN in the samples they were dried in a speed vac at 60 °C for 25 minutes. After, 20 µl of (Alcohol dehydrogenase 1) ADH1 (10 fmol/µl in 2.5 % ACN, 0.01 % formic acid (FA)) was pipetted into each sample. The samples were transferred to auto-sampler tubes in preparation for LC-MS.

2.11.2.2 Liquid Chromatography-Mass Spectrometry

Samples were loaded on to a Symmetry C18 5 µm, 2 cm x 180 µm trap column (Waters, Milford, MA) in 2.5 % ACN, 0.1 % (v/v) formic acid via. Separation was conducted at 35 ºC through a BEH C18 1.7 µm, 25 cm x 75 µm analytical reverse phase column (Waters, Milford, MA) using a linear gradient from 2.5 % to 37.5 % acetonitrile in 0.1 % (v/v) formic acid over 60 minutes at a flow rate of 300 nL/min.

The mass spectrometer was operated in a data-dependent positive ESI mode at a resolution of >10,000 FWHM. Prior to sample analysis, the ToF analyser was calibrated using fragment ions of Glu-1-fibrinopeptide B from 50 to 1990 m/z. LC-MS profiling recorded peptides between 350 m/z and 1500 m/z using MS survey scans of 0.9 second duration with an inter-scan delay of 0.1 seconds. Equivalent data-dependent tandem mass spectrometry (MS/MS) spectra were collected from the control samples with no D_2O label. MS/MS spectra of fragment ions were recorded over 50-2000 m/z for the 5 most abundant precursors ions of charge 2+ or 3+ detected in the survey scan. Precursor fragmentation was achieved by collision induced dissociation (CID) at an elevated (20-40 eV) collision energy over a duration of 0.25 second scan an inter-scan delay of 0.05 seconds. A dynamic exclusion window was set to 30 seconds to avoid repeat selection of prominent ions. Acquisition was switched from MS to MS/MS mode when the base peak intensity (BPI) exceeded a threshold of 30 counts. MS mode was restored when the TIC in the MS/MS channel exceeded 7500 counts/s or when 1 second (5 scans) were acquired.

2.11.2.3 Protein Profiling using QIP Progenesis

Both MS and MS/MS spectra were imported into Progenesis QIP software (Waters Corp. Milford, MA). Spectra were aligned using prominent ion features (mean ± SD per chromatogram: 455 ± 42) as vectors to provide a common reference chromatogram. An analysis window of 15-105 minutes and 350-1500 m/z was selected. This encompassed a total of 32,824 features with charge states of +2, +3 or +4. The MS data (peptide abundances) was log transformed and normalised by inter-sample abundance ratio. MS/MS spectra were exported in Mascot generic format and searched against the UniProt database (2018) restricted to 'mus musculus' (17,006

sequences) using a locally implemented Mascot (www.matrixscience.com) server (version 2.2.03). The enzyme specificity was: trypsin allowing 1 missed cleavage, carbamidomethyl modification of cysteine (fixed), deamidation of asparagine and glutamine (variable), oxidation of methionine (variable) and an m/z error of ± 0.3 Da. The false discovery rate based on decoy database search was 1.88 %. The Mascot output (xml format), restricted to non-homologous protein identifications was recombined with MS profile data in Progenesis. Peptide features with MOWSE scores <30 (MudPIT scoring) were excluded.

2.11.2.4 Fractional Synthesis Rate Calculations

As mentioned in **section 2.11.1** the D_2O incorporation, or fractional synthesis rate (FSR) was calculated by the reciprocal decline of the monoisotopic peak (m_0), which follows the exponential decay equations.

Equation 1:

$$\chi_t = \chi_{t1} \times e^{-kt}$$

k = rate of decay
χ = molar fraction (m_0)
t = prior labelling period
t1 = post labelling period
e = exponential

The rate (k) of decay was calculated from the change in molar fraction (χ) of the monoisotopic peak period times (t0-t1). Then, the rate of decay of m_0 was normalised by the number of exchangeable H positions based on the peptide sequence (MS2) and the level of enrichment (4 %: 0.04 D_2O).

Equation 2:

$$k = 1/(t1-t) \times \ln(\chi_t) - \ln(\chi_{t1})$$

k = rate of decay
χ = molar fraction (m_0)
t = prior labelling period
t1 = post labelling period
ln = natural log

Equation 2.8: Equations used to determine the FSR of peptides. 1: The rate of decay from change of molar fraction. 2: Rate of decay normalised by exchangeable H position.

2.10 Statistical Analysis and Graphical Representations

All the data are displayed as mean ± standard deviation (SD), unless differently stated in the specific section. All of the statistical analyses were completed on SPSS Predictive Analytics Software (v.25, IBM Corporation, New York, USA). All C_2C_{12} experiments were based on n=3, which are referred to as technical repeats throughout the thesis. Technical repeats due to the cell line originating from one mouse muscle. When comparing two group means, a t-test was used. When multiple groups of means were required, analysis of variance (ANOVA) was used. For ANOVA's, the data sets were checked for normal distribution and appropriate correction factors was used. Greenhouse-Geiser or Huyn-Feldt correction factors were used if the data violated the assumption of sphericity. If a significant main effect or interactions were apparent, then Bonferroni post-hoc pairwise comparison test was used. Significance was set at p ≤ 0.05. The majority of figures were designed using Prism (v8, GraphPad, La Jolla, CA, USA) or Microsoft Excel (v.2016).

Chapter 3: Influence of Replicatively Ageing and Nutrition on Myoblast Migration

The work contained in this Chapter has been published:

3.1 Abstract

Introduction: Cell migration is central to skeletal muscle repair following damage. Leucine and HMB are supplements consumed for recovery from muscle damaging exercise in humans, however, their impact on muscle cell migration with age is not yet understood. The aim was to investigate the impact of leucine and HMB on control and replicatively aged myoblast repair. The hypothesis was that replicatively aged cells would be less able to repair wounds vs. control, and supplements would enhance efficient wound closure in both control and replicatively aged cells.

Methods: Replicatively aged and control myoblasts were scratch-damaged and migration velocity, directionality and distance assessed over 48 h in the absence and presence of leucine (10 mM) or HMB (10 mM) ± PI3K/Akt (LY294002 10 µM), ERK (PD98059 5 µM) or mTOR (rapamycin 0.5 µM) inhibition.

Results: Replicatively aged cells displayed significantly increased velocities, directionality and distance migrated (all $P < 0.001$) vs. control. Leucine and HMB significantly increased ($P < 0.001$) the same parameters in control cells. The supplements were with smaller, albeit significant impact on aged cell velocity ($P < 0.001$) and in the presence of HMB only, distance ($P < 0.05$). Inhibitor studies revealed that, PI3K and ERK activation were essential for velocity, directionality and migration distance of aged cells in basal conditions, whereas mTOR was important for directionality only. While PI3K activation was critical for all parameters in control cells ($P < 0.001$), inhibition of ERK or mTOR improved, rather than reduced, control cell migration distance. Enhanced basal velocity, directionality and distance in aged cells required ERK and PI3K activation. By contrast, in control cells, basal migration was underpinned by PI3K activation, and facilitated by leucine or HMB supplementation, to migration levels seen in aged cells.

Conclusion: These data suggest that replicatively aged myoblasts are not anabolically resistant per se, but are capable of efficient repair, underpinned by altered signaling pathways, compared with unaged control myoblasts.

3.2 Introduction

During the human lifespan, a gradual loss of skeletal muscle mass and strength occurs, referred to as sarcopenia. While muscle mass and strength in young individuals can be preserved through nutritional supplementation, it is reported that muscle in older adults displays a level of anabolic resistance (Breen and Phillips, 2011). The capacity of the muscle to regenerate following exercise induced muscle damage is reportedly impaired in ageing rodents and humans (Brooks *et al.*, 1988; Faulkner *et al.*, 1991). It is reported that altered satellite cell behaviour may negatively impact not only on muscle mass and strength, but also on the muscle regeneration processes (Welle, 2002; Shefer *et al.*, 2006; Day *et al.*, 2010; Bigot *et al.*, 2015).

Recently, interest has arisen relating to the use of nutraceuticals to facilitate muscle growth. Data suggest old muscle may be anabolically resistant and require higher concentrations of protein to elicit a hypertrophic response versus young muscle (Breen *et al.*, 2011). Leucine, an essential AA, is reportedly a potent anabolic agent (Koopman *et al.*, 2006) and is also consumed following damaging exercise, with the aim to improve muscle regeneration (Farup *et al.*, 2014). Recent studies have investigated the effects of leucine administration on myoblast fusion (Areta *et al.*, 2014; Dai *et al.*, 2015) and demonstrated that increasing leucine in a dose responsive manner (5 and 16.5 mM) stimulated the mTOR signaling pathway and the phosphorylation of P70S6K, resulting in significantly increased myoblast fusion. Furthermore, in young recreationally active males, whey protein, which contains high doses of leucine (8 g per 100 g), increased muscle satellite cell number at 48 h post eccentric damage, compared with control (Farup *et al.*, 2014).

HMB, a metabolite of leucine, is increasing in popularity as an ergogenic aid for muscle recovery and regeneration. HMB studies in human myoblasts and rodents demonstrate positive effects on satellite cell proliferation, differentiation and survival, following MAPK/ERK and PI3K/Akt activation (Kornasio *et al.*, 2009; Vallejo *et al.*, 2016). Supplementation of human myoblasts with HMB (0-85 mM) stimulated cell proliferation via the MAPK/ERK pathway and induced differentiation via the PI3K/Akt pathway (Kornasio *et al.*, 2009). Further studies by Vallejo *et al.* (2016) investigated

the impact of HMB on C_2C_{12} myoblasts (25-125 µM) and on the contractile force of ageing murine soleus muscle (514 mg/kg). HMB treatment increased C_2C_{12} myoblast proliferation and myoblast viability. In mice, HMB prolonged force generation and reduced the amount of time for peak muscle contraction following damage (Vallejo *et al.*, 2016). Together, these studies indicated that leucine and HMB could impact positively on muscle differentiation, survival and function.

Adequate skeletal muscle mass and function are essential in supporting human health and well-being (Sharples *et al.*, 2015). However, the molecular regulators of skeletal muscle cell migration are relatively understudied, despite the fact that skeletal muscle has a remarkable ability to regenerate. Understanding the signalling pathways that regulate myoblast migration, direction and velocity is therefore important in advancing capacity to promote skeletal muscle regeneration. Evidence exists supporting the role of the Rho family, in regulating satellite cell migration (Raftopoulou *et al.*, 2004). Upstream of the Rho family is the PI3K/Akt pathway, which we demonstrated, when inhibited, resulted in impaired myoblast migration (Dimchev *et al.*, 2013). Furthermore, the MAPK/ERK pathway is also reportedly involved in efficient myoblast migration, albeit findings are somewhat equivocal (Leloup *et al.*, 2007; Ranzato *et al.*, 2009; Al-Shanti *et al.*, 2011).

Given a global drive to reduce/refine animal research, relevant cell models are required to inform future *in vivo* studies. To this end, our laboratory have developed a myoblast model, with application to ageing muscle cell behaviour (Sharples *et al.*, 2011). Using a process of replicative ageing, C_2C_{12} murine skeletal muscle cells were subjected to 58 population doublings versus parental control and were reported to display impaired differentiation both in 2-D and 3-D models (Sharples *et al.*, 2011, 2012; Deane *et al.*, 2013). While these cells have been extensively characterised with regards to hypertrophy and atrophy and compare well with replicatively aged human cells (Bigot *et al.*, 2008), human and rodent cells isolated from ageing muscle (Lees *et al.*, 2006, 2009; Bigot *et al.*, 2008; Léger *et al.*, 2008; Pietrangelo *et al.*, 2009) and muscle biopsy tissue derived from older individuals (Welle *et al.*, 2003; Léger *et al.*, 2008), little research has focused on their ability to repair damage. Furthermore, although the potential of nutraceuticals in muscle preservation is being avidly investigated (Phillips *et al.*, 2009), the question remaining to be challenged is whether

nutraceuticals elicit a beneficial impact on muscle cell migration and repair and whether this is compromised with ageing.

Therefore, the aim of this study is to investigate the impact of leucine and HMB on control and aged skeletal muscle cell repair. The objectives are: 1. To determine the migration capacity of replicatively aged (but not senescent) C_2C_{12} skeletal muscle cells versus controls that have not undergone any population doublings relative to aged cells. 2. To investigate the impact of the nutritional supplements leucine and HMB on migration capacity and; 3. To begin to determine relevant signalling pathways (Akt, ERK and mTOR) that may be important for successful migration and wound closure. We hypothesised that: 1) replicatively aged (P46-P48; 'replicatively aged') myoblasts would be less efficient at damage repair versus unaged controls (P12-P16, 'control'); 2) leucine and HMB would increase the migration potential in control but not aged cells and; 3) that the Akt and ERK, but not mTOR (given its critical role in myoblast fusion) pathways would be required for effective migration in both models.

3.3 Methods

3.3.2 Cell Culture

Commercially available C_2C_{12} mouse skeletal myoblasts were purchased from ATCC and passages 12-16 (referred to as 'control') and passages 44-48 (replicative aged and referred to as 'aged'; (130-140 population doublings)) were used in this study. For standardised cell culture procedures, see **section 2.2.**

3.3.3 Damage Protocol and Cell Treatments

Once 80 % confluency was attained, cells were typsinised, counted and seeded at 100,000 cells/ml on gelatinised six or twelve well plates (Nunc, Roskilde, Denmark) and grown to 80 % confluence. Cells were washed once with PBS prior to an established *in-vitro* wound/repair model to assess migration in myoblasts via applying a damaging scratch to monolayer cells as previously reported by our group (Dimchev *et al.*, 2013; Owens *et al.*, 2015). Cells were washed twice with PBS to remove any debris, prior to dosing in DM in the absence or presence of leucine (10 mM) or HMB (10 mM). Doses were selected following basal dose response studies (0-10 mM). In addition, signaling pathways, in the absence or presence of leucine or HMB, were manipulated with: LY294002 (10 µM), inhibitor of PI3K signalling, PD98059 (5 µm), inhibitor of ERK signalling or rapamycin (0.5 µM) inhibitor of mTOR (Dimchev *et al.*, 2013; Hatfield *et al.*, 2015). For inhibitor studies, cells were allowed to quiesce for 30 minutes, in DM, prior to addition of respective inhibitors for 30 minutes, followed by supplements for up to 48 h. All cell experiments were repeated 3 times in duplicate.

3.3.4 Wound Healing Assay and Migration Analysis

For detailed methods on wound/repair healing assays and analysis, see **section 2.3.** In brief, microscopic images were obtained from two points within each wound, every 30 minutes for 48 h at 10x magnification. For the analysis of cell migration dynamics, the directionality, accumulated distance and velocity were determined using TIF image stacks and Image J software (IBIDI, Munich, Germany).

3.3.5 Cell Fixation and Preparation for FLOW Cytometry

Flow cytometry was performed to simultaneously assess multiple phosphoproteins in relevant cell samples (Schubert *et al.*, 2009; Sharples *et al.*, 2011). At 80 % confluence, the cells were washed, damaged and quiesced prior to dosing. The cells were extracted and fixed as described in **section 2.5.3**. Cells were then stored at -20 °C until further analyses by flow cytometry. The cells were washed, centrifuged and re-suspended in flow buffer **(see section 2.7.2)**. The anti-human/mouse phospho-AKT (S473; APC; 675/25 nm; 0.5 µg), anti-human/mouse phospho-ERK1/2 (T202/Y204; Alexafluor 488; 533/30 nm; 0.03 µg) and anti-human/mouse phospho-mTOR (S2448; PerCP; 670/LP nm; 0.125 µg) antibodies (Thermo Fisher Scientific inc, Waltham, USA) were added to each sample and incubated at RT in the dark for 60 minutes. The cells were washed and re-suspended three more times before analysis via flow cytometry **(see section 2.7.2)**.

3.3.6 Statistical Analysis

SPSS Predictive Analytics Software (version 23; IBM) was used for all statistical analyses. Data were assessed and normal distribution confirmed. For the comparison of replicative aging (control vs. aged C_2C_{12} cells) vs. supplements (DM alone, leucine, HMB) a two by three-way ANOVA was used, where significant main effects and interactions were present, the Bonferroni post hoc pairwise comparisons test was used. For within test comparisons, either, independent t-tests, or one-way ANOVA was used. All data are presented as mean $\pm$ SD and significance as ≤ 0.05.

3.4 Results

3.4.1 Improved Migration in Replicatively Aged vs. Control C_2C_{12} Skeletal Muscle Cells

Following scratch damage, aged and control cell migration into the wound site was measured over 48 h (Figure 3.1). In contrast to our hypothesis, under basal conditions in replicatively aged vs. control cells respectively, there was a 1.27-fold increase in cell velocity (0.28 ± 0.07 μm/min vs. 0.22 ± 0.07 μm/min; $P < 0.001$; Figure 3.2A), a 1.27-fold increase in directionality (0.71 ± 0.12 vs. 0.61 ± 0.17; $P < 0.001$; Figure 3.2B) and a 1.29-fold increase in overall migration distance (802 ± 202 μm vs. 622 ± 188 μm; $P < 0.001$; Figure 3.2C). This increased migration in the replicatively aged cells was associated with altered phosphorylation of Akt, ERK, and mTOR (Figure 3.3A, 3.3B and 3.3C, respectively). In replicatively aged cells ERK activation was significantly increased ($P < 0.05$) vs. control cells at 15 minutes and while still elevated at 60 minutes, significance was not attained. Akt phosphorylation was not different between the two cell groups at 15 minutes. However, while Akt phosphorylation decreased in the unaged controls to 60 minutes where it plateaued to 120 minutes, it increased over the time course in the replicatively aged cells reaching significance ($P < 0.05$) vs. control at 120 minutes. Finally, mTOR phosphorylation did not significantly change over the time course assessed in replicatively aged or control cells and no significant differences were observed between the two models.

Replicatively Aged   **Control**

0h
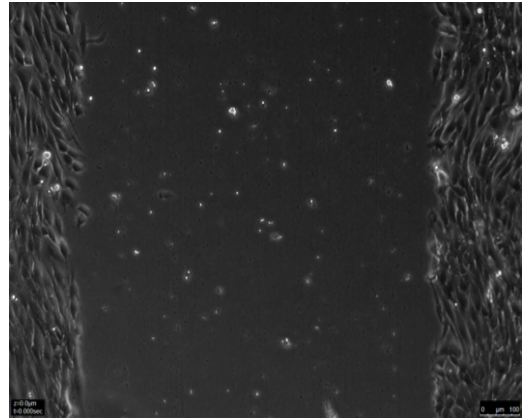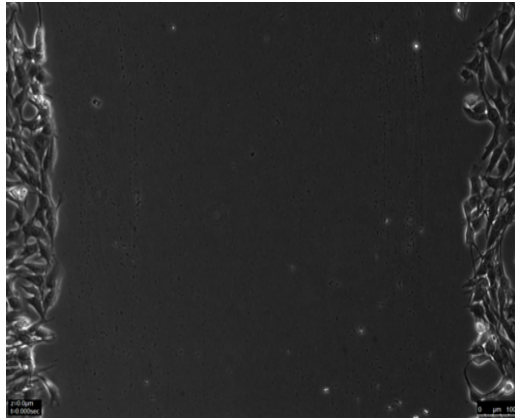
24h
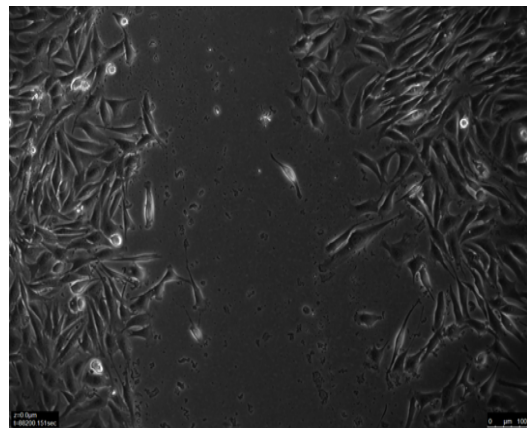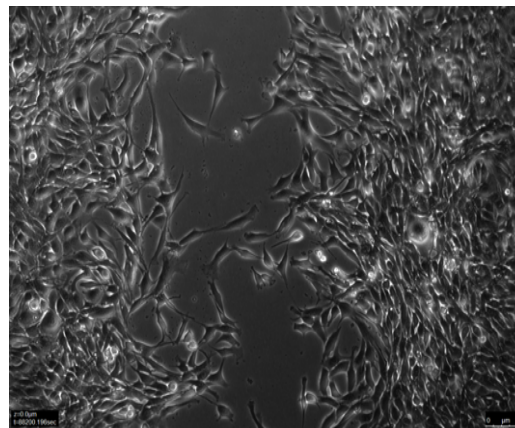
48h
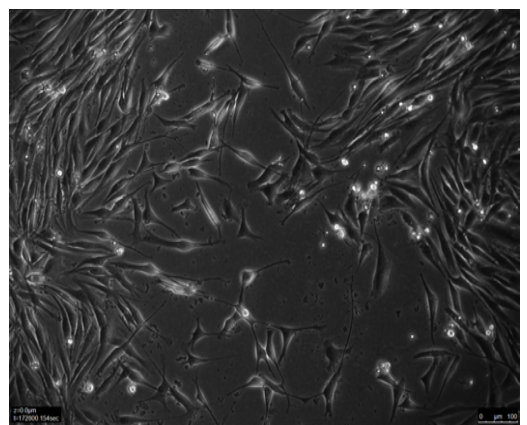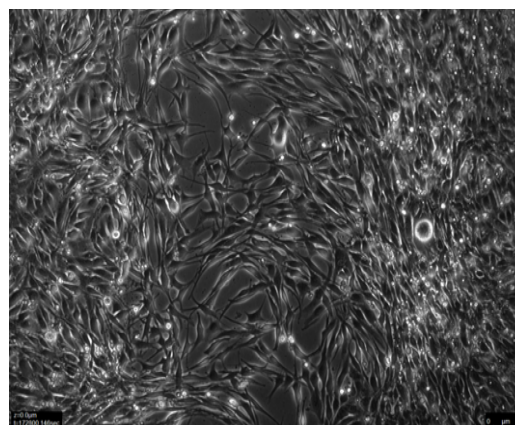
Figure 3.1. Images to show the difference between aged and control cells at 0 h, 24 h and 48 h.
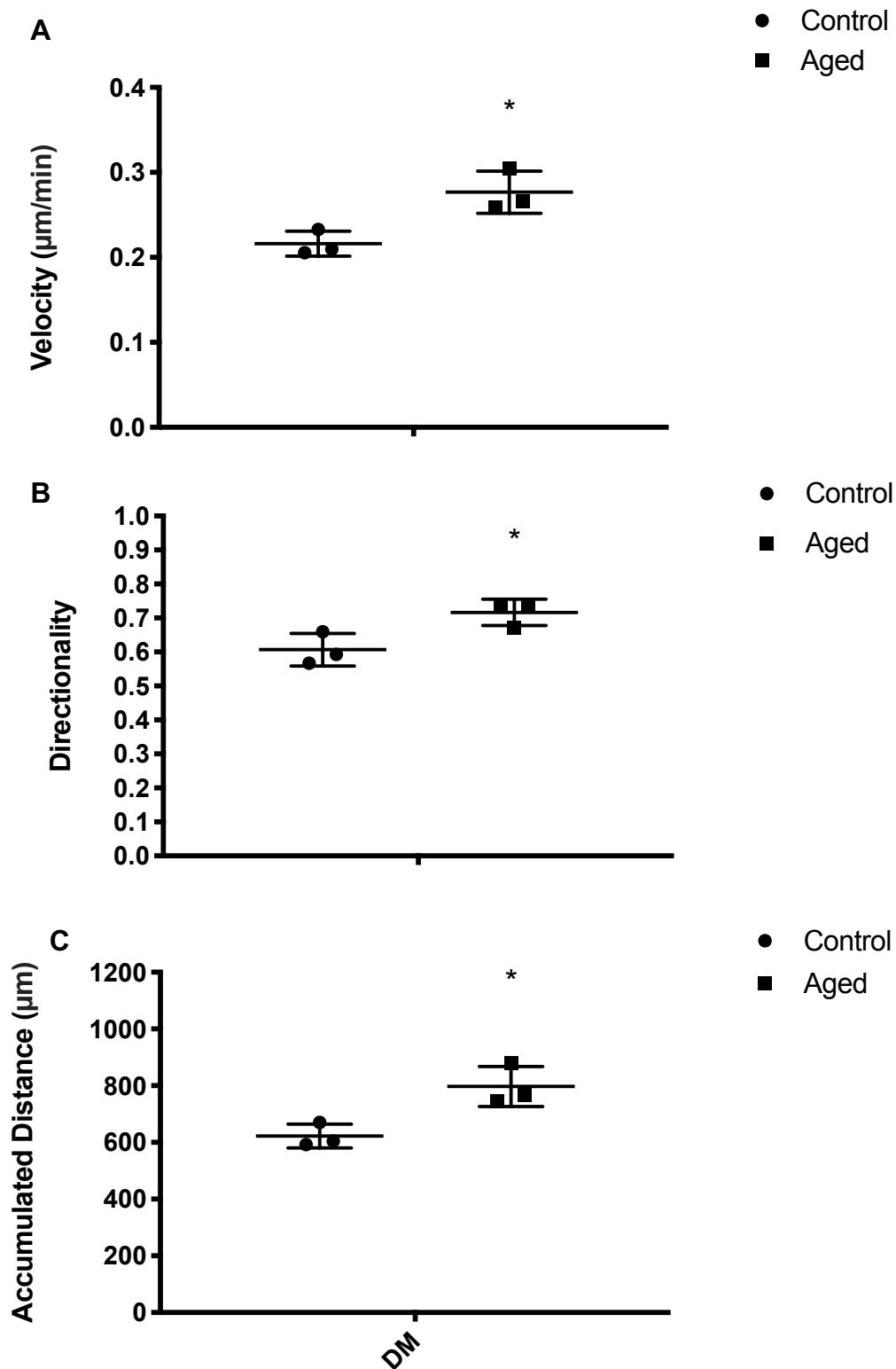
Figure 3.2. Cell velocity (A), directionality (B) and accumulated distance (C) between the aged and control over 48 h. The data is shown as mean with SD. Significance is set at P < 0.05, and the significance between aged vs. control was indicated using *. The experiment consisted of 3 repeats all in duplicate.
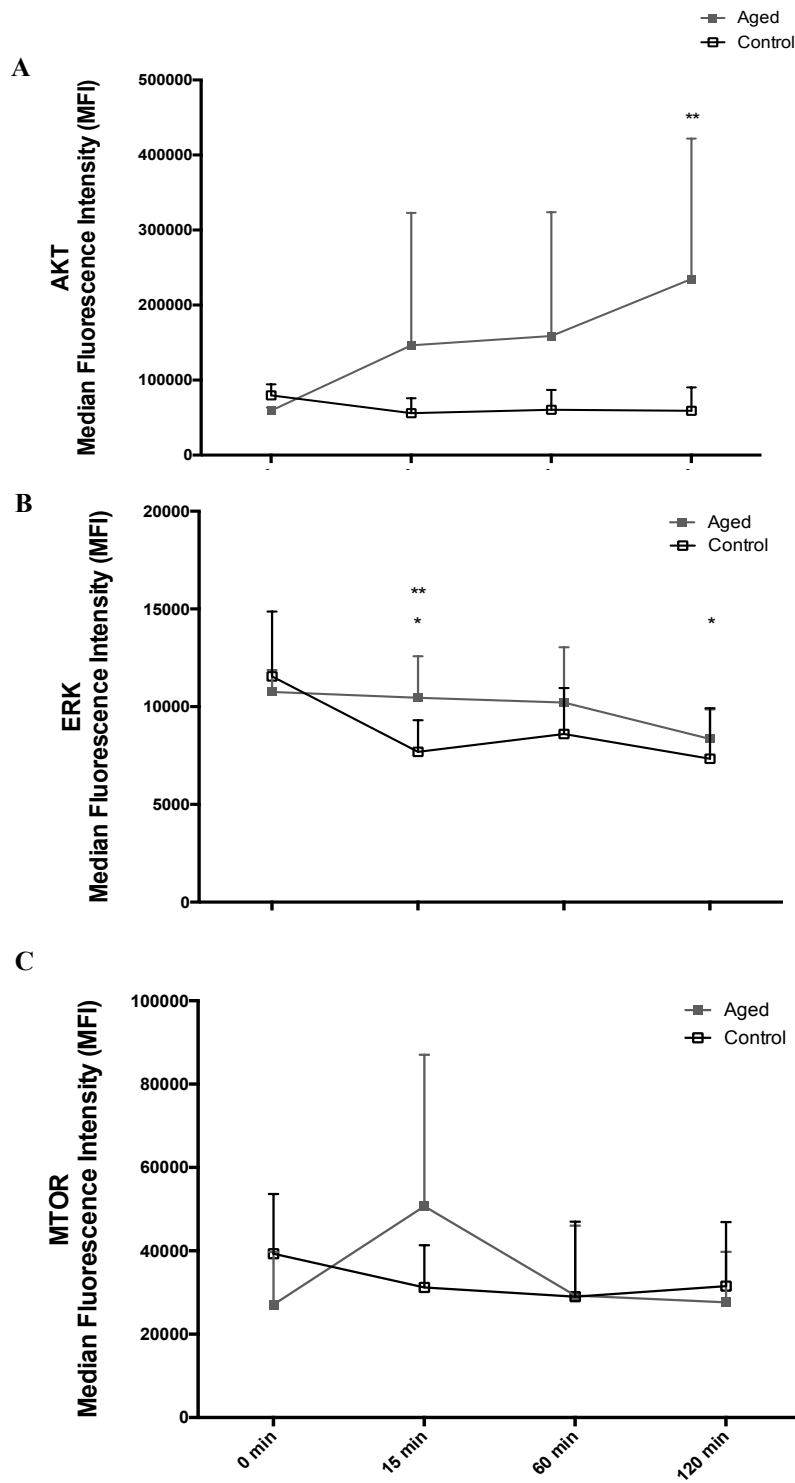
Figure 3.3. Line charts illustrating the differences in the phosphorylation of Akt (A), ERK (B) and mTOR (C) molecules between the aged and control over 120 minutes. The data is shown as mean with SD. Significance is set at P < 0.05. Significance was indicted vs. 0 minutes (*) and vs. corresponding time-point (**). The experiment consisted of 3 repeats all in duplicate.

Wishing to determine whether the altered signalling profiles evident between the cell models may impact on improved migration in the replicatively aged model, inhibitor studies were performed. Cell velocity was 2.8-fold (0.28 ± 0.07 μm/min vs. 0.10 ± 0.04 μm/min; P < 0.001), directionality, 1.5-fold (0.71 ± 0.12 vs. 0.49 ± 0.20; P < 0.001) and overall migration distance, 2.4-fold (802 ± 202 μm vs. 332 ± 123 μm; P < 0.001) greater in the absence vs. presence of the PI3K inhibitor, LY294002, respectively (Figure 3.4). Similarly, when replicatively aged cells were incubated with the ERK inhibitor (PD98059), cell velocity was 1.3-fold (0.28 ± 0.07 μm/min vs. 0.21 ± 0.08 μm/min; P < 0.05), directionality, 1.1-fold (0.71 ± 0.12 vs. 0.64 ± 0.17; P < 0.001) and accumulated distance 1.3-fold (802 ± 202 μm vs. 618 ± 219 μm; P < 0.001) higher under control vs. inhibitor conditions, respectively (Figure 3.4). Indeed, in the presence of PD98059, migration potential of the replicatively aged cells was reduced to that of control cells, the latter under control conditions. Finally, under aged control vs. mTOR inhibition (rapamycin administration), despite a small reduction in velocity vs. untreated aged control (Figure 3.4), significance was not attained (0.24 ± 0.07 μm/min vs. 0.28 ± 0.07 μm/min). Compared with untreated aged control cells in the presence of rapamycin, directionality was significantly reduced by 1.15-fold (0.71 ± 0.12 vs. 0.62 ± 0.17; P < 0.001), however, this was not sufficient to significantly reduce overall migration distance (802 ± 202 μm vs. 697 ± 213 μm).

Having determined central roles for PI3K/Akt and ERK in all parameters of replicatively aged cell migration and mTOR in directionality, equivalent studies were performed in the control cell model (Figure 3.4). Similar to the replicatively aged cells, compared with control, when incubated with PI3K/Akt inhibitor (LY294002), cell velocity was 1.6-fold (0.22 ± 0.07 μm/min vs. 0.14 ± 0.06 μm/min, P < 0.001), directionality, 1.6-fold (0.61 ± 0.17 vs. 0.38 ± 0.18, P < 0.001) and accumulated migration distance, 1.45-fold (622 ± 188 μm vs. 437 ± 174 μm; P < 0.001) higher under control vs. inhibitor conditions, respectively. By contrast, compared with control, in the presence of ERK inhibition via PD98059 administration, cell velocity (0.22 ± 0.07 μm/min vs. 0.21 ± 0.08 μm/min) directionality (0.61 ± 0.17 vs. 0.57 ± 0.15) and overall migration distance (622 ± 188 μm vs. 678 ± 217 μm; P < 0.05), were not altered (Figure 3.4). Therefore, while ERK inhibition reduced the migration potential of replicatively aged cells to control

capabilities; it was without impact on control cell migration. Finally, in complete contrast to the replicatively aged cell model, compared with control, when control cells were incubated with mTOR inhibitor, rapamycin, cell velocity was 1.4-fold (0.22 ± 0.07 μm/min vs. 0.31 ± 0.06 μm/min; $P < 0.001$) higher. Directionality, which was reduced in aged cells, was unaltered (0.61 ± 0.17 vs. 0.62 ± 0.16), however, in line with increased velocity in control cells with rapamycin, overall migration distance was significantly increased by 1.4-fold (622 ± 188 μm vs. 884 ± 180 μm; $P < 0.001$) vs. control. Indeed, the enhanced migration potential of control cells in the presence of rapamycin now was equivalent to that of aged cells (velocity and distance) under control conditions (Figure 3.4).

Under basal conditions, inhibition of PI3K using LY294002 resulted in a significant reduction in replicatively aged cell migration velocity vs. control cells (0.10 ± 0.04 μm/min vs. 0.14 ± 0.06 μm/min; $P < 0.001$; Figure 3.4A), significantly reduced control cell directionality vs. replicatively aged (0.38 ± 0.18 vs. 0.49 ± 0.20; $P < 0.001$; Figure 3.4B) and resulted in an overall reduction in migration distance of replicatively aged vs. unaged cells (332 ± 123 μm vs. 437 ± 174 μm; $P < 0.001$; Figure 3.4C). By contrast, when administration of ERK inhibitor, PD98059, there were no significant differences between control and replicatively aged cell velocity (0.21 ± 0.08 μm/min vs. 0.21 ± 0.08 μm/min; Figure 3.4A). However, despite cell directionality being reduced in control vs. replicatively aged cells basally (0.57 ± 0.15 vs. 0.64 ± 0.17; $P < 0.05$; Figure 3.4B), overall migration distance was significantly lower in aged vs. control cells with ERK inhibition (618 ± 219 μm vs. 678 ± 217 μm; $P < 0.05$; Figure 3.4C). Finally, the impact of rapamycin on cell velocity was greater in control vs. replicatively aged cells (0.31 ± 0.06 μm/min vs. 0.24 ± 0.07 μm/min; $P < 0.001$; Figure 3.4A) and despite no differences in cell directionality (Figure 3.4B), rapamycin resulted in a significantly increased migration distance in control vs. replicatively aged cells (884 ± 180 μm vs. 697 ± 213 μm; $P < 0.001$; Figure 3.4C).
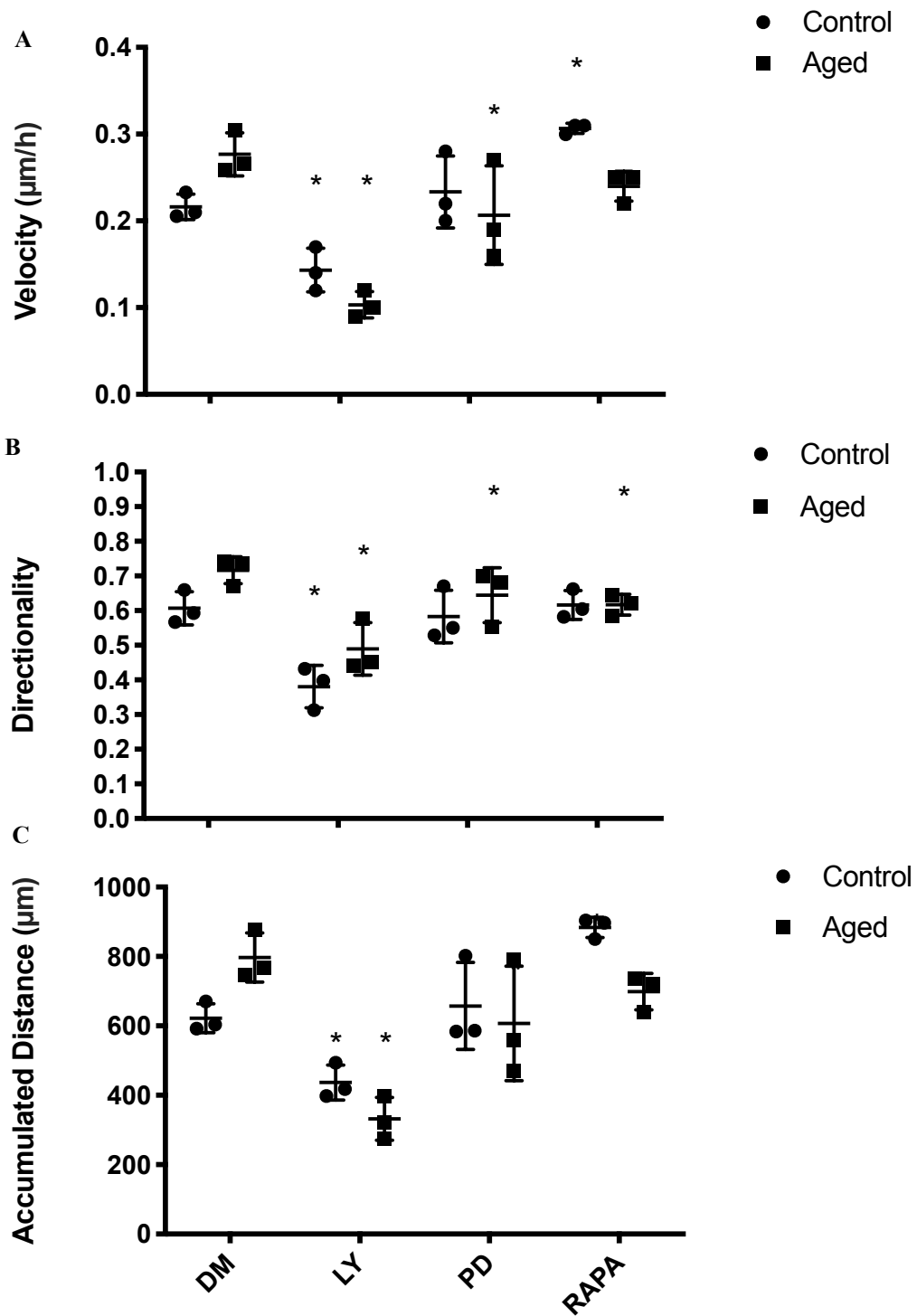
Figure 3.4. Cell velocity (A), directionality (B) and accumulated distance (C) in the aged and control vs. LY294002, PD98059 and rapamycin. The data is shown as mean with SD. Significance is set at P < 0.05, and the significance between the inhibitors vs. basal aged and control cells, was indicated using *. The experiment consisted of 3 repeats all in duplicate.

3.4.2 Effect of Leucine and HMB supplementation on Murine C_2C_{12} Skeletal Muscle Cells Migration

To determine whether aged cell migration could be enhanced dose response experiments indicated there was significant closure in the 5 ($P < 0.05$) and 10 mM ($P < 0.001$) dose in all experiments vs. control (Figure 3.5). Treatment with leucine (10 mM) and HMB (10 mM) were performed. When supplemented with leucine, there was a small but significant 1.07-fold increase in replicatively aged cell velocity (0.30 ± 0.07 µm/min vs. 0.28 ± 0.07 µm/min; $P < 0.001$) and a small but significant 0.97-fold decrease in directionality (0.67 ± 0.13 vs. control 0.71 ± 0.12; $P < 0.05$) vs. untreated control. Together, these changes were not sufficient to impact on overall migration distance, which was not different from untreated aged control (Figure 3.6). In the presence of HMB, there was a small but significant 1.15-fold increase in velocity (0.32 ± 0.07 vs. 0.28 ± 0.07 µm/min; $P < 0.001$), no impact on directionality and an overall 1.15-fold increase in migration distance vs. untreated aged control (921 ± 215 µm vs. 802 ± 202 µm; $P < 0.05$).

In contrast, to replicatively aged cells, it was hypothesised, that migration of control cells would be increased when supplemented with leucine or HMB. In the presence of leucine, cell velocity was significantly increased by 1.4-fold, (0.31 ± 0.09 µm/min; vs. 0.22 ± 0.07 µm/min; $P < 0.001$) vs. untreated control, directionality was unaltered and overall migration distance increased by 1.4-fold (883 ± 250 µm vs. 622 ± 188 µm; $P < 0.001$). Indeed, in the presence of leucine, the enhanced velocity (0.31 ± 0.09 µm/min) and overall migration distance (883 ± 250 µm) of control cells were now not significantly different from velocity (0.30 ± 0.07 µm/min) and migration distance (871 ± 202 µm) of replicatively aged cells with leucine (Figure 3.6). Similar to leucine, in control cells, HMB supplementation resulted in a 1.36-fold increase in velocity (0.30 ± 0.08 µm/min vs. 0.22 ± 0.07 µm/min; $P < 0.001$) vs. untreated control, no impact on directionality and a 1.41-fold increase in overall migration distance (878 ± 219 µm vs. 622 ± 188 µm; $P < 0.001$). Despite improved migration, in the presence of HMB, replicatively aged cells still displayed increased cell velocity (0.32 ± 0.07 µm/min vs. 0.30 ± 0.08 µm/min; $P < 0.05$), directionality (0.68 ± 0.14 vs. 0.62 ± 0.17; $P < 0.001$)

and overall migration distance (920± 215 µm vs. 878 ± 219 µm; P < 0.05) vs. control cells, respectively (Figure 3.6).
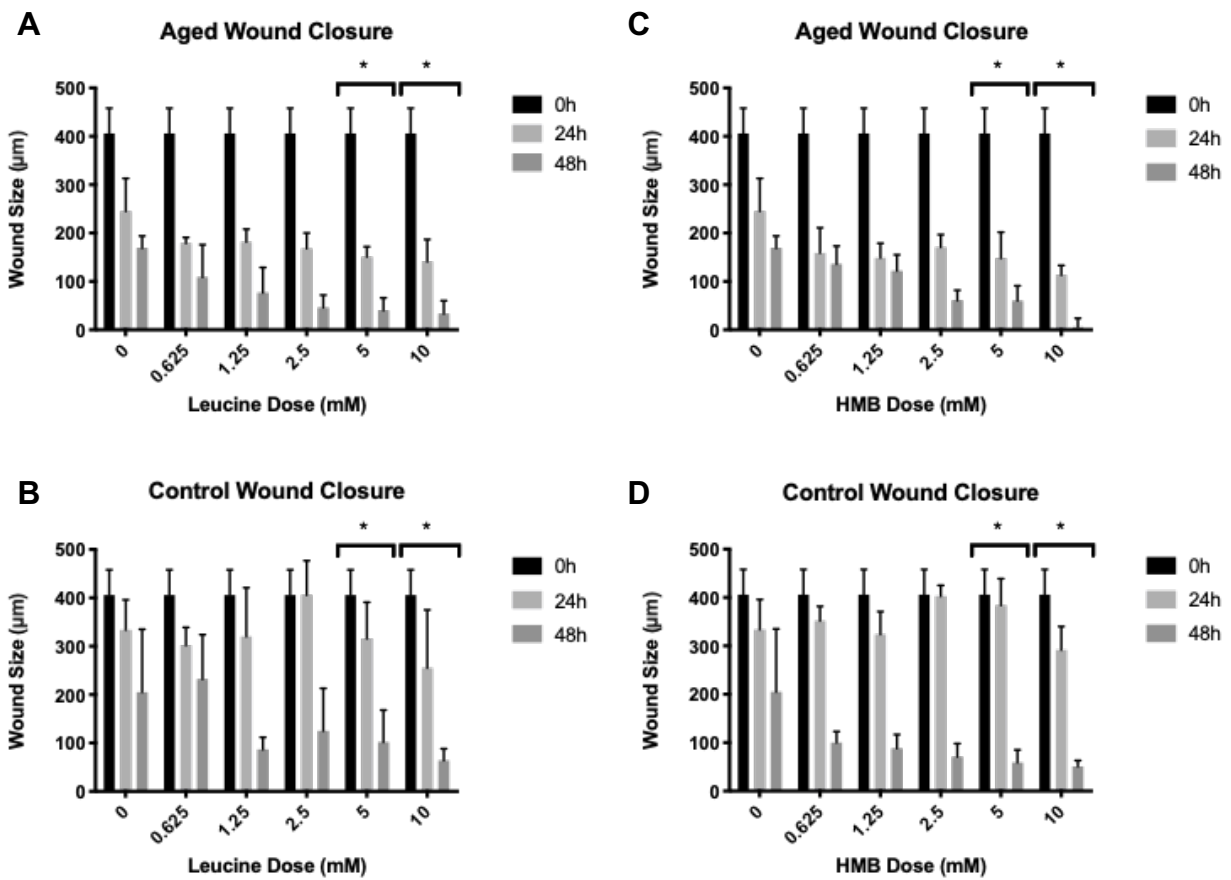
Figure 3.5. Bar charts illustrating differences between aged (A, C) and control (B,D) cells in the presence dose responses of leucine (A, B) and HMB (C,D) on wound size. Data is represented as means and SD, significance (⌐*⌐) is dose vs. control and set as (P < 0.05). The experiment consisted of 3 repeats all in duplicate.
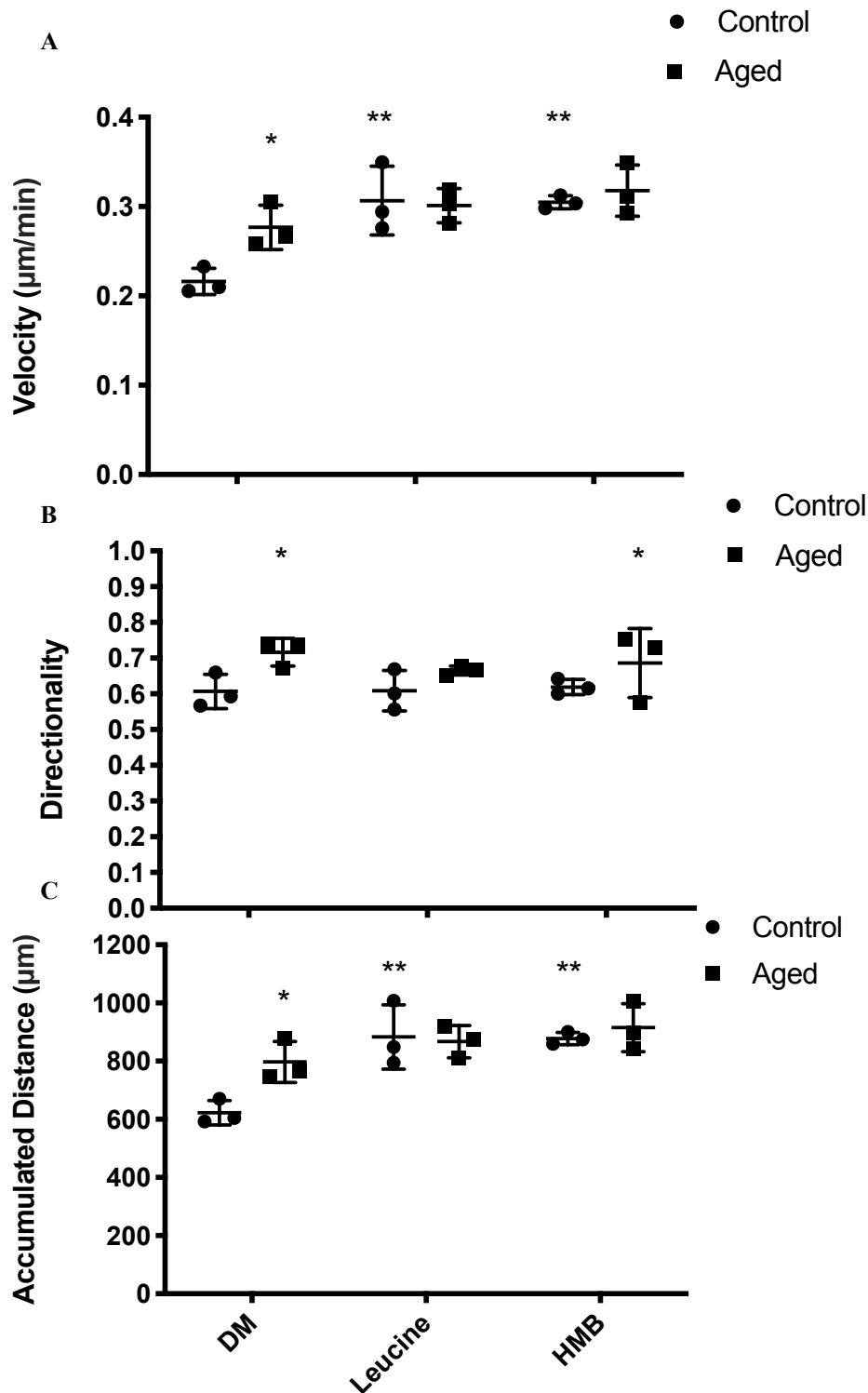
Figure 3.6. Cell velocity (A), directionality (B) and accumulated distance (C) in the aged and control vs. leucine and HMB. The data is shown as mean with SD. Significance is set at P < 0.05, and the significance between the supplements vs. basal aged and control cells, was indicated using *. The significance between the aged vs. control was indicated using **. The experiment consisted of 3 repeats all in duplicate.

3.4.3 Proposed Signalling Pathways that Regulate Cell Migration

Having identified the impact of leucine and HMB on cell migration, the next step was to investigate their impact on relevant signalling molecules. In line with the small impact that these supplements had on replicatively aged cell migration, there was little impact on Akt, ERK or mTOR activation vs. untreated aged control. Indeed, over a 2 h time course, despite small changes in signalling profiles, no significant differences were evident between untreated replicatively aged control vs. leucine or vs. HMB treatment (Figure 3.7).

Given the limited impact of leucine or HMB replicatively aged cell migration or on PI3K/Akt, ERK or mTOR activation vs. aged cell controls, the hypothesis to be challenged next was that these supplements would not rescue inhibited cell velocity, directionality, overall migration distance in the presence of LY294002, PD98059 or rapamycin (Figure 3.8, A-C), respectively. Indeed, replicatively aged cell velocity was significantly blocked by LY294002 in the absence (0.10 ± 0.04 µm/min; $P < 0.001$) or presence of leucine (0.12 ± 0.06 µm/min; $P < 0.001$) or HMB (0.12 ± 0.05 µm/min; $P < 0.001$) vs. untreated aged control (0.30 ± 0.07 µm/min). There was no significant difference between LY294002 alone vs. LY294002 with leucine or with HMB, indicating that there was no rescue of cell velocity by supplements in the presence of reduced PI3K/Akt activation (Figure 3.8A). Similar to these data, when treated with LY294002 directionality was significantly reduced in the absence (0.49 ± 0.20; $P < 0.001$) or presence of leucine (0.52 ± 0.19; $P < 0.001$) or HMB (0.54 ± 0.22; $P < 0.001$) vs. untreated aged control (0.71 ± 0.12; Figure 3.9A). Finally, overall migration distance in the presence of LY294002 was significantly reduced in the absence (332 ± 123 µm; $P < 0.001$) or presence of leucine (388 ± 157 µm; $P < 0.001$) or HMB (399 ± 167 µm; $P < 0.001$) vs. untreated replicatively aged control (802 ± 202 µm; Figure 3.10A). Interestingly and in contrast to our hypothesis, there was a small but significant increase in overall migration distance, compared with LY294002, when co-incubated with either supplement ($P < 0.05$).

As with PI3K/Akt inhibition, when replicatively aged cells were treated with PD98059, velocity was significantly decreased in the absence (0.21 ± 0.08 µm/min; P < 0.05) or presence of leucine (0.24 ± 0.06 µm/min) or HMB (0.23 ± 0.08 µm/min), vs. untreated aged control (0.28 ± 0.07 µm/min; Figure 3.8B). Similarly, directionality was significantly reduced in the absence (0.64 ± 0.17; P < 0.001) or presence of either leucine (0.67 ± 0.15; P < 0.001) or HMB (0.68 ± 0.15; P < 0.001) vs. untreated replicatively aged control (0.71 ± 0.12; Figure 3.9B). Overall migration distance was also significantly blunted when incubated with PD98059 (618 ± 219 µm; P < 0.001) vs. untreated replicatively aged control (802 ± 202 µm; Figure 3.10B). Interestingly there was a small but significant increase in overall migration distance, compared with PD98059 alone, when co-incubated with either supplement (P < 0.01).

Rapamycin conditions were not significantly different (0.24 ± 0.07 µm/min) in cell velocity (Figure 3.8C) vs. untreated replicatively aged control (0.28 ± 0.07 µm/min) and were not altered by co-incubation with leucine (0.26 ± 0.06 µm/min) or HMB (0.29 ± 0.07 µm/min). Furthermore, rapamycin in absence (0.62 ± 0.17; P < 0.001) or presence of leucine (0.64 ± 0.16; P < 0.001) or HMB (0.65 ± 0.14; P < 0.001) significantly reduced the cell directionality vs. untreated replicatively aged control (0.71 ± 0.12; Figure 3.9C). The overall migrated distance in the presence of rapamycin (697 ± 213 µm; Figure 3.10C) was not significantly different to untreated replicatively aged control (802 ± 202 µm), this was sustained in the presence of leucine (757 ± 159 µm) or HMB (849 ± 205 µm). Compared to rapamycin alone, the co-incubation of leucine did not significantly increase overall distance, whereas HMB was able to promote increases in overall distance (P < 0.001).

Together these data suggest that indeed the ability of leucine or HMB to rescue replicatively aged cell migration in the presence of inhibited PI3K/Akt or ERK signalling is compromised. Given the improved basal migration in control cells supplemented with leucine or HMB and the roles that PI3K/Akt and ERK appear to play in control cell migration, the next hypothesis to be tested was that these supplements may rescue inhibited cell migration in the presence of PI3K/Akt and ERK but not mTOR inhibition.

Control cell velocity was significantly reduced with LY294002 treatment, in the absence (0.14 ± 0.06 µm/min; P < 0.001) of supplements vs. untreated control (0.22 ± 0.07 µm/min). In the presence of leucine, but not HMB, cell velocity was increased vs. LY294002 (0.19 ± 0.06 µm/min; P < 0.001), which was not significantly different from control (Figure 3.8A). The directionality of control cells was significantly blocked when inhibited with LY294002 (0.38 ± 0.18; P < 0.001) vs. untreated control (0.61 ± 0.17; Figure 3.9A). Co-incubation with leucine or HMB, respectively, rescued directionality vs. LY294002 alone (0.51 ± 0.16; P < 0.001; 0.46 ± 0.21; P < 0.05). The co-incubation with HMB was rescued back to control, as there was no significant difference. Despite improvements in cell velocity and directionality, through co-incubation with supplements and the small increases in overall migration distance (Figure 3.10A), neither leucine (495 ± 205 µm) or HMB (476 ± 206 µm) were able to significantly increase overall migration distance vs. LY294002 alone (437 ± 174 µm).

Cell velocity did not change when inhibited with PD98059 (0.21 ± 0.08 µm/min) vs. control (0.22 ± 0.07 µm/min); it is not therefore surprising that co-incubation in the presence of either leucine (0.24 ± 0.06 µm/min; P < 0.05) or HMB (0.23 ± 0.08 µm/min; P = 0.032) resulted in improved cell velocity vs. control alone (Figure 3.8B). PD98059 in the absence or presence of supplements was without impact on directionality (Figure 3.9B), however when compared with control (622 ± 188 µm; Figure 3.10B), migration distance was improved with PD98059 (678 ± 217 µm; P < 0.05) in the absence or presence of leucine (756 ± 217 µm; P < 0.001) or HMB (742 ± 256 µm; P < 0.001).

In control cell following rapamycin treatment, there was an increase in cell velocity (0.31 ± 0.06 µm/min; P < 0.001) vs. control (0.22 ± 0.07 µm/min), which was further enhanced in the presence of leucine (0.34 ± 0.08 µm/min; P < 0.001) or HMB (0.35 ± 0.08 µm/min; P < 0.001) vs. untreated control (Figure 3.8C). Indeed, when compared with rapamycin alone, leucine (P < 0.05) or HMB (P < 0.001) co-incubation both also significantly increased cell velocity vs. rapamycin alone. Cell directionality was unaltered by rapamycin or by rapamycin plus either supplement (Figure 3.9C), however in the presence of rapamycin, the significant increase in migration distance (884 ± 180 µm; P < 0.001) vs. control (622 ± 188 µm; Figure 3.10C), was further enhanced in the presence of leucine (970 ± 232 µm; P < 0.001) or HMB (1010 ± 227

µm; P < 0.001). Indeed, these increases were significantly higher than rapamycin alone for both co-incubations with leucine (P < 0.05) or HMB (P < 0.001).

Given the unexpected potential of mTOR inhibition, via rapamycin, to improve not reduce cell migration, particularly in control cells and wishing to determine possible compensatory mechanisms, which may be involved in this adaptation, the cells were incubated with rapamycin and the phosphorylation of Akt, ERK and mTOR were analysed. In both replicatively aged and control cells, rapamycin led to a significant decrease in mTOR phosphorylation. Rapamycin treated replicatively aged cells had suppressed Akt phosphorylation vs. control, there was a significant decrease at 15 minutes (P < 0.05) vs. 0 minutes, but not at any other time points (Figure 3.11A). There was no difference between ERK (Figure 3.11B) and mTOR (Figure 3.11C) in replicatively aged cells until 60 minutes, where activity decreased in control, and increased with rapamycin. Similar to Akt, mTOR phosphorylation was greatly suppressed with rapamycin treatment vs. control over 120 minutes. In control cells, Akt phosphorylation was also significantly reduced with rapamycin treatment at 15, 60 and 120 minutes vs. 0 minutes (P < 0.05; P < 0.05; P < 0.05 respectively; Figure 3.11D). The activation of ERK was reduced and suppressed until 60 minutes (Figure 3.11E). At 120 minutes ERK activation spiked, which is contrary to the treatments. Rapamycin treated cells significantly reduced mTOR phosphorylation at 15 minutes (P < 0.05) and 60 minutes (P < 0.05) vs. 0 minutes (Figure 3.11F). At 120 minutes, the levels increase back to baseline and at 15 minutes, there was a significant difference between control vs. rapamycin treatment (P < 0.05).
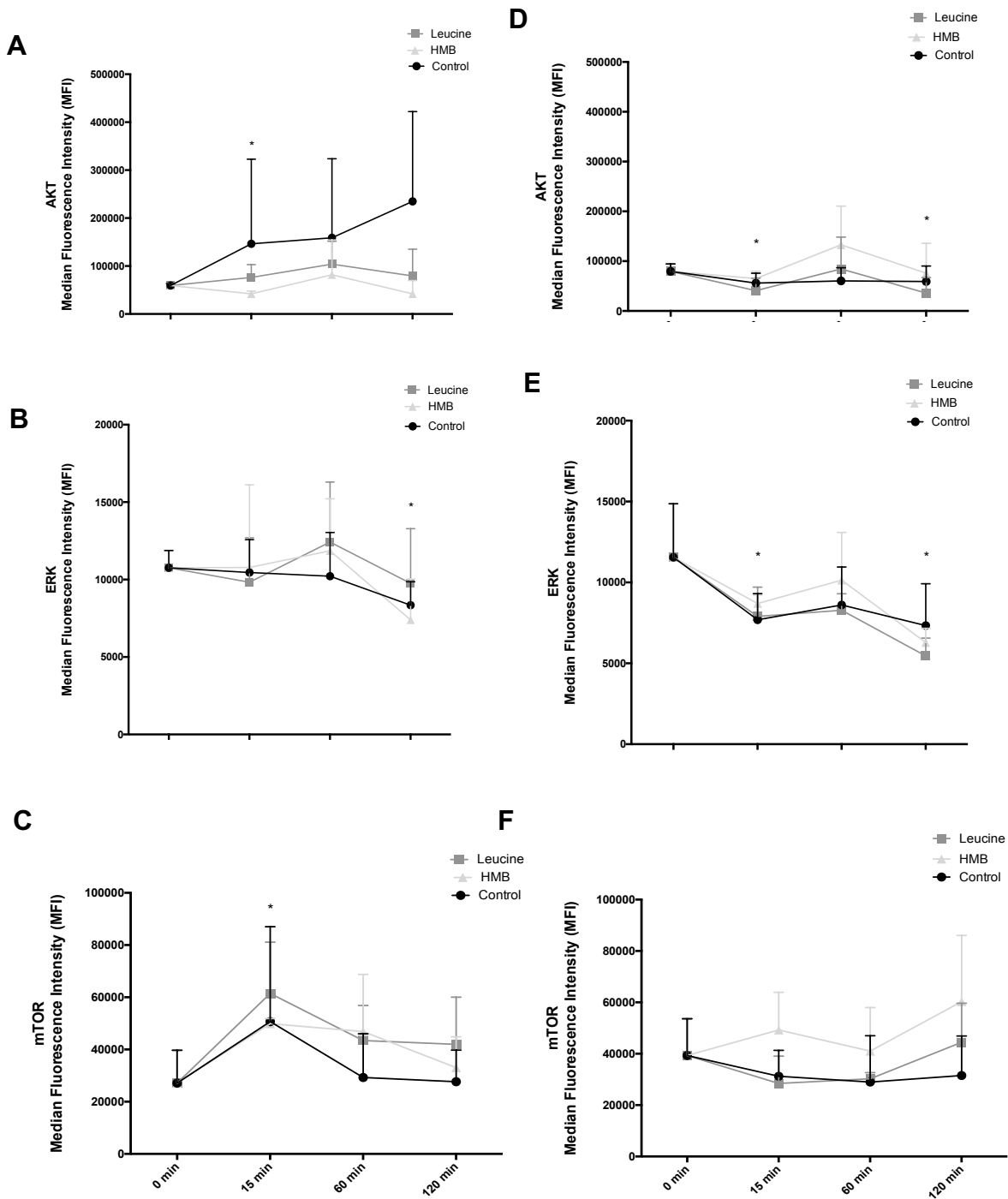
Figure 3.7. Line charts illustrating the differences in the phosphorylation of aged Akt (A), ERK (B) and mTOR (C) and control Akt (D), ERK (E) and mTOR (F) molecules, with cells treated with leucine and HMB over 120 minutes. The data is shown as mean with SD. Significance is set at P < 0.05 and was indicted vs. 0 minutes (*) time-point. The experiment consisted of 3 repeats all in duplicate.
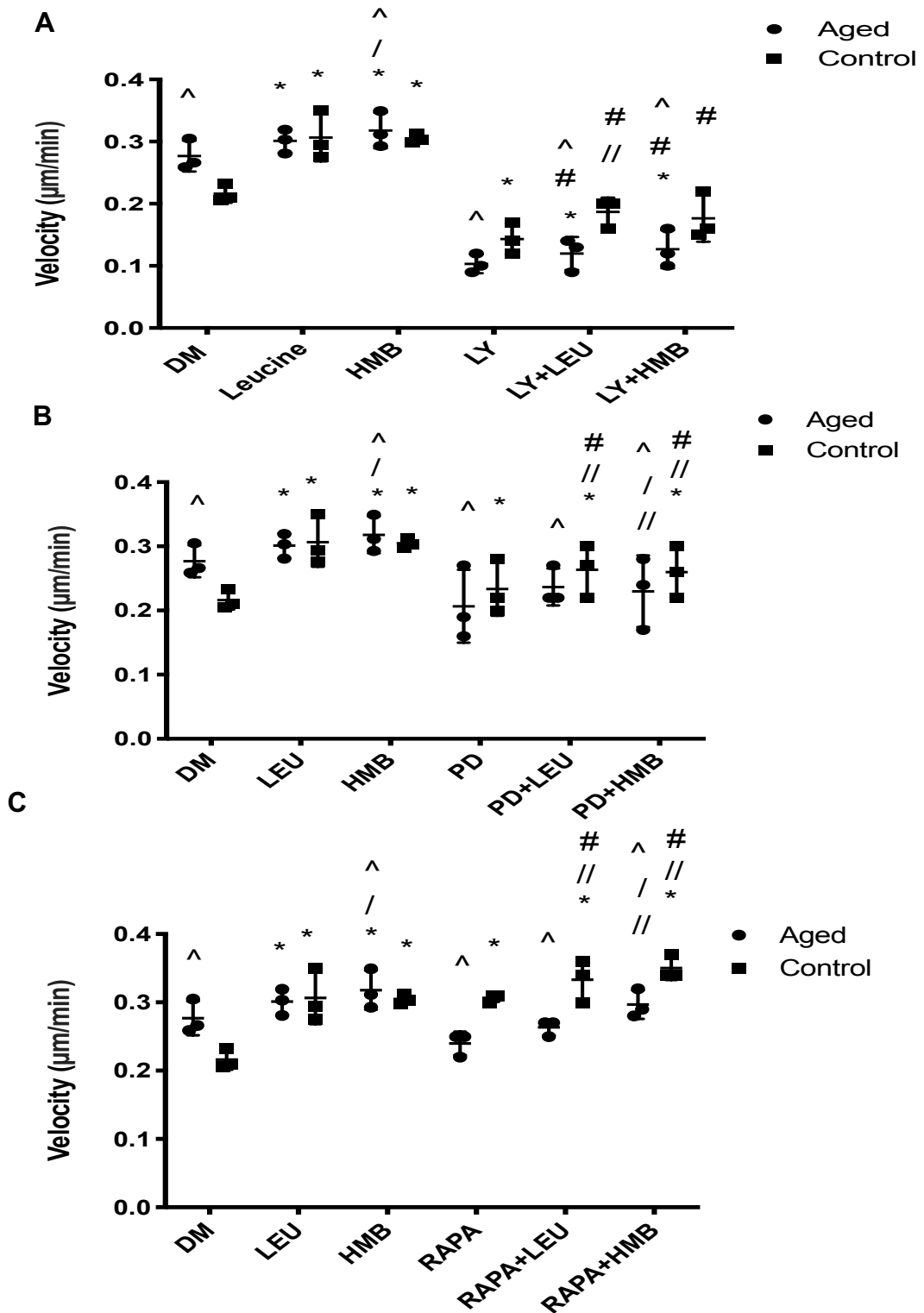
Figure 3.8. Cell velocity with the inhibition of LY294002 (A), PD98059 (B), and rapamyocin (C) in the presence or absence of leucine and HMB over 48 h. The data is shown as mean with SD. Significance is set at P < 0.05. Significance was shown as: aged vs. control (^), vs. control (*), vs. inhibitor (//)), leucine vs. HMB (/) and inhibitor with supplement vs. supplement alone (#). The experiment consisted of 3 repeats all in duplicate.
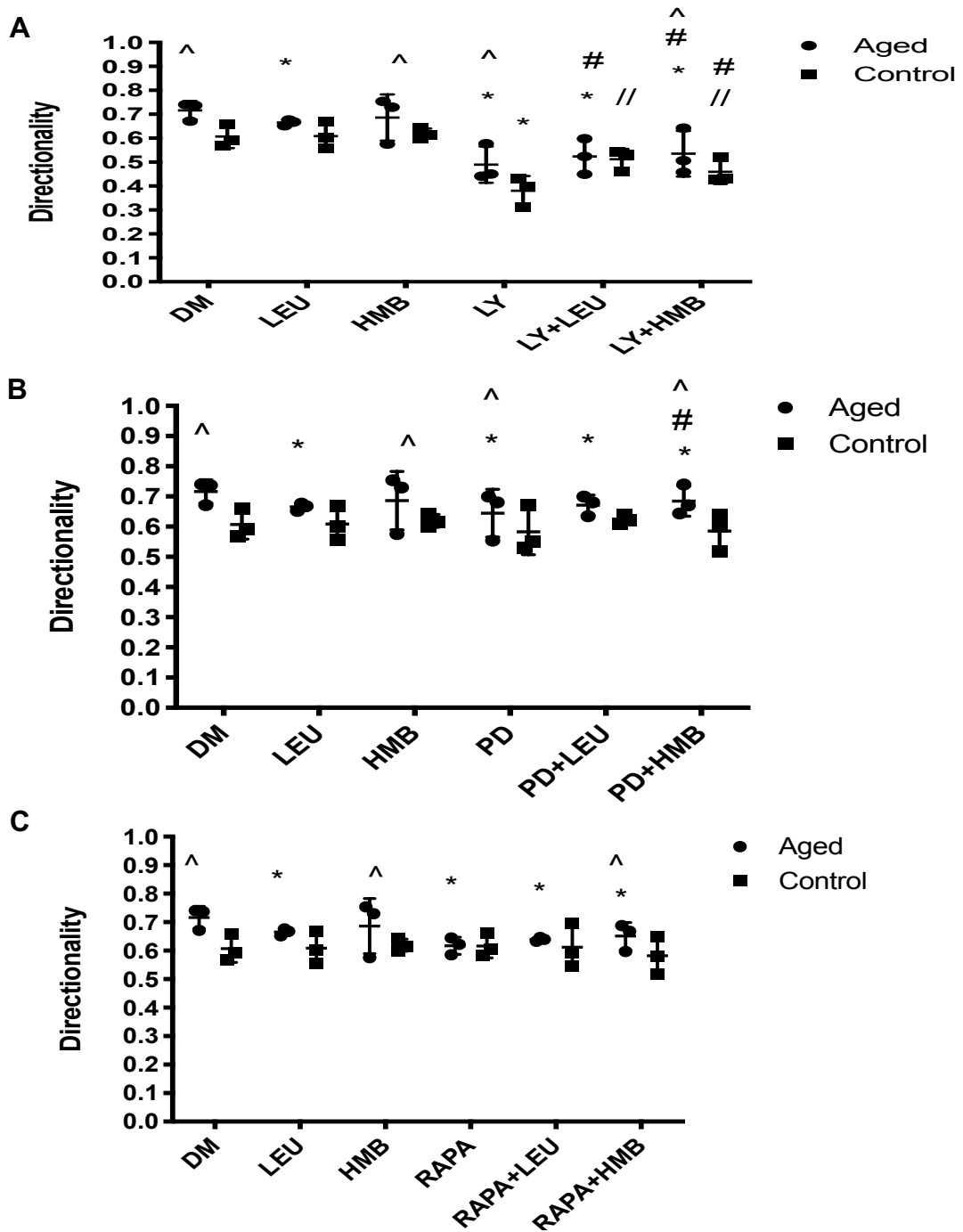
Figure 3.9. Cell directionality with the inhibition of LY294002 (A), PD98059 (B), and rapamyocin (C) in the presence or absence of leucine and HMB over 48 h. The data is shown as mean with SD. Significance is set at P < 0.05. Significance was shown as: aged vs. control (^), vs. control (*), vs. inhibitor (//)), leucine vs. HMB (/) and inhibitor with supplement vs. supplement alone (#). The experiment consisted of 3 repeats all in duplicate.
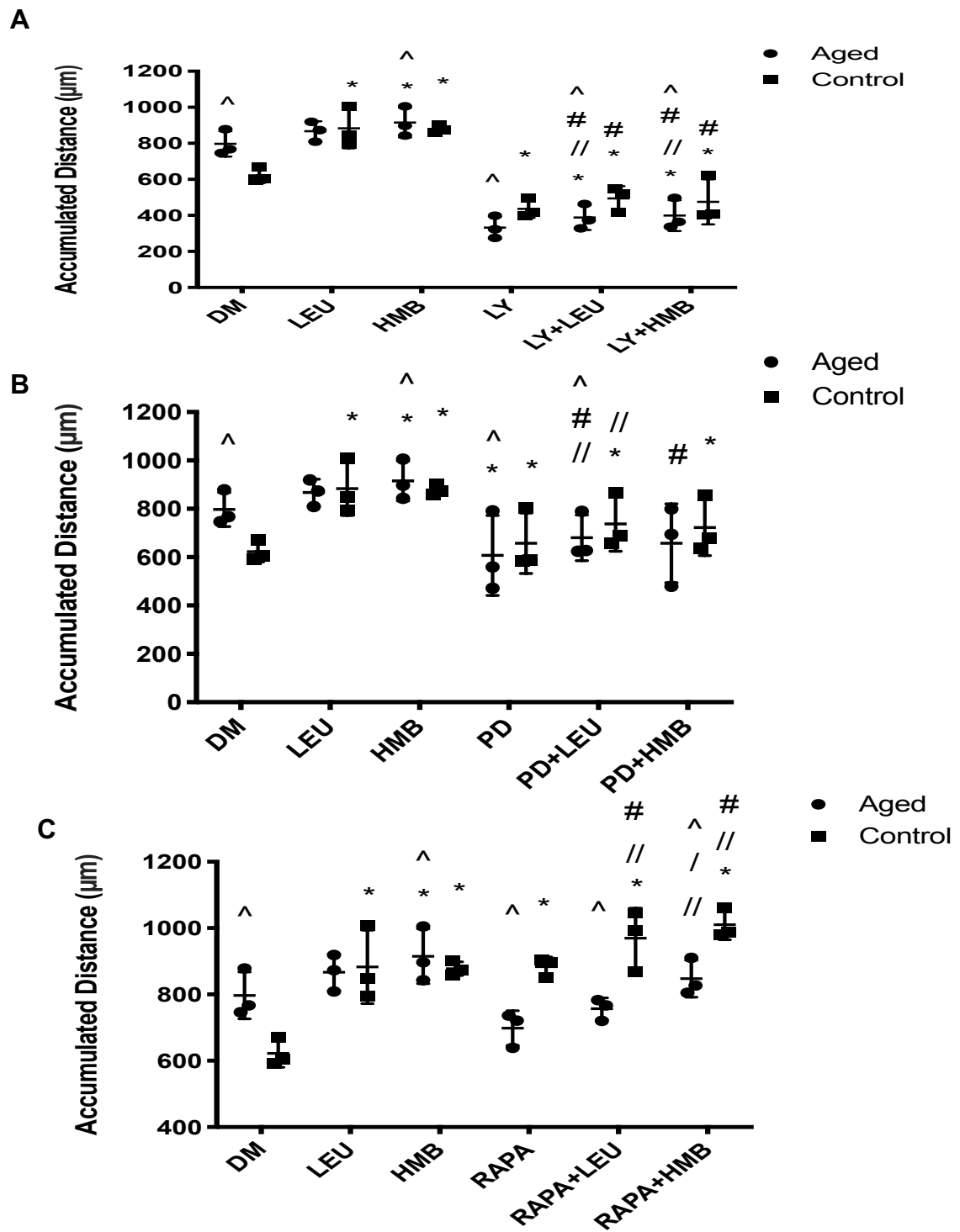
Figure 3.10. Cell accumulated distance with the inhibition of LY294002 (A), PD98059 (B), and rapamyocin (C) in the presence or absence of leucine and HMB over 48 h. The data is shown as mean with SD. Significance is set at P < 0.05. Significance was shown as: aged vs. control (^), vs. control (*), vs. inhibitor (//)), leucine vs. HMB (/) and inhibitor with supplement vs. supplement alone (#). The experiment consisted of 3 repeats all in duplicate.
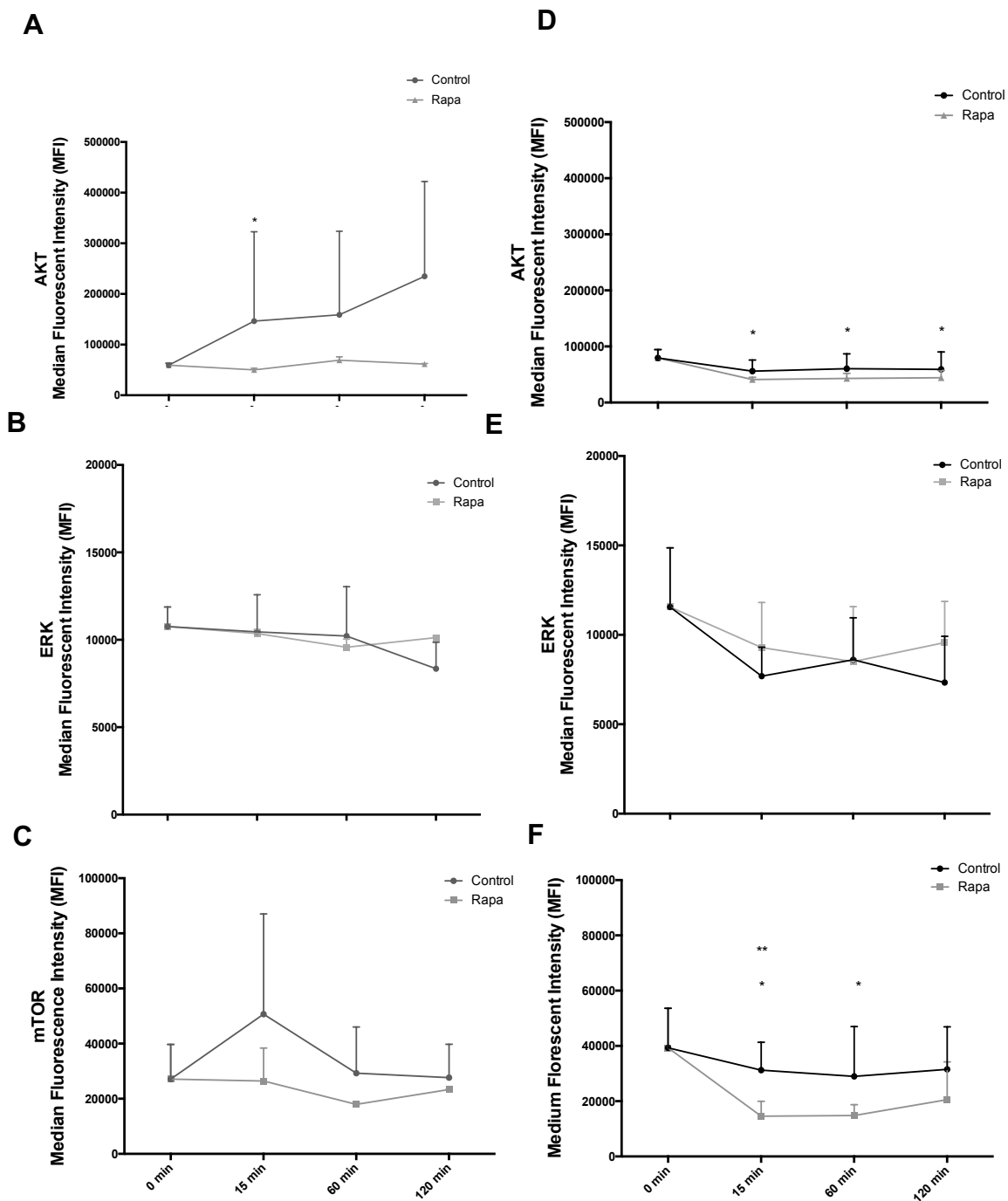
Figure 3.11. Line charts illustrating the differences in the phosphorylation of aged Akt (A), ERK (B) and mTOR (C) and control Akt (D), ERK (E) and mTOR (F) molecules, with cells treated with rapamycin over 120 minutes. The data is shown as mean with SD. Significance was indicted vs. 0 minutes (*) and vs. corresponding time-point (**). The experiment consisted of 3 repeats all in duplicate.

3.5 Discussion

The aim of this study was to determine the capacity of replicatively aged vs. non-replicated control cells to migrate, the signalling mechanisms underpinning this capacity and whether leucine and/or HMB could impact models of skeletal myoblast repair. We hypothesised that: 1) replicatively aged (P46-P48; "replicatively aged") myoblasts would be less efficient at damage repair versus control (P12-P16; "control"); 2) leucine and HMB would increase the migration potential in control but not aged cells and; 3) that the PI3K and ERK but not mTOR pathways would be required for effective basal migration in both models.

The main outcome of this investigation and in contrast to hypothesis 1., was that under basal conditions, the aged passaged cells closed the wound more quickly compared to their control counterparts. This was evident in the overall velocity, directionality and accumulated distance of the cells. However, in accordance with our hypothesis 2., the supplementation of leucine or HMB enhanced the migration potential of control cells compared to the aged cells. Interestingly, the enhanced migration of control cells, in the presence of supplements, resulted in overall migration distances equivalent to those obtained in replicatively aged cells in the absence of supplements, suggesting the control cells were "catching up" with aged cells, following supplementation. Finally, in accordance with hypothesis 3., Akt and ERK were important for basal migration in both models, but in contrast to predictions, mTOR inhibition, not activation, enabled facilitated wound repair in the absence or presence of supplements and most markedly in control vs. replicatively aged cell models.

To date, when studying the impact of age and nutrition on muscle adaptation, the majority of published research has focused on sarcopenia (Churchward-Venne *et al.*, 2014), the progressive loss of muscle mass and strength with age and on anabolic resistance in aged individuals (Burd *et al.*, 2013). However, it is also reported that the capability of the muscle to regenerate in the aged individuals is impaired, compared with control counterparts (Jang *et al.*, 2011). *In vitro*, mechanistic studies to underpin this latter observation are, however, currently sparse. Owens *et al.* (2015) investigated the impact of vitamin D on muscle regeneration in primary human muscle cells, and

reported average control migration rates equivalent to those in this model (666 ± 288 vs 622 ± 188 µm). Our data challenge our hypothesis of impaired migration with age, with aged cells migrating more efficiently than control ones, perhaps as a result of improved P13K/Akt and ERK signalling. Activation of these pathways have been reported to stimulate Rac and formation of lamellipodia and filapodia protrusions which cause the cell to move (Raftopoulou & Hall, 2004). The improved wound closure is not a result of cellular replication, with previous studies using mitomycin-C to block proliferation in unaged and aged myoblasts reporting migration capabilities which remain intact (Falcone *et al.*, 1984; Dimchev *et al.*, 2013). Replicatively aged C_2C_{12} myoblasts also retain telomeres (Yaffe and Saxel, 1977; Holt *et al.*, 1996; O'Connor *et al.*, 2009) and express decreased levels of IGF-I and Akt phosphorylation (Benbassat *et al.*, 1997; Léger *et al.*, 2008) similar to aged primary muscle stem cells. The absence of a response to leucine and HMB supplementation in replicatively aged cells may arise as a result of optimised migration under basal conditions this is supported via the observation that when control cells are supplemented with either leucine or HMB, migration is significantly improved, but only to levels seen in untreated replicatively aged cells.

To substantiate this theory, in both cell models, when the PI3K/Akt pathway was inhibited, the cell velocity, directionality and accumulated distance all decreased, suggesting that this pathway is integral to myoblast migration. It's basal enhancement in the replicatively aged vs. control cells may account for improved migration under control conditions. Neither leucine nor HMB were able to rescue reduced migration in the presence of LY294002, suggesting the fundamental role of this pathway in effective migration of myoblasts. Interestingly, while PD98059 reduced basal velocity and distance migrated in replicatively aged cells, it was without impact in control cells extending our observations to suggest that PI3K and ERK function together to facilitate increased migration in replicatively aged vs. control cells. Under inhibitor conditions and unlike PI3K inhibition, co-incubation with leucine or HMB incurred partial rescue to the replicatively aged cell velocity and migration distance. By contrast, while basal velocity and overall migration distance were not negatively impacted by PD98059 in control cells, the facilitated migration velocity and distance in the presence of leucine or HMB was significantly reduced, compared with either supplement alone. Therefore, while partial rescue can be incurred via supplementation in replicatively aged cells

when ERK is inhibited, the capacity of control cells to respond to supplements is reduced in the absence of ERK activation, despite no impact on basal cell migration potential. These data suggest both shared and divergent pathways underpinning aged vs. control myoblast migration.

Dai *et al.* (2015) recently researched the effects of leucine on rat satellite cell proliferation and differentiation. The authors reported that leucine promoted proliferation and differentiation through the mTOR-MyoD signalling pathway. Research reinforcing these results demonstrated that leucine starvation led to inhibition of myoblast differentiation (Averous *et al.*, 2012). Areta *et al.* (2014) also demonstrated the benefits on supplementing leucine on C_2C_{12} muscle cell growth. Research by Kornasio *et al.* (2009) is the only study, to the author's knowledge, to investigate the effects of HMB on aged myoblast activity. This study suggested that HMB stimulated myoblast proliferation, differentiation and survival compared to control, with both the PI3K/Akt and ERK/MAPK signalling pathways involved in these processes. Cell migration was not assessed. Further, studies by Kornasio *et al.* support the concept that HMB has beneficial effects on the proliferation and differentiation of myoblasts, through the MAPK/ERK and PI3K/Akt pathways (Kornasio *et al*., 2009; Vallejo *et al*., 2016). Although migration in the presence of supplements was not investigated in these reports, data from Dimchev *et al.* (2013) suggest that the ability of myoblasts to migrate depends on the PI3K/Akt and ERK/MAPK pathways (Dimchev *et al*., 2013).

The data from our study support the hypothesis that when inhibiting the PI3K/Akt pathway with LY294002, the cell velocity, directionality and accumulated distance is reduced. Previous studies have supported this finding (Suzuki *et al.*, 2002; Kawamura *et al.,* 2004; Sharples *et al.*, 2011; Dimchev *et al.,* 2013). Raftopoulou *et al.* (2004) suggested that the PI3K/Akt pathway is integral in the development of cellular protrusions. Moreover, Kawamura *et al.* (2004) demonstrated that the PI3K/Akt pathway is essential for cell migration through lamellipodial formation, which is important in cell directionality and velocity (Raftopoulou *et al.* (2004)). It is apparent therefore, that the PI3K/Akt pathway is integral for myoblast migration, irrespective of the replicative status of the myoblasts. This may not be the case for ERK activation, where ERK activity appears important for improved migration of the replicatively aged

cells, but not control, in this study. However, the data underpinning a role for ERK in myoblast migration are equivocal. For instance, Leloup *et al.* (2007) suggested that the ERK/MAPK pathway was responsible for stimulating growth factor mediated stimulation of myoblast migration. Conversely, Ranzato *et al.* (2009) suggested that it was primarily Akt and p38 MAPK signalling proteins that stimulated myoblast migration not the ERK pathway. Whereas, other research has also supported the notion that the ERK/MAPK pathway was involved in cell migration (Al-Shanti *et al.*, 2011; Dimichev *et al.*, 2013). The differences in studies could be attributed to the dose of inhibitor used as well as the myoblast models, alternatively, this apparent controversy warrants further investigation, as it may have important implications for cellular need, for example, fusion in the control vs. migration in the replicatively aged models.

Intriguingly, and not reported in the Kornasio study (Kornasio *et al.*, 2009), when rapamycin was added to the wound model detailed in this manuscript, it was with no impact on basal migration of aged cells, but significantly increased, not decreased, cell velocity and basal migration of control cells, which were both further increased with co-incubations of leucine or HMB. The mTOR pathway is largely regarded to be integral for MPS and is stimulated by both exercise and protein ingestion, and is further increased when both are combined (Hawley *et al.*, 2011). Further research proposes that leucine is the primary initiator of MPS (Churchward-Venne *et al.*, 2012). The mTOR target is downstream of the PI3K and Akt signalling cascades which then stimulate S6K which leads to MPS (Sharples *et al.*, 2015). The impact of this pathway on muscular hypertrophy and muscle wasting is well known (Sharples *et al.*, 2015), however, the impact on cell migration has not been studied. These observations would suggest that mTOR activation is detrimental to control cell migration, but integral to myoblast hypertrophy/fusion (Averous *et al.*, 2012; Areta *et al.*, 2014; Dai *et al.*, 2015), again raising the concept of differential drivers of cellular behaviour with age. Indeed, the data derived in this study suggest that the PI3K/Akt pathway is an integral pathway, shared in control and aged cell migration, that ERK further enhances replicatively aged cell migration, but that mTOR reduces control cell migration. These changing signalling pathways may underpin the adaptation that appears to have occurred as a result of replicative ageing.

3.6 Conclusion

Taken together, basally, the replicatively aged cells migrate more quickly than control myoblasts, potentially at the expense of efficient fusion. However, with the supplementation of leucine and HMB, the capacity of the control cells to migrate is increased to that of the replicatively aged cells. This implies that the control cells are more responsive to the supplements or that maximal migration capacity has been attained in replicatively aged cells under basal conditions and therefore supplements cannot improve their migration capability. In control myoblasts, it is the PI3K/Akt pathway that appears central for migration. However, our data show that the ERK/MAPK pathway is less important for control myoblast migration, where the results in the literature are still equivocal. Activation of both pathways are required for replicatively aged myoblast migration. The results are interesting, showing that this pathway, when activated, could reduce control myoblast migration, perhaps to ensure successful MPS and hypertrophy. Differential activation of the PI3K/Akt, ERK/MAPK and mTOR pathways appear to underpin the differences observed in control or supplemented control and replicatively aged myoblast migration. Although these findings provide a mechanistic insight on the C_2C_{12} cell line, further research is required to validate and translate these findings into responses in in young and older humans post damaging exercise.

Chapter 4: Influence of Replicatively Ageing and Nutrition on Myoblast Fusion

4.1 Abstract

Introduction: With ageing the ability to retain skeletal muscle mass and function declines (sarcopenia), with associated "anabolic resistance" being reported. However, the impact of anabolic nutraceuticals has not been studied locally in ageing models of skeletal muscle cells. The aim was therefore to implement models of cellular ageing in the absence or presence of leucine or HMB to improve myoblast fusion. The hypothesis to be challenged was that serially aged cells would show compromised fusion but that this would be rescued by amino acid supplementation, when compared with control.

Methods: Control and replicatively aged myoblasts were supplemented with 10 mM leucine or HMB. Myotube formation was assessed morphologically and biochemically (CK, LDH) intercellularly (Akt, mTOR, ERK, p38 signalling) and gene expression all at 0 h, 24 h and 96 h.

Results: Although control cells showed significant fusion with time and increased with leucine and HMB supplementation (all $P < 0.001$), replicatively aged myoblasts did not fuse in the absence or presence of supplementation and displayed significant reductions in CK ($P < 0.05$) and significant increases in LDH ($P < 0.05$) vs. control. Akt, mTOR and ERK signalling over 24 h were all significantly decreased (all $P < 0.05$). Significant suppression of myogenin, IGF-I, IGF-II (all $P < 0.05$) and relative increases in myostatin were observed in replicatively aged vs. control. However, replicatively aged cells treated with leucine significantly ($P < 0.05$) increased Akt signalling at 120 minutes compared to untreated controls. Also, HMB significantly increased (both $P < 0.05$) Akt and mTOR at 120 minutes compared to untreated control. These levels reduced to baseline at 24 h, whereas, increases were evident at 24 h. No significant difference was observed in AA transporters between replicatively aged and control.

Conclusion: Replicatively aged myoblasts failed to fuse basally and with supplementation. Basally, suppressed levels of Akt, mTOR, ERK, myogenin, IGF-I, IGF-II that were involved in muscle hypertrophy were observed in replicatively aged. Replicatively aged myoblasts signalling responded to supplements and AA transporter gene expression, with no impact on fusion.

4.2 Introduction

Skeletal muscle adapts significantly throughout the human lifespan, displaying features of growth (hypertrophy), loss (atrophy) and repair. In younger individuals, muscle hypertrophy occurs throughout childhood and is evident as a consequence of regular resistance exercise and appropriate nutrition (Churchward-Venne *et al*., 2012). In contrast, sarcopenia is defined as the loss of muscle mass and strength with age (Breen and Philipps, 2011). Furthermore, skeletal muscle reportedly displays 'anabolic resistance' in sarcopenic individuals (Breen and Philipps, 2011). Critically, the ability of the muscle to repair and regenerate following injury is initiated by the satellite cell (Hill *et al*., 2003). The majority of literature reports that number and function of the satellite cells is reduced with age (Welle, 2002; Shefer *et al*., 2006; Day *et al*., 2010; Bigot *et al*., 2015). Research to further enhance skeletal muscle adaptation, including improved hypertrophy and reduced sarcopenia are important for the following: developing/maintaining strength, performance, health, metabolism, injury reduction, improved functionality, and reducing other related atrophic diseases such as Duchenne muscular dystrophy (McGlory and Phillips, 2015).

The ability of satellite cells to fuse is regulated by signalling cascades that include two main molecules: Akt and mTOR. It is widely accepted that mTOR activation induces downstream targets p70S6K and 4E-BP1 (Bodine *et al*., 2001). Activation of this pathway eventually increases muscle replication, MPS and muscle growth. Downstream of these signalling pathways, multiple genes are expressed which are implicated in myoblast fusion and growth, including: myogenin, myostatin, IGF-I/IGF-II, DNA-binding protein inhibitor (ID3), actin-histidine N-methyltransferase (SETD3), phosphatidylinositol 3-kinase catalytic subunit type 3 (PIK3C3), FOXO3 and E3 ubiquitin-protein ligase (URB5) (Hameed *et al.*, 2004; Al-Shanti and Stewart, 2008; Seaborne *et al.*, 2018, 2019). In addition, genes important for cell-cell contact, (cadherin) CDH1 and matrix remodelling (disintegrin and metalloproteinase domain-containing protein 10 (ADAM10)) (Seals and Courtneidge, 2003; Maretzky *et al.*, 2005) are also key to myoblast migration, fusion and hypertrophy.

Nutraceuticals, including protein supplements, are commonly consumed to enhance cell growth. Evidence suggests that leucine increases hypertrophy of murine C_2C_{12} myoblasts (Talvas *et al.*, 2006; Averous *et al.*, 2012; Areta *et al.*, 2014) and of primary pre-term rat satellite cells (Dai *et al.*, 2015). Studies supplementing these cells with leucine, concluded that inducing p70S6K and 4E-BP1 phosphorylation was the primary regulatory mechanism of muscle growth (Areta *et al.*, 2014; Dai *et al.*, 2015). Furthermore, increases were observed in myogenic gene expression, such as myogenin and MyoD after 2 mM of leucine supplementation in differentiating primary myoblasts from limb preterm rat muscle (Dai *et al.*, 2015). *In vivo,* Farup *et al.* (2014) took biopsies from young males that were supplemented with whey protein containing 23 g/d of BCAAs over 168 h. The authors demonstrated increased satellite cell numbers following 150 unilateral eccentric contractions (Farup *et al.*, 2014), compared with placebo control. Evidentially, supplementation with leucine stimulates muscle growth, via increased satellite cell responses. The expression of the leucine transporter, solute carrier family 7 member 5 (SLC7A5) and its heterodimer complex protein, solute carrier family 3 member 2 (SLC3A2) activate mTOR signalling (Dickinson and Rasmussen, 2013), which is involved in muscle hypertrophy (Churchward-Venne *et al.*, 2012).

HMB, a metabolite of leucine, is ingested to aid muscle recovery (Wilson *et al.*, 2009). Similar to leucine, published evidence suggests that HMB supplementation increases satellite cell proliferation, differentiation and survival in humans and promotes cell proliferation, viability and prevents reductions in muscle force in rodents following muscle dissection and electric stimulation (Kornasio *et al.*, 2009; Alway *et al.*, 2013; Vallejo *et al.*, 2016). Extensive evidence exists in both human and rodent cell models that the activation of the PI3K/Akt and p38 MAPK and ERK, pathways are important not only myoblast proliferation, but also migration and fusion (Brown *et al.*, 2017: Foulstone *et al.*, 2003: Al-shanti *et al.*, 2008). These pathways have also been reported to be involved following supplementation with 85 mM of HMB in differentiating primary myoblast from one 5-year-old infant (Kornasio *et al.*, 2009). Further, Vallejo *et al.* (2016) also demonstrated that C_2C_{12} myoblast proliferation and viability were increased with 25-125 µM HMB. Therefore, evidence indicates that HMB also aids muscle recovery and regeneration.

However, these studies focussed on the effect of leucine and HMB in young rodents, or myoblasts isolated from young cohorts. In aged models, there is limited evidence focusing on the impact of leucine or HMB supplementation on muscle adaptation, *in vivo* or *in vitro*. Recently, findings from our group demonstrated that replicatively aged myoblasts had increased basal migration compared to control cells (Brown *et al*., 2017). Leucine and HMB supplementation (10 mM) increased migration distance in both replicatively aged and non-passaged control myoblasts, but with a greater impact in control cells (Brown *et al*., 2017). In aged rats, leucine (1.35 g/d) and HMB (3.4 g/kg/d) supplementation improved satellite cell proliferation and muscle regeneration (Alway *et al.*, 2013; Pereira *et al.*, 2014). Twenty to twenty-four-month-old rats were supplemented with 1.35 g/kg/d leucine for 3-day before cyro-lesion of the soleus and for 10-day post damage (Pereira *et al.*, 2014). The authors observed increased satellite cell proliferation and increased levels of ubiquinated proteins in the old rats compared to 2-month rats (Pereira *et al.*, 2014). In addition, 34-month-old rats, which were treated with 340 mg/kg of HMB for 7-day prior, during 14-day immobilisation and during a 14-day recovery (Alway *et al.*, 2013), displayed increased satellite cell proliferation following Akt activation compared to control. Evidence is sparse, but early indications suggest that leucine and HMB benefit both young and aged muscle regeneration, calling into question the notion of anabolic resistance as a general phenotype.

To assess aged and young myoblast growth, we developed a model with an application to ageing muscle cell behaviour (Sharples *et al*., 2011). As recently described (Brown *et al*., 2017), C_2C_{12} murine skeletal muscle cells were subjected to 58 population doublings and displayed reduced differentiation capacity (Sharples *et al*., 2011, 2012; Deane *et al*., 2013). Therefore, using this replicatively aged model, the question that remains to be challenged is whether leucine and HMB can impact skeletal muscle cell adaptation, with a specific focus on fusion, where data are sparse. Such studies would begin to provide evidence relating to the specificity, if any, of anabolic resistance with age.

The overarching aim of this programme of work was to utilise nutritional supplements to improve cell growth and fusion in control and replicatively aged murine myoblasts. The central objective was to examine the impact of protein supplements on hypertrophy in control and replicatively aged cell models. The underpinning objectives were: 1. To establish whether replicatively aged and control C_2C_{12} murine myoblasts fuse under control conditions. 2. To determine the impact of leucine and HMB on myoblast fusion and 3. To investigate the underlying mechanisms involved in myoblast fusion. We hypothesised that: 1. Control myoblasts would fuse under basal conditions, whereas replicatively aged myoblasts would not. 2. Leucine and HMB would further increase control hypertrophy and stimulate the initiation of fusion in replicatively aged C_2C_{12} cells; 3. That mTOR, Akt and ERK phosphorylation would be increased in control myoblasts stimulated with leucine and HMB supplementation compared to replicatively aged myoblasts and 4. That there would be reduced gene expression in IGF-I/II, myogenin, SLC7A5 and SLC3A2 which would underpin compromised fusion.

4.3 Methods

4.3.1 Cell Culture

All standardised cell culture procedures were previously described in **section 2.2.1.** Briefly, cells were seeded in 6 well plates and grown to 80 % confluency.

4.3.2 Cell Differentiation and Dosing Strategy

Once cells attained 80 % confluency, cells were washed twice in PBS and dosed in DM which was used as a control. Leucine and HMB dose response studies (0-10 mM) were performed. The higher dose of 10 mM leucine and HMB were used. Cells were dosed at 0 h only and cultured for 96 h to enable alignment and fusion to form myotubes (Figure 4.1). All experiments were repeated 3 times in duplicate.
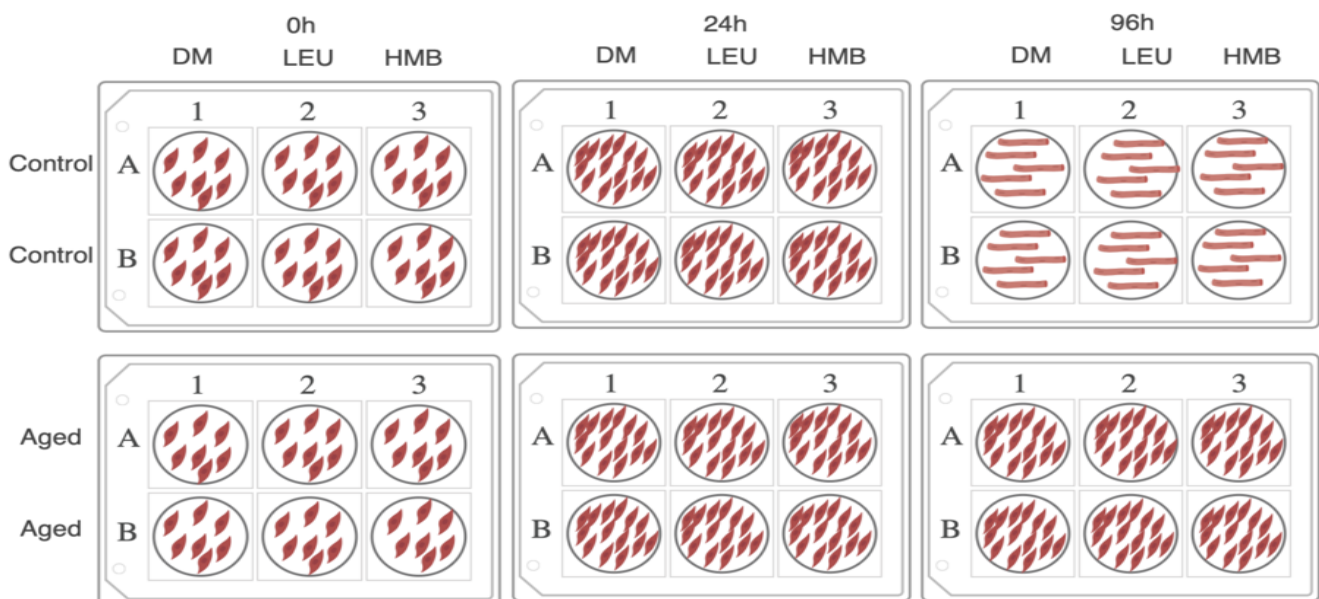
Figure 4.1. Schematic that represents that cell culture experimental design.

Control and replicatively aged myoblasts were differentiated over 96 h. The cells were dosed with 10 mM of leucine and HMB. Lack of cell fusion at 96 h was based on Sharples *et al*. (2011) observations. All experiments were repeated 3 times in duplicate.

4.3.3 Cell Fixation and Morphological Analysis

At 96 h, the cells were fixed for morphological analyses (**see section 2.4.1**). Briefly, cells were washed and fixed in 70 % ethanol and stored at 4 °C. Three microscopic images were randomly acquired per well at 10x and 20x magnification using a Leica DMB 6000 microscope (microscope (Leica Biosystems GmbH, Nussloch, Germany). In total, 18 microscopic images per magnification per treatment were captured. For morphology analyses, 10x magnification microscopic images were exported in TIF format and analysed using Image J software (IBIDI, Munich, Germany). For analysis pixels were converted using the 'set scale' function in image J software. Myotubes were defined as containing 3 or more myonuclei per myotube. All myotubes within each field of view were assessed for four myotube characteristics: 1) myonuclear number 2) length 3) diameter and 4) area.

4.3.4 Creatine Kinase Activity

At 0 h, 48 h and 96 h, CK activity was analysed as a marker of muscle cell differentiation/fusion (as described previously (Foulstone *et al*., 2003; Al-Shanti *et al*., 2008; Sharples *et al*., 2013)). Replicatively aged and control C_2C_{12} myoblasts were washed with PBS, prior to lysing in TMT, for further details **see section 2.6.5**. Briefly, 10 µl TMT cell lysate were analysed in duplicate using 96-well UV plates. Two hundred µl CK reaction reagent was added to the samples using a multichannel pipette. The change in absorbance was monitored continuously over 20 minutes using ELISA plate reader (Biotek, USA) at a wavelength of 340 nm.

4.3.5 Cytotoxicity Assay-Lactate Dehydrogenase

At time points 0 h, 24 h, 48 h, 96 h, 150 µl supernatant was harvested from each well. Then, 50 µl of sample was utilised for the LDH assay (**see section 2.6.8**), according to manufacturer instructions (Roche, Germany). Briefly, samples were incubated with 50 µl reaction mix prior to incubation in the dark at RT for 30 minutes. The samples were analysed using spectrophotometry at 492 nM absorbance and using an ELISA plate reader (Biotek, USA).

4.3.6 Cell Fixation and Preparation for Flow Cytometry

Flow cytometry was performed to simultaneously assess multiple phosphoproteins (**see section 2.5.3 and 2.7.2**). Briefly, prior to dosing, but following transfer to DM, all the cells were left to quiesce for 30 minutes. This timepoint was designated as time 0 minutes. The cells were then treated experimentally as above, with timepoints for harvest at: 0 minutes, 15 minutes, 60 minutes, 120 minutes and 24 h. The cells were extracted, fixed and the antibodies bodies were added. The same antibodies used in the **section 4.2.4** with the addition of the anti-human/mouse phosphor-P38 MAPK (T180/Y182; PE; 585/40 nm; 0.06 µg). The cells were washed a further three times and the samples were analysed using flow cytometry.

4.3.7 RNA Extraction, Isolation and RT-PCR

Total RNA was extracted at 0 h, 24 h and 96 h by lysing in 250 µl TRIzol reagent. For detailed RNA isolation procedure, refer to **section 2.8.2**. Briefly, chloroform was added to separate RNA from DNA and protein. Isopropanol was the added to precipitate the RNA from chloroform. The supernatant was removed, and ethanol was added to the pellet, which was left air dry. Between each stage centrifugation steps were taken. Then, the samples were assessed using Nanodrop spectrophotometer 3000 at 230 nm, 260 nm and 280 nm (pooled 260/280: 2.00 ± 0.10 nm: CV 4.95 %). Samples were diluted 10-fold in RNA storage solution. In total, 70 ng RNA was used per reaction, in a total reaction volume of 20 µl per sample, which contained 11.2 µl master mix (10 µl Quanitfast SybrGreen, 1 µl primer, 0.2 µl RT) and 8.8 µl RNA sample. Samples were analysed on rotor-gene Q PCR machine using a one-step protocol (see **section 2.8.2**). For C_T values, a threshold was set at 0.1 for all genes. The amplification efficiencies were also analysed, with values 80-100 % proposed as efficient. To relativise C_T values to 0 h control and reference gene (RP2β) the delta delta C_T equation was used (Livak & Schmittgen, 2001). For between variables (age), the replicatively aged expression was also relativized to control cells at 0 h. This is displayed as 'age-control' on figures. Finally, the details of genes analysed, basal C_T values and differences between aged and control basal values are displayed in Table 4.1.

Table 4.1 Gene name, basal Ct values and significance between groups.

Gene	Basal Aged C_T Values	Basal Control C_T Values	Significance (basal C_T) (P < 0.05)
RP2β (Polr2b)	23.47 ± 1.29	23.56 ± 1.38	NS
Myogenin	32.19 ± 1.43	21.82 ± 0.73	P < 0.001
Myostatin	30.18 ± 2.04	32.36 ± 3.04	NS
IGF-I	31.93 ± 0.82	28.10 ± 0.57	P < 0.001
IGF-II	32.10 ± 1.54	26.71 ± 1.08	P < 0.001
ID3	25.38 ± 0.71	24.42 ± 1.38	NS
SETD3	28.95 ± 1.44	28.65 ± 1.57	NS
PIK3C3	23.95 ± 1.36	22.54 ± 0.74	NS
FOXO3	24.83 ± 0.95	24.52 ± 1.23	NS
URB5	18.01 ± 0.61	17.86 ± 0.76	NS
ADAM10	21.72 ± 0.58	22.24 ± 0.73	NS
CDH1	27.54 ± 1.02	28.53 ± 1.43	NS
SLC7A5	18.46 ± 0.94	18.39 ± 0.83	NS
SLC3A2	23.17 ± 1.57	24.00 ± 0.83	NS

4.3.8 Statistical Analyses

For the comparison of replicative aging (control vs. replicatively aged) vs. supplements (DM, leucine and HMB) a two by three-way ANOVA with Bonferroni post-hoc pairwise comparision. Comparisons between control vs. replicatively aged cells over time without treatment a repeated two-way between ANOVA was employed. In control and replicatively aged only with leucine and HMB supplementation over time, two-way within ANOVA was used. A repeated two-way ANOVA was implemented in control, replicatively aged in the absence and presence of leucine and HMB over time. Where relevant, comparing individual groups at one time point, independent T-tests were implemented. All data are presented as mean ± SD and significance as ≤ 0.05.

4.4 Results

4.4.1 Impaired Fusion in Replicatively Aged vs. Control Myoblasts

To confirm whether replicatively aged and control myoblasts fused under basal conditions, microscopic images were captured at 0 h, 24 h and 96 h. Observations from these images supported our hypothesis that replicatively aged myoblasts would not fuse vs. control myoblasts (Figure 4.2). These data substantiate previously published observations relating to fusion capacity of the cells (Sharples *et al.*, 2011).

Replicatively aged at 96h

Control at 96h
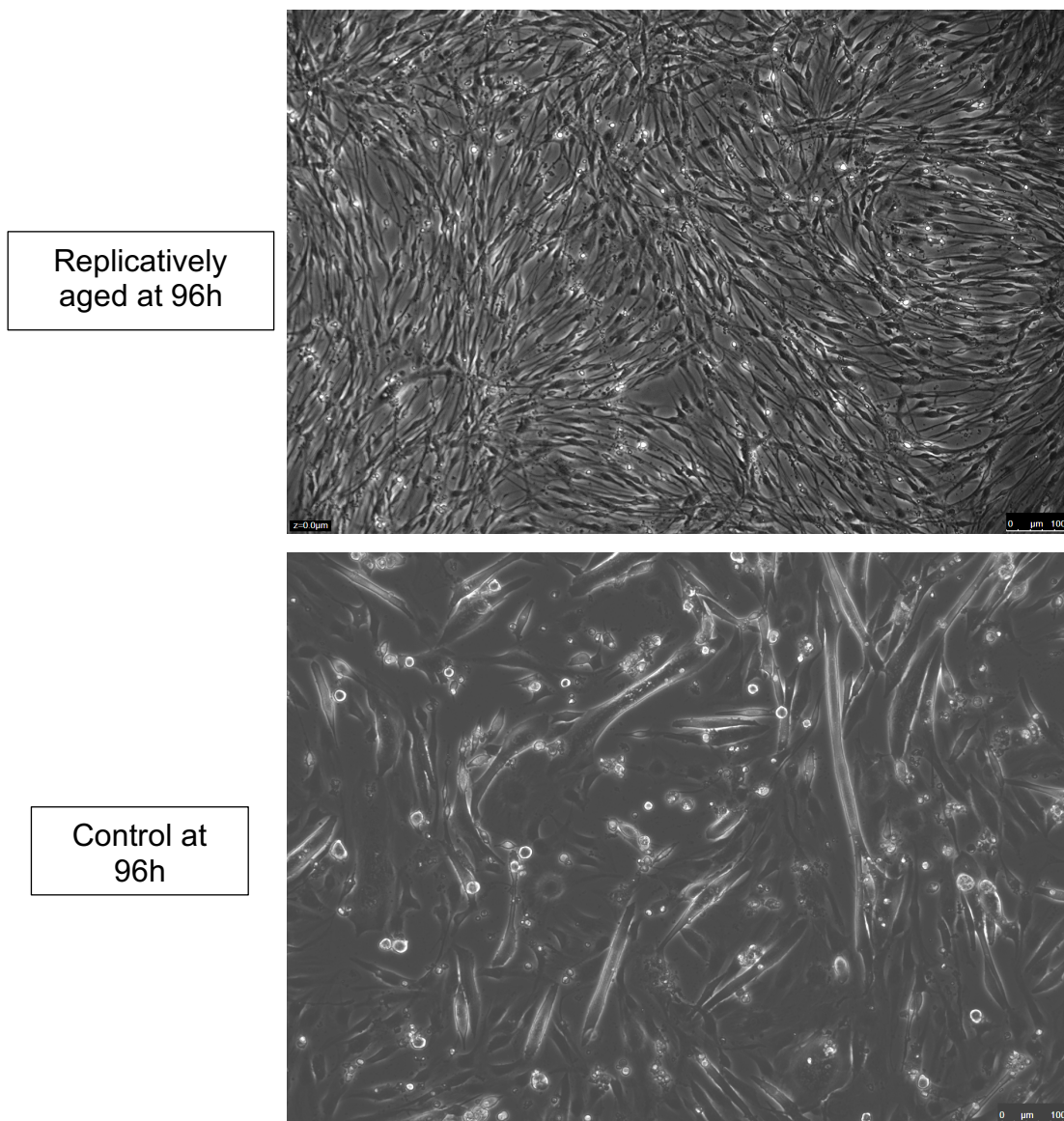
Figure 4.8. Morphological representation of replicatively aged and control myoblasts. Magnification 10x, scale 100 μm, n = 18 images.

4.4.2 Reduced Creatine Kinase Activity in Replicatively Aged Myoblasts vs. Control

There was no significant difference in CK activity at 0 h between replicatively aged (26 $\pm$ 6 U.l^{-1}) and control (33 $\pm$ 12 U.l^{-1}) myoblasts. At 96 h, CK activity of replicatively aged (45 $\pm$ 2 U.l^{-1}) myoblasts was significantly reduced (P < 0.05; Figure 4.3) by 6-fold vs. control (268 $\pm$ 27 U.l^{-1}).
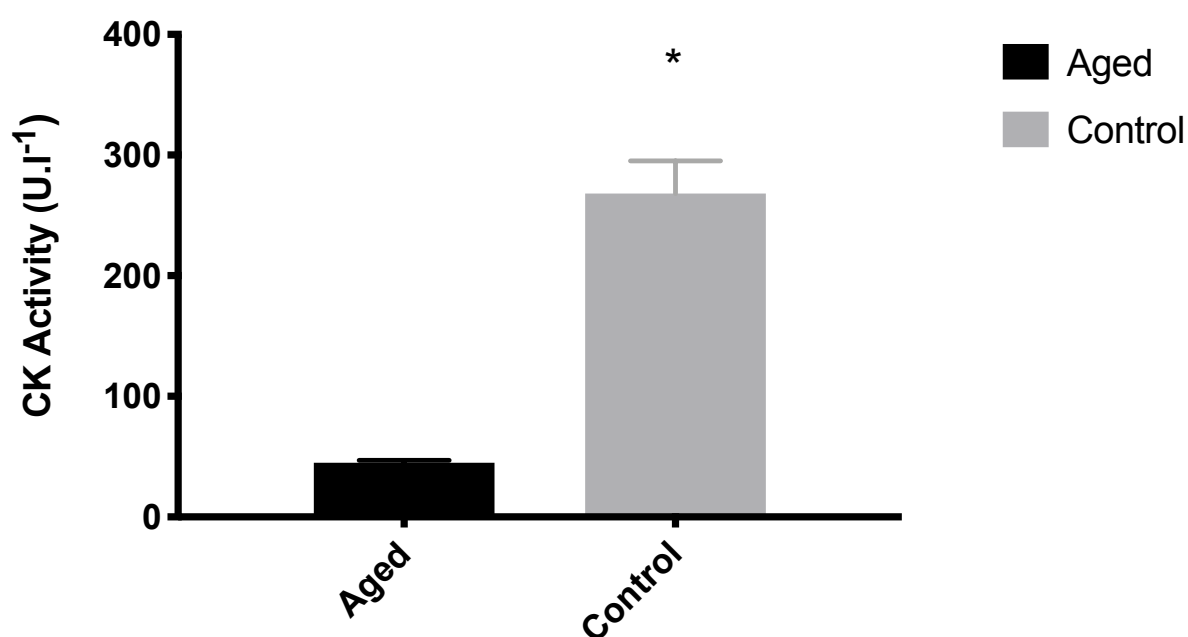
Figure 4.9. Creatine kinase activity at 96h between replicatively aged and control myoblasts. Data reported as mean $\pm$ SD. Significance (*) is set at P < 0.05. Experiments N = 3 all in duplicate.

4.4.3 Proposed Signalling Pathways that Stimulate Myotube Formation Basally

In order to ascertain the mechanisms underpinning reduced fusion capacity of replicatively aged cells, the next step was to investigate the impact of replicative ageing on signalling proteins involved in myotube formation.

Akt phosphorylation in replicatively aged cells, showed no difference from 0 h to any other timepoint (Figure 4.4A). However, there was a significant reduction in Akt activation in replicatively aged cells at 24 h vs. 15 minutes ($P < 0.05$) and a trend towards significance vs. 60 minutes ($P = 0.054$). In control myoblasts, again there was no difference in Akt activation at any time vs. 0 h. As in aged cells, there were significant increases at 120 minutes ($P < 0.05$) and 24 h ($P < 0.05$) vs. 15 minutes. When comparing replicatively aged myoblasts vs. control there was a significant suppression in Akt phosphorylation at 0 h ($P < 0.05$) and 24 h ($P < 0.05$), in replicatively aged vs. control myoblasts.

There were no significant differences in mTOR phosphorylation with time, in replicatively aged cells (Figure 4.4B). In control myoblasts, there was a significant difference over time ($P < 0.05$), with significant decreases from 0 h-15 minutes ($P < 0.05$) and 60 minutes ($P < 0.05$). There was a significant increase in mTOR phosphorylation at 24 h ($P < 0.05$) vs. 15 minutes, when activation returned to baseline levels. As with Akt phosphorylation, there was a significant reduction in mTOR phosphorylation in replicatively aged vs. control myoblasts at 0 h ($P < 0.05$) and 24 h ($P < 0.05$).

As with mTOR, there was no change in ERK phosphorylation over time in replicatively aged cells (Figure 4.4C). By contrast, in control cells ERK phosphorylation increased over 24 h, with significance being attained vs. 0 h at 120 minutes ($P < 0.05$) and 24 h ($P < 0.05$). Increased ERK phosphorylation at 24 h was also significantly higher than all other timepoints (15 minutes; $P < 0.05$, 60 minutes; $P < 0.001$ and 120 minutes; $P < 0.05$). The progressive rise in ERK activation with time in control cells resulted in a

significant difference at 24 h between replicatively aged myoblasts vs. control (P < 0.001).

There was no significant difference in p38 activation within control or aged cells over time and no differences evident between replicatively aged and control myoblasts at any time (Figure 4.4D).
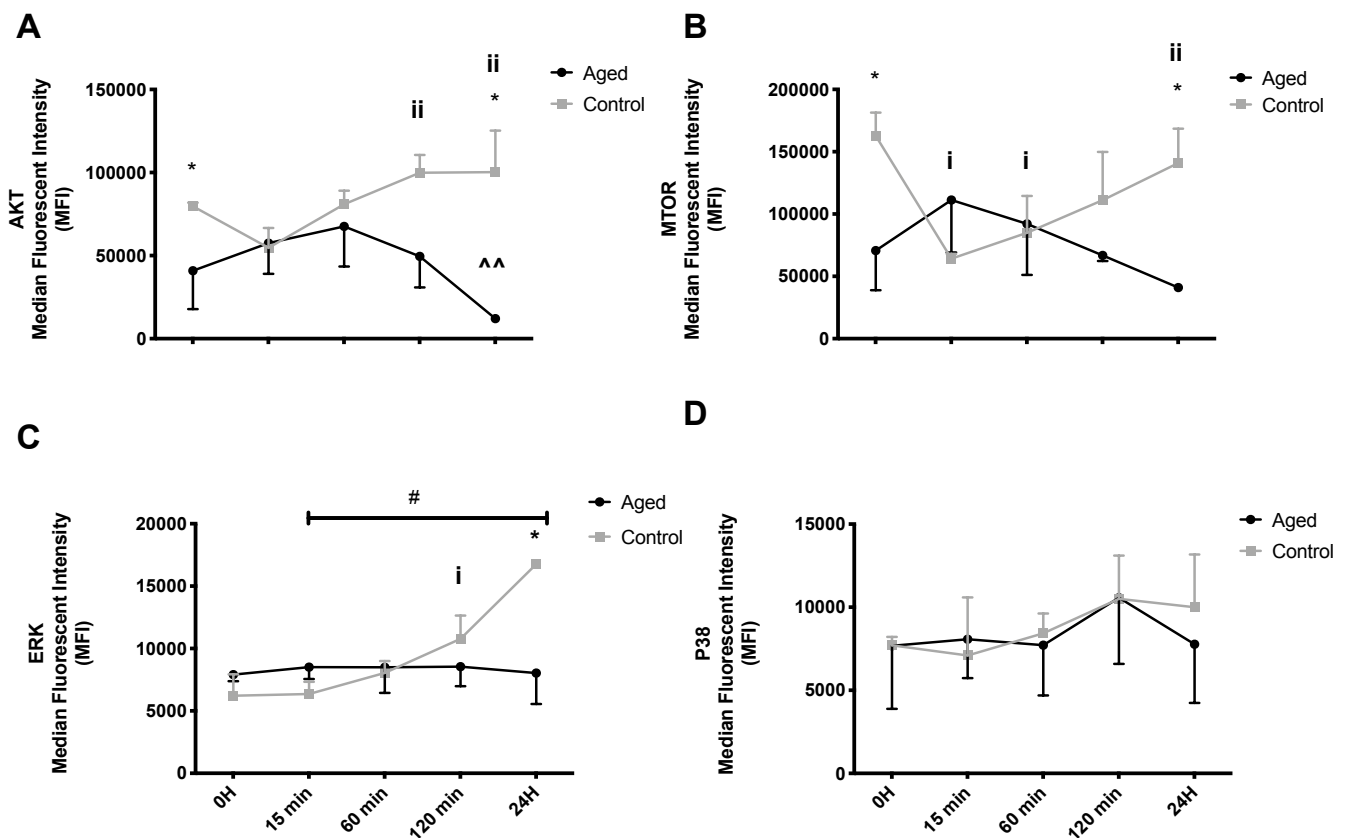
Figure 4.4 Akt (A), mTOR (B), ERK (C) and P38 (D) signalling between replicatively aged and control myoblasts over 24 h. Data reported as mean $\pm$ SD. Significance is set at P < 0.05. Significance reported as: between age (*); 15 minutes vs. other time point in aged (^^); pre vs. other time point in control (i); 15 minutes vs. other time point in control (ii) and 15 minutes, 60 minutes and 120 minutes vs. 24 h (⌐—#—⌐). Experiments N = 3 all in duplicate.

4.4.4 Gene Expression in Replicatively Aged and Control Myoblasts

Having determined adaptations are evident in Akt, ERK and mTOR activation in control vs. aged myoblasts, downstream molecular mechanisms were next assessed. Genes related to muscle differentiation (myogenin, myostatin, ID3, IGF-I and IGF-II, SETD3, PIK3C3, FOXO3 and URB5), adhesion/cell-cell interaction (ADAM10 and CDH1) and amino acid transporters (SLC7A5 and SLC3A2) were investigated, in an attempt to further define altered fusion capacity of the cells. Comparisons were made within replicatively aged and control myoblasts vs. their own 0 h baseline (within adaptations) as well as replicatively aged normalised to control (between adaptations).

4.4.4.1 Genes Implicated in Muscle Growth and Hypertrophy:

Myogenin gene expression increased significantly by 7-fold at 96 h ($P < 0.05$) in aged cells (within) when compared with baseline. By contrast, in control cells myogenin gene expression (within) initially decreased significantly by 9-fold ($p < 0.05$) at 24 h before increasing significantly by 4-fold ($p < 0.05$) at 96 h vs. baseline. However, due to significant reductions in myogenin expression at baseline in aged vs. control ($P < 0.001$; Table 4.1), when normalised to control (between) relative myogenin expression was significantly reduced in aged by 1000-fold ($p < 0.05$) and 200-fold ($p < 0.05$) at 24 h and 96 h respectively (Figure 4.5A), when compared to control baseline. Significant reductions of 74-fold ($P < 0.05$) and 714-fold ($P < 0.05$) were also evident when aged (between) were compared with control at 24 h and 96 h respectively.

Myostatin gene expression (within) decreased significantly by 4-fold at 24 h ($P < 0.05$) in aged cells (within) when compared with baseline. By contrast, in control cells, myostatin gene expression (within) increased significantly by 9-fold ($p < 0.05$) at 24 h, before returning to baseline levels at 96 h. Due to higher, but not significant gene expression levels of aged vs. control cells, when normalised to control (between) relative myostatin expression did not change at 24 h, but increased significantly by 12-fold ($P < 0.05$) at 96 h (Figure 4.5B), when compared to control baseline. There was a signficiant reduction of 7-fold ($P < 0.05$) at 24 h between aged (between) compared to control.

IGF-I gene expression (within) increased significantly by 9-fold at 24 h (P < 0.05) and 8-fold at 96 h (P < 0.05) in aged cells (within) when compared with control baseline (Figure 4.5C). Significant 6-fold (P < 0.05) increases in IGF-I gene expression (within) in control cells were also evident at 24 h and 20-fold increases by 96 h (P < 0.05) vs. control baseline. Due to significant reductions in IGF-I mRNA expression in aged vs. control cells at control baseline (P < 0.001; Table 4.1), when normalised to control (between) no significant differences in relative IGF-I expression vs. control baseline were evident at 24 h or 96 h. Significant reductions of 10-fold (P < 0.05) and 19-fold (P < 0.05) were also evident when aged (between) were compared with control at 24 h and 96 h respectively.

IGF-II gene expression (within) increased signficantly by 27-fold (P < 0.05) and 26-fold (P < 0.05) at 24 h and 96 h, respectively, in aged cells when compared with baseline (Figure 4.5D). In contrast, in control cells, there were no differences in gene expresion (within) at 24 h, however, at 96 h, there was a significant, 33-fold increase in expression vs. baseline (P < 0.05). Due to significant reductions in IGF-II mRNA expression in aged vs. control cells at baseline (P < 0.001; Table 4.1), when normalised to control (between) no significant differences in relative IGF-II expression vs. baseline were evident at 24 h or 96 h. There was a signficiant reduction of 52-fold (P < 0.05) at 96 h between aged (between) compared to control.

ID3 gene expression (within), was significantly elevated by 8-fold at 24 h (P < 0.05) vs. baseline but there was no difference at 96 h (Figure 4.6A), returning to baseline levels, in aged cells. By contrast, no difference in ID3 expression, vs. baseline, was evident in control cells at either timepoint. However, when normalised to control (between), there was a significant increase by 4-fold at 24 h (P < 0.05) which returned to baseline by 96 h. There was a signficiant reduction of 8-fold (P < 0.05) at 24 h between aged (between) compared to control.

SETD3, PIK3C3, FOXO3 and UBR5 gene expression showed no statistical differences basally (Table 4.1), with age or time (data not shown).

<u>4.4.4.2 Genes Involved in Cell-Cell Adhesion</u>

Adam10 gene expression did not change in aged cells at either time-point. In control cells there was a significant, 100-fold reduction ($P < 0.05$) in gene expression at 24 h, which returned to baseline levels by 96 h (Figure 4.6B). When normalised to control (between), there was no difference in gene expression compared to baseline at 24 h or 96 h. However, when compared to control at 24 h, aged showed a 142-fold increase ($P < 0.05$).

CDH1 gene expression showed no statistical differences basally (Table 4.1), with age or time (data not shown).

<u>4.4.4.3 Amino Acid Transporter Gene Expression</u>

SLC7A5 gene expression showed no statistical differences basally (Table 4.1), with age or time (data not shown).

SLC3A2 gene expression did not change in aged vs. baseline, with time. In control cells, no difference was evident at 24 h, however, a significant 11-fold increase in expression ($P < 0.05$) was evident at 96 h (Figure 4.6C). When normalised to control (between), no difference compared to baseline was evident.

To summarise, distinct differences between replicatively aged and control myoblasts included: low levels of CK activity, blunted Akt, ERK and mTOR signalling and the relative suppression of the gene expression of myogenin, IGF-I and IGF-II and relative increases in myostatin.
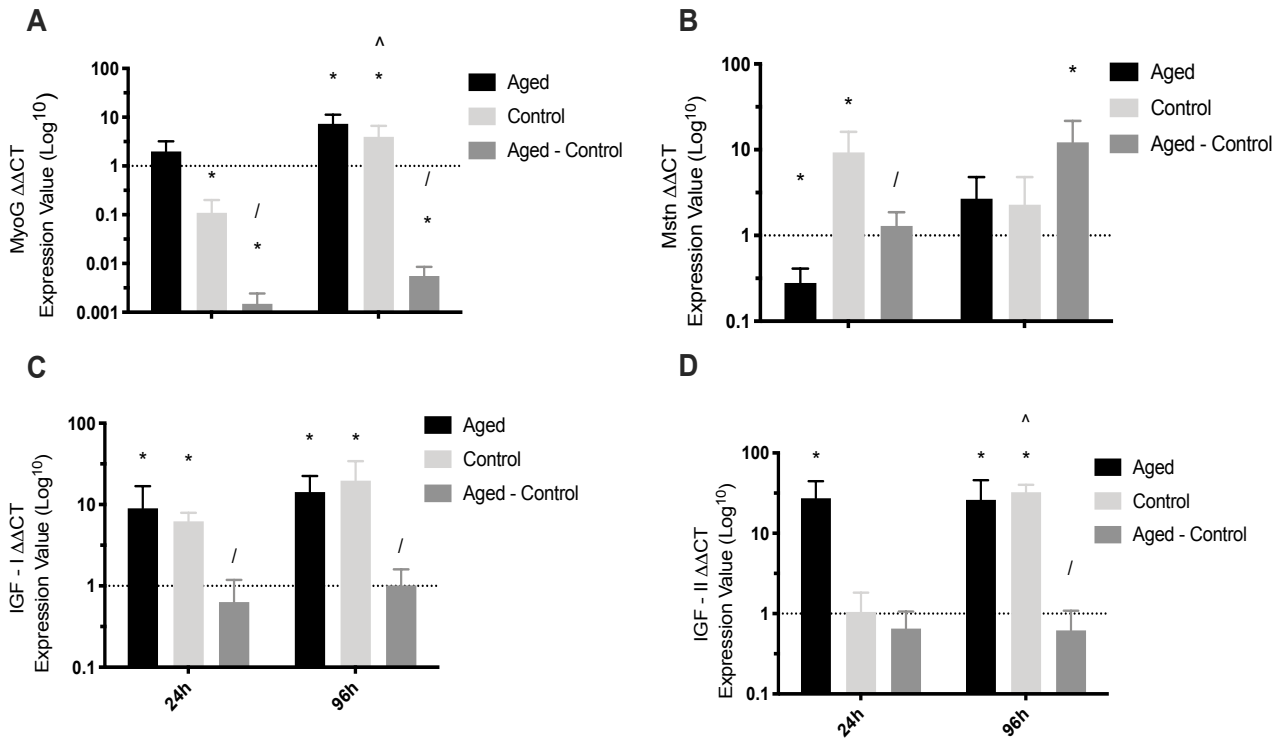
Figure 4.5. Gene expression values of myogenin (A), myostatin (B), IGF-I (C) and IGF-II (D) in replicatively aged and control myoblasts. 'Aged-Control' is defined as aged relative to control. Data reported as mean $\pm$ SD. Significance is set at $P < 0.05$. Cell age vs. own baseline (*); difference over time (^) and control vs. aged-control (/) Experiments N = 3 all in duplicate.
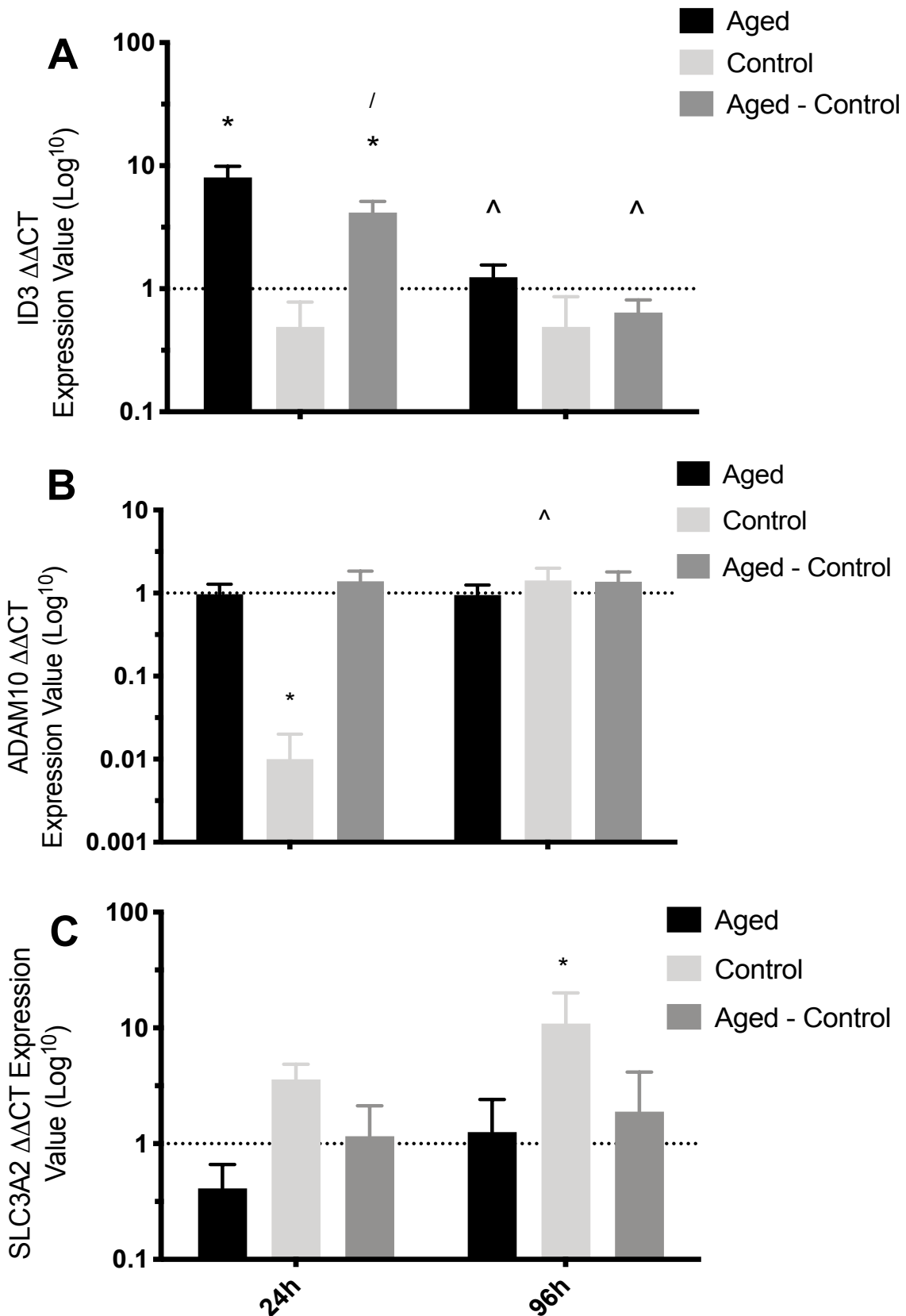
Figure 4.6. Gene expression values of ID3 (A), ADAM10 (B) and SLC3A2 (C) in replicatively aged and control myoblasts. 'Aged-Control' is defined as aged relative to control. Data reported as mean ± SD. Significance is set at $P < 0.05$. Cell age vs. own baseline (*); difference over time (^) and control vs. aged control (/). Experiments N = 3 all in duplicate.

4.4.5 Impact of Leucine and HMB Supplementation on Myoblast Fusion

Since there were no significant differences in expression of the basal AA transporters studied in aged vs. control cells (Table 4.1) and no differences with age or time for SLC7A5 and only a reduction in expression of SLC3A2 at 96 h in aged vs. control (between), the impact of leucine and HMB on muscle fusion was investigated, to ascertain whether these supplements could rescue the blunted hypertrophic response of replicatively aged myoblasts. Initial studies determined the doses of leucine and HMB to be used in control cells (Figure 4.7). Data illustrate that leucine doses of >2.5 mM leucine significantly (all $P < 0.05$) increase myotube length, diameter and area vs. DM (Figure 4.7). Also, data show that HMB >1.25 mM significantly increase (all $P < 0.05$) myotube length, diameter and area of control cells and that doses vs. DM (Figure 4.7). As a consequence of this beneficial hypertrophic effect, further studies were initiated to determine the impact of these supplements on both cell models.
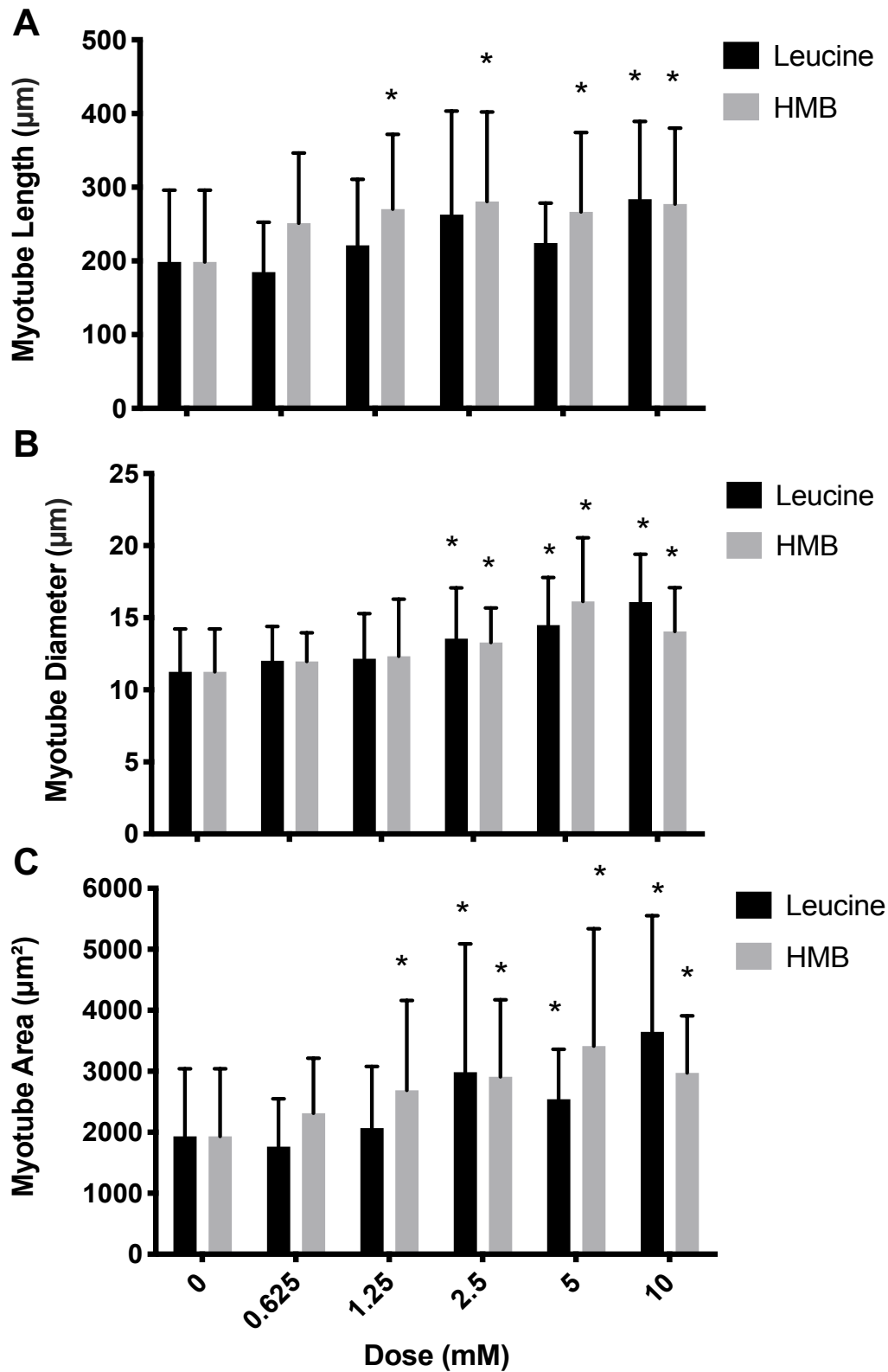
Figure 4.7. Dose-response experiments with leucine and HMB in myotube length (A), diameter (B) and area (C). Data reported as mean ± SD and significance set at $p < 0.05$. Dose vs. no dose (*). Experiments N = 3 all in duplicate and 18 images taken per data bar.

Control
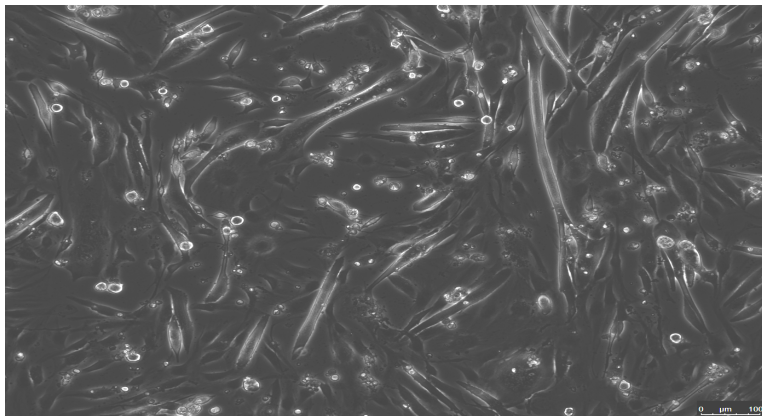
Leucine
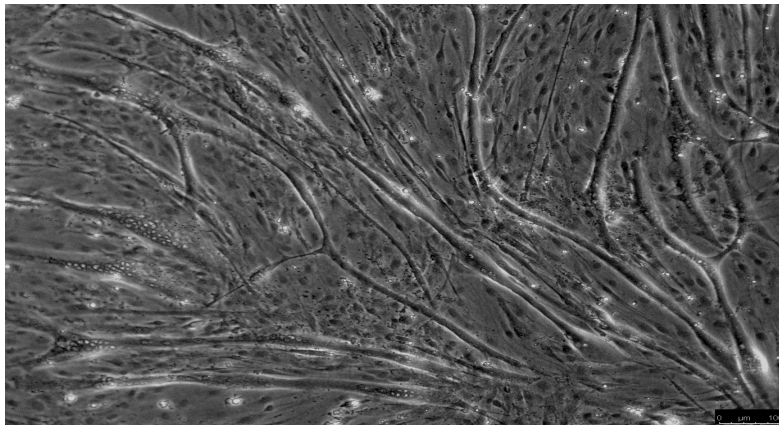
HMB
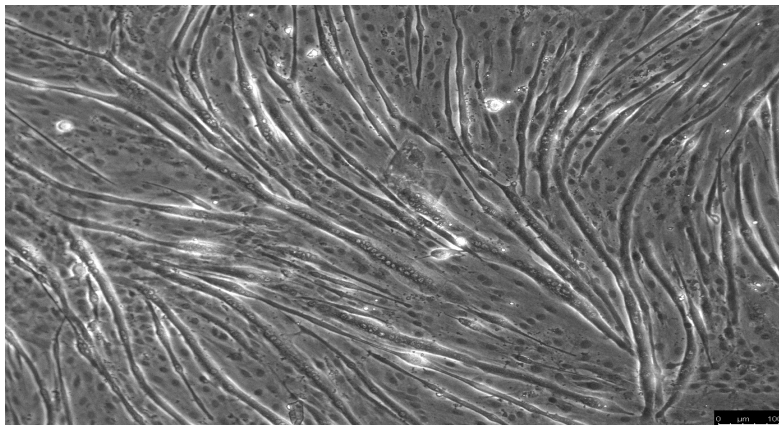
Figure 4.8. Images in control myoblasts in the presence and absence of leucine and HMB. The first row contains no supplements, the second row were treated with 10 mM of leucine and third row treated with 10 mM HMB. All experiments were N = 3 in duplicate equally 18 images in total.

4.4.6 The Effect of Leucine and HMB on Signalling Pathways Involved in Myoblast Fusion

In the presence of leucine and HMB at 120 minutes, there were 2.4-fold (P < 0.05) and 2.5-fold (P < 0.05) increases in Akt activation, respectively, vs. untreated replicatively aged cells at the same time (Figure 4.9A). By 24 h, leucine supplementation was no different to untreated replicatively aged cells, however, Akt activation was sustained in the presence of HMB (3.8-fold, P < 0.05). In contrast, control cells Akt phosphorylation in the presence of leucine significantly decreased by 5.9-fold from 0 h to 15 minutes (P < 0.05) and vs. untreated control cells (P < 0.05). This was rescued by 5.8-fold at 60 minutes (P < 0.05) and from 15 minutes to 24 h (P < 0.05) by 8.2-fold (Figure 4.9B). In contrast to leucine, there was no impact of HMB on Akt activation, vs. untreated control.

In replicatively aged myoblasts HMB supplementation significantly increased mTOR activation at 120 minutes with HMB vs. leucine (P < 0.05; 1.9-fold) and untreated replicatively aged cells (P < 0.05; 2.5-fold). In addition, HMB treatment increased activation significantly at 120 minutes vs. 0 h (P < 0.05) by 2.4-fold. There was no difference with leucine supplementation on mTOR phosphorylation in replicatively aged myoblasts over 24 h (Figure 4.9C). There was also no impact of leucine or HMB on control myoblast mTOR activation (Figure 4.9D).

ERK phosphorylation, replicatively aged myoblasts in the presence of leucine or HMB showed no significant differences over 24 h, which mirrored basal trends (Figure 4.9E). Control cells supplemented with leucine and HMB emulated the basal response (Figure 4.9F). In addition, there was no impact of leucine and HMB on p38 phosphorylation in replicatively aged and control myoblasts over 24 h (Figure 4.9G/H).

In summary, leucine and HMB activate Akt phosphorylation in replicatively aged myoblasts compared to basal levels. With HMB supplementation only, mTOR phosphorylation was increased in replicatively aged. This suggests that Akt and mTOR are impacted by leucine and HMB in replicatively aged.
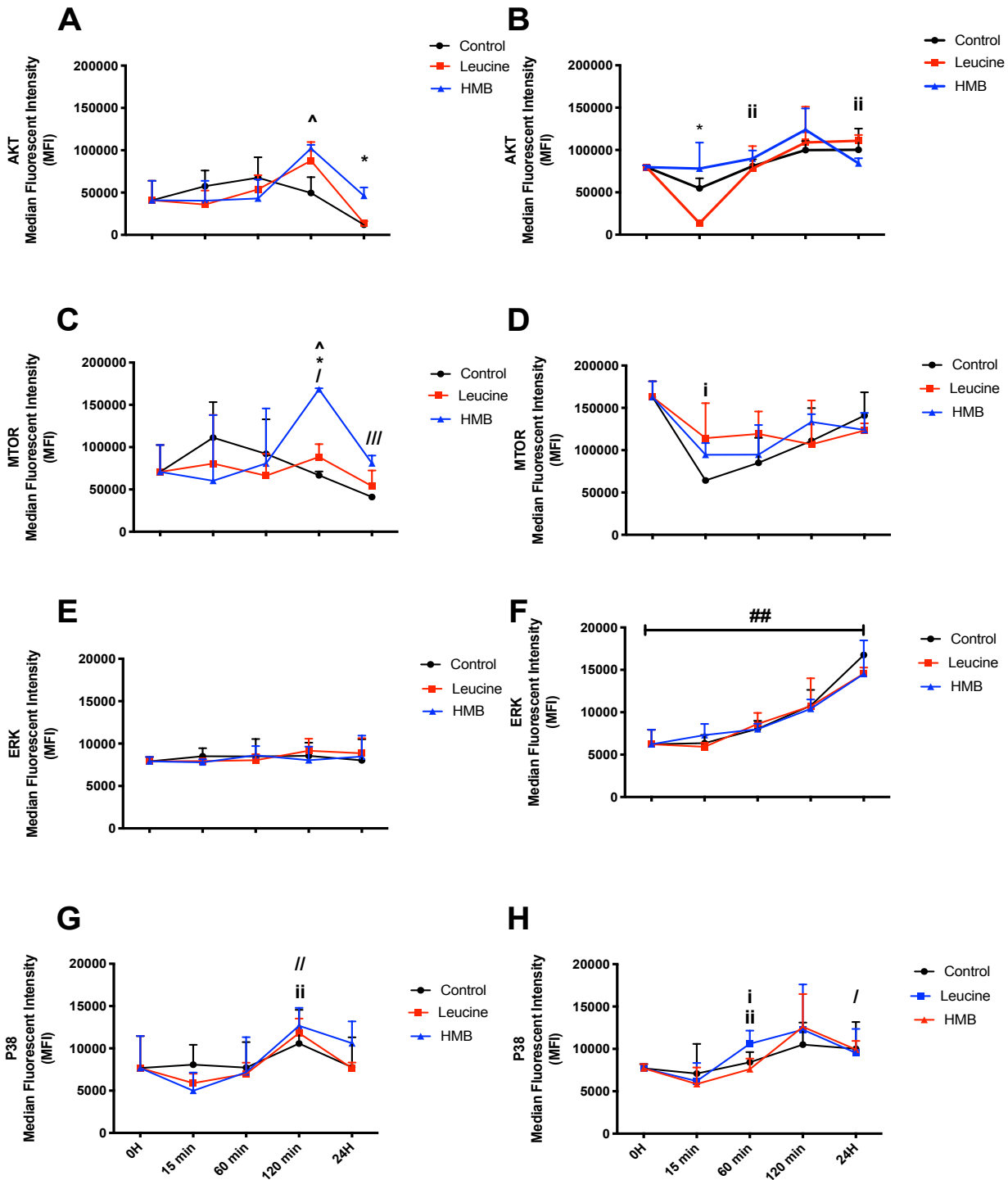
Figure 4.9. Replicatively Aged Akt (A), mTOR (C), ERK (E) and P38 (G) signalling. Control Akt (B), mTOR (D), ERK (F) and p38 (H) signalling. Data reported as mean ± SD. Significance set at P < 0.05. Leucine 0 h vs. other time-point (i); leucine 15 minutes vs. other time-point (ii); HMB 0 h vs. other time-point (/); HMB 15 minutes vs. other time-point (//); HMB 120 minutes vs. other time-point (///); between untreated control and supplement at specific time-point (*); between supplement at specific time-point (^). Experiments N = 3 all in duplicate.

4.4.7 Adaptations in Gene Expression Following Leucine and HMB Supplementation in Replicatively Aged and Control Myoblasts

4.4.7.1 Genes Implicated in Muscle Growth:

The changes in myogenin expression already reported in aged cells (Figure 4.10) was unchanged at any time by supplementation with leucine or HMB. Similarly, changes already reported for control cells (Figure 4.10) were unaltered by addition of leucine or HMB. In myostatin gene expression, leucine and HMB significantly ($P < 0.05$) decreased control myoblast by 5-fold and 7-fold respectively. There was no other impact of leucine and HMB on myostatin gene expression in replicatively aged (Figure 4.11). The was no impact of leucine and HMB on IGF-I gene expression that was already reported basally (Figure 4.12) in replicatively aged and control myoblasts.

Next, IGF-II gene expression in aged cells and in the presence of leucine at 24 h was without impact (Figure 4.13A). In contrast, HMB treatment significantly ($P < 0.05$) reduced gene expression by 8-fold vs. DM at 24 h. By 96 h, there was no difference in either supplement group (Figure 4.13B). In control cells at both 24 h and 96 h there was no impact of either supplement. There was no impact of leucine on normalised (between) IGF-II gene expression at 24 h and 96 h vs DM (Figure 4.13). However, HMB treatment significantly decreased gene expression at 24 h and 48 h (both $P < 0.05$) by both 8-fold vs. DM. Lastly, there was no impact of leucine and HMB on ID3, SEDT3, PIK3C3, FOXO3 and URB5 gene expression in either aged, control or normalised group.
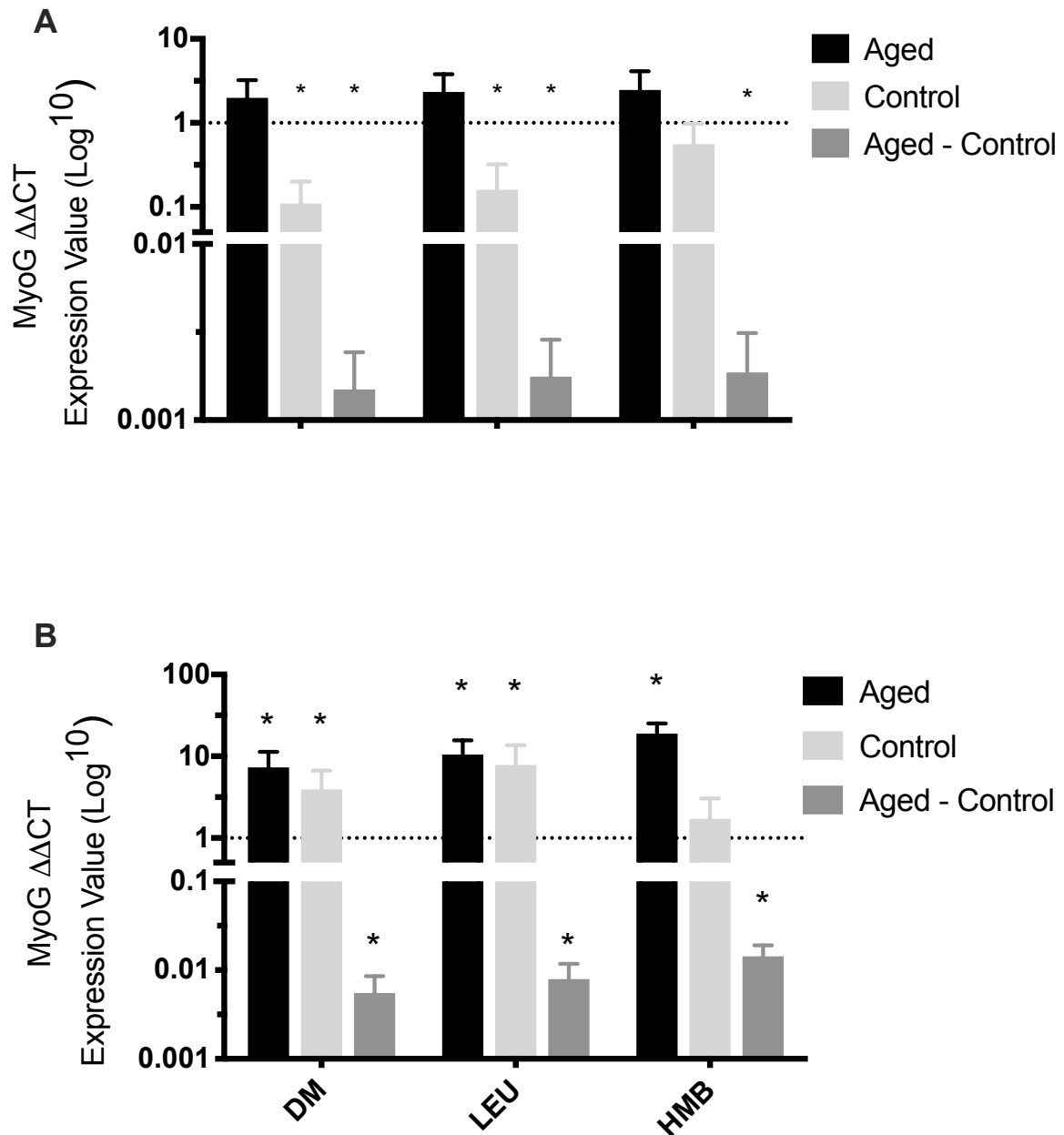
Figure 4.10. Myogenin gene expression in replicatively aged and control myoblasts. 'Aged-Control' is defined as aged relative to control. Gene expression in the absence and presence of leucine and HMB is presented. Myogenin at 24 h (A), 96 h (B) is reported as mean ± SD. Significance is set at $P < 0.05$. Significance reported: cell age vs. baseline (*). Experiments N = 3 all in duplicate.
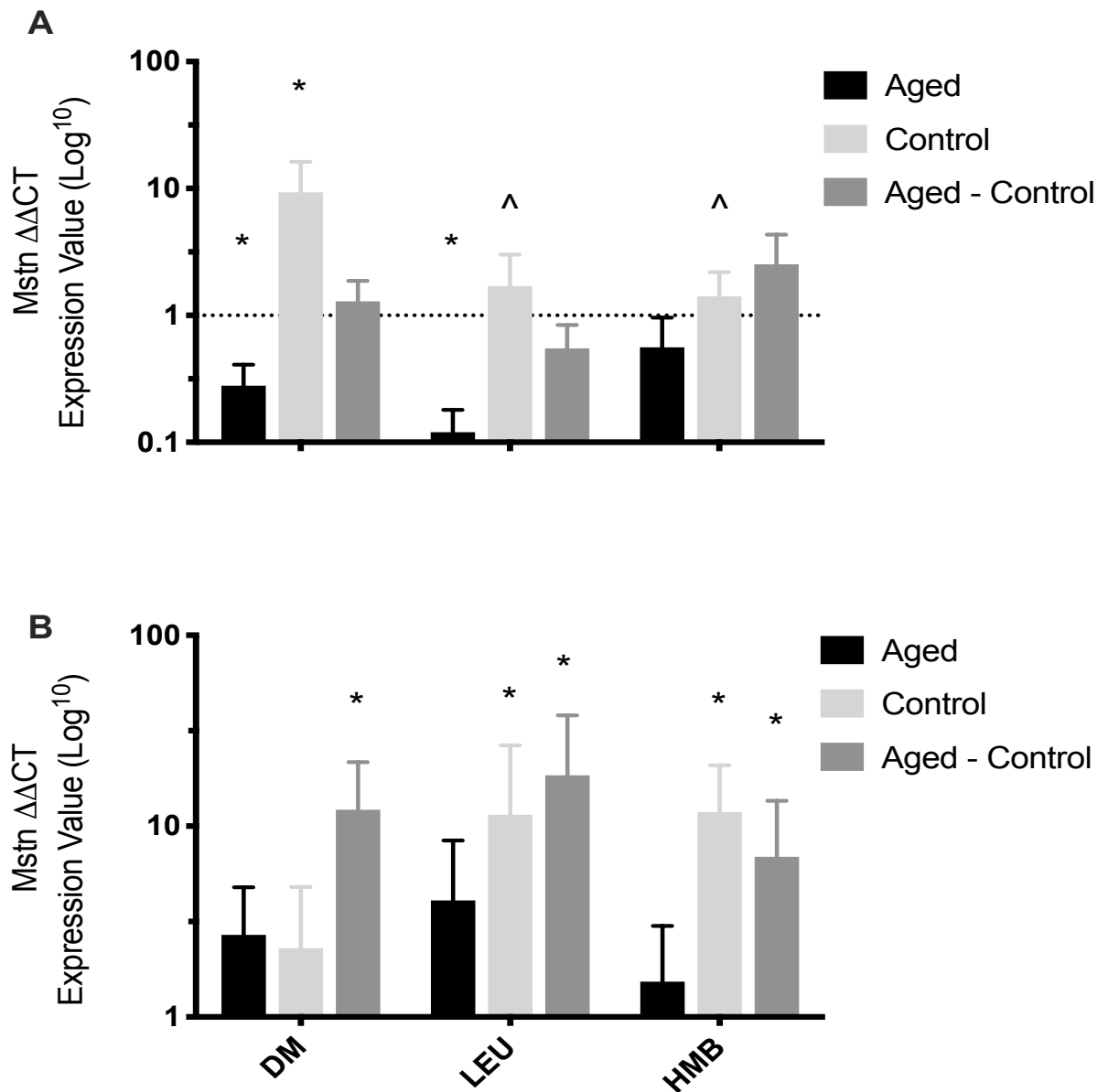
Figure 4.11. Myostatin gene expression in replicatively aged and control myoblasts. 'Aged-Control' is defined as aged relative to control. Gene expression in the absence and presence of leucine and HMB is presented. Myostatin at 24 h (A), 96 h (B) is reported as mean $\pm$ SD. Significance is set at $P < 0.05$. Significance reported: cell age vs. baseline (*) and ^ supplements vs. DM. Experiments N = 3 all in duplicate.
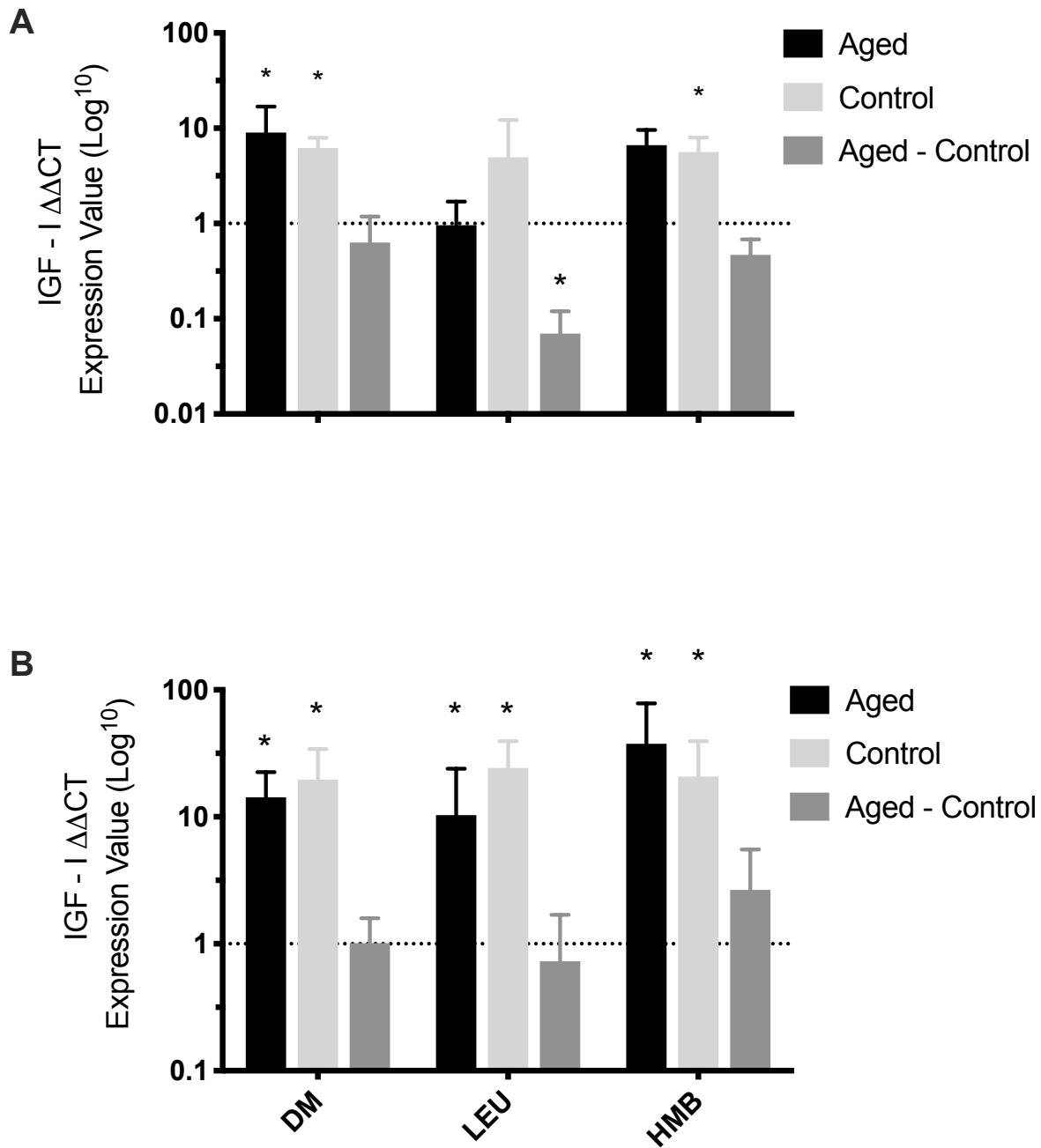
Figure 4.12. IGF-I gene expression in replicatively aged and control myoblasts. 'Aged-Control' is defined as aged relative to control. Gene expression in the absence and presence of leucine and HMB is presented. IGF-I at 24 h (A), 96 h (B) is reported as mean $\pm$ SD. Significance is set at $P < 0.05$. Significance reported: cell age vs. baseline (*). Experiments N = 3 all in duplicate.
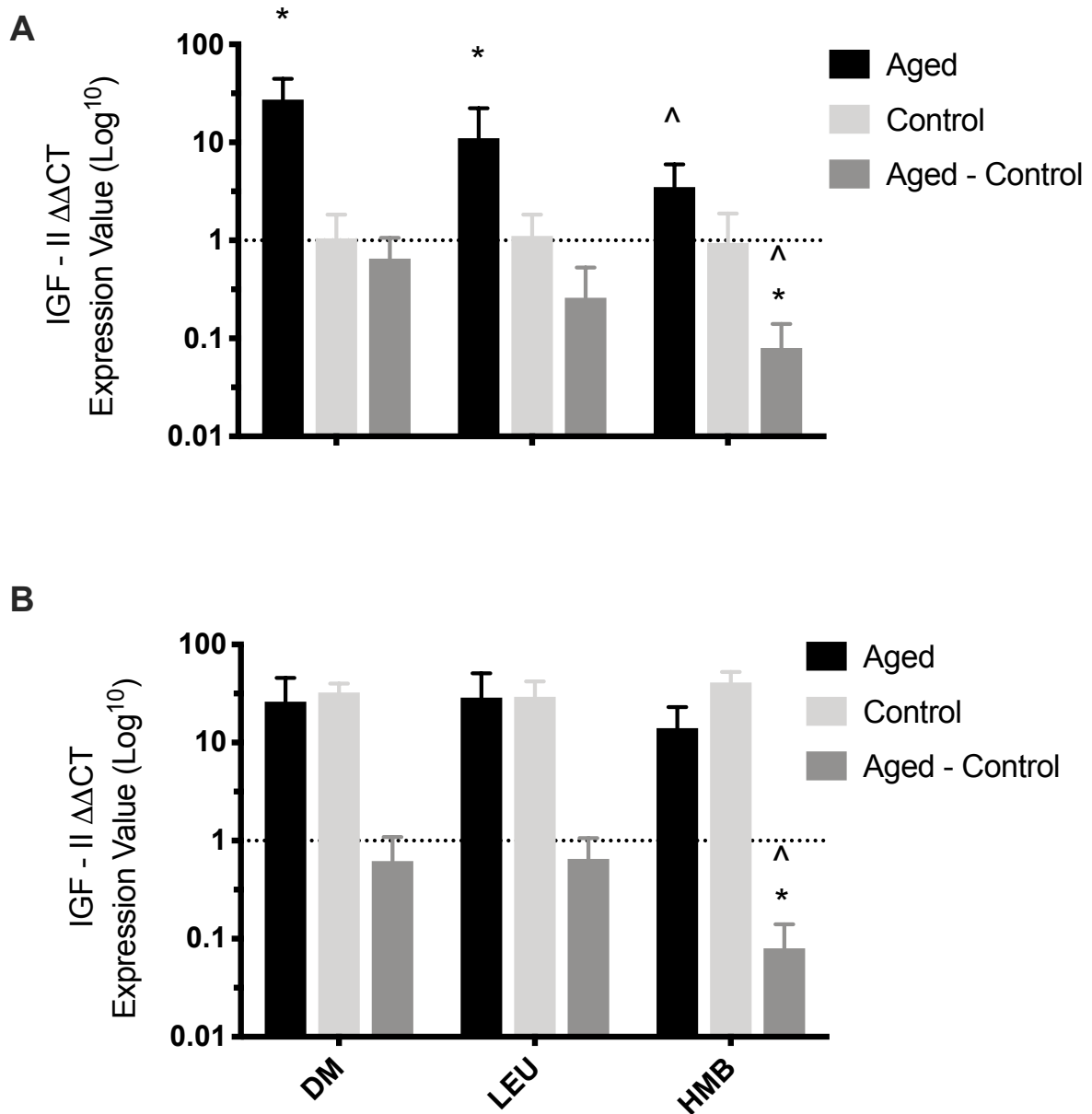
Figure 4.13. IGF-II gene expression in replicatively aged and control myoblasts. 'Aged-Control' is defined as aged relative to control. Gene expression in the absence and presence of leucine and HMB is presented. IGF-II at 24 h (A), 96 h (B) is reported as mean $\pm$ SD. Significance is set at $P < 0.05$. Significance reported: cell age vs. baseline (*) and ^ supplements vs. DM. Experiments N = 3 all in duplicate.

<u>4.4.7.2 Genes Implicated in Cell-Cell Interactions and Cell Adhesion:</u>

The integrin CHD1 reported no differences across all variables. There was also no impact of leucine and HMB supplementation on ADAM10 gene expression in replicatively aged cells at either 24 h or 96 h (Figure 4.14). However, at 24 h in control cells leucine ($P < 0.05$) and HMB ($P < 0.05$) significantly increased expression by 164-fold and 69-fold vs. DM.

<u>4.4.7.3 Genes Involved in Amino Acid Transportation:</u>

There was no impact of leucine and HMB on SLC7A5 gene expression in replicatively aged. In addition, leucine was without effect in SLC3A2 gene expression at 24 h or 96 h in aged (Figure 4.15). However, at 24 h, HMB significantly reduced (all $P < 0.05$) aged (between) SLC3A2 gene expression vs. DM by 10-fold.

From these data, replicatively aged myoblasts do respond to leucine and HMB at signalling and gene level. Albeit, surprising responses at gene level with reduction in IGF-II in response to HMB, despite increases with Akt and mTOR signalling. This therefore encouraged further experiments to ascertain whether these conflicts in signals enabled fusion or not. Therefore, the next section is fusion with HMB and leucine supplementation in control and replicatively aged metabolic enzymes CK and LDH.
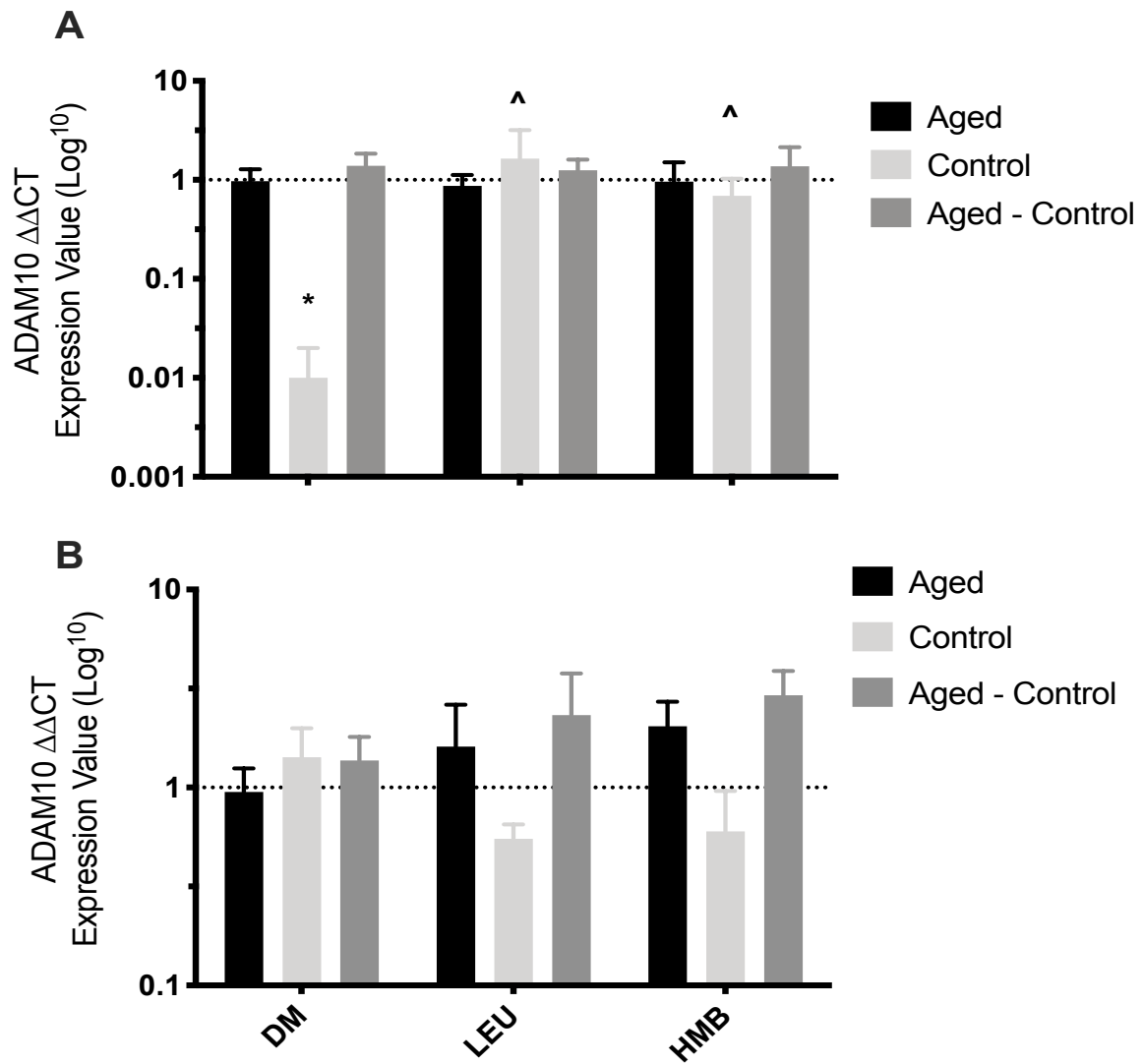
Figure 4.14. ADAM10 gene expression in replicatively aged and control myoblasts. 'Aged-Control' is defined as aged relative to control. Gene expression in the absence and presence of leucine and HMB is presented. ADAM10 at 24 h (A), 96 h (B) is reported as mean $\pm$ SD. Significance is set at $P < 0.05$. Significance reported: cell age vs. baseline (*): supplements vs. DM (^). Experiments N = 3 all in duplicate.
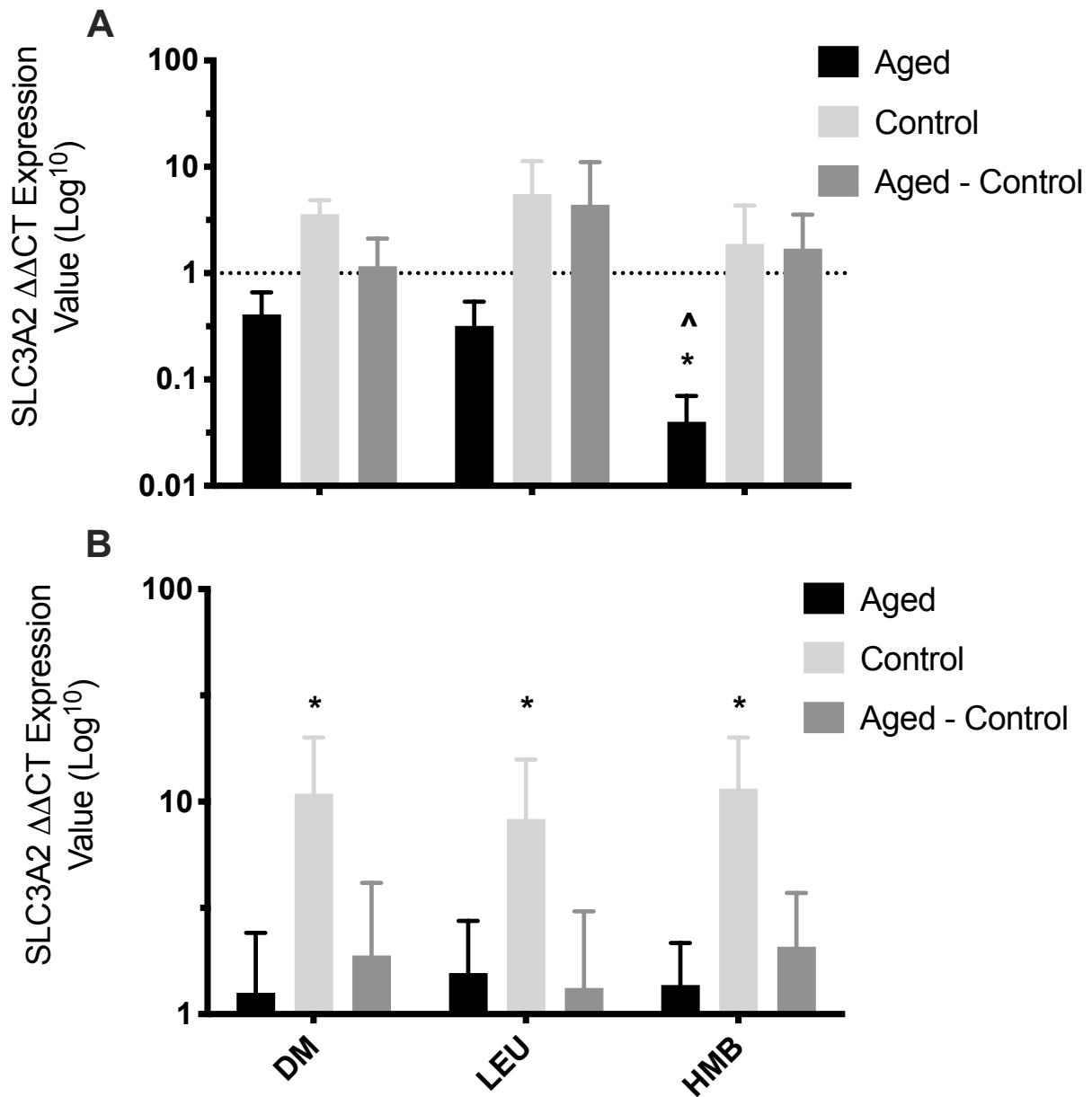
Figure 4.15. SLC3A2 gene expression in replicatively aged and control myoblasts. 'Aged-Control' is defined as aged relative to control. Gene expression in the absence and presence of leucine and HMB is presented. ADAM10 at 24 h (A), 96 h (B) is reported as mean ± SD. Significance is set at $P < 0.05$. Significance reported: cell age vs. baseline (*): supplements vs. DM (^). Experiments N = 3 all in duplicate.

4.4.8 Impact of Leucine and HMB on Creatine Kinase Activity

At 0 h, there was no significant difference in CK activity between replicatively aged (26 ± 6 U.l^{-1}) and control (33 ± 12 U.l^{-1}) myoblasts. At 96 h, as supported by the morphological analysis in replicatively aged cells (Figure 4.16A), CK activity remained at basal levels and did not change in the presence or absence of leucine or HMB (Figure 4.16B). Following 96 h in control cells, CK activity was significantly increased in all culture conditions (Figure 4.16). However, contrary to morphological outcomes at 96 h, where both leucine and HMB resulted in increased myotube area, only HMB treatment resulted in significant 1.37-fold increase ($P < 0.05$) in CK activity vs. untreated control, perhaps as a consequence of increased myotube size following this treatment only (Figure 4.7). Given the absence of increased CK activity in aged cells, it is not surprising that control cells had significantly higher CK activity levels at 96 h (5.96, $P < 0.001$; 5.68, $P < 0.001$ and 7.47, $P < 0.001$) under control, leucine and HMB interventions, respectively (Figure 4.16).

A

Control

Leucine

HMB

147
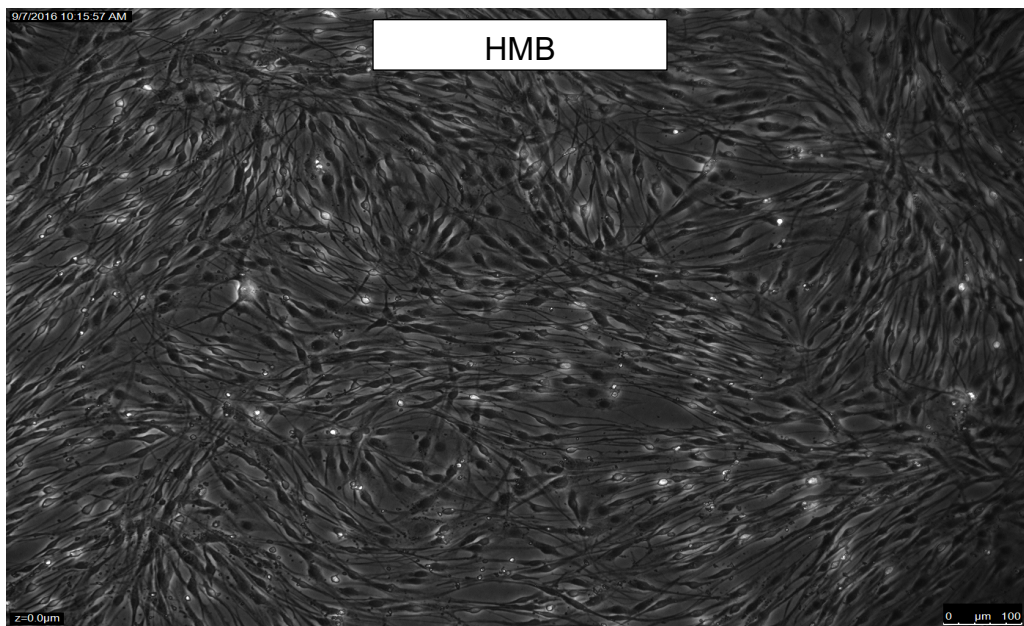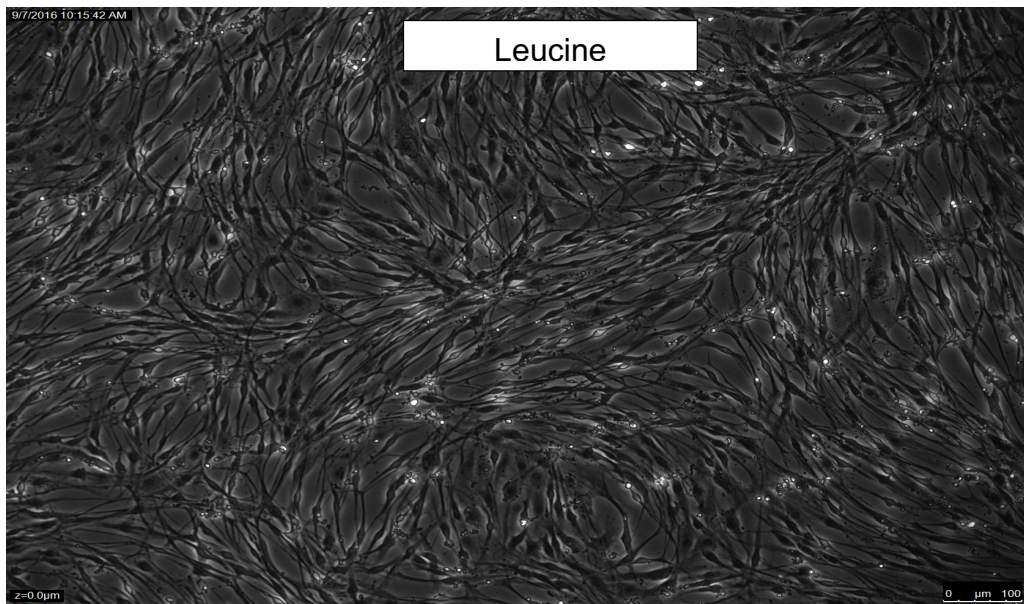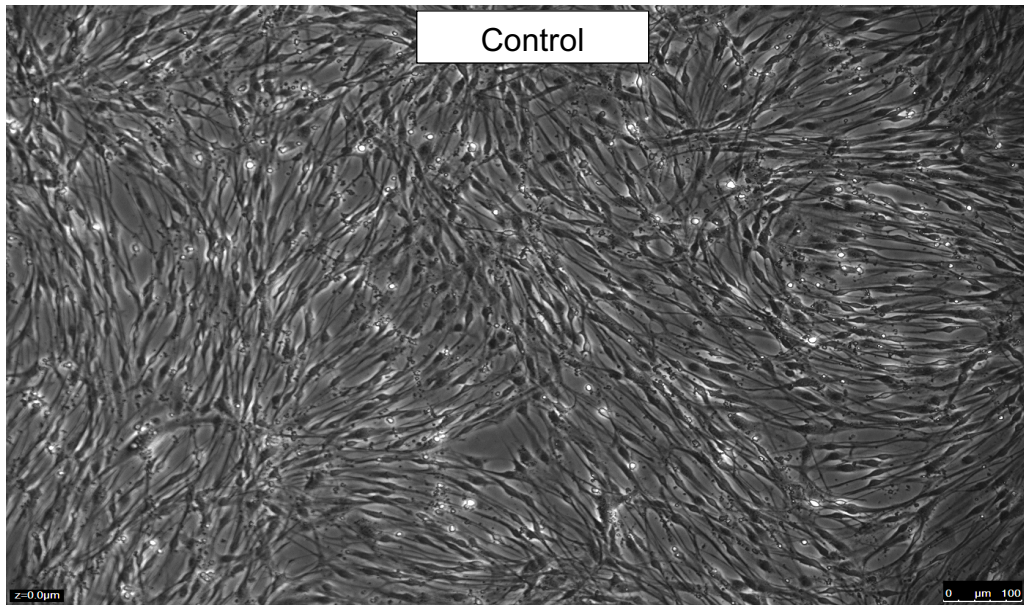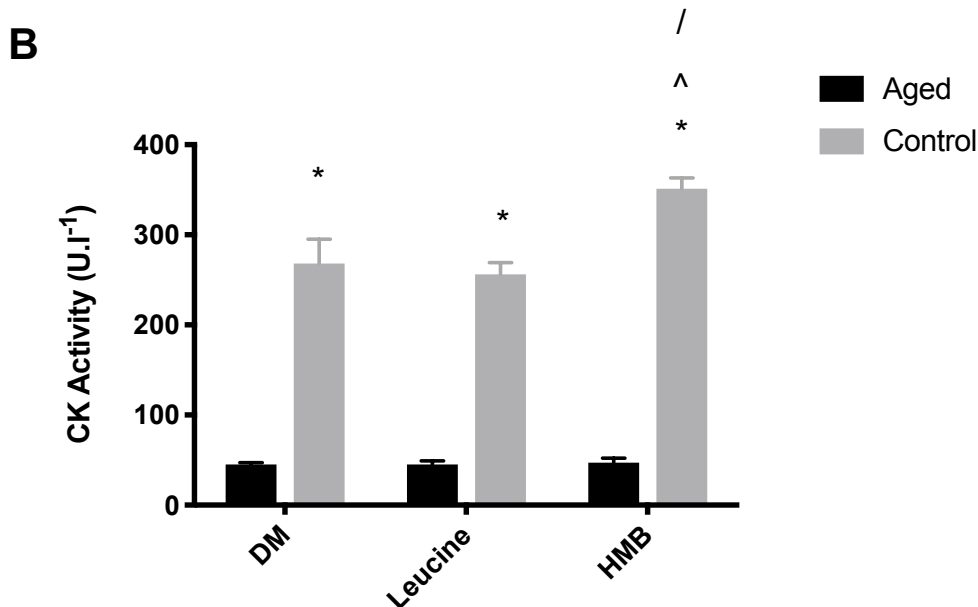
Figure 4.16. Morphology (A) in replicatively aged cells in the absence and presence of leucine and HMB. Creatine kinase activity (B) in replicatively aged and control myoblasts at 96 h. Cells were treated with 10 mM of leucine and HMB. Data is reported as mean ± SD. Significance is set at P < 0.05. Significant difference between age (*), DM vs. HMB (^) and leucine vs. HMB (/). Experiments N = 3 all in duplicate. Scale 0-100 μm.

4.4.9 Lactate Dehydrogenase Increases in Replicatively Aged was Suppressed with Leucine

In replicatively aged cells between 24 h-48 h and 48 h-96 h there were significant 10.8-fold and 4.2-fold increase in LDH secretion (P < 0.001). In addition, in control myoblasts between 24 h-48 h and 48 h-96 h there was significant 2.3-fold and 9.0-fold increases (both P < 0.001) in LDH. There were no differences in LDH activity at 24 h in replicatively aged vs. control myoblasts. However, at 48 h and 96 h there was significant (both P < 0.001) increases in LDH in replicatively aged compared to control, by 8.5-fold and 3.5-fold respectively. Leucine significantly attenuated (P < 0.05) the increases in LDH at 48 h and 96 h compared to DM by 3.2-fold and 1.5-fold. There was no impact of HMB. In addition, there was no impact of leucine or HMB on control cells at 24 h, 48 h and 96 h (Figure 4.17). Whereas, with leucine supplementation,

LDH secretion in replicatively aged was significantly increased (P < 0.05) at 48 h and 96 h compared to control by 3.3-fold and 1.5-fold respectively. This significant LDH increase (P < 0.01) was also observed with HMB supplementation at 48 h by 8.5-fold and 96 h by 4.6-fold in replicatively aged compared to control.

Summary of these data is that the inability of replicatively aged myoblasts to fuse is not rescued with leucine or HMB supplementation, perhaps as a consequence of altered signalling. Leads to the question of what else could be occurring, as a consequence of enhanced Akt and mTOR signalling. Altered metabolism is another potential output, therefore assessed LDH levels in the cell supernatant. Determined that the significant increase in LDH in the supernatant in replicatively aged cells vs. control, was reduced in the presence of leucine, but not HMB, in replicatively aged cells. Although the mechanisms not fully understood. These data and those derived from wound healing studies suggest that while the cells do not improve fusion, they are not resistant to anabolic stimuli, as illustrated in these studies. Underpinning mechanisms remain to be further clarified.
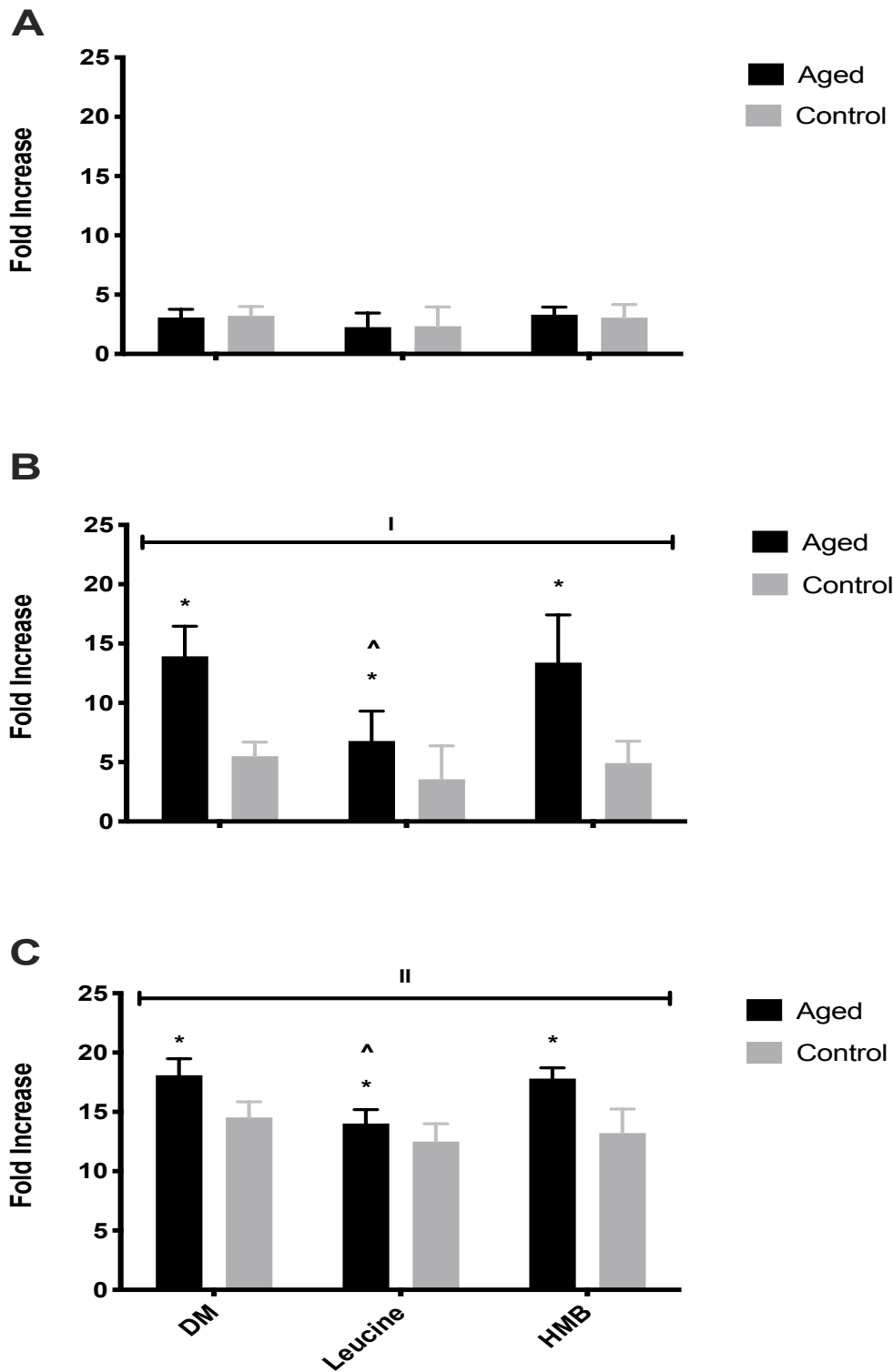
Figure 4.17. Lactate dehydrogenase activity at 24 h (A), 48 h (B) and 96 h (C) in replicatively aged and control myoblasts in the absence and presence of 10 mM leucine and HMB. Data reported as mean ± SD. Significance set at $P < 0.05$. Significance represented as: replicatively aged vs. control (*); supplement vs. DM (^); 24 h vs. 48 h (⊢——⊣: 48 h vs. 96 h (⊢——⊣). Experiments N = 3 all in duplicate.

4.5 Discussion

The overarching aim of this programme of work was to utilise nutritional supplements to improve hypertrophy in control and replicatively aged murine myoblasts. The central objective was to examine the impact of protein supplements on hypertrophy in control and aged cell models. We hypothesised that: 1. Control myoblasts would fuse under basal conditions, whereas replicatively aged myoblasts would not. 2. Leucine and HMB would further increase control hypertrophy and stimulate the initiation of fusion in replicatively aged C_2C_{12} cells; 3. That mTOR, Akt and ERK phosphorylation would be increased in control myoblasts stimulated with leucine and HMB supplementation compared to replicatively aged myoblasts and 4. That there would be reduced gene expression in IGF-I/II, myogenin, SLC7A5 and SLC3A2 which would underpin compromised fusion.

4.5.1 Replicatively Aged Myoblasts Do Not Fuse Under Basal Conditions vs. Control

Replicatively aged myoblasts underwent serial passaging (Sharples *et al*., 2011), and these cells display characteristics similar to those of aged primary human myoblasts (Bigot *et al*., 2008). We accepted our hypothesis, that basally, replicatively aged myoblasts would not fuse vs. unaged controls. Morphologically, in replicatively aged myoblasts after 96 h, no myotubes formed compared to control cells. This has previously been shown by our group (Sharples *et al*., 2011). The authors identified reduced CK in replicately aged myoblasts (Sharples *et al*., 2011), which was in line with our findings. Which is in contrast to isolated primary human myoblasts do fuse (Bigot *et al*., 2008; Foulstone *et al*., 2004), albeit forming smaller myoblasts than cells from young donors. These findings indicate that basally, replicatively aged myoblasts do not fuse, supported by significant attenuation of CK concentrations.

Therefore, we aimed to establish the intracellular signalling responses underpinning adaptations of replicatively aged myoblasts compared to unaged controls. In the literature, Akt-mTOR, MAPK-ERK and MAPK-p38 signalling pathways contribute to myoblast differentiation (Li *et al.*, 2000; Foulstone *et al*., 2004; Al-Shanti and Stewart,

2008). Akt phosphorylation in replicatively aged cells was significantly decreased compared to control cells. Supporting our hypothesis, mTOR phosphorylation was impaired in replicatively aged cells compared to unaged controls. In muscle hypertrophy, it is well established that the mTOR pathway is integral (Saxton and Sabatini, 2017). The inhibition of mTOR, dosing with rapamycin in C_2C_{12} myoblasts, have reported lack of myotube formation in (Erbay and Chen, 2001). Indeed, in aged individuals and rodent models, it was proposed that autophagy (programmed recycling of proteins) was increased (Kim *et al.*, 2011) which inhibits mTOR by activating AMPK phosphorylation via ULK1 (Kim *et al.*, 2011). This data supports the findings in this study that lack of myotube formation in-part could be due supressed Akt/mTOR signalling.

The MAPK-ERK and p38 pathways are involved in activating cell differentiation (Li *et al.*, 2000; Foulstone *et al.*, 2004; Al-Shanti and Stewart, 2008; Kim *et al.*, 2009). Data in this study indicate that ERK activation was suppressed in replicatively aged cells compared to control. ERK was reported to activate Raptor, a substrate of mTORC1 through activating p90RSK (Romeo *et al.*, 2012), which resulted in improved muscle differentiation (Romeo *et al.*, 2012). The findings from our study suggest that there were no changes in p38 phosphorylation. Other studies report increased p38 phosphorylation increases in cell differentiation by inhibiting ERK 1/2 (Al-Shanti and Stewart, 2008). Further mechanisms for p38's role in muscle differentiation have been reported through phosphorylation of p38-γ (Gillespie *et al.*, 2009; Lassar, 2009). However, we did not distinguish between different isoforms, that could initiate different signalling pathways (Wang *et al.*, 2008). Therefore, reduced Akt, mTOR and ERK signalling could prevent replicatively aged myoblast fusion, to ascertain downstream mechanisms, gene expression was measured.

For muscle growth, the expression of myogenin, myostatin IGF-I, IGF-II, ID3, SETD3, PIK3C3, URB5 and FOXO3 were measured. Myogenin was well established to be involved in muscle cell differentiation (Hasty *et al.*, 1993). Myogenin was increased by the suppression of pro-proliferation of myogenic regulatory factors (e.g. MyoD) Rawls *et al.*, 1998). In our model it was reported that replicatively ageing supresses myogenin compared to unaged controls (Sharples *et al.*, 2011), this corresponds with the findings

of the data from this study. The negative regulator in muscle growth, myostatin, was reported in many ageing studies that analysed gene expression (McKay *et al.*, 2012). Our results indicate, that over time myostatin increased in aged cells when normalised to control cells. It was reported that as myostatin increases, the myogenic regulators of differentiation (MyoD and Myogenin), as well as CK (Ríos *et al.*, 2013) are inhibited. The lack of CK and myogenin in replicatively aged cells in our study could be due to these mechanisms. The growth factors, IGF-I and IGF-II are also essential for myoblast differentiation, resulting in the activation of the Akt-mTOR signalling pathway (Hughes *et al.*, 2016). IGF-I in replicately aged cells, but not control, was suppressed over time. This supports the literature, that IGF-I was integral in unaged myoblast fusion and likely activates Akt-mTOR as supported by the signalling results in this and other studies (Hughes *et al*., 2016). The reduction of IGF-I in aged cells coincides with reduction in Akt leading to suppression of fusion, with control cells reporting opposite effects. Moving forward, IGF-II expression at 96 h was significantly reduced in replicatively aged cells compared to untreated controls. IGF-II regulates MyoD by recruiting specific coactivators and controls terminal differentiation (Stewart *et al.*, 1996). Overall, from the outcomes from this study, and also supported by the literature, our data suggest that in replicately aged myoblasts, suppression in IGF-I and IGF-II, with reduced downstream signalling and altered expression of myogenic regulatory factors could impair myotube formation.

Further, ID3 is a helix-loop helix protein that is proposed to inhibit muscle cell differentiation (Melnikova *et al.*, 1999). At 24 h, replicatively aged myoblasts increased ID3 gene expression which was reduced by 96 h, back to baseline. It was reported that cells upregulate ID3 to block differentiation (Al-Shanti *et al*., 2008). However, this was contradictory to the fact that the control cells also expressed increased ID3 expression throughout, and still fused. Conversely, it was proposed that ID3 interacts with IGF-II to regulate the rate of differentiation (Navarro *et al.*, 2001; Al-Shanti and Stewart, 2008), via a feed forward loop. However, it would be expected that as IGF-II expression increased over 96 h, so would ID3 in control cells, our results show no change in ID3 expression, warranting further investigation as to its role in control cell fusion. The identification of novel proteins (SETD3, URB5 and PIK3C3) were measured as a result of interesting findings from Seaborne *et al* (2018 & 2019) and others (Wilkinson *et al.*, 2019; Zhao *et al.*, 2019). The expression of these three genes

showed no differences between replicatively aged and unaged cells, or over 96 h. However, the basal C_T values for PIK3C3 and URB5 suggest that these proteins were highly expressed in both replicatively aged and unaged cells. Future studies should aim to identify the specific function of these genes in relation to different biological processes, under varying conditions. Moreover, FOXO3 is a protein which triggers cell apoptosis and autophagy (Sanchez *et al.*, 2012). Our results show no impact of age or time on FOXO3 expression, which together with cell counting and morphology data (both of which indicate an absence of apoptosis) suggest that the process of apoptosis/autophagy does not underpin the absence of fusion in replicatively aged cells.

For myoblasts to fuse into myotubes, the interactions between neighbouring cells and their environment are required (Przewoźniak *et al.*, 2013). However, no changes in ADAM10 and CDH1 were reported between replicatively aged and control myoblasts. From these data, it can be proposed that the complete lack of replicatively aged myoblasts to fuse under basal conditions was due to changes in the gene expression (IGF-I, IGF-II, myogenin, myostatin) of key regulatory proteins with suppressed signalling from the IGF-I or insulin receptors preventing correct expression of myogenic regulatory factors. Therefore, one of the challenges was to combat this impairment in fusion. In this study, given the data in humans which suggests nutritional supplements can enhance hypertrophy, we performed the same measures as above, but in the presence of leucine and HMB.

4.5.2 Effects of Leucine and HMB Supplementation on Myoblast Fusion

Protein consumption is reported to simulate muscle hypertrophy (Churchward-Venne *et al.*, 2012). The primary AA involved in activating muscle growth is leucine (Breen and Churchward-Venne, 2012). Its metabolite is commonly consumed within the public domain, with the aim of also initiating muscle growth, or in ageing individuals, delaying sarcopenia (Breen and Philipps, 2011). However, very little evidence exists that investigates the *in vitro* cellular responses to protein supplementation. Therefore, we hypothesised that leucine and HMB would increase both control and replicatively

aged myoblast fusion. The hypothesis was both accepted and rejected, where both AAs stimulated control myoblast fusion, but did not rescue fusion in replicately aged cells.

To further investigate the impact of leucine and HMB on control and replicatively aged myoblasts, we investigated intracellular signalling pathways. Leucine and HMB increased Akt phosphorylation in replicatively aged cells at 120 minutes. In addition, HMB increased mTOR phosphorylation at 120 minutes. This provided evidence that the signalling cascades responded to supplementation in both cell models, however, it did not rescue myotube formation in replicatively aged cells. The overall reduction in mTOR activation in replicatively aged was also blunted during ageing (Selman *et al.*, 2009). In control cells, leucine and HMB rapidly increased mTOR phosphorylation which signals translational machinery stimulating MPS, and myotube formation (Areta *et al.*, 2014; Dai *et al.*, 2015), again confirming the cells are responding to supplements, but not with fusion. By contrast, ERK and p38 signalling were not altered with supplementation in replicatively aged or control cells. From these data, it is clear that the replicatively aged cells are responding to amino acid supplementation via improved signalling through Akt and mTOR, however, this was not sufficient to rescue fusion. To further establish the underlying mechanisms that leucine and HMB exhibit on muscle cell fusion, gene expression was undertaken.

Leucine and HMB had no effect on myogenin expression in both replicatively aged and control myoblasts. Some literature has reported that leucine improves mRNA expression of MyoD, which was involved in initial muscle differentiation, but this was not investigated in this study (Dai *et al.*, 2015). Interestingly, there was no impact of supplements on IGF-I gene expression and surprisingly HMB suppressed increases in IGF-II gene expression seen basally, and with leucine supplementation potentially via a feedforward loop to prevent excessive fusion. In addition, against our hypothesis, expression levels of the two large AA transporters were equivalent in both models, underpinning the capacity of both to respond to amino acid supplementation. Overall, the cells are able to respond to AA supplementation with altered signalling profiles evident in the aged myoblasts also, however, this was not sufficient to rescue the blocked differentiation in replicatively aged myoblasts.

Finally, we investigated the impact of supplementation on metabolic enzymes CK and LDH. There was no impact of leucine and HMB on CK response in replicatively aged cells, and a significant increase in CK activity in controls in response to supplements, confirming the data thus far. Interestingly, the replicatively aged cells produced increased concentrations of LDH into the supernatant suggested an increased toxic environment. Surprisingly, leucine inhibited replicatively aged increases in LDH, with no effect with HMB. Typically, increased LDH secretion is associated with apoptosis (Chan *et al.*, 2013). However, this did not occur in our model (see images), and there was no increase in FOXO3 gene expression (involved in apoptosis: Sanchez *et al.*, 2012). Also, other research reported no impact on cell death basally in replicatively aged cells (Brown *et al.*, 2017; Sharples *et al.*, 2011). Therefore, we are completing additional experiments to ascertain the mechanisms behind the increase in secretion of LDH in replicatively aged cells and the ability of leucine to attenuate this response.

4.6 Conclusion

Taken together, control cells responded positively to supplementation with increased fusion, while replicatively aged myoblasts failed to fuse compared to unaged controls, despite supplements increasing Akt and mTOR activation in this model. Suppressed levels of myogenin, IGF-I/II gene expression were not rescued by AA supplementation and require further intervention. The impact of leucine on reducing LDH activity also warrants further investigation, perhaps from a metabolic perspective in replicatively aged myoblasts.

Chapter 5: Dynamic Proteomic Profiling on Replicatively Aged Myoblasts and Myotubes

5.1 Abstract

Introduction: Dynamic proteome profiling is the measurement of protein abundance and synthesis within a tissue or cell. Replicatively aged cells do not fuse basally and myoblast fusion is integral for efficient regeneration and growth. Therefore, the aim was to establish the proteome of replicatively aged myoblasts and myotubes to enable interventions targeting impairments in myoblast fusion.

Methods: Differentiating replicatively aged and control myoblasts were lysed at 0 h, 24 h, 72 h and 96 h. Deuterium oxide (D_2O) was added to myoblasts from 0 h-24 h and myotubes from 72 h-96 h. Proteins were digested and loaded through liquid chromatography mass spectrometry (LC-MS) to measure relative abundance and consequently calculate the fractional synthesis rate (FSR) (via D_2O incorporation).

Results: Replicatively aged myoblasts had 33 ribosomal proteins with significantly lower ($P < 0.01$) abundance vs. control. There were 10 metabolic enzymes with significantly greater ($P < 0.01$) abundance in replicatively aged myoblasts vs. control. Nine contractile proteins with significantly lower abundance ($P < 0.01$) in replicatively aged myotubes vs. control. Replicatively aged myoblasts and myotubes had significantly lower FSR (both $P < 0.01$) vs. control myoblasts and myotubes. Both control and replicatively aged myoblasts contained significantly greater (both $P < 0.01$) FSR compared to age-matched myotubes.

Conclusion: Replicatively aged myoblasts and myotubes had reduced abundance of ribosomal and contractile proteins, some that were involved in muscle differentiation. Replicatively aged cells suggest increased energy demands from greater abundance of glycolytic enzymes. Finally, replicatively aged cells protein turnover was reduced compared to control. Therefore, interventions to increase FSR could increase the abundance of ribosomal and contractile proteins involved in muscle differentiation.

5.2 Introduction

The proteome consists of the entire complement of proteins within a cell, tissue or organism. Proteomics is the term used for high-throughput protein investigations, which often use mass spectrometry. Dynamic profiling involves the analysis of the abundance and synthesis rate of proteins on a protein by protein basis (Camera *et al.*, 2017). Protein dynamic profiling is more complex and challenging than well-established protein abundance measurements or techniques for studying post-translational modifications. Dynamic measurement requires methods of labelling proteins as they are synthesised, for instance, stable isotopes and stable isotope-labelled amino acids.

In particular, the stable isotope labelling by amino acids (SILAC) can be used to identify protein abundances and turnover rates (Ong *et al.*, 2002; Cambridge *et al.*, 2011). SILAC requires the growth of two populations of cells, one cell population containing 'light isotope' medium which contains the natural isotope abundance. The other cell population contains 'heavy isotope' media which contains the amino acid of the researcher's choice (Ong and Mann, 2007). For the 'heavy isotopes' to fully incorporate into the cells, usually five cell doublings are required (Zhu *et al.*, 2002). The samples from unlabelled ('light isotope') and labelled ('heavy isotope') are mixed, then analysed by mass spectrometry. Indeed, studies that use 'dynamic' SILAC (Cambridge *et al.*, 2011) exchanges the media between cells to measure protein turnover. However, the SILAC method is time consuming and expensive. Also, incomplete incorporation of heavy medium contributes to signal of light label affecting quantitation accuracy (Deng *et al.*, 2019). In addition, only one label is incorporated into each peptide, which reduces sensitivity. Also, the identification between light and heavy isotopes complicates analysis and takes up more analytical space. Therefore, we dosed cells with D_2O which offers insight into synthesis and abundance of individual proteins over time (Camera *et al*., 2017).

D_2O labelling becomes incorporated into the majority of amino acids (Busch *et al.*, 2006). From an administration perspective, in human studies, D_2O can be administered via drinking water over a number of days and it is non-hazardous at

enrichment concentrations less than 20 % MPE (Barbour, 1937). Previous studies have administered D_2O in rodents and cells with enrichment of 4 % (Busch *et al.*, 2006; Miller *et al.*, 2015; Foletta *et al.*, 2016). After supplementation of D_2O, the H-C bonds of amino acids become labelled intracellularly via de-novo synthesis and transamination (Busch *et al.*, 2006). Thus, the major advantage of this labelling is that biological processes are not affected, for example, amino acid metabolism and membrane transport (Busch *et al.*, 2006). In addition, the incorporation of D_2O is irreversible after the amino acid has been incorporated into a polypeptide (Busch *et al.*, 2006; Kasumov *et al.*, 2013) which enables D_2O to tag newly synthesised proteins. In summary, D_2O incorporation has the advantage in investigating the protein turnover in skeletal muscle and cells in both rodents and humans.

Understanding the abundance and synthesis rates of individual proteins via D_2O administration enables an in-depth insight to skeletal muscle adaptation, in relation to, for example, exercise, nutrition, muscle diseases and aging. In relation to this thesis, understanding the regenerative process in C_2C_{12} myoblast differentiation and our model of replicatively ageing (Sharples *et al.*, 2011). Indeed, previous research has labelled D_2O in humans, rodents and cells (Brook *et al.*, 2015; Foletta *et al.*, 2016; Hesketh *et al.*, 2016; Camera *et al.*, 2017). In 10 males, research has shown muscle protein synthesis to increase 18 % after 3 weeks of unilateral leg extension exercises with D_2O incorporation (Brook *et al.*, 2015). In addition, Camera *et al.* (2017) researched the effect of resistance training and high fat diet on muscle protein synthesis, degradation and abundance. In the control condition, skeletal muscle proteins exhibited range of synthesis rates, therefore, average rates on mixed muscle proteins may be insufficient to fully capture muscle protein dynamics. Indeed, in the resistance training group, displayed proteins that underwent increased synthesis, but the protein abundance did not change, due to changes in degradation (Camera *et al.*, 2017). This study demonstrates the in-depth analysis of individual protein abundance, turnover and breakdown in humans. In rodents, Hesketh *et al.* (2016) were the first to investigate protein synthesis via D_2O incorporation on individual proteins across different striated muscles. Results provided insights to varying proteins such as albumin, actin, creatine kinase and ATP synthase having markedly different synthesis rates in heart, diaphragm, soleus and extensor digitorium longus (Hesketh *et al.*, 2016).

Currently, only two studies (Foletta *et al*., 2016: Miller *et al*., 2015), to the authors knowledge, have labelled C_2C_{12} myoblasts with deuterium and reported average synthesis rates. Foletta *et al*. (2016) labelled proliferating and non-proliferating C_2C_{12} cells with D_2O, and measured turnover in myoblasts and myotubes, stating that myoblast turnover was higher than myotubes. Miller *et al*. (2015) developed a mathematical model that aimed to identify different labelling periods on C_2C_{12} myotubes and to measure synthesis rates at the individual protein level. The authors labelled and isolated the myoblasts for 2-day, 4-day and 7-day. The authors reported that the turnover was greater during the shorter timeframe (e.g. 2-day) compared to longer periods (7-day) providing evidence that cells also have broad range of turnover rates (Miller *et al*., 2015).

In **chapter 5**, we reported that replicatively aged fusion was significantly impaired compared to control via the suppression of signalling molecules and gene expression involved in myoblast differentiation. Therefore, the aim of this study was to investigate the abundance and turnover of individual proteins to establish targets for subsequent interventions. The objectives were firstly, to determine the abundance and FSR of proteins involved in myoblast differentiation. Secondly, to determine the protein profile in replicatively aged myoblasts that do not fuse basally. The hypothesis were 1: that myoblasts have greater FSR compared to myotubes and 2: replicatively aged myoblasts and myotubes lacked abundance of proteins involved in myoblast fusion.

5.3 Methods

5.3.1 Cell Culture

All standardised cell culture procedures were previously described in **section 2.2.1.** Briefly, cells were seeded in 6 well plates and grown to 80 % confluency.

5.3.2 Cell Differentiation and Dosing Strategy

After cells had attained 80 % confluency they were washed twice in PBS and then cultured in DM. Isotopic labelling of newly synthesised proteins was achieved by supplementing the DM with 4 % (v/v: 99 % MPE: Foletta *et al*., 2016: Miller *et al*., 2015) sterilised D_2O (Sigma-Aldrich, Dorset, UK) over a period of 24 h. Labelling of myoblasts began immediately, i.e. during the first 0-24 h of differentiation, whereas myotubes were labelled from 72 h to 96 h after transfer into DM. Each condition was repeated in triplicate alongside non-labelled cells that were differentiated in media that did not contain D_2O (Figure 5.1).
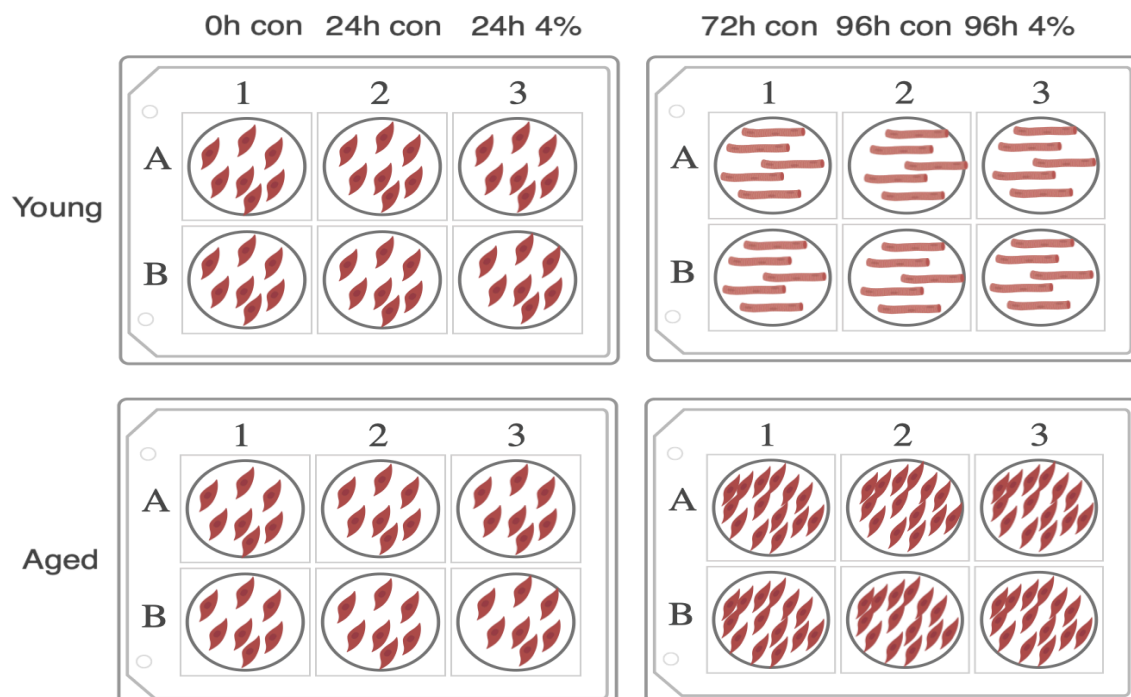
Figure 5.1. Schematic to illustrate cell culture experiment design.

5.3.3 Cell Extraction

Cells were collected by cell scraping at 0 h, 24 h, 72 h and 96 h after exchange in to DM and lysed in 250 µl RIPA buffer (**see section 2.5.4**). Samples were collected into labelled 1.5 ml Eppendorf tubes and stored at -80 °C until further analyses.

5.3.4 Protein Assay

The quantification of total protein was measured on the lysed samples using the Pierce BCA protein assay kit was used and manufacturer's guidelines were followed (**see section 2.6.2**). BSA standards were prepared by serial dilution of 2 mg/ml to 0.03 mg/ml and 20 µl of sample was added to each well. All the samples were pipetted in duplicate and then 200 µl of working agent was added to each well. The samples were incubated at 37 °C for 60 minutes. Finally, the samples were scanned at an absorbance of 595 nM. Protein concentrations of cell samples were interpolated from the standard curve via linear regression calculation.

5.3.5 Cell Preparation and Liquid Chromatography-Mass Spectrometry

For detailed proteomic methods, refer to **section 2.9.2**. Briefly, extracts containing 100 ug of protein were digested using the FASP method (Wiśniewski *et al.*, 2009). Samples containing 4 µg peptides, were desalted using C_{18} Zip-tips (Millipore, Billercia, MA, USA) following the manufacturer's instructions. Then, 20 µl of 2.5 % ACN, 0.1 % FA containing 10 fmol/µl yeast ADH1 was added to samples. The samples were transferred to autosampler tubes in preparation for LC-MS and both MS and MS/MS spectra were imported into Progenesis QIP software (Waters Corp. Milford, MA). Spectra were aligned using prominent ion features (mean ± SD per chromatogram: 455 ± 42) as vectors to provide a common reference chromatogram. The MS data (peptide abundances) was log transformed and normalised by inter-sample abundance ratio. MS/MS spectra were exported in Mascot generic format and searched against the UniProt database.

5.3.6 Data and Statistical Analysis

The log transformed MS data were used to investigate differences in protein abundance between myoblasts and myotubes as well as control and replicatively aged cells using one-way ANOVA and Bonferroni post hoc pairwise comparison. FSR was calculated from the ratio of unlabeled and labelled peptide mass isotopomer peaks, for full details see section **(2.9.1 and 2.9.2)**. Differences in FSR of proteins between myoblasts and myotubes together with control and replicatively aged, a one-way ANOVA and Bonferroni post hoc correction was used. Each peptide spectral match (PSM) that is selected contains some degree of error, and incorrect PSMs could be identified. The false discovery rate (FDR) is a measure of incorrect PSMs among all accepted PSMs (Aggarwal and Yadav, 2016). In essence, it is a global estimate of the false positives present in results obtained by database search algorithms (Benjamini and Hochberg, 1995). However, this communicates nothing about confidence of the individual PSMs. Thus, the q-value which is a minimum FDR cut off of a specific PSM can be accepted, providing a direct measure of significance of a specific PSM in relation to a complete dataset (Storey and Tibshirani, 2003). To control FDR, P-value distributions were used to calculate q-values and a criterion FDR of <10 % was set. This statistical approach considers the biological variation across each protein and is more sophisticated than arbitrarily implementing a threshold based on fold-change.

5.4 Results

5.4.1 The Abundant Proteins Identified in Control Myoblast to Myotube Differentiation Were Not Observed in Replicatively Aged

Label-free quantification was used to measure protein abundances in control myoblasts compared to myotubes and replicatively aged myoblasts compared myotubes. Proteomic analysis encompassed 237 proteins and 56 proteins exhibited a significant (P < 0.01: 10 % FDR) difference in abundance between control myoblasts and myotubes (Figure 5.2A). Twenty-five proteins were significantly (P < 0.01: 10 % FDR) different between myoblasts and myotubes that had been replicatively aged (Figure 5.2B).

There were 15 ribosomal proteins with significantly greater (P < 0.01: 10 % FDR) abundance in control myoblasts vs. control myotubes (Figure 5.2A: Table 5.2). There was significantly greater (P < 0.01: 10 % FDR) abundance of 8 contractile proteins in control myotubes vs. control myoblasts (Figure 5.2A). Those contractile proteins were: actin (ACTC), filamin-C (FLNC), myosin-3 (MYH3), nestin (NEST), spectrin alpha chain (SPTN1), desmin (DESM), clathrin heavy chain 1 (CLH1) and tubulin beta-3 Chain (TBB3). By contrast, there were 8 metabolic enzymes with significantly higher (P < 0.01: 10 % FDR) abundance in control myotubes compared to control myoblasts. These 8 proteins included: ADP/ATP translocase (ADT2), ATP synthase subunit beta (ATPB), NADH-cytochrome B5 reductase 3 (NB5R3), PRA1 Family Protein 3 (PRAF3), and aldo-keto reductase family 1 Member B1 (ALDR), ATP synthase alpha (ATPA), ATP synthase subunit F (ATPK) and elongation factor 1 beta (EF1B). The greater abundance of ribosomal, contractile and metabolic proteins in control myoblast and myotubes were not observed in replicatively aged cells (Figure 5.2: Table 5.2).

There was 9 common proteins that were significantly (P < 0.01: 10 % FDR) greater in abundance in control and replicatively aged myoblasts compared to aged matched myotubes (Figure 5.3). Whereas, there was three proteins (ADT2, FLNC, NEST) that were significantly (P < 0.01: 10 % FDR) greater in abundance in control and replicatively aged myotubes compared to aged matched myoblasts (Figure 5.3).
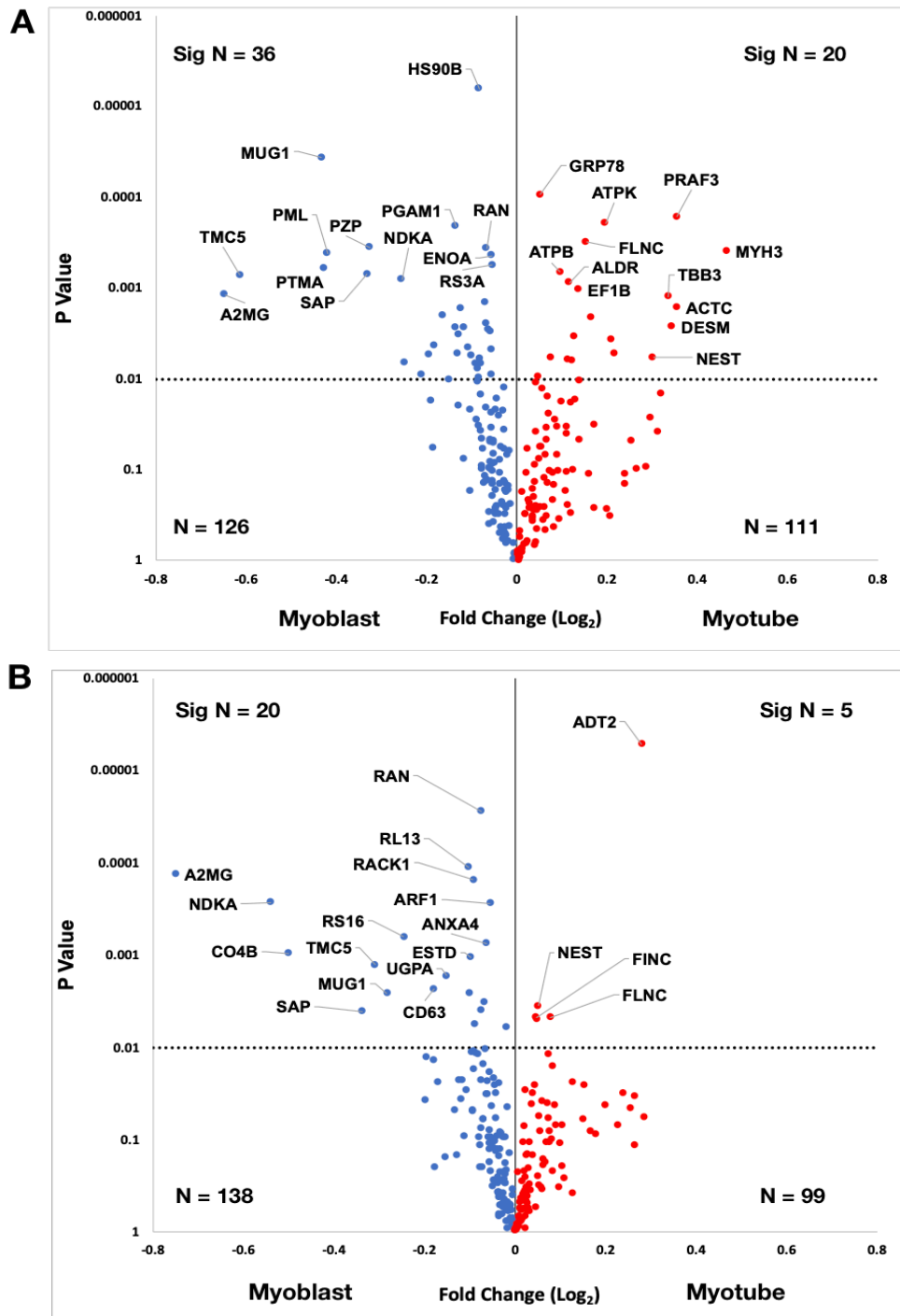
Figure 5.2. Differences in relative abundances (N = 237) between control (A) and replicatively aged (B) myoblasts and myotubes.

The relative abundance changes (fold change, log_2) were plotted against P-values from one-way ANOVA and reported in a volcano plot. Myoblasts at 0 h was compared to myotubes at 72 h. Proteins that were statistically significant if the false discovery rate (FDR) was 10 % (above P < 0.01 line). Protein labels represent UniProt knowledgebase identifier.
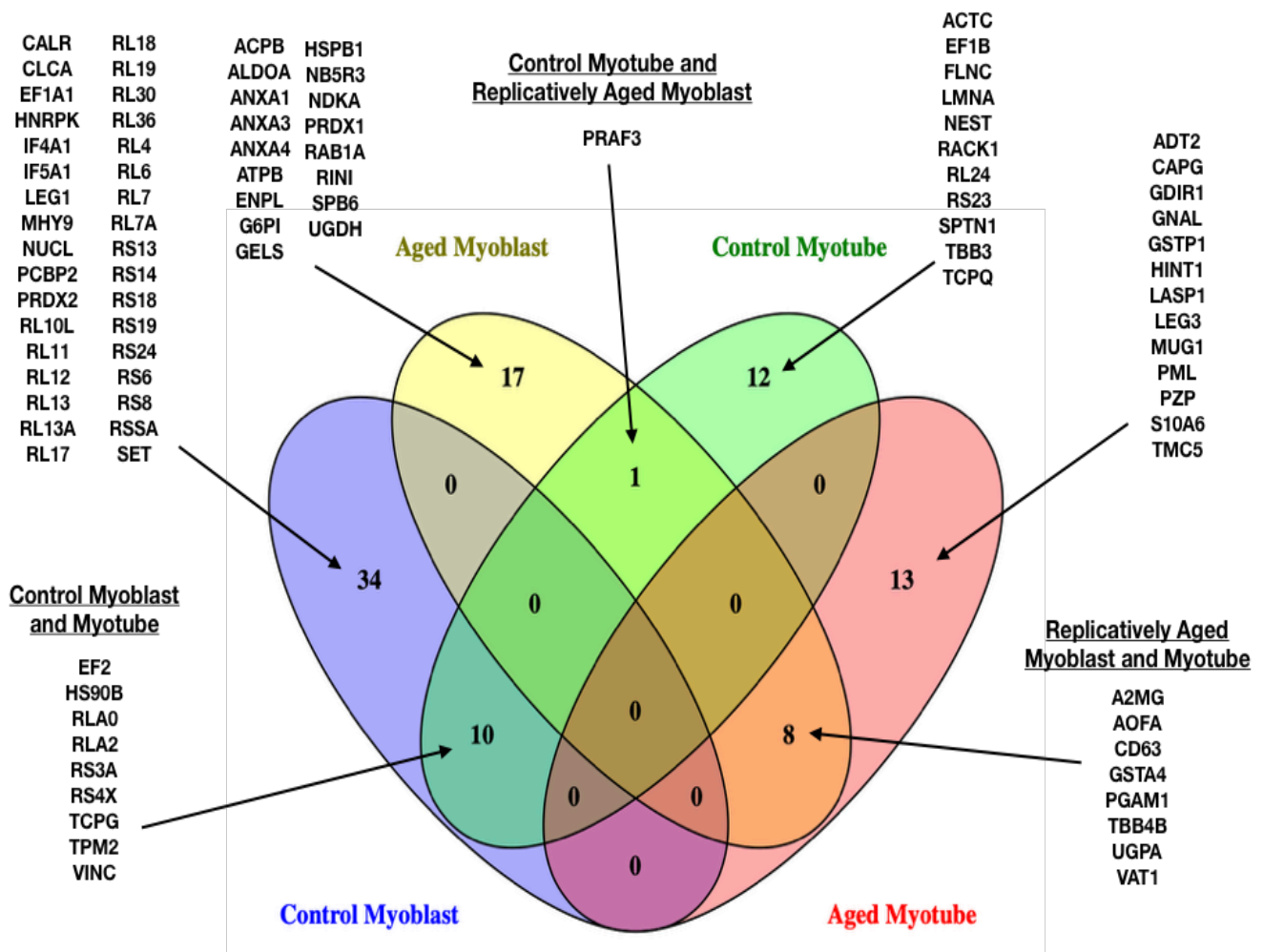
Figure 5.3. Venn diagram reporting common proteins when comparing control and replicatively aged myoblasts compared to myotubes.

Proteins significantly greater (P < 0.01: FDR 10 %) in comparisons between cell phenotype. Venn diagrams created using Venny online software (Oliveros, 2007).

5.4.2 Fractional Synthesis Rates were Greater in Control and Replicatively Aged Myoblasts vs. Aged-Matched Myotubes

The average FSR in control myoblasts (0.558 ± 0.275 %/h) was significant greater (P < 0.001: 22%) than control myotubes (0.458 ± 0.419 %/h). Similarly, the average FSR in replicatively aged myoblasts (0.470 ± 0.314 %/h) was significant greater (P < 0.001: 87%) than replicatively aged myotubes (0.252 ± 0.230 %/h) (Table 5.1).

Table 5.1. FSR of Control and Replicatively Aged Myoblasts and Myotubes.

	Mean FSR ± SD (%/h)	
	Myoblast	Myotube
Control	0.558 ± 0.275*^	0.458 ± 0.419^
Replicatively Aged	0.470 ± 0.341*	0.252 ± 0.230

Significant increase (P < 0.05) in myoblast compared to myotubes (*).
Significant increase (P < 0.05) in control compared to replicatively aged (^).

There were 124 proteins with relatively greater FSR in control myoblasts compared to 23 in control myotubes (Figure 5.4A). The protein galectin-1 (LEG1), 14-3-3 protein zeta/delta (1433Z), protein S100-A10 (S10AA) and 60S ribosomal protein L36 (RL36) had significantly (P < 0.01: 10 % FDR) greater rates of synthesis in control myoblasts compared to control myotubes.

Lastly, 112 proteins were relatively greater in protein FSR in replicatively aged myoblasts compared to 37 in replicatively aged myotubes (Figure 5.4B). There was 12 statistically significant (P < 0.01: 10 % FDR) proteins with higher FSR in replicatively aged myoblasts compared to replicatively aged myotubes. There were 3 contractile proteins (actin (ACTB), moesin (MOES), myosin light polypeptide 6 (MYL6)) and 3 metabolic enzymes (alpha-enolase (ENOA), ATPB and glyceraldehyde-3-phosphate dehydrogenase (G3P)). Whereas, in replicatively aged myotubes, there were 3 proteins with significantly higher (P < 0.01: 10 % FDR) FSR compared to myoblasts. These 3 proteins were 60S ribosomal protein L7a (RLA7), 60S ribosomal protein P2 (RLA2) and annexin A2 (ANXA2).
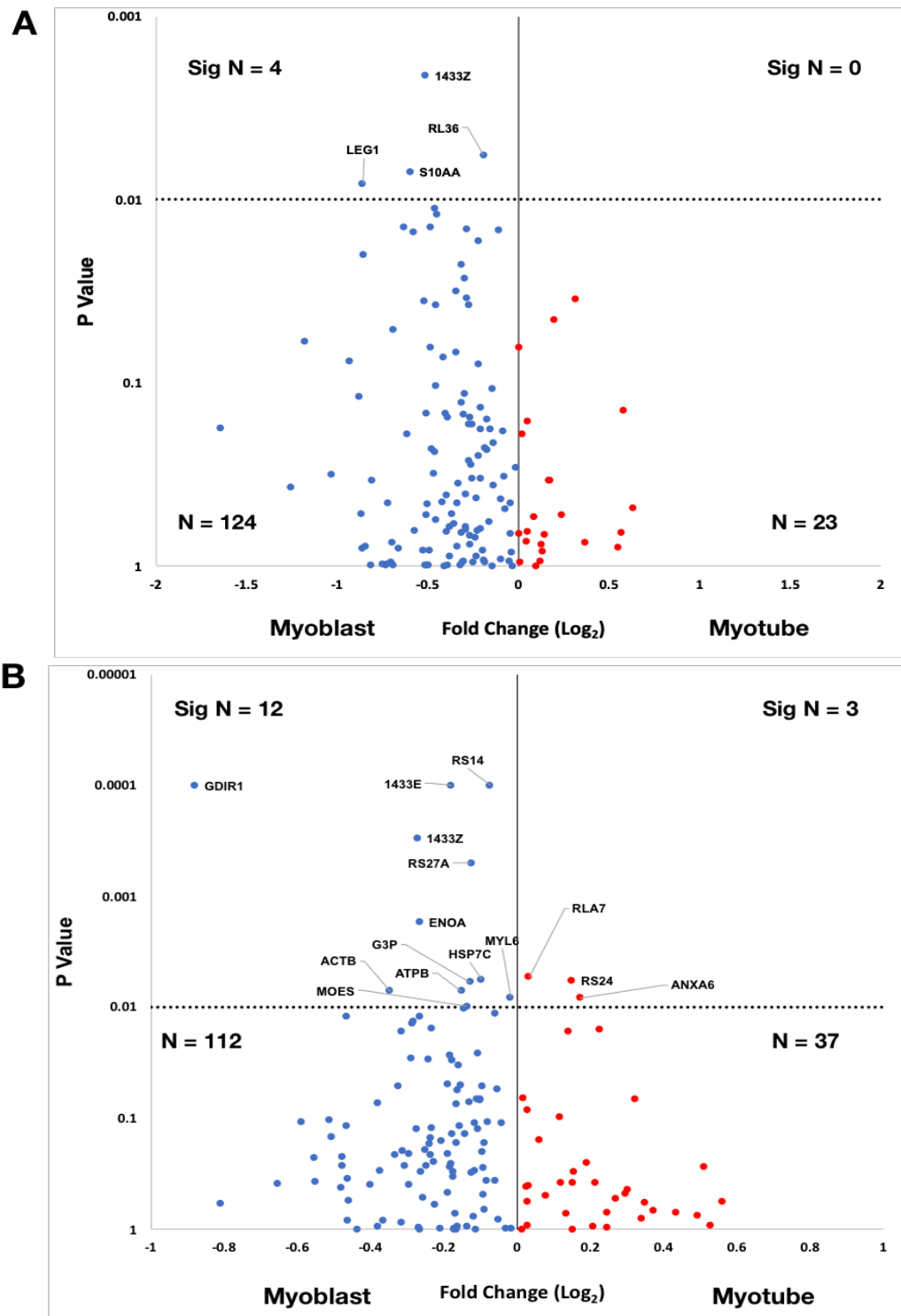
Figure 5.4. Differences in FSR between control (A) and replicatively aged (B) myoblasts and myotubes.

The FSR fold change ($\log_2$) were plotted against P-values from one-way ANOVA and reported in a volcano plot. Myoblasts and myotubes were labelled for 24 h (0 h-24 h and 72 h-96 h). Proteins that were statistically significant if the false discovery rate (FDR) was 10 % (above P < 0.01 line). Protein labels represent UniProt knowledgebase identifier.

5.4.4 Contractile and Ribosomal were Relatively more Abundant in Control vs. Replicatively Aged Myoblasts and Myotubes

Following abundance and FSR during differentiation from myoblasts to myotubes in both control and replicatively aged. Abundance was compared between control and replicatively aged in myoblasts and myotubes. In total, the volcano plots compared 237 proteins between myoblasts and myotubes (Figure 5.5). Seventy proteins exhibited a significant ($P < 0.01$: 10 % FDR) difference in abundance in control myoblasts and replicatively aged myoblasts (Figure 5.5A). Whereas, 44 proteins demonstrated significant ($P < 0.01$: 10 % FDR) difference in abundance between control myotubes and replicatively aged myotubes (Figure 5.5B).

In control myoblasts there was 33 ribosomal proteins with significantly greater ($P < 0.01$: 10 % FDR) abundance compared to replicatively aged myoblasts (Figure 5.5A: Table 5.2). In contrast, there was only the ribosomal protein nucleoside diphosphate kinase A (NDKA) with significantly higher ($P < 0.01$: 10 % FDR) abundance in replicatively aged myoblasts compared to control myoblasts (Figure 5.5A). Alternatively, there was 10 metabolic enzymes in replicatively aged myoblasts that had significantly greater ($P < 0.01$: 10 % FDR) relative abundance compared to control myoblasts (Figure 5.5A). These included: fructose-bisphosphate aldolase A (ALDOA), amine oxidase A (AOFA), ATPB, glucose-6-phosphate Isomerase (G6PI), glutathione s-transferase A4 (GSTA4), NB5R3, phosphoglycerate Mutase 1 (PGAM1), PRAF3, UTP-glucose-1-phosphate uridylyltransferase (UGPA) and UDP-glucose 6-dehydrogenase (UGDH).

Further, in control myotubes there was 7 ribosomal proteins with significantly greater ($P < 0.01$: 10 % FDR) relative abundance compared to replicatively aged myotubes (Figure 5.5B). These included: elongation factor 2 (EF2), 60S ribosomal protein 24 (RL24), 60S acidic ribosomal protein P0 (RLA0), RLA2, 40S ribosomal protein S23 (RS23), 40S ribosomal protein S3a (RS3A) and 40S ribosomal protein S4X (RS4X). In addition, there was 9 contractile proteins with significantly higher ($P < 0.01$: 10 % FDR) abundance in control myotubes compared to replicatively aged myotubes (Figure 5.5B). For instance: ACTC, FLNC, tropomyosin beta chain (TPM2), vinculin

(VINC), TBB3, NEST, MYH3, SPTN1 and translationally-controlled tumor protein (TCTP). Whereas, in replicatively aged myotubes, there were 6 metabolic enzymes with significantly higher (P < 0.01: 10 % FDR) in relative abundance compared to control myotubes (Figure 5.5B). These 6 metabolic enzymes included: ADT2, AOFA, GSTA4, PGAM1, UGPA and glutathione s-transferase P1 (GSTP1).

Ten proteins were significantly (P < 0.01: 10 % FDR) greater in abundance in both control myoblasts and myotubes compared to replicatively aged myoblasts and myotubes (Figure 5.6). Five of those proteins were ribosomal and included: EF2, RLA2, RS4X, RLA0 and RS3A. In addition, 8 shared proteins were significantly (P < 0.01: 10 % FDR) greater in abundance in both replicatively aged myoblasts and myotubes (Figure 5.6) compared to control myoblasts and myotubes. Four of those proteins were metabolic and included: AOFA, GSTA4, PGAM1, UGPA.
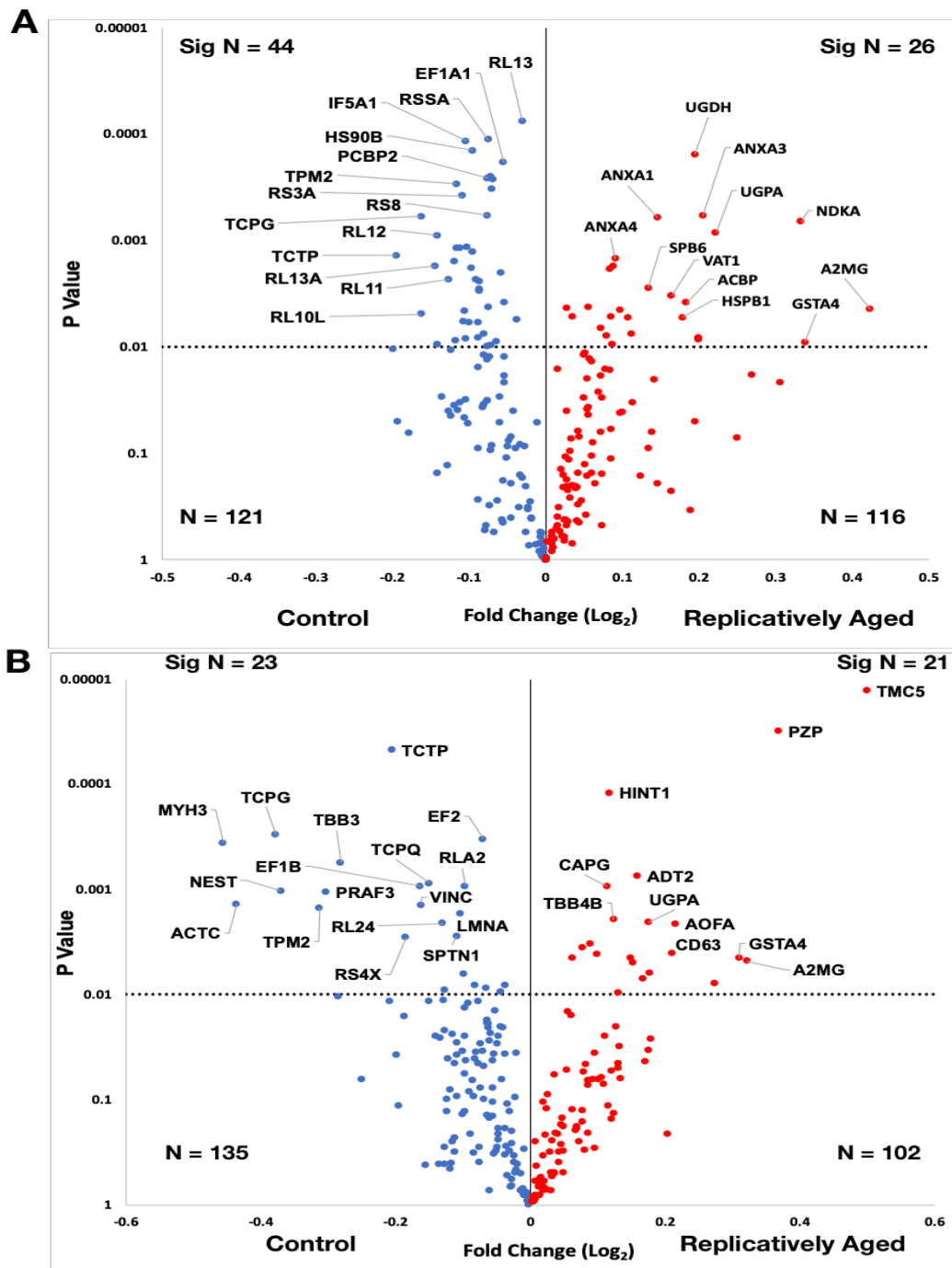
Figure 5.5. Differences in relative abundances (N = 237) between control and replicatively aged myoblasts (A) and myotubes (B).

The relative abundance changes (fold change, $\log_2$) were plotted against P-values from one-way ANOVA and reported in a volcano plot. Replicatively aged and control myoblast at 0 h and myotube at 72 h were compared. Proteins that were statistically significant if the false discovery rate (FDR) was 10 % (above P < 0.01 line). Protein labels represent UniProt knowledgebase identifier.

ACTC LMNA
ALDR MYH3
ATPA NB5R3
ATPB PRAF3
ATPK SPTN1
CLH1 TBB3
DESM TCPG
EF1B TPM2
GRP78

ANXA4
ANXA5
ARF1
CD63
CNN3
CO4B
RAB1A
RL13
RS16
RSSA
UGPA

ENOA PGAM1
FLNA PML
GSTA4 PTMA
HINT1 PZP
HS90A RL10L
HS90B RL12
HS97C RL6
IF5A1 RL7A
KPYM RS12
LDHA RS3A
LEG3 RS6
NPM SET
NUCL TCPB
PCBP2

Control Myotube

Aged Myoblast

17

11

0

0

0

27

0

0

2

CLCA
FINC

0

0

0

9

3

Control and Replicatively Aged Myoblasts

A2MG
ESTD
MUG1
NDKA
PRDX1
RACK1
RAN
SAP
TMC5

0

0

0

Control Myoblast

Aged Myotube

Control and Replicatively Aged Myotubes

ADT2
FLNC
NEST

Figure 5.6. Venn diagram reporting common proteins when comparing control vs. replicatively aged myoblasts and myotubes.

Proteins significantly greater (P < 0.01: FDR 10 %) in comparisons between cell phenotype. Venn diagrams created using Venny online software (Oliveros, 2007).

5.4.5 Fractional Synthesis Rate is Reduced in Replicatively Aged Myoblasts and Myotubes Compared to Control Myoblasts and Myotubes

FSR of mixed proteins in control myoblasts (0.558 ± 0.275 %/h) was significantly (P < 0.001) greater (19 %) than in replicatively aged myoblasts (0.470 ± 0.314 %/h) (Table 5.1). Similarly, the FSR of mixed proteins in control myotubes (0.458 ± 0.419 %/h) was significantly (P < 0.001) greater (82 %) than replicatively aged myotubes (0.252 ± 0.230 %/h) (Table 5.1).

Protein by protein analysis, in control myoblasts highlighted 110 proteins with relatively greater FSR compared to replicatively aged myoblasts (Figure 5.7A). In replicatively aged myoblasts, 40 proteins were relatively higher in FSR compared to control myoblasts (Figure 5.7A). However, only 6 proteins were significantly (P < 0.01: 10 % FDR) higher in FSR in control myoblasts vs. replicatively aged myoblasts (Figure 5.7A). In control myoblasts there were contractile (vimentin (VIME)), mitochondrial (long-chain specific acyl-dehydrogenase (ACADL) and four binding proteins (acyl-CoA-binding protein (ACPB), 1433E, ANXA2 and phosphatidylethanolamine-binding protein 1 (PEBP1). Whereas, in replicatively aged myoblasts there was only RLA2 that had significantly (P < 0.01: 10 % FDR) greater FSR vs. control myoblasts (Figure 5.7A).

Interestingly, results indicate that there were 130 proteins in control myotubes with relatively higher FSR compared to replicatively aged myotubes (Figure 5.7B). In control myotubes, 6 proteins had significantly (P < 0.01: 10 % FDR) higher FSR rate compared to replicatively aged myotubes. Proteins included: ACPB, 1433E, myosin regulatory light chain 12B (ML12B), voltage-dependent anion-selective channel protein 1 (VDAC1), heterogeneous nuclear ribonucleoproteins A2/B1 (ROA2) and 40S ribosomal protein S2 (RS2). By contrast, there was only 22 proteins in replicatively aged myotubes with relatively greater FSR compared to control myotubes, none reached significance (Figure 5.7B).
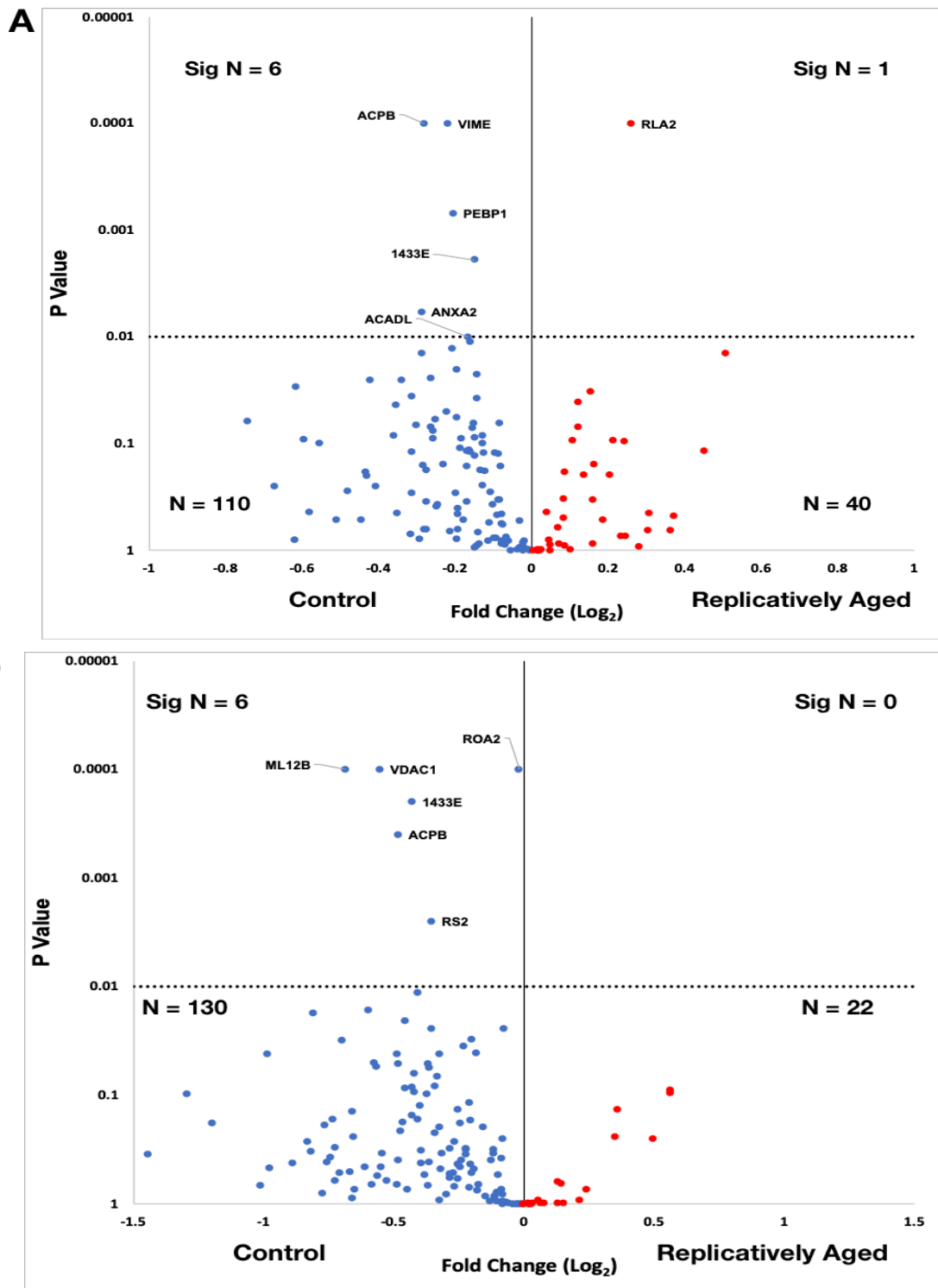
Figure 5.7. Differences in FSR between control and replicatively aged myoblasts (A) and myotubes (B).

The FSR fold change ($\log_2$) were plotted against P-values from one-way ANOVA and reported in a volcano plot. Myoblasts and myotubes were labelled for 24 h (0 h-24 h and 72 h-96 h respectively). Proteins that were statistically significant if the false discovery rate (FDR) was 10 % (above P < 0.01 line). Protein labels represent UniProt knowledgebase identifier.

Table 5.2. Protein accession, function and evidence to support the role in myoblast differentiation.

Name	Accession	Function	Figure	Role in Myoblast Differentiation?	Reference
Ribosomal Proteins					
<u>Transcription</u>					
Heterogeneous Nuclear Ribonucleoprotein K	HNRPK	Pre-mRNA binding protein	5.5A*	Y	Chen *et al*. (2017); Liu *et al*. (2017)
Protein PML	PML	Transcription, apoptosis and senescence	5.5B* + 5.2A^	Y	Butler *et al*. (2009)
Heterogeneous nuclear ribonucleoproteins A2/B1	ROA2	Transcription, RNA nuclear export and binds to telomeric DNA sequences	5.7B*	Y	Chen *et al*. (2017); Liu *et al*. (2017)
40S Ribosomal Protein S16	RS16	RNA binding	5.2B*	N	
60S ribosomal protein L7a	RLA7	RNA binding and transcription	5.4B^	N	
60S Ribosomal Protein L30	RL30	RNA binding	5.5A*	N	
40S Ribosomal Protein S19	RS19	Pre mRNA binding	5.5A*	N	
60S Ribosomal Protein L7A	RL7A	RNA binding	5.5A* + 5.2A*	N	
40S Ribosomal Protein S14	RS14	RNA binding	5.5A* + 5.4B*	N	
60S Acidic Ribosomal Protein P0	RLA0	RNA binding	5.5A* + 5.5B*	N	

Protein	Gene	Function	Spot(s)	Novel	Reference
Protein SET	SET	Apoptosis, transcription, nucleosome assembly and histone chaperoning	5.5A* + 5.5B*	N	
40S Ribosomal Protein S4, X Isoform	RS4X	RNA binding	5.5A* + 5.5B*	N	
40S Ribosomal Protein S3a	RS3A	Transcription	5.5A* + 5.5B* + 5.2A*	N	
60S Acidic Ribosomal Protein P2	RLA2	Elongation in protein synthesis	5.5A* + 5.5B* + 5.7B^	N	
60S Ribosomal Protein L12	RL12	Binds to 26S ribosomal RNA	5.5A* + 5.2A*	N	
60S Ribosomal Protein 24	RL24	RNA binding	5.5B*	N	
Histidine Triad Nucleotide-Binding Protein 1	HINT1	Nucleotide binding and regulation of transcription	5.5B^ + 5.2A*	N	
Translation					
40S Ribosomal Protein S6	RS6	mRNA binding	5.5A* + 5.2A*	Y	Corrick *et al.* (2015)
60S Ribosomal Protein L17	RL17	Cytoplasmic translation	5.5A*	N	
60S Ribosomal Protein L18	RL18	Cytoplasmic translation	5.5A*	N	
Eukaryotic Initiation Factor 4A-1	IF4A1	mRNA binding to the ribosome	5.5A*	N	
60S Ribosomal Protein L11	RL11	mRNA binding	5.5A*	N	
60S Ribosomal Protein L7	RL7	Translation	5.5A*	N	

40S Ribosomal Protein S13	RS13	mRNA binding	5.5A*	N	
40S Ribosomal Protein S	RS8	Translation	5.5A*	N	
40S Ribosomal protein S12	RS12	Translation	5.5A*	N	
Eukaryotic Translation Initiation Factor 5A-1	IF5A1	Involved in translation elongation	5.5A* + 5.2A*	N	
60S Ribosomal Protein L10-like	RL10L	Translation	5.5A* + 5.2A*	N	
60s Ribosomal Protein L6	RL6	mRNA binding	5.5A* + 5.2A*	N	
60S Ribosomal Protein L13	RL13	Translation	5.5A* + 5.2B*	N	
60S Ribosomal Protein L36	RL36	Cytoplasmic translation	5.5A* + 5.4A*	N	
40S Ribosomal Protein S23	RS23	mRNA binding	5.5B*	N	
Ribosome Biosynthesis					
Nucleophosmin	NPM	Ribosome biogenesis, histone assembly and cell proliferation	5.4A*	Y	Cammas *et al*. (2014)
Elongation Factor 1 Alpha 1	EF1A1	Ribosomal biosynthesis	5.5A*	Y	Ruest *et al*. (2002)
Elongation factor 2	EF2	Ribosomal translocation during translation elongation	5.5A* + 6.5B*	Y	Ruest *et al*. (2002)
60S Ribosomal Protein L19	RL19	rRNA binding	5.5A*	N	
60S Ribosomal Protein L4	RL4	rRNA binding	5.5A*	N	

40S Ribosomal Protein S18	RS18	rRNA binding	5.5A*	N	
40S Ribosomal Protein S24	RS24	Pre-rRNA processing	5.5A* + 5.4B^	N	
Nucleolin	NUCL	Ribosome assembly and pre-rRNA transcription	5.5A* + 5.5B*	N	
Other					
Nucleoside Diphosphate Kinase A	NDKA	Synthesis of nucleoside triphosphates	5.5A^ + 5.2A* + 5.2B*	Y	Lombardi *et al.* (1995)
60S Ribosomal Protein L13A	RL13A	Associated with ribosomes and is component of GAIT complex	5.5A^ + 5.2A* + 5.2B*	N	
40S Ribosomal Protein SA	RSSA	Cell-cell adhesion and laminin receptor	5.2B* + 5.5A*	N	
GTP-binding Nuclear Protein Ran	RAN	Nucleocytoplasmic transport. Import and export of proteins and RNA	5.2A* + 5.2B*	N	
Ubiquitin - 40S ribosomal protein S27a	RS27A	Protein ubiquitination and ligase binding	5.4B*	N	
40S ribosomal protein S2	RS2	Cellular response to IL-4, FGF binding and enzyme binding	5.7B*	N	
Myofibrillar Proteins					
Muscle Contraction					
Desmin	DESM	Muscle intermediate filament involved in muscle structure and function	5.2A^	Y	Gard *et al.* (1980); Wietzer *et al.* (1995); Li *et al.* (1994)

Calponin-3	CNN3	Binds to actin, calmodulin, troponin C and tropomyosin	5.2B*	Y	Shibukawa et al. (2013), (2010); Daimon et al. (2013)
Clathrin Light Chain A	CLCA	Binds to actin and required for sarcomere organisation	5.2B^	Y	Hosino et al. (2013); Isobe et al. (2018)
Actin	ACTB	Muscle contraction	5.4B*	Y	Nowak et al. (2009); O'Connor et al. (2008); Spangenburg et al. (2004); Swailes et al. (2004)
Myosin-9	MYH9	Cytoskeletal reorganisation	5.5A*	Y	Cooper et al. (2004); Devlin et al. (1978)
Clathrin Heavy chain 1	CLH1	Binds to actin and required for sarcomere organisation	5.5A* + 5.2A^	Y	Towler et al. (2004); Hosino et al. (2013)
Vinculin	VINC	Actin filament involved in cell matrix and cell-cell adhesion	5.5A* + 5.5B*	Y	Ren et al. (2008); Tay et al. (2010)
Tropomyosin Beta Chain	TPM2	Muscle contraction by binding to actin filaments	5.5A* + 5.5B* + 5.2A^	Y	Wiles et al. (2015); Lin et al. (1986)
Gelsolin	GELS	Binds to actin and regulates actin	5.5A^	Y	Schloz et al. (1995)
Actin	ACTC	Muscle contraction	5.5B* + 5.2A^	Y	Nowak et al. (2009); O'Connor et al. (2008); Spangenburg et al. (2004); Swailes et al. (2004)

Protein	Gene	Function			Reference
Myosin-3	MYH3	Muscle contraction	5.5B* + 5.2A^	Y	Cooper *et al.* (2004); Devlin *et al.* (1978)
Filamin-C	FLNC	Links with actin and cytoskeletal reorganisation	5.5B* + 5.2A^ + 5.2B^	Y	Dalkilic *et al.* (2006)
LIM and SH3 Domain Protein	LASP1	Regulation of actin and cytoskeletal activity	5.5B^	Y	Robinson *et al.* (2003); Tannu *et al.* (2004)
Moesin	MOES	Connects actin cytoskeleton to plasma membrane, cell shape determination, membrane transport, signal transduction and regulates T and B cell homeostasis	5.4B*	N	
Myosin light polypeptide 6	MYL6	Muscle contraction	5.4B*	N	
Myosin regulatory light chain 12B	ML12B	Regulation of contractile activity, triggers actin polymerisation and binds to calcium	5.7B*	N	
Other					
Tubulin Beta-4B Chain	TBB4B	Constituent of microtubules	5.5A* + 5.5B^	Y	Keller *et al.* (2007); Lewis *et al.* (1988)
Spectrin Alpha Chain	SPTN1	Calcium-dependant movement of cytoskeleton	5.5B* + 5.2A^	Y	Duan *et al.* (2018)
Tubulin Beta-3 Chain	TBB3	Constituent of microtubules	5.5B* + 5.2A^	Y	Keller *et al.* (2007); Lewis *et al.* (1988)
Nestin	NEST	Disassembles vimentin intermediate filaments	5.5B* + 5.2A^ + 5.2B^	Y	Zhong *et al.* (2008); Kachinsky *et al.* (1994);

182

Vimentin	VIME	Intermediate filament that is attached to the nucleus, endoplasmic reticulum and mitochondria and involved in protein binding/signalling	5.7A*	Y	Vaittinen et al. (2001) Wu et al. (2007); Vaittinen et al. (2001)
Translationally-controlled Tumor Protein	TCTP	Calcium binding and microtubule stabilisation	5.5A* + 5.5B*	N	
Protein S100-A6	S10A6	Calcium sensor, modulator and cellular calcium signalling	5.5B*	N	

Metabolic Enzymes					
<u>Glycolysis</u>					
L-lactate Dehydrogenase A Chain	LDHA	Catalyses pyruvate to lactate	5.2A*	Y	Zhu et al. (2013); Willkomm et al. (2014); Ohno et al. (2018); Ohno et al. (2019)
ATP Synthase Alpha	ATPA	Mitochondrial membrane ATP synthase producing ATP from ADP	5.2A*	Y	Sin et al. (2016); Moyes et al. (1997); Webster et al. (1990).
ATP Synthase Subunit F	ATPK	Mitochondrial membrane ATP synthase producing ATP from ADP	5.2A*	Y	Sin et al. (2016); Moyes et al. (1997); Webster et al. (1990)
Fructose-bisphosphate Aldolase A	ALDOA	Role in glycolysis and gluconeogenesis	5.5A^	Y	Casciola et al. (2012)

Protein	Abbreviation	Function	Samples	Known?	References
ATP Synthase Subunit Beta	ATPB	Mitochondrial membrane ATP synthase producing ATP from ADP	5.5A^ + 5.2A^ + 5.4B*	Y	Sin *et al.* (2016); Moyes *et al.* (1997); Webster *et al.* (1990)
Pyruvate Kinase	KPYM	Glycolytic enzyme involved in generating ATP.	5.2A*	N	
Alpha-Enolase	ENOA	Multifunctional enzyme, involved in glycolysis	5.2A* + 5.4B*	N	
Aldo-keto Reductase Family 1 Member B1	ALDR	Catalyses NADPH-dependant reduction	5.2A^	N	
Glyceraldehyde - 3 - phosphate dehydrogenase	G3P	Glycolysis, nuclear functions, modulates organisation of cytoskeleton, transcription, RNA transport, DNA replication and apoptosis	5.4B*	N	
Glucose-6-phosphate Isomerase	G6PI	Involved in glycolysis	5.5A^	N	
Other					
UDP-glucose 6-dehydrogenase	UGDH	Role in the biosynthesis of glycosaminoglycans	5.5A^	N	
NADH-Cytochrome B5 Reductase 3	NB5R3	Desaturation and elongation of fatty acids	5.5A^ + 5.2A^	N	
PRA1 Family Protein 3	PRAF3	Regulates intracellular taurine and glutamate	5.5A^ + 5.5B* + 5.2A*	N	
Amine Oxidase A	AOFA	Functions in metabolism of neuroactive amines in CNS	5.5A^ + 5.5B^	N	
Glutathione S-transferase A4	GSTA4	Catalyses conjugation of hydrophobic and electrophilic compounds	5.5A^ + 5.5B^ + 5.2A*	N	

184

Phosphoglycerate Mutase 1	PGAM1	Catalyses 3- and 2-phosphoglycerate with 2,3-biphosphoglycerate	5.5A^ + 5.5B^ + 5.2A*	N	
UTP-glucose-1-phosphate Uridylyltransferase	UGPA	Central role in glucosyl donor in metabolic pathways	5.5A^ + 5.5B^ + 5.2B*	N	
Elongation Factor 1 Beta	EF1B	Initiate exchange of GDP to GTP	5.5B* + 5.2A^	N	
Glutathione S-transferase P1	GSTP1	Catalyses conjugation of hydrophobic and electrophilic compounds	5.5B^	N	
ADP/ATP Translocase 2	ADT2	Exchanges cytoplasmic ADP with mitochondrial ATP	5.5B^ +5.2A^ + 5.2B^	N	
Long - chain specific acyl - CoA dehydrogenase	ACADL	Mitochondrial fatty acid beta oxidation.	5.7A*	N	

Chaperone and Protein Binding Proteins

Chaperone Proteins

Heat Shock Protein 90 Alpha	HS90A	Molecular chaperone that promotes structural maintenance and signal transduction	5.2A*	Y	Yun and Matts (2005a), (2005b); Wagatsuma *et al*. (2011)
Heat Shock Protein Cognate 71 kDa Protein	HSP7C	Molecular chaperone involved in multiple cellular processes	5.2A* + 5.4B*	Y	Grossi *et al*. (2011)
Endoplasmic Reticulum Chaperone	GRP78	Chaperone protein folding in endoplasmic reticulum	5.2A^	Y	Grossi *et al*. (2011): Brinkmeier and Ohlendieck (2014).
Heat Shock Protein 90-Beta	HS90B	Molecular chaperone that promotes structural	5.5A* + 5.5B* + 5.2A*	Y	Yun and Matts (2005a), (2005b):

					Wagatsuma *et al.* (2011)
		maintenance and signal transduction			
T-complex Protein Subunit Beta	TCPB	Chaperone protein involved in the folding of proteins in ATP hydrolysis	5.2A*	N	
Calreticulin	CALR	Calcium binding chaperone protein that regulates endoplasmic reticulum	5.5A*	N	
T-complex Protein 1 Subunit Gamma	TCPG	Component of chaperone complex that assists in protein folding	5.5A* + 5.5B* + 5.2A^	N	
Endoplasmin	ENPL	Chaperone that transports secreted proteins	5.5A^	N	
Heat Shock Protein Beta 1	HSPB1	Chaperone protein involved in stress resistance and actin organisation	5.5A^	N	
Ras-related Protein Rab-1A	RAB1A	Intracellular membrane trafficking	5.5A^ + 5.2B*	N	
T-complex Protein 1 Subunit Theta	TCPQ	Component of chaperone complex that assists in protein folding	5.5B*	N	
Protein Binding					
ADP-ribosylation Factor 1	ARF1	GTP binding protein involved in protein trafficking	5.2B*	Y	Pajcini *et al.* (2010)
14-3-3 protein zeta/delta	1433Z	Adapter protein involved in multiple signalling pathways	5.4A* + 5.4B*	N	
Poly-binding Protein 2	PCBP2	Immune function	5.5A* + 5.2A*	N	
Acyl-COA-binding Protein	ACBP	Intracellular carrier of acyl-CoA esters	5.5A* + 5.7A* + 5.7B*	N	

186

Annexin A4	ANXA4	Calcium binding protein	5.5A^ + 5.2B*	N	
Phosphatidylethanolamine - binding protein 1	PEBP1	ATP binding, serine protease inhibitor and inhibitor of MEK.	5.7A*	N	
14-3-3 protein epsilon	1433E	Signalling and binding protein in multiple areas.	5.7A* +5.7B* + 5.4B*	N	
Other Proteins					
Prosaposin	SAP	Initiates ERK signalling and G protein binding	5.2A* + 5.2B*	Y	Li *et al*. (2013)
Annexin A5	ANXA5	Calcium channel activity and cell signal transduction	5.2B*	Y	Leikina *et al*. (2013)
Fibronectin	FINC	Bind cell surfaces and various compounds including collagen, fibrin, heparin, DNA, and actin.	5.2B^	Y	Salmeron-Sanchez *et al*. (2011); Vaz *et al*. (2012)
Galectin-1	LEG1	Regulates apoptosis, and cell differentiation	5.5A* + 5.4A*	Y	Chan *et al*. (2006); Goldring *et al*. (2002); Georgiadis *et al*. (2007)
Annexin A1	ANXA1	Immune system, resolution of inflammation	5.5A^	Y	Bizzarro *et al*. (Bizzarro *et al*., 2010) and (2012); Leikina *et al*. (2013) and (2015).
Annexin A3	ANXA3	Inhibitor of phospholipase A2	5.5A^	Y	Duval *et al*. (2006)
CD63 Antigen	CD63	Cell surface receptor of TIMP1 and activates cell signalling cascades	5.5A^ + 5.5B^ + 5.2B*	Y	Zhou *et al*. (2011); Giancotti *et al*. (1997)

Protein	Gene	Function		Reference
Prelamin-A/C	LMNA	Nuclear assembly, chromatin organisation and telomere dynamics	5.5B* + 5.2A^	Y	Frock *et al.* (2006)
Guanine Nucleotide-Binding Protein	GNAL	Modulator/transducer in transmembrane signalling	5.5B^	Y	Clark *et al.* (2010)
Rho GDP-dissociation Inhibitor 1	GDIR1	Controls Rho protein homeostasis	5.5B^ + 5.4B*	Y	Wei *et al.* (1998); Charrasse *et al.* (2002)
Voltage - dependent anion - selective channel protein 1	VDAC1	Forms channel through mitochondrial outer membrane and plasma membrane, channel that triggers apoptosis	5.7B*	Y	Barbieri *et al.* (2011); Khalek *et al.* (2014)
Prothymosin Alpha	PTMA	Mediates immune function	5.2A*	N	
S-formylglutathione Hydrolase	ESTD	Detoxification of formaldehyde	5.2A* + 5.2B*	N	
Complement C4-B	CO4B	Classical complement pathway	5.2B*	N	
Protein S100-A10	S10AA	Regulates ANXA2 monomer phosphorylation	5.4A*	N	
Annexin A6	ANXA6	Associate with CD21, calcium release from intracellular stores.	5.4B^	N	
Peroxiredoxin-2	PRDX2	Role in cell protection against oxidative stress	5.5A*	N	
Ribonuclease Inhibitor	RINI	Regulates angiogenesis	5.5A^	N	
Serpin B6	SPB6	Inhibitor of cathepsin G	5.5A^	N	
Peroxiredoxin-1	PRDX1	Protects cells against oxidative stress	5.5A^ + 5.2A* + 5.2B*	N	

Protein Name	Abbreviation	Function	Location	
Synaptic Vesicle Membrane Protein VAT1-1 Homolog	VAT1	Negative regulator of mitochondrial fusion	5.5A^ + 5.5B^	N
Alpha-2-macroglobulin	A2MG	Inhibitor of proteinases and transmembrane protein	5.5A^ + 5.5B^ + 5.2A* + 5.2B*	N
Receptor of Activated Protein C Kinase 1	RACK	Scaffolding protein involved in assembly and regulation of signalling molecules	5.5B* + 5.2A* + 5.2B*	N
Macrophage-capping Protein	CAPG	Reversibly blocks actin filament binding and involved in macrophage function	5.5B^	N
Galectin-3	LEG3	Member of lectin family and is important in cell-cell adhesion	5.5B^ + 5.2A*	N
Pregnancy Zone Protein	PZP	Protein complex binding and proteinase inhibitor	5.5B^ + 5.2A*	N
Murinoglobulin-1	MUG1	Inhibitors of serine-type endopeptidases	5.5B^ + 5.2A*	N
Transmembrane Channel-like Protein 5	TMC5	Ion channel activity	5.5B^ + 5.2A*	N
Annexin A2	ANXA2	Calcium regulated binding protein, heat stress involvement.	5.7A*	N

Abundance and FSR with greater significant ($P < 0.01$: 10 % FDR) proteins were reported in the volcano plots (Figures 2,4,5,7). Not all proteins were labelled on the volcano plots, therefore, they were reported in the above table and split into protein categories. Evidence detailing the proteins function in myoblast differentiation was highlighted. The location of each protein in the relevant figure was highlighted. The * indicates negative $\log_2$ and ^ indicates positive $\log_2$ on the volcano plot.

5.5 Discussion

The aim of this chapter was to investigate proteomic differences associated with the relative lack of fusion of replicatively aged myoblasts compared to young (control) counterparts. The major findings of this study are that early (0-24 h) during the differentiation process replicatively aged myoblasts have a lesser abundance of ribosomal proteins. Later (72-96 h) replicatively-aged myotubes have a lesser abundance of myofibrillar proteins. In addition, significant differences in protein synthesis rates between the conditions suggest that these findings impact on the ability for replicatively aged myoblasts to fuse into myotubes.

Label-free quantification indicated that control myoblasts contained fifteen ribosomal proteins that are reported in myoblast differentiation, which included: 40S ribosomal protein S6 (RS6), NDKA and nucleophosmin (NPM) (Lombardi *et al.*, 1995; Cammas *et al.*, 2014; Corrick *et al.*, 2015). For instance, reduced RS6 content and subsequently anabolic signalling and the lack of myotube formation was reported by Corrick *et al*. (2015) which supplemented serum from burn victims onto 30-year-old primary myoblasts. This suggests that RS6 protein is important for primary cell differentiation. Further, Kislinger *et al*. (2005) investigated the relative abundance of proteins across a time-course during myoblast differentiation using gel-free tandem mass spectrometry. The majority of proteins identified were nuclear and ribosomal, similar to our findings. In addition, there was also a distinct lack of myofibrillar proteins in myoblasts compared to myotubes. Tannu *et al*. (2004) also investigated protein abundance between myoblasts and myotubes. The authors fractionated multiple proteins via 2D-PAGE and then ran targeted proteins on mass spectrometry. Similar results found multiple proteins involved in transcription (Table 5.2). However, both of these studies also found highly abundant proteins involved in chromatin remodelling, which is important in myoblast differentiation (Delgado *et al.*, 2003).

In control myotubes, there was a greater abundance of myofibrillar proteins compared to myoblasts, which was expected as myofibrillar proteins are used in muscle contraction observed in mature myotubes (Fujita *et al.*, 2007a). The proteins ACTC, CLH1, FLNC, MYH3 and TPM2 are all integral for muscle contraction but also have

roles in myoblast differentiation (Cooper *et al.*, 2004; Dalkilic *et al.*, 2006; Nowak *et al.*, 2009; Hoshino *et al.*, 2013; Wiles *et al.*, 2015). For instance, Dalkilic *et al.* (2006) differentiated myoblasts into myotubes and inhibited FLNC RNA. However, the authors reported severe defects in myogenesis and myoblast formation (Dalkilic *et al.*, 2006). Furthermore, analysis of the C_2C_{12} proteome reported proteins with higher abundance in myotubes, including ACTC, MYH3 and DESM (Kislinger *et al.*, 2005), corresponding to our findings. Although in that study, additional myosin proteins were identified compared to our study. In addition, Tannu *et al.* (2004) also suggested that myotubes accumulated greater abundance of proteins involved with actin binding, including multiple tropomyosin isoforms.

Furthermore, our results also indicated that there was higher abundance of ATP synthase isoforms in control myotubes compared to myoblasts. ATP synthase catalyses the final step of oxidative phosphorylation and is also involved in muscle differentiation (Sin *et al.*, 2016). Sin *et al.* (2016) reported that inhibiting ATP synthase with oligomycin, impacted oxidative phosphorylation and myoblast differentiation. However, equivocal findings of protein abundance of ATP synthase are reported in the literature, with results indicating higher abundance in four isoforms of ATP synthase in myotubes (Kislinger *et al.*, 2005), similar to our findings. In contrast, Tannu *et al.* (2004) reported no differences in ATP synthase protein abundance between myoblasts and myotubes using two-dimensional gel electrophoresis. However, this method reports proteoforms (transcriptional and post-translational variations and products of a protein), not proteins. However, the evidence and findings from this study indicate that greater abundance of ribosomal proteins is integral for early myoblast differentiation, whereas contractile and metabolic proteins in myotube formation. In replicatively aged myoblast differentiation, there was a distinct lack of these protein groups which arguably negatively affects myoblast formation.

To understand the protein turnover during early stage differentiation and myotube formation, myoblasts and myotubes were labelled with D_2O for 24 h. Overall, control myoblasts had significantly greater (22 %) FSR compared to control myotubes. This implies that during early differentiation, proteins within myoblasts are undergoing relatively greater protein turnover compared to control myotubes, with synthesising at constant rate. In support of our findings, Cambridge *et al.* (2011) concluded that

myotubes had reduced turnover rates compared to myoblasts using the SILAC method. Converting FSR to protein half-life, which was reported by Cambridge *et al*. (2011), 143 identical proteins from both data sets were compared. The median half-life in Cambridge *et al*. (2011) was 85.5 $t_{1/2}$ compared to 170.1 $t_{1/2}$ in our study. The discrepancies in results could be the passage of cells, the lower passage have increased myogenic potential, forming larger myotubes (Sharples *et al*., 2011). However, the passage is not indicated in the Cambridge *et al*. (2011) study. In addition, the experimental days during differentiation impact myotube size, for instance, 96 h in this study compared to 144 h (Cambridge *et al*., 2011).

Moreover, Foletta *et al*. (2016) labelled myoblasts and myotubes with D_2O and reported increased FSR in myoblasts (3.1 %/h) compared to myotubes (1.7 %/h). These FSR were greater than those observed in this study as myoblast was 0.56 %/h and myotube was 0.46 %/h. However, it is not known the amount of proteins that were synthesised, that could have impacted the FSR. Miller *et al*. (2015) also surmised that myoblasts (~1 %/h) had greater turnover when dosed with 4 % compared to myotubes (~0.6 %/h), although they labelled for 48 h compared to 24 h compared to our study. Therefore, although discrepancies between values, the early evidence does demonstrate that there is greater FSR in control myoblasts compared to control myotubes, which support our hypothesis. This is the first study to investigate the FSR rates of replicatively aged myoblasts compared to replicatively aged myotubes. Similar to control, there was a significantly greater FSR in replicatively aged myoblasts compared to replicatively aged myotubes. Importantly however, the difference between replicatively myoblasts and myotubes (87 %) is considerably greater than the magnitude of difference (22 %) between control myoblasts and myotubes. Therefore, we identified differences in protein abundance and FSR between replicatively aged and control in both myoblasts and myotubes.

In control myoblasts compared to replicatively aged myoblasts, there was 33 ribosomal proteins that had a relatively higher abundance compared to replicatively aged. Interestingly, RS6 was significantly greater in control myoblasts, and is involved differentiation, as mentioned earlier (Corrick *et al*., 2015) compared to replicatively aged myoblasts. Calculating the absolute synthesis rate would determine whether the control myoblasts are producing much greater amounts of proteins through increased

ribosomal capacity. In addition, the control myoblasts and myotubes contained higher abundance of VINC and TPM2 compared to replicatively aged myoblasts and myotubes and were involved in muscle differentiation (Tay *et al.*, 2010; Wiles *et al.*, 2015). Wiles *et al.* (2015) inhibited USP19 in L6 muscle cells which decreased myogenin, tropomyosin expression and impaired muscle differentiation.

Interestingly, replicatively aged myoblasts and myotubes had a higher abundance of metabolic enzymes compared to control myoblasts and myotubes. The glycolytic enzymes linked to myoblast differentiation, ATPB and ALDOA (Casciola-Rosen *et al.*, 2012; Sin *et al.*, 2016) were involved in ATP production (Burniston *et al.*, 2014). This suggests that replicatively aged myoblasts have a greater capacity to resynthesise ATP, which may match the demand for increased energy requirements during ageing (Zhang *et al.*, 2018). Replicatively aged myoblasts were differentiated over 72 h and did not fuse **(see chapter 5)**. In these myotubes, there was seven metabolic enzymes compared to control myotubes. Only PGAM1 was involved in glycolysis, but not linked to muscle differentiation (Burniston *et al.*, 2014). Supporting our hypothesis, reduced abundance of ribosomal, contractile proteins and possible higher abundance of metabolic enzymes producing ATP are linked to lack of fusion in replicatively aged myotubes.

There was a significantly greater FSR in control myoblasts and control myotubes compared to replicatively aged myoblasts and myotubes. On a protein by protein basis, there was no ribosomal proteins with significantly greater FSR compared to control myoblasts. Whereas, in replicatively aged, FSR was greater in RLA2 which interestingly, was greater in abundance in control myoblasts and myotubes compared to replicatively aged (Table 6.2). However, future experiments are required to determine whether this protein is involved in myoblast differentiation. The myofibrillar protein VIME has significantly greater FSR in control myoblasts compared to replicatively aged myoblasts. VIME is located near the nucleus, endoplasmic reticulum and mitochondria and is involved in cell adhesion and signalling (Ivaska *et al.*, 2007) together with myoblast differentiation (Vaittinen *et al.*, 2001; Wu *et al.*, 2007). Interesting that VIME was the most abundant protein across all independent groups, with no significant difference observed (data not shown).

In myotubes, there was six proteins with greater FSR in control myotubes compared to replicatively aged myotubes, with ROA2 and VDAC1 involved in myoblast differentiation (Barbieri *et al.*, 2011; Khalek *et al.*, 2014; Liu *et al.*, 2017). Interestingly, VDAC1 is an anion channel on the mitochondrial outer membrane, which triggers apoptosis (programmed cell death) (Khalek *et al*., 2014). Whereas, ROA2 is a heterogeneous nuclear ribonucleoprotein involved in transcription and binding to DNA on telomeric sequences (Chen *et al.*, 2017). In addition, although not evidenced in myoblast differentiation, the protein ACPB was significantly greater in FSR in both control myoblasts and myotubes compared to replicatively aged myoblasts and myotubes. ACPB, a protein that binds short and long chain esters with high affinity, was also significantly greater in abundance in replicatively aged myoblasts compared to control myoblasts. Therefore, difference between protein abundance and FSR could be due to other processes such as post transcriptional, translational and degradation regulation (Vogel and Marcotte, 2012) which was not measured in this study but requires further investigation.

5.6 Conclusion

To conclude, replicatively aged myoblasts lacked abundance of ribosomal proteins compared to control myoblasts. Also, replicatively aged myotubes had reduced abundance of contractile proteins compared to control myotubes. Interestingly, the greater abundance of metabolic enzymes in replicatively aged myoblasts and myotubes implies energy demand was increased, which requires further investigation. Indeed, the diminished FSR rate in replicatively aged myoblasts and myotubes likely contributes to reduced abundance of essential proteins. Therefore, the data from study indicates that impairments in replicatively aged fusion was a result of reduced FSR and the production of essential ribosomal and contractile proteins.

Chapter 6: Repair and Recovery Following Eccentric Contractions in Young Males and Females: Impact of Leucine and HMB

6.1 Abstract

Introduction: The majority of exercise regimes involve eccentric contractions that result in DOMS as a result of muscle damage. In sedentary and recreationally active individuals, the sensation of DOMS can affect engagement with unaccustomed exercise. In order to recover from eccentric exercise, repair and regeneration of muscle is integral. The protein supplements, leucine and HMB, are reported to aid recovery from exercise. Therefore, the aim was to reduce the sensation of DOMS and improve skeletal muscle repair and recovery. The hypothesis was 1: leucine and HMB will benefit muscle repair and recovery compared to control after dynamic exercise and 2: leucine and HMB will attenuate markers associated with exercise and stimulate cytokines involved with muscle repair and recovery compared to control.

Methods: Seventy-one healthy recreationally active males (n = 43) and females (n = 28) completed 5 sets of 20 drop jumps. The participants were split into three groups (control, leucine and HMB). The leucine and HMB group consumed 3 g/d supplement from 1 day prior to the exercise protocol and for 14 days post-intervention. Muscle soreness, squat jumps, chair rises, ROM and serum samples were collected at pre, post, 24 h, 48 h, 7-day and at 14 days. Blood lactate (pre and post), CK and cytokines were measured.

Results: Significant increases (all $P < 0.05$) in muscle soreness (peak 6-fold: 48 h) and CK (peak 69 %) were observed over 48 h in males with and without leucine and HMB supplementation. No impact of supplements on muscle function and performance in male or females. Significant increases in soreness ($P < 0.05$: peak 6-fold) but not CK was observed in females, with no difference between group. Concentrations of IL-7 significantly increased ($P < 0.05$: 2.6-fold) at day 7 and increases in IL-8 in male controls compared to females. Leucine significantly increased (both $P < 0.05$) IL-7 concentrations in females at pre and 48 h (8-fold) post exercise compared to males.

Conclusion: There was increased soreness in males and females but only elevated CK in males. Functional measures declined as a result of damage but were not impacted by supplementation. Leucine and HMB also did not improve skeletal muscle repair following eccentric exercise. Systemically the intervention induced an immune response, which was different between males and females and which was impacted by supplements.

6.2 Introduction

Globally, exercising is known to have multiple physiological benefits (Neufer *et al.*, 2015). The majority of exercise regimes and sports predominately involve eccentric contractions compared to concentric or isometric (Proske and Allen, 2005). Multiple eccentric contractions result in DOMS (Howatson and Van Someren, 2008). In sedentary and recreationally active populations, this sensation of DOMS adversely affects motivation to exercise for prolonged periods. Therefore, individuals explore ways of minimising DOMS. These include: nutraceuticals, pharmaceuticals, ice baths and massage among others (Howatson and Van Someren, 2008). The supplements leucine and HMB are commonly consumed and literature reports benefits on muscle recovery and attenuation of DOMS (Kirby *et al.*, 2012; Wilson *et al.*, 2009).

Exercise causes microinjury within skeletal muscle and disrupting the structural integrity of muscle membranes (Mackey *et al.*, 2011). In detail, sarcomere disruption misaligns Z-line formation. Also, sarcolemma trauma activates satellite cells (Hill *et al.*, 2003). Other affected components include myofibrils, T-tubules, cytoskeleton proteins and the sarcoplasmic reticulum (Clarkson *et al.*, 1986). These insults result in the initiation of the repair phase, which involves the infiltration of inflammatory immune cells to 1) remove neurotic tissue; 2) activate satellite cells. The immune cells primarily involved in the repair phase are neutrophils, which secrete IL-1β, IL-6, TNF-α and macrophages (Chen and Shan, 2019). The first phase of inflammation usually occurs within 48 h. The second phase includes recovery and adaptation and occurs from 48 h-14 days. Between phases, the inflammatory state changes from pro-inflammatory to anti-inflammatory via macrophages (Varga *et al.*, 2016). This also coincides with changes in satellite cell behaviour from activation and proliferation to differentiation and fusion (Chen and Shan, 2019). The recovery phase involves regeneration of muscle fibres and full repair of skeletal muscle. Adaptation occurs in the latter stages although the evidence supporting satellite cells involvement is still debatable (Serrano *et al.*, 2008; Petrella *et al.*, 2008). The impact of leucine and HMB on aspects of these mechanisms is not known.

Leucine supplementation results in AA transport into skeletal muscle, subsequently activating signalling cascades involved in MPS (Dickinson and Rasmussen, 2011). Leucine in particular is reported to be integral in initiating MPS, through increased mTOR activation (Hawley *et al.*, 2006). However, whether this cellular increase in MPS translates to muscle repair, recovery and physiological outcomes is not clear. Also, it is debatable which AA supplement is the most efficient in reducing DOMS and stimulating adaptation. Other supplements of interest in the sporting world include BCAA and whey protein (Shimomura *et al.*, 2010; Buckley *et al.*, 2010) and are reported to have benefits in muscle recovery. Although more data is required to substantiate these findings in different populations and using real world exercise regimes.

HMB, the metabolite of leucine, is not naturally produced in the body. Endogenously, only 5 % of leucine is metabolised into HMB in the liver (Zanchi *et al.*, 2011). Therefore, HMB is commonly supplemented with the rationale that the benefits are similar to that of leucine. To date, however, only a selection of studies have investigated the effect of HMB on eccentric exercise (Wilson *et al.*, 2009: Wilson *et al.*, 2013: Padden-Jones *et al.*, 2011: Van-Someren *et al.*, 2005). Wilson *et al.* (2009) supplemented HMB in young males that performed 55 knee extensions on both legs. However, no impact of HMB was observed over 72 h on force gain, pain reduction or CK activity. Alternatively, Wilson *et al.* (2013) investigated the effects of 3 g of HMB before and for 48 h post resistance exercise session in young males which consisted of 3 sets of 12 repetitions of exercises including squats, deadlifts and pull ups. The authors concluded that HMB decreased CK activity and perceived pain. Rather than repair and regenerate following dynamic exercise, however, the majority of reported studies are based on muscle building training regimes and specifically muscle hypertrophy where the findings are equivocal (Wilson *et al.*, 2014; Lowery *et al.*, 2016; Teixeira *et al.*, 2018, 2019).

As a result of the limited and contrasting information, a need for further research is required, to ascertain whether AA supplementation may impact on reducing recover or facilitating repair, following eccentric exercise. This study therefore attempts to address the question of supplementation and adaptation. In addition, it also focused on recruiting both males and females, as current research is frequently performed with males. Since males are stronger and contain increased muscle mass (Hicks *et al.*,

2001), different endocrine and metabolic responses (Hill and Smith, 1993), a need to study adaptation in females is key, as extrapolations from one population to the other would not necessarily be valid. Furthermore, Albert *et al.* (2006) reported that men fatigue at a quicker rate than women and therefore, women recover more quickly (Flores *et al.*, 2011).

The aim of this study is to reduce the sensation of DOMS and improve skeletal muscle repair and recovery using leucine or HMB supplementation following dynamic exercise. The objectives are to 1: investigate the impact of leucine and HMB on skeletal muscle repair and recovery and 2: uncover some of the physiological and inflammatory mechanisms of skeletal muscle repair and recovery. The hypotheses to be challenged are 1: leucine and HMB will benefit muscle repair and recovery compared to control after dynamic exercise and 2: leucine and HMB will attenuate markers associated with exercise and stimulate cytokines involved with muscle repair and recovery compared to control.

6.3 Method

6.3.1 Participants

Seventy-one healthy and recreationally active males (n=43) and females (n=28) voluntarily took part in the study. Participant characteristics are reported in table 6.1. To reach 80 % statistical power, n=9 in each group was required. Statistical power was based on Kirby *et al.* (2011) study which investigated the effects of leucine supplementation on indices of muscle damage. The exclusion criteria stated they did not complete more than two gym sessions a week and no leg training, and they did not complete strenuous endurance exercise that would cause unaccustomed eccentric damage (e.g. downhill running). In addition, participants were not allowed to partake in the study if they had DOMS within the last 6 months. Following a health screening questionnaire, if participants agreed to take part, they signed a consent form. The study was approved by Liverpool John Moores Research Ethics Committee (16/SPS/007). The samples stored were in line with Human Tissue Act regulations.

Table 6.1 Subject characteristics in each group. Data displayed as mean ± SD.

Group	Gender	Number	Age (years)	Height (cm)	Weight (cm)
Control	Male	19	22 ± 2	178.0 ± 5.1	74.28 ± 8.33
Control	Female	10	23 ± 2	162.0 ± 6.2	58.25 ± 7.54
Leucine	Male	15	22 ± 4	175.7 ± 5.4	71.59 ± 7.90
Leucine	Female	9	22 ± 2	163.3 ± 7.3	57.54 ± 9.57
HMB	Male	9	23 ± 4	176.6 ± 7.1	75.40 ± 9.30
HMB	Female	9	21 ± 2	164.3 ± 9.5	63.19 ± 13.07

There was no significant difference within genders in age, height and weight.

6.2.2 Study Design

The design of this study was a randomised control trial (RCT). The study compromised of 3 groups (control, leucine and HMB) with each group containing at least 9 males and 9 females. The study period covered 15 days (Figure 6.1). There was one day (day -1) allocated to supplement preloading and familiarisation. Familiarisation consisted of participants being demonstrated and trying all the measures outlined

below, excluding blood collection. The participants completed 10 drop jumps to practice and understand the technique required for the exercise protocol. Baseline measures (pre), exercise protocol and post measures (post) were completed on day 0. For 14 days, the participant took supplements or nothing (control) and soreness measures. At the timepoints: pre, post, 24 h, 48 h, 7 days and 14 days post damage, the participant came into the laboratory and completed performance, functional measures and gave a blood sample (Figure 6.1). The measures included: blood sample collection, squat jump, range of motion (ROM), chair rises and pain score.
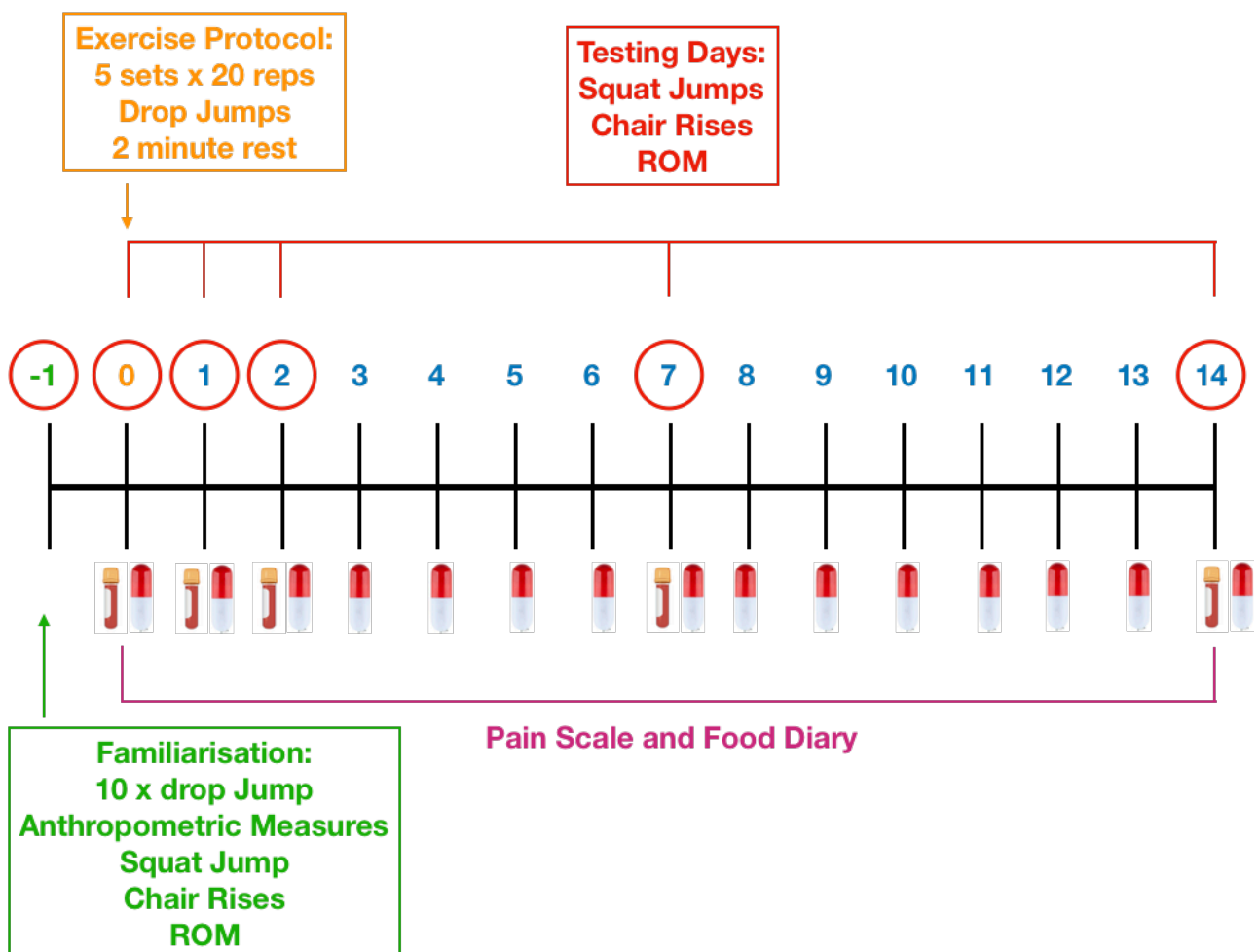
Figure 6.10. Schematic to demonstrate the experimental design of the current study.

6.3.3 Anthropometry

On the first day (day -1), all participants attended the laboratory where their body mass (kg) and height (cm) were recorded. For body mass, the participants were instructed

to take off their shoes and any heavy items before standing on a digital scale (Seca 704, Birmingham, UK). For height, participants were asked to take off shoes, stand under a portable stadiometer (Seca 213, Birmingham, UK) and breath in before measurement was taken.

6.3.4 Muscle Performance and Function Measures

Squat jumps were measured as an indicator of lower extremity power. The participant stood on a jump mat (Probotics, Inc, Huntsville, USA) with feet shoulder width apart and hands on hips. When instructed, the participants lowered themselves into a squat position (knees approximately flexed to 90 °) and held this position for 3 seconds. The time was recorded via stopwatch by the researcher. When 3 seconds elapsed, the participants were instructed to jump maximally, whilst maintaining hands on hips. They performed the squat jump three times, and *an* average was recorded.

Chair rises were performed to assess functional movement. The participants were asked to stand in front of a 40 cm box and stand with feet shoulder width apart and their hands on hips. To complete one chair rise, the participant was asked to sit on the box and stand back to the starting position. The participant executed as many chair rises as possible within 30 seconds. The total number achieved was recorded.

To assess the flexibility around the joint, ROM was measured. The participant was asked to sit on a chair with their knees at a 90 ° angle. The lateral epicondyle of the femur was palpated, and the centre of the goniometer was placed on this bony landmark. The goniometer was separated to 90 ° and the participant was asked to maximally extend and flex their leg three times each. A value was recorded for each movement and an average of maximum flection or extension was recorded.

The participants were asked to rate their perceived muscle soreness of the lower extremity. They were provided with a visual analogue scale (VAS) with 0 = no soreness and 10 = worst possible soreness. This was recorded from day 0 to day 14.

6.3.5 Supplementation Protocol

The participants either took no supplement (control), leucine or HMB over the 15-day study period. The doses selected were based on recommended daily allowance (RDA). For the leucine group, this consisted of 3 capsules per day, which equalled 3000 mg/d. The HMB consumed 6 capsules per day, which also equalled 3000 mg/d. The supplements were purchased from Myprotein (Cheshire, UK). The participants were asked to take either 1 (leucine) or 2 (HMB) supplements with each meal. They were also asked to maintain habitual nutritional intake and refrain from additional supplements.

6.3.6 Eccentric Exercise Protocol

On day 0, the participants completed an eccentric exercise protocol. The protocol consisted of 100 drop jumps which was split into 5 sets of 20 repetitions. The period between each repetition was maximum 10 seconds and between set was 2 minutes. To allow participants to become familiarised with the protocol, on day -1, 10 drop jumps were performed. The participant was asked to stand on the 40 cm box, with hands on their hips and to drop off the box. The participant landed on a jump mat, with feet shoulder width apart whilst not moving their hands. On impact, the participants immediately bent knee angle to approximately 90 ° and propelled themselves upward and landing with feet shoulder width apart. Each jump was recorded, and participants were encouraged to maintain maximal effort and technical form.

6.3.7 Blood Collection

Blood samples were taken from two locations, finger and the antecubital vein. At the timepoints pre, 48 h and 7-day samples were taken from the antecubital vein. Whereas, at post, 24 h and 14-day the finger was used. From the vein, samples were collected in 10 ml serum BD vacutainers, left on ice for 30 minutes. The finger prick blood samples were collected in 500 µl microvette and also left for 30 minutes on ice. All samples were centrifuged at 2000 rpm (800 g) for 10 minutes at 4 °C. This was to separate the serum from the blood clot. The serum was aliquoted into Eppendorf tubes

and both the blood clot and serum were stored at -80 °C in a coded format that would not enable the participants to be identified.

6.3.8 Blood Analysis

Pre and immediately post the drop jump protocol, blood lactate was measured. From a finger prick site, a blood droplet was collected into a lactate strip and a reading was obtained using a lactate analyser (Nova, Lactate Plus, Massachusetts, USA). From the stored serum samples, CK, a marker of muscle damage, was measured at all time points. In 96 well plates, 20 µl of sample was added in each well, followed by 180 µl CK reaction reagent. The plate was incubated for 5 minutes at 37 °C. The change in absorbance was monitored continuously over 20 minutes using ELISA plate reader (Biotek, USA) at a wavelength of 340 nm **(see section 2.6.5)**. Protein concentrations of multiple cytokines from the serum were measured using a CBA Kit (BD Biosciences). The timepoints measured were pre, 24 h, 48 h and 7 days. This technique uses fluorescent pre-mixed capture beads incubated with PE conjugated antibodies against specific cytokines which are analysed via flow cytometry. The cytokines measured were: interleukins (1β, 2, 3, 4, 6, 7, 8, 10, 17α) and tumor necrosis factor receptor 1 alpha (TNFr-1α). For more details **see section 2.7.3**.

6.3.9 Statistical Analysis

For all comparisons, a 3-way mixed ANOVA and Bonferroni post hoc pairwise comparison used. The between subject comparisons were between gender and supplement. The within subject comparisons were over the time course. Independent t-tests were utilised for comparisons between pre and baseline values. Statistical analysis was performed using SPSS version 25 (SPSS, Chicago, IL, USA). All data was represented as mean ± SD, unless mentioned otherwise.

6.4 Results

6.4.1 Male Demographics

There were no significant differences between male groups in participant height, weight and age (Table 6.1). For all measures, there were no significant differences between familiarisation and pre time points. Therefore, all comparisons were made to pre (0 h). The following studies were undertaken to ascertain the impact of drop jumps on biochemical, functional, immune adaptations over 14 days, in healthy males and females in the absence or presence of leucine or HMB. Data are presented below, initially for males, then females and finally as a comparison. Study time is subdivided into damage (0-48 h) and repair (48 h-14 days) phases to align with adaptations that would occur following eccentric exercise.

6.4.2 Blood Lactate Increases Post Exercise in Men

In males, at 0 h, there were no significant differences between groups. Immediately post eccentric contractions (100 drop jumps), there were significant increases in blood lactate in all groups ($P < 0.05$). From pre to post, blood lactate rose 3.0-fold from 1.2 ± 0.5-3.6 ± 1.8 mmol/L in the control, increased 2.1-fold from 1.4 ± 0.7-3.0 ± 1.6 mmol/L in the leucine and increased 2.1-fold from 1.5 ± 1.0-3.2 ± 1.4 mmol/L in the HMB group. There was no significant difference between supplements post exercise (Figure 6.2). The comparable rise in blood lactate levels is indicative that all male participants are working at comparable exercise intensities.

Figure 6.11. Male blood lactate responses from pre to post in control, leucine and HMB groups. Data displayed as average ± SD. Significance (*) represents pre vs. post and set at P < 0.05.

6.4.3 Muscle Soreness and Creatine Kinase Increase in Repair Phase in Men

Muscle soreness (perceived) was measured as a marker of the severity of repeated eccentric contractions (Figure 6.3). In all male participants, soreness significantly increased from baseline to post intervention (P < 0.05), regardless of the group. Soreness peaked in controls (6-fold increase; P < 0.05) at 48 h, plateaued in the leucine group from post to 48 h (5-fold increase; P < 0.05) and peaked in the HMB group at 24 h (5-fold increase; P < 0.05). In all groups, soreness returned to baseline levels by 7 days (Fig 6.3A-C). There was no significant difference in muscle soreness between groups.

To consolidate these findings, CK was measured as a serum marker of muscle damage. The data trends were similar to muscle soreness (Figure 6.3). In the control and leucine group (Figures 6.3A and B), there were significant increases from pre to 24 h (69 %; $P < 0.05$: 46 %; $P < 0.05$ respectively) and in the control group the elevation continued, with a significant increase also evident from post to 24 h (35 %; $P < 0.05$). In contrast, there was no increase in CK activity in the HMB group at any time, despite the increase in soreness (Figure 6.3C). In addition, all CK values returned to baseline levels by 48 h in control and 24 h in leucine supplemented groups. There was no significance difference in CK between groups.

Together these data suggest that the intervention was sufficient to incur muscle trauma, as evidenced by the increased soreness. Elevations in CK in control and leucine groups, mirror the soreness data. The absence of an increase in CK in the HMB group is interesting and warrants further consideration, suggesting that while pain has not been positively impacted, CK release has been.

Figure 6.3. Representation of muscle soreness and CK response in control (A) or in leucine (B) and HMB (C). Red line graph and text boxes represent muscle soreness, whereas, blue bars and text boxes represent CK. Significance was set at $P < 0.05$. Significant comparisons: a: pre, b: post, c: 24 h, d: 48 h vs other time points.

6.4.4 Differing Responses in Performance and Functional Measures over the Repair and Recovery Phase in Men.

Having determined that the intervention implemented resulted in increased pain and CK activity in the circulation (not for HMB), the next step was to assess the impact on performance after 100 drop jumps, squat jump height was measured. At baseline, average squat jump height was (47.2 ± 7.3 cm), with no differences between groups. There was no significant decrease in squat jump height during the first 48 h post exercise (the repair phase (0 h-48 h)), regardless of treatment. During the recovery phase (48 h-14-day), there was again, no significant difference between groups, however, the leucine group showed a significant 16 % increase in jump height at 14 day vs. immediately post exercise (P < 0.05); importantly, this increase did not result in a difference from baseline (Figure 6.4A).

The number of chair rises completed over 30 seconds was used as a functional measure in response to multiple drop jumps. There was no impact of exercise on chair rises from 0 h-48 h (Figure 6.4B) in any group. Similarly, there were no differences between groups across the 14-day intervention period. Within group measures, were however evident for the control group, with significant increases at 7-day vs. post and 24 h (16 % P < 0.05, 16 %, P < 0.05), respectively. By 14 days, chair rises in the control group were significantly greater than all-time points to 48 h (0 h (11 %), post (20 %), 24 h (20 %) and 48 h (11 %) (all P < 0.05)). In the presence of leucine, chair rises increased significantly (P < 0.05) vs. baseline at 7-day (12 %) and 14-day (14 %). By contrast, HMB treatment was without significant impact on chair rises across the whole study period, despite no differences apparent between groups.

Muscle tightness and flexibility was investigated post eccentric damage by measuring the extension and flexion around the knee joint (Figure 6.5A and B). In male control group, there was no significant impact of muscle contractions on extension over time. In contrast, with leucine supplementation, there was a small but significant improvement from post to 48 h (P < 0.05). There were also small significant increases from post to 7-day and 14-day (P < 0.05) and from 24 h-14-day (P < 0.05). HMB supplementation demonstrated no changes in extension over time (Figure 6.5A).

Between groups at pre, the HMB group was significantly reduced vs. control ($P < 0.05$). At day 7, the extension was significantly reduced in HMB vs. leucine group ($P < 0.05$). With flexion, there was no significant changes over time or with supplementation (Figure 6.5B).

Thus, from the results above, the intervention protocol did not reduce muscle performance or function over the repair phase (0 h- 48 h) and there was no attenuation of supplements. However, during the longer recovery period (0 h vs. 7-day/14-day), improvements in muscle performance and function were evident (Figure 6.4 and 6.5). However, despite specific changes within groups, there were no differences between groups, suggesting that improvements evident may have been as a result of practice, rather than supplementation per se.
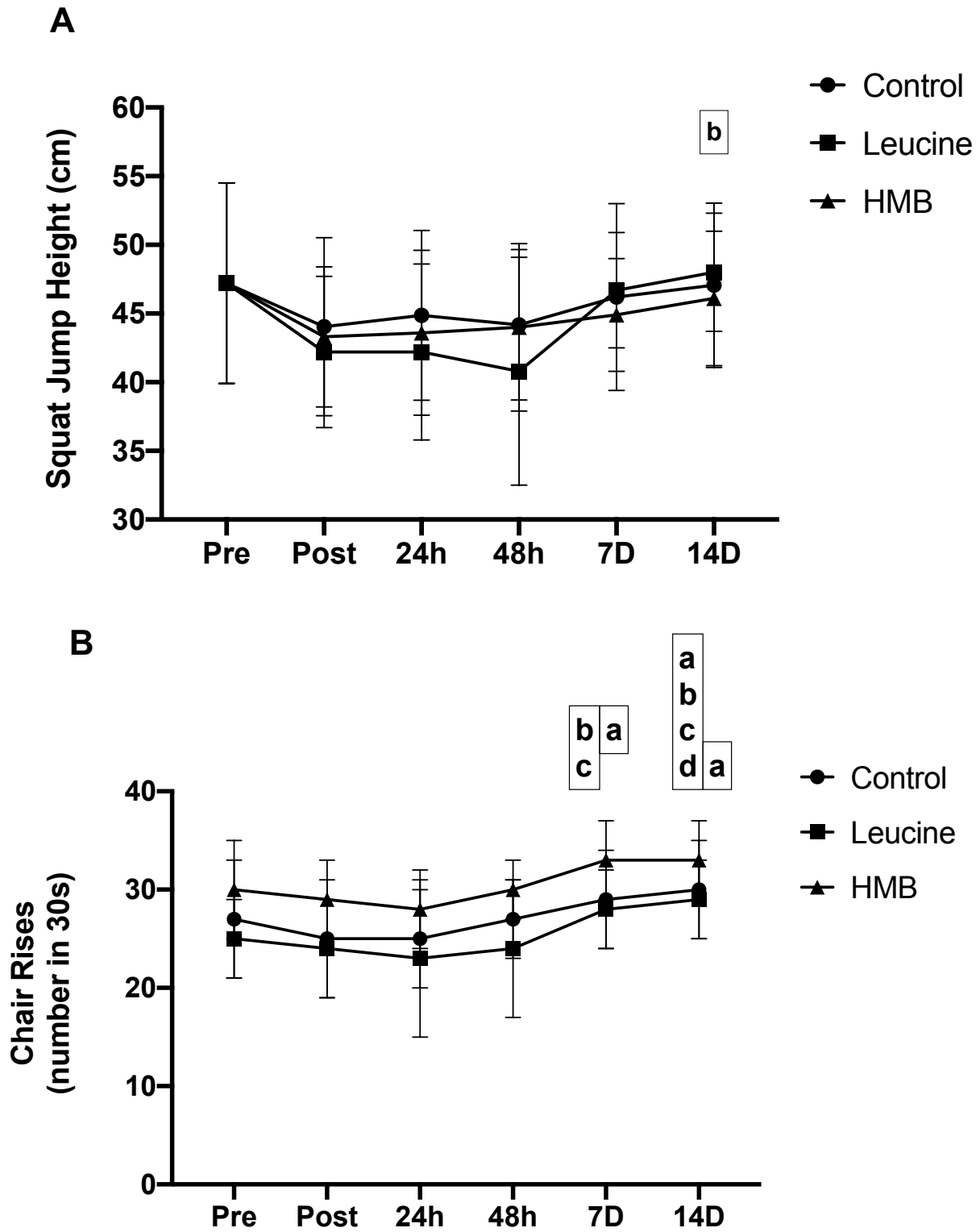
Figure 6.4 Squat jumps (A) and chair rises (B) over time in males in the absence or presence of leucine and HMB. Data displayed as average ± SD. Significance was set at P < 0.05. Significant comparisons: a: pre, b: post, c: 24 h, d: 48 h vs. other time points.
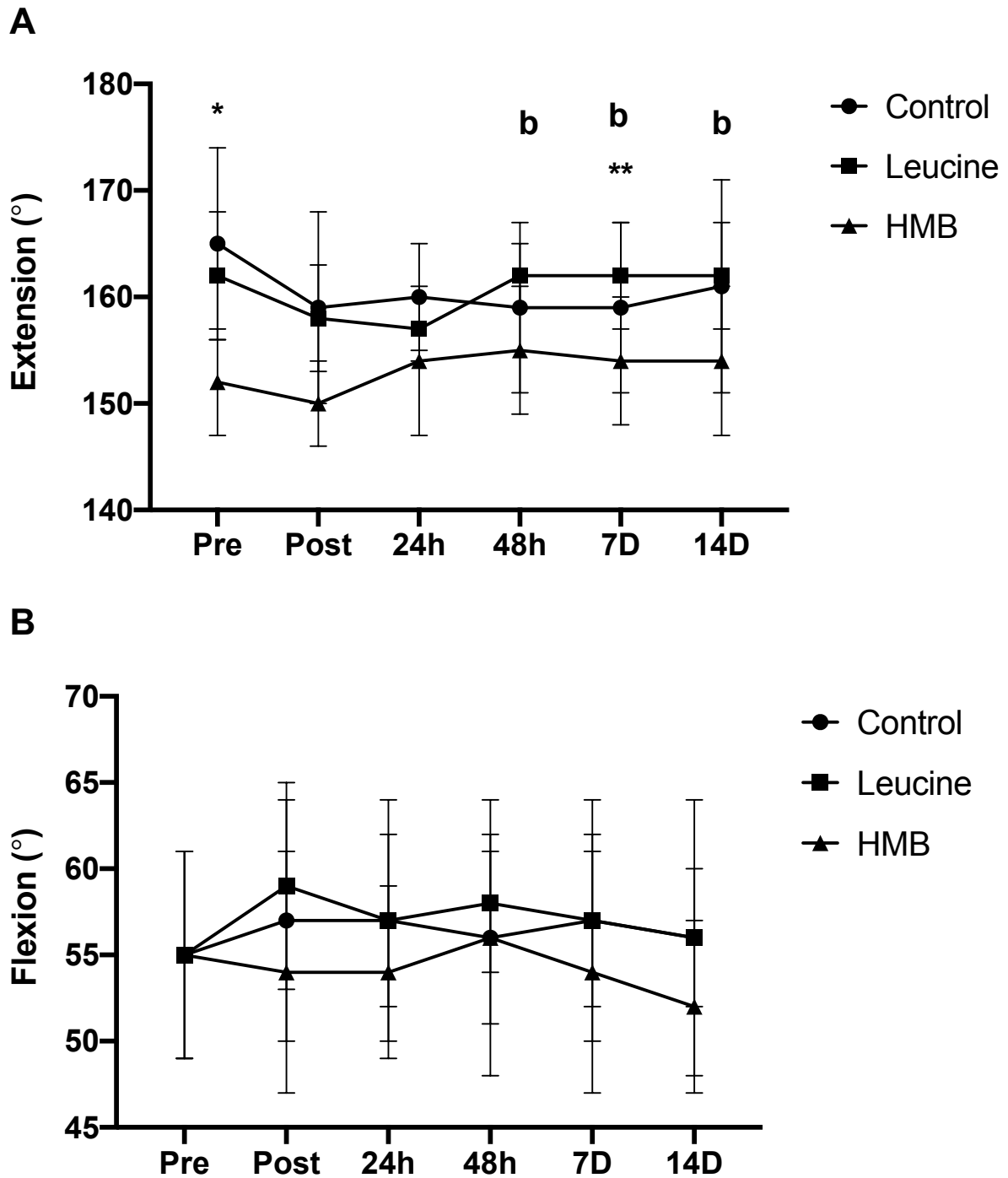
Figure 6.5 Extension (A) and Flexion (B) over time in males in the absence or presence of leucine and HMB. Data displayed as average ± SD. Significance was set at $P < 0.05$. Significant comparisons: b: post vs. other time points; *: control vs. HMB and ** leucine vs. HMB.

6.4.5 Female Demographics

There were no significant differences between female groups in participant height, weight and age (Table 6.1.) For all measures there was no significant differences between familiarisation and pre time point. Therefore, all comparisons were made to pre (0 h).

6.4.6 Female Responses to Eccentric Contractions in the Absence and Presence of Leucine and HMB.

There was no difference between groups at 0 h (Figure 6.6) in blood lactate. From pre to post there were significant elevations (all $P < 0.05$) in all groups, with the control group increasing from 1.3 ± 0.6-3.6 ± 1.8 mmol/L, the leucine group from 1.2 ± 0.9-5.0 ± 2.6 mmol/L and the HMB group from 1.1 ± 0.7-3.5 ± 1.5 mmol/L. There was no significant difference between groups at the post timepoint.

There were significant increases in muscle soreness in all groups (Figure 6.7A-C), with control and leucine groups, showing significant increases (all $P < 0.05$) from pre vs. post (both 4-fold), vs. 24 h (both 5-fold) and vs. 48 h (5-fold; 6-fold respectively). In the HMB group, significant increases (all $P < 0.05$) from pre vs. post (4-fold), 24 h (4-fold) and 48 h (3-fold). There were significant differences at 48 h between leucine and HMB (leucine 3-fold higher; $P < 0.05$). In all groups, there were significant decreases in pain scores from 48 h to 7-day and 14-day, with all values returning to baseline levels.

Average squat jump height was (32.3 ± 4.9 cm), similar differences were evident regardless of treatment group (leucine group males vs. females (44.5-30.0 cm; 33 % difference $P < 0.05$) and HMB group (44.9-33.3 cm; 26 % difference $P < 0.05$) and were retained across time. Further, the average number of chair rises in females was 24 ± 5. There were no differences between groups at baseline. In the control group, number of chair rises did not change as a result of the intervention. Whereas, in the leucine and HMB groups, there was a significant rise in number of chair rises completed from pre to 7-day (both 14 %; $P < 0.05$) and 14-day in the HMB group ($P <$

0.05; 17 %). Also, significant increases (P < 0.05) were observed from post to both 7-day (18 %) and 14-day (21 %) in the HMB group. Despite these changes within the supplement groups, there were no significant differences between groups (Appendix 2). Moreover, muscle tightness and flexibility was investigated post eccentric damage by measuring the extension and flexion around the knee joint. With the exception of the female control group, where there was a small (3 %) but significant decline in muscle extension from pre to 24 h (P < 0.05), there were no other significant differences observed in either flexion or extension across time and between groups (Appendix 2).
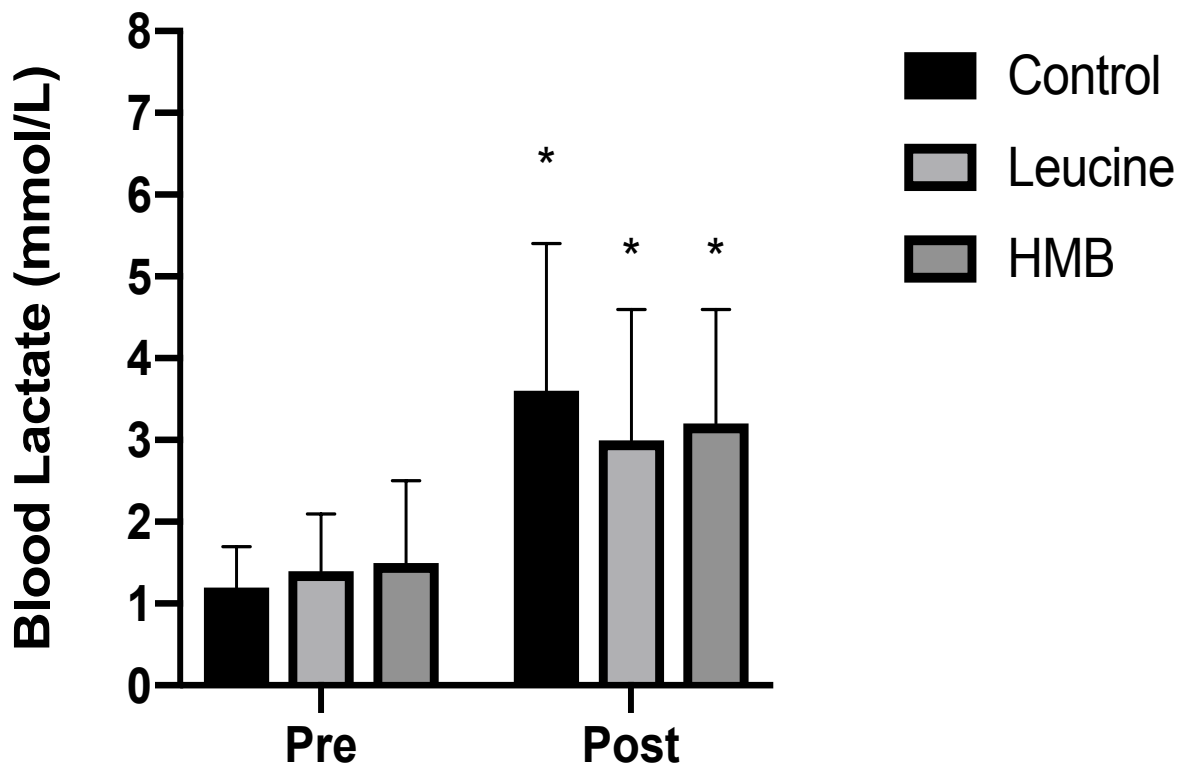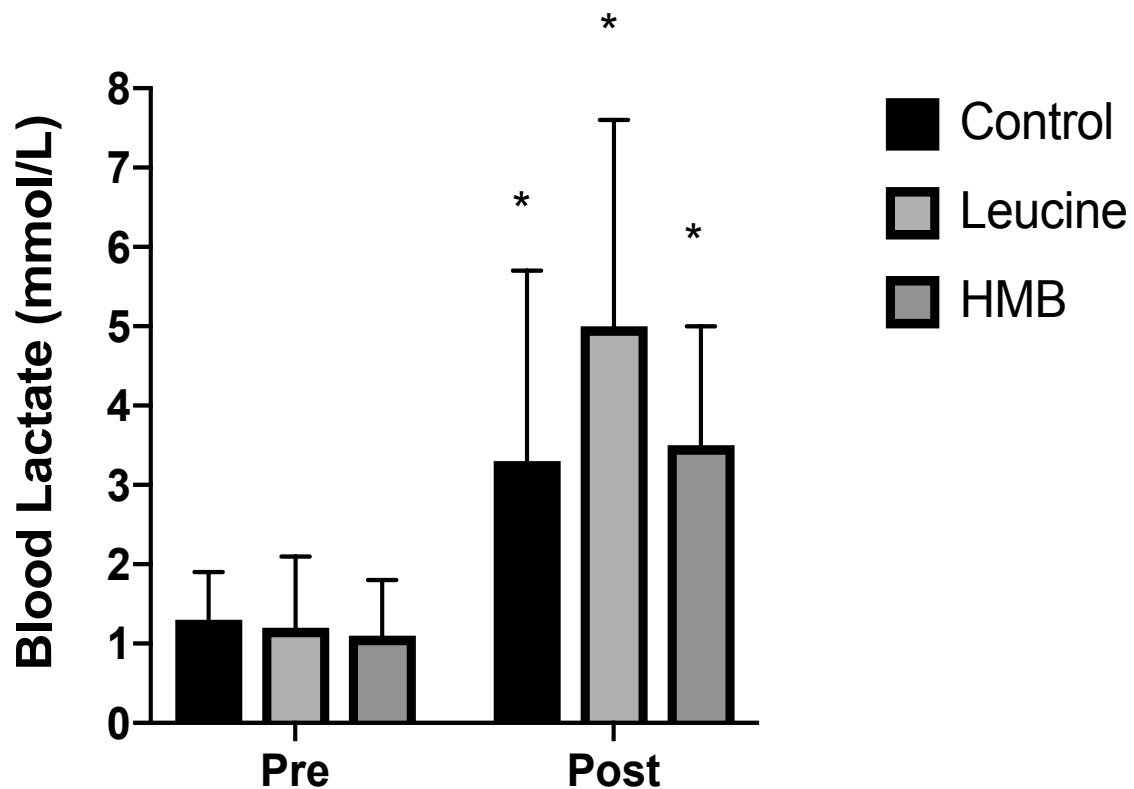

Figure 6.12. Female blood lactate responses from pre to post in control, leucine and HMB groups. Data displayed as average ± SD. Significance (*) represents pre vs. post and set at P < 0.05.

6.4.7 Blood Lactate Increased Post Exercise with Leucine in Females vs. Males

Data suggest that blood lactate responses were comparable in the females, regardless of intervention and indeed increases in the females were comparable to those seen in the males. There were no significant differences in lactate levels between gender in the control or HMB groups. However, in the leucine group, lactate levels were significantly lower ($P < 0.05$) in males vs. females post eccentric damage (3.0 ± 1.6-5.0 ± 2.6 mmol/L).

6.4.8 Increases in Muscle Soreness with Differing Responses CK in Females vs. Males

Trends in muscle soreness evident in the females were similar to those seen in the males, indeed there were no significant differences in muscle soreness in males vs. females in any group or across any time point.

In complete contrast to data derived in the males, CK activity levels in the females did not increase over time in any groups (Figure 6.7). There were also no differences between groups in the females (Figure 6.7A-C). In the control male vs. female groups (Figure 6.8A), CK activity was significantly increased (all $P < 0.05$) at post (64 %), 24 h (79 %) and 48 h (55 %). There were similar increases in the male leucine group (Figure 6.7B), with significant (all $P < 0.05$) increases at post (74 %) and 24 h (62 %) vs. females. In the HMB group, there were no differences at post, however, there were significant increases (both $P < 0.05$) at 24 h (50 %) and 48 h (65 %). In addition, there were significant elevations in the control group (both $P < 0.05$) in male CK vs. females at 7-day (43 %) and 14-day (63 %). In the leucine group, there were significant increases at 7-day ($P < 0.05$; 44 %). No difference was seen at 7-day and 14-day in the HMB group (Figure 6.8C).

To conclude, muscle soreness increased in female participants in response to a multiple eccentric contractions during the first 48 h following intervention, before returning to baseline levels over the following recovery period to 14 days. Unlike the

CK data in males, which increased in the absence or presence of leucine and HMB during the first 48 h, there were no increases in CK activity in the females at any time or in any group. Nevertheless, the increases in pain experienced and elevations in lactate levels warranted further investigation in terms of functional impact, if any, in females.
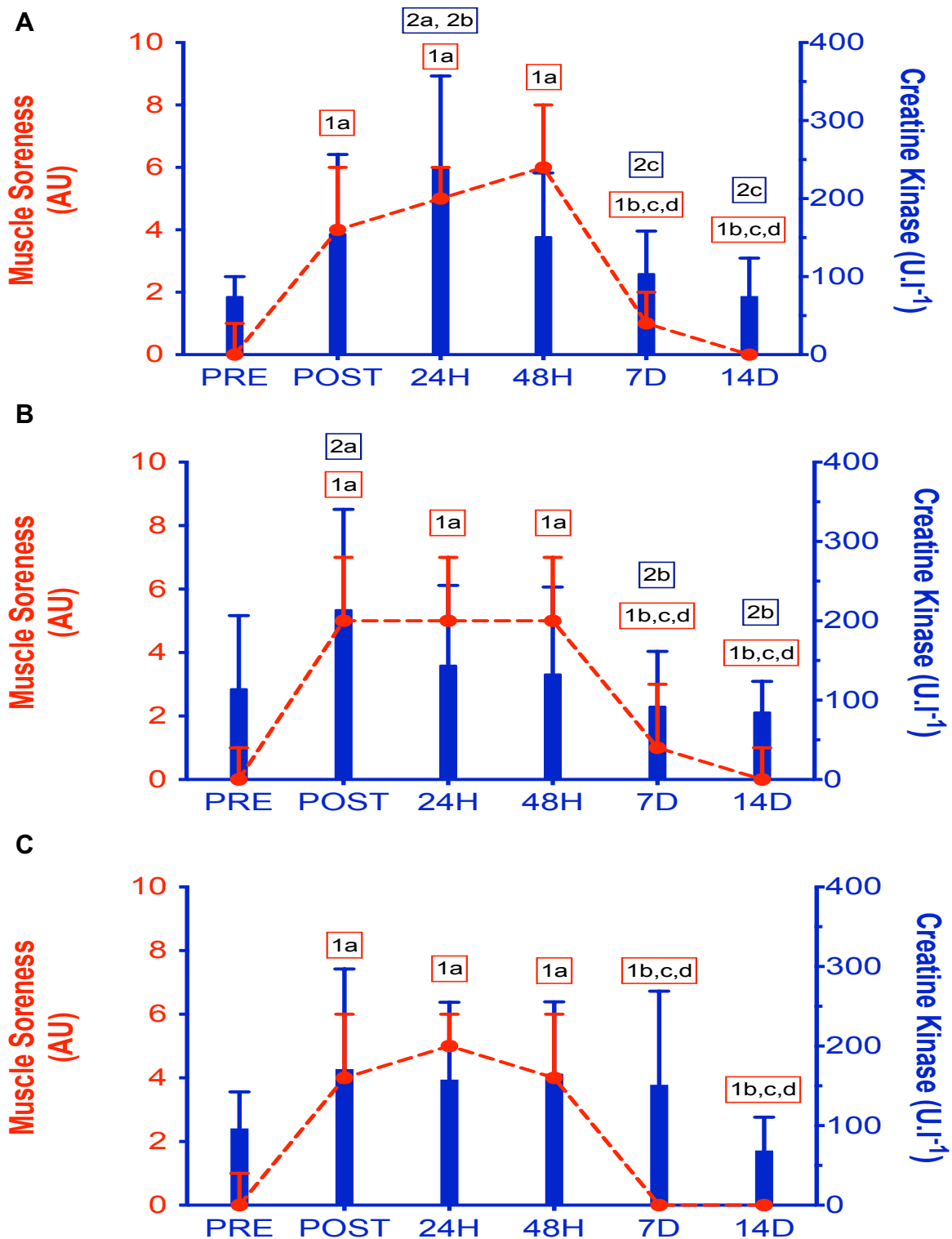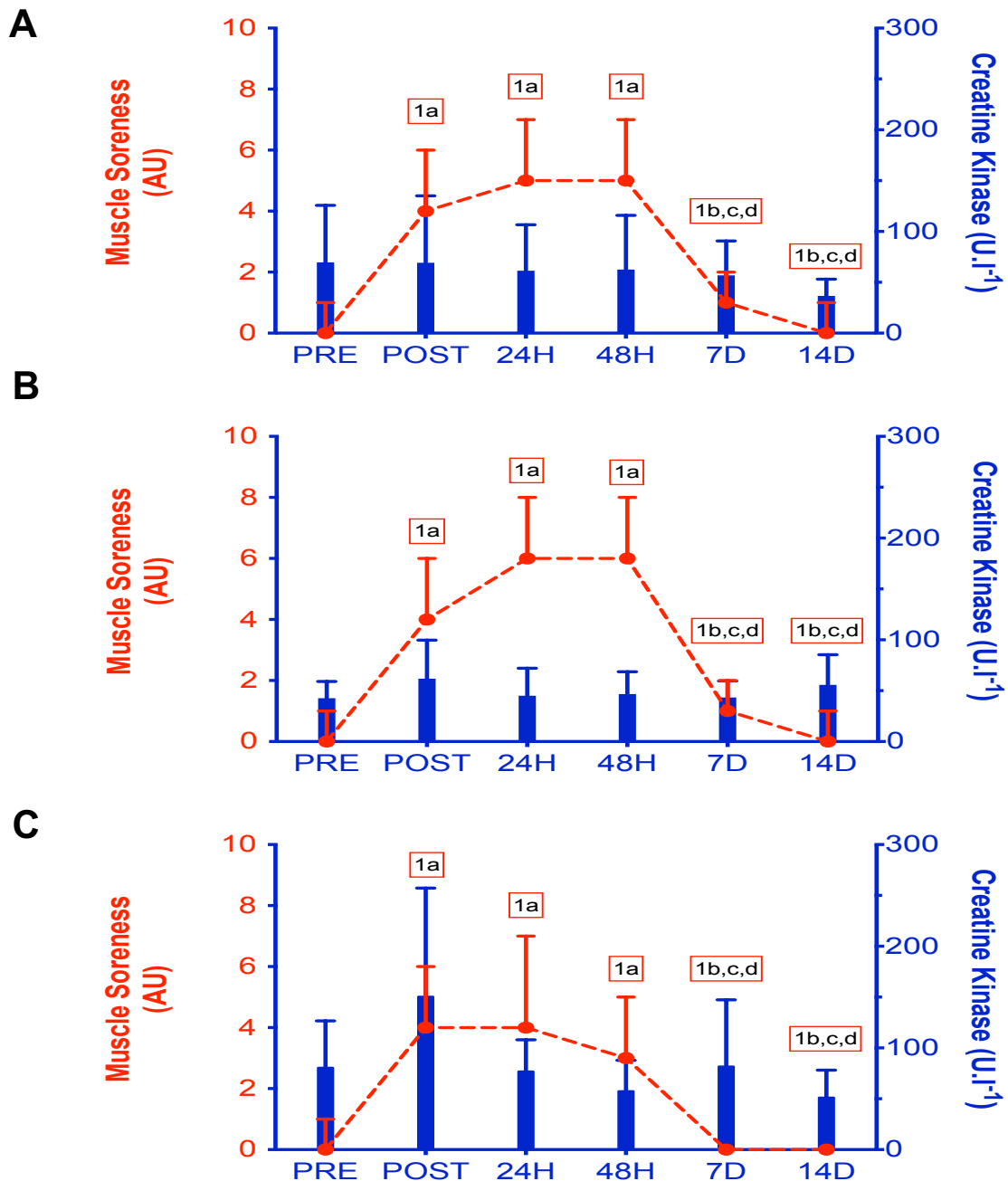

Figure 6.7. Representation of muscle soreness and CK response in control (A) or in leucine (B) and HMB (C). Red line graph and text boxes represent muscle soreness, whereas, blue bars and text boxes demonstrate CK. Significance was set at $P < 0.05$. Significant comparisons: a: pre, b: post, c: 24 h, d: 48 h vs other
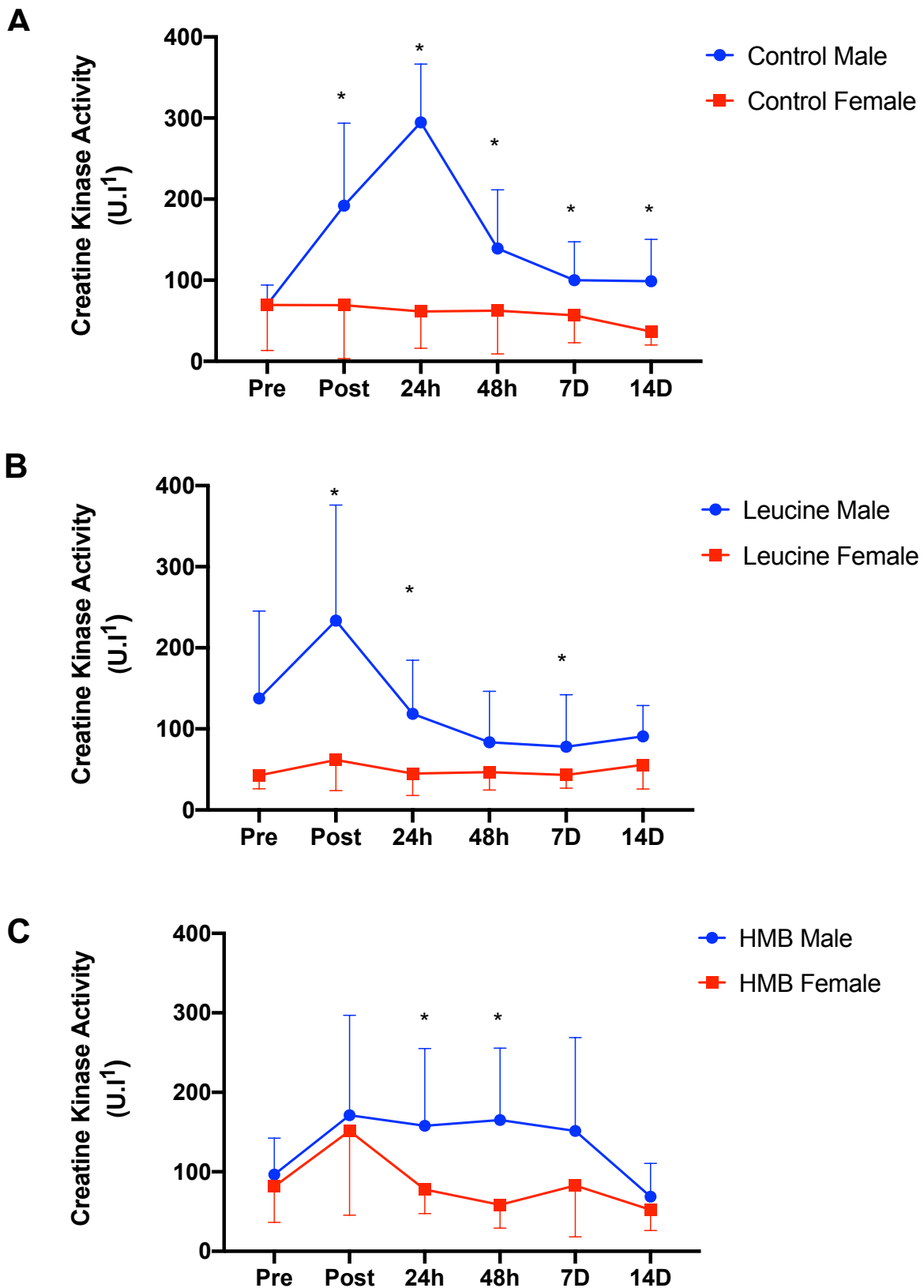
Figure 6.8. CK differences between males and females in control (A), leucine (B) and HMB (C) groups over 14-day. Data presented as mean ± SD. Significance (*) was between male vs. female and set at $P < 0.05$.

6.4.9 Eccentric Contractions and Supplement Impact on Performance and Function in Females and Males

In females, average squat jump height was (32.3 ± 4.9 cm), which was 36 % lower than in males (P < 0.05); As with males, there was also no impact of repeated drop jumps and supplements across all time points on squat jump performance (Appendix 2).

Males performed equivalent (P < 0.05) higher of chair rises under control (27 ± 6) and leucine (25 ± 6) conditions vs. females (24 ± 7; 25 ± 6 respectively) across all times. By contrast, in the presence of HMB, the numbers of chair rises were greater this was as a result of a reduction in the average number performed in males (30 ± 4) vs. females (25 ± 6). Despite this reduction in the number of chair rises in the male HMB group it was not significantly different from the other male groups across time (Appendix 2).

Furthermore, in the control and HMB group, extension was significantly greater (both P < 0.05) in males vs. females at pre (Appendix 2). In the control and leucine group, a significantly greater (both P < 0.05) degree of extension occurred in the males vs. females at 14-day only. Moving on, there was no significant difference between gender in flexion within the control group (Appendix 2). In the leucine group, male flexion was significantly (all P < 0.05) higher vs. females at all time points apart from at pre. There was no difference between males and females in the HMB group over time.

6.4.10 Gender Differences in Cytokine Concentrations with Supplementation

The data derived thus far provide interesting similarities and differences between males and females in terms of responses to damaging exercise protocols. Both genders had similar levels of lactate following exercise, regardless of control or supplement groups and both genders had similar pain profiles, independent of supplements. In contrast, while the male participants experienced significant increases in CK activity post damaging exercise, the female participants did not. Functional deficits as a consequence of the exercise intervention were small in both groups. However, the significant difference in CK warrants further investigation from an inflammatory perspective between the genders. If damage in males has a differing biochemical marker profile to that in females, is the inflammatory response also different?

Several cytokines were measured, including: interleukins 1β, 2, 3, 4, 6, 7, 8, 10, 17α and tumor necrosis factor receptor 1 alpha (TNFr-1α). However, only IL-7, IL-8 and TNFr-1α either showed detectable concentrations or significance (Figure 6.9). In response to the eccentric exercise protocol, IL-7 levels were unchanged in females, but increased with time in control male participants, with a significant, 2.6-fold increase being evident at 7 days ($P < 0.05$; Figure 6.9A). However, with leucine and HMB supplementation, profiles were altered. Under these conditions, IL-7 levels, when compared with baseline, were suppressed (leucine) or at basal levels (HMB) in males over the 7-day period and increased in the females, such that for leucine supplementation, females had significantly higher concentrations of IL-7 vs males over the first 48 h (8.0-fold increase $P < 0.05$) and for HMB, approximate 2.2-fold increases were evident at 48 h and 7 days in females vs. males, however, significance was not achieved (Figure 6.9A). There is a potential role for IL-7 in accelerated wound healing, as a result of enhanced cellular migration (Bartlett *et al.*, 2016).

The IL-8 is a chemoattractant for polymorphonuclear cells and may have a role in accelerating wound healing (Engelhardt *et al.*, 1998). Under control conditions, IL-8, levels increased 1.7-fold in males over the first 48 h, like IL-7, attaining higher

concentrations than those evident in females (significance not attained; Figure 6.9B)). In the presence of leucine and in contrast to IL-7, IL-8 concentrations remained at baseline levels for all time points and in both genders (Figure 6.9B). In the presence of HMB, IL-8 levels were variable, with no differences evident over time or between genders, again, different to IL-7 profiles. Finally, TNFr-1α concentrations were increased 2-fold in males vs. females under control conditions at 24 h post injury. As with IL-7, in the presence of leucine or HMB, levels of TNFr-1α were increased in female vs. males, with differences most marked in the presence of leucine at 48 h (2.2-fold) and in the presence of HMB at 7 days (2.6-fold; Figure 6.9C).

In summary, with supplementation there were increases in IL-7 and TNFR-1 concentrations, however under control conditions, males had higher cytokine levels than females.
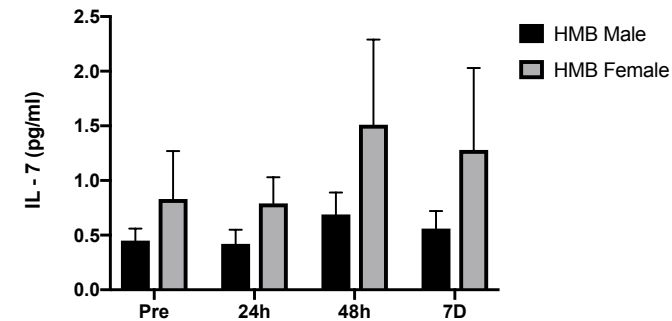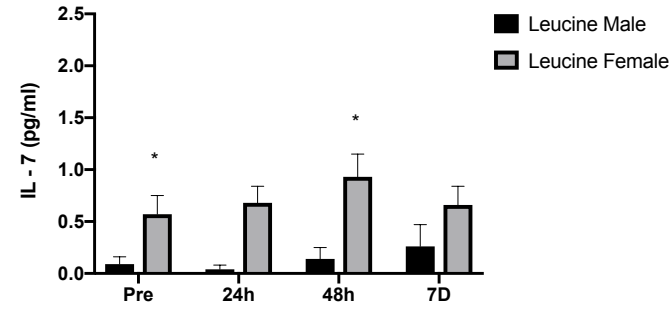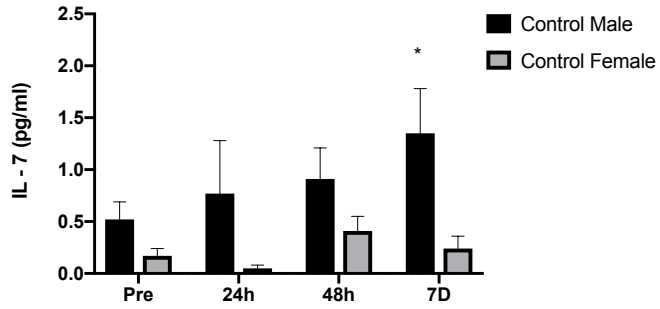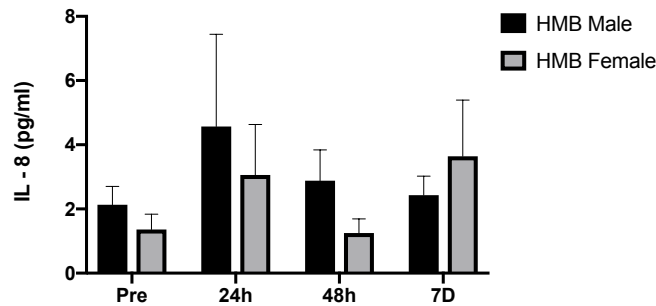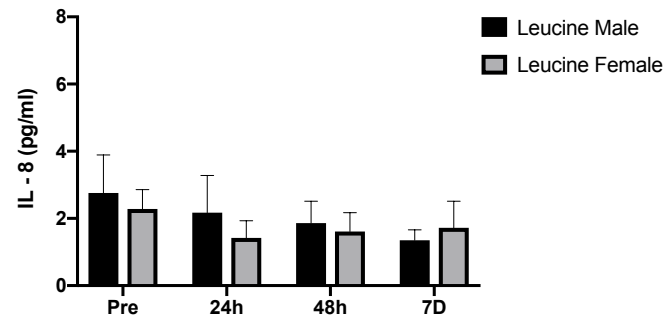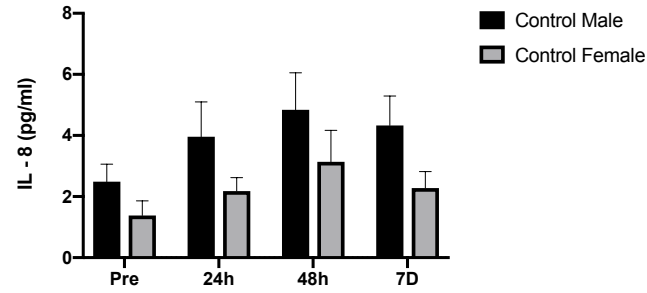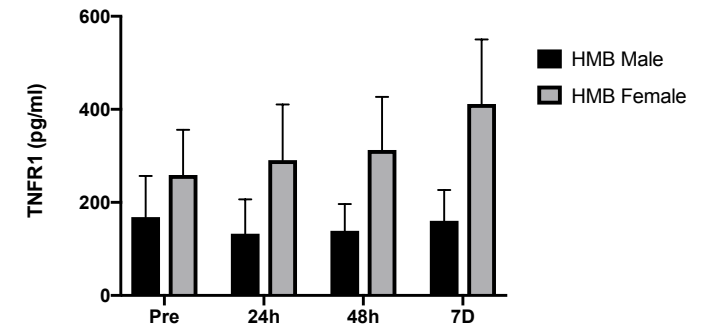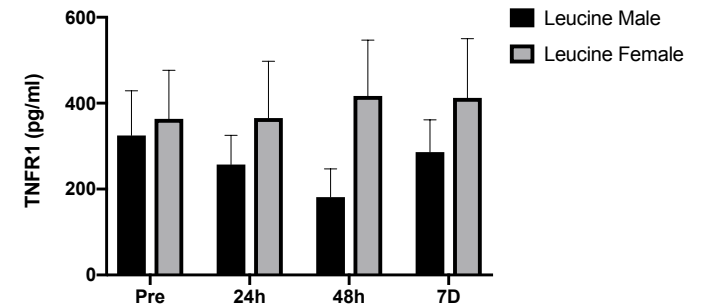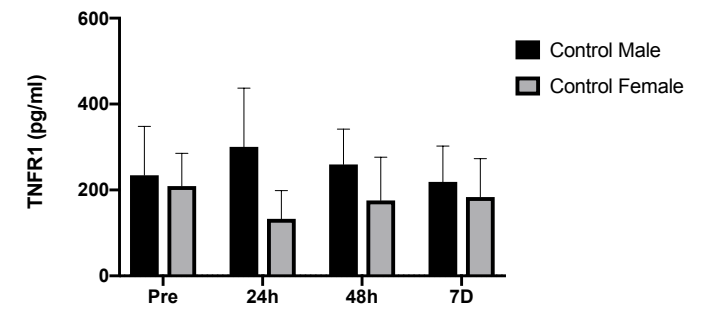
Figure 6.9 Gender comparisons in three different cytokines in control (first row), leucine (second row) and HMB (third row). The cytokines IL-7 (A), IL-8 (B) and TNFR1 (C) were displayed with mean ± SEM. Significance (*) was between male vs. female and set at P < 0.05.

6.5 Discussion

The aim of this study was to induce muscle damage using a drop jump protocol and following muscle injury, to reduce DOMS and improve skeletal muscle repair and recovery with leucine and HMB supplementation. The objectives were to 1: investigate the impact of leucine and HMB on skeletal muscle repair and recovery and 2: uncover the physiological and inflammatory mechanisms during skeletal muscle repair and recovery. The hypothesis to be challenged were 1: leucine and HMB benefited muscle repair and recovery compared to control after muscle injury and 2: leucine and HMB attenuated muscle damage markers and stimulate cytokines involved with muscle repair and recovery compared to control.

6.5.1 Eccentric Contractions Cause Elevations in Blood Lactate, Soreness and CK but No Impact on Function or Performance in Males

In males, blood lactate rose in response to eccentric contractions, suggesting that intensity was increased and comparable among participants. Soreness and CK activity, a commonly used indirect marker of muscle damage were measured (Brancaccio *et al.*, 2007). The findings provide evidence that in all groups the protocol caused increases in both soreness and CK activity over the repair phase. These levels return to baseline during the muscle recovery phase. Similar to these findings, most studies report increases in both muscle soreness and CK activity over 48 h (Jackman *et al.*, 2010; Kirby *et al.*, 2012). Kirby *et al.* (2011), performed 100 drop jumps in male participants, from a height of 60 cm. However, the participants also completed 10 repetitions x 6 sets of leg press exercises. The authors reported no attenuation with leucine (250 mg/kg/d) on muscle soreness and CK activity (Kirby *et al.*, 2011). With HMB supplementation, Wilson *et al.* (2013) reported reduction of CK activity and muscle soreness with HMB (3 g/d; same concentration as in our study) after intensive resistance training session in young males. In another study, HMB mitigated CK concentrations compared to placebo at 72 h after 55 knee

extensions, but the level did not reach baseline (Wilson *et al.*, 2009). Padden-Jones *et al.* (2001) observed similar findings with HMB supplementation in muscle soreness after 24 maximal elbow extensions, the study however did not measure CK activity. Whereas, Van-Someren *et al.* (2005) reported an increase in CK activity in the placebo but not the HMB (3 g/d) group, after 3 sets of 10 bicep curls at 70 % 1 repetition max. Therefore, findings across studies differ and the results in this thesis illustrate that physiologically there was no impact of leucine or HMB on CK or soreness after eccentric exercise in males. However, the impact of 100 drop jumps on blood lactate, muscle soreness and CK warranted further investigation, in the absence or presence of supplementation, to determine the impact on muscle function and performance.

There was no difference in squat jump height or number with leucine or HMB supplementation, compared to controls, over the first 48 h. In contrast, Kirby *et al.* (2011) observed significant decreases in jump height in both placebo and leucine groups. Finding differences may be due to the increased severity in the study by Kirby *et al.* (2011), which reported significant force losses measured by MVC. The limitation to this study was not measuring MVC which is suggested to be the most reliable and valid marker of damage (Damas et al., 2015). However, at day 14, our results indicate that leucine supplementation increased squat jump height compared to immediately post. This demonstrates that the protocol did cause slight decreases immediately post exercise, and leucine rescued and improved this reduction, as no significant difference was observed in the control group. There was no impact with HMB supplementation. Therefore, these findings suggest that there is limited impact of supplementation on squat jump height in the repair and recovery phase following a drop jump protocol.

Similar to performance, there was no difference in the muscle function during 48 h with leucine and HMB supplementation, compared with control. There is no comparative evidence reporting influence of supplementation on chair rises, warranting further investigations. Van Someren *et al.*, (2005) reported no effect of HMB supplementation on ROM, which coincides with our findings. Interestingly, during muscle recovery, in the control and leucine group there

was an increased number of chair rises compared to pre and increased extension compared to post and 24 h. This provides evidence that chair rises and extensions can improve over 14 days, however, the lack of a between group difference suggests this may be a learning effect, rather than a specific effect of the supplement per se.

Although the exercise protocol caused elevations in blood lactate, soreness and CK over the repair phase in males, there was no impact of leucine and HMB supplementation on these measures or on muscle function and performance. However, whether there is an effect of leucine and HMB on muscle function and performance during the recovery phase requires further investigation following one bout of eccentric exercise.

6.5.2 No Impact of Eccentric Contractions on CK in Females, but Comparable Responses on Blood Lactate, Function and Performance to Males

Similar to males, blood lactate levels significantly increased from pre to post, with no attenuation with leucine or HMB. Muscle soreness significantly increased in all groups over 48 h, then reduced during the recovery phase. Evidence indicates that with BCAA administration, muscle soreness is attenuated in females after 7 sets of 20 squats (Shimomura *et al*., 2010). We hypothesised that in females, CK and muscle soreness would increase in response to eccentric exercise. There was no change in CK in response to 100 drop jumps in the absence or presence of supplementation. Shimomura *et al*. (2010) also reported no difference in CK and myoglobin in either the placebo or BCAA group. Although both exercise protocols were different (100 drop jumps vs. 140 squats), the eccentric movements were similar as they both involved squatting to 45 degrees. It is not known if increasing the severity of muscle damage, for instance, downhill running or electrical stimulation would impact the CK response differently in females and whether this would be altered with supplementation.

However, a limitation of this study is that we did not control for menstrual cycle, via measuring blood oestrogen or for questions within the screening questionnaire. The differing phases of the menstrual cycle could affect musculotendinous stiffness in female participants (Eiling *et al.*, 2007). In addition, CK was significantly lower in high oestrogen group compared to control (Carter et al., 2001). Therefore, higher levels of oestrogen during menstrual cycle could have protective effects in response to muscle damage (Clarkson and Hubal, 2001). However, some report no impact of menstrual cycle on tendon mechanical properties (Burgess *et al.*, 2009; Kubo *et al.*, 2009) and no impact on CK or soreness (Miles and Schneider, 1993; Sorichter *et al.*, 2001). The literature is not clear, with different damaging protocols and levels of damage eliciting different outcomes, e.g. some indicating protective effect, and some not (Clarkson and Hubal, 2001). Although, menstrual cycle might have an effect on CK, soreness increased post exercise, this remains to be determined.

Muscle soreness between males and females was not different in any group, which is supported by previous research (Rankin *et al.*, 2015). Further, this study reported large difference in CK response between male and female over 14 days in control and leucine groups. In contrast, Rankin *et al*. (2015) reported no difference in any groups in CK over 72 h with 6 sets of 10 repetitions of hamstring contractions. Differences between protocols and muscle groups could influence CK results, but also CK protocols. Research in sport science is understudied in females (Costello *et al.*, 2014). Reinforcing the demand for more research in the female population, as there are differences between genders, as findings in this study indicate.

In addition, we observed no changes in muscle performance in the absence and presence of leucine or HMB. Shimomoura *et al*. (2010) did not measure squat jumps but suggested that BCAA supplementation attenuated force loss with 140 squats. However, our results suggest no decline in muscle performance from the exercise protocol. Surprisingly, muscle function during muscle recovery reported significant increases in the number of chair rises performed with both leucine and HMB supplementation compared to pre and

post levels. Although increases were observed with groups, the differences were not significant between groups. Muscle injury did reduce muscle extension at 24 h in the control group, suggesting that leucine and HMB attenuated muscle stiffness in the hamstrings.

Previous research suggests that after multiple drop jumps, males demonstrate increased levels of force production at baseline (Hubal *et al.*, 2008). However, post exercise, relative changes were similar between men and women (Hubal *et al.*, 2008). Our results support this evidence, in that there was no difference between males and females in performance and muscle function in the absence and presence of leucine and HMB. There was also no difference between males and females with regard to muscle soreness, performance and function. By contrast, there was a considerable difference in CK response to eccentric contraction which required further investigation into muscle inflammation.

6.5.3 Comparisons in Inflammation Between Male and Females in the Presence of Leucine and HMB

For the majority of cytokines measured, the eccentric protocol or supplements caused no elevation in cytokine concentrations. However, there were increases in IL-7, IL-8 and TNFr1-α over the 7 days. In males, there was an exponential increase in IL-7 compared to females over time, which reached significance at day 7. To the authors knowledge, there are no reports investigating IL-7 response to eccentric exercise. However, Haugen *et al.* (2010) provide evidence that IL-7 was produced by primary skeletal muscle myotubes and is reported to activate T-cells which are important during satellite cell activation and the inflammatory process (Chen and Shan, 2019). In addition, IL-7 levels were increased in wounded keratin cells compared to unwounded (Bartlett *et al.*, 2015) and were believed to be involved in improved keratinocyte migration. Interestingly, in our study, the IL-7 profiles were altered with leucine and HMB supplementation, IL-7 concentrations increased in females compared to males. Although data are scarce, evidence does indicate that higher levels of IL-7 support immune cell recruitment and cell migration.

Similar to IL-7, IL-8 is reported to be involved in cell migration during wound healing, specifically, in leukocyte infiltration (Engelhardt *et al.*, 1998). Our results indicate that in the control group, males have increased concentrations compared to females and peak at 48 h, which is similar to the CK profile. Our results further suggest that leucine and HMB suppress the increases in IL-8, in both males and females. In contrast, Peake *et al.* (2005) also measured IL-8 over 24 h and observed no increase, however, it is not known whether the concentrations would increase post 24 h. Finally, it is well known that TNF-α is produced by macrophages and T-cells and has multiple synergistic roles in the removal of necrotic tissue, satellite cell activation and proliferation (Chen and Shan, 2019). Therefore, the TNF-α receptor, TNFr1-α concentration in serum was measured as an indirect marker for TNF-α. TNFr1-α concentrations were significantly increased at 48 h in males compared to females, also similar to the CK results. However, as with IL-7, leucine and HMB reversed the TNFr1-α response. Townsend *et al.* (2013) also reported an attenuation with HMB (3 g/d) of TNFr1-α following a resistance exercise training session in males. In summary, in control group, males had greater cytokine concentrations, whereas with supplementation this response was reversed for IL-7 and TNFR-1 concentrations in females.

6.6 Conclusion

To conclude, the data from this study suggest that leucine and HMB supplementation did not improve skeletal muscle repair following multiple eccentric contractions in males or females. Comparison between genders indicated that males had increased CK levels compared to females, although muscle soreness levels were not different. Finally, cytokine activity data suggest that males had increased concentrations compared to females under control conditions, but that this cytokine response was altered with leucine and HMB supplementation, whether this directly influenced the local cellular adaptations is unknown.

Chapter 7: Thesis Synthesis Chapter

7.1 Chapter Purpose

The purpose is to amalgamate the previous chapters of this thesis and discuss the major findings, strengths and limitations. From these outcomes, future research topics will be outlined and finally, this thesis will be concluded.

7.2 Thesis Aims and Objectives

7.2.1 The overarching aim of this thesis was:

To utilise amino acid supplementation as an intervention to reduce damage and/or facilitate growth and repair in skeletal muscle using *in vivo* (objective 1) and *in vitro* (objectives 2-4) models.

7.2.2 The objectives of each study were as follows:

1: To reduce the sensation of DOMS and improve skeletal muscle repair and recovery with leucine and HMB supplementation following dynamic eccentric exercise.

2: To investigate the impact of leucine and HMB on control and replicatively aged skeletal muscle cell repair.

3: To determine the impact of nutritional supplements on myotube formation in control and replicatively aged murine myoblasts.

4: To investigate the dynamic protein profiling on replicatively aged and control myoblasts and myotubes.

7.3 General Discussion of Major Thesis Outcomes

Replicatively Aged and Control C2C12 Cell Migration and Fusion with Leucine and HMB.

The main outcome identified was replicatively aged myoblasts migrated with greater efficiency compared to control cells. This finding was in contrast to our hypothesis which was based on the majority of previous literature reporting that aged satellite cell function is impaired (Welle, 2002). This was the first study to directly measure migration. Mechanistically, Akt and ERK signalling were important for basal replicatively aged cell migration. Whereas, only Akt signalling was increased in control myoblasts, which is similar to the reported literature (Suzuki *et al*., 2000, Kawamura *et al*., 2004, Al-Shanti *et al*., 2011, Dimchev *et al*., 2013). However, contrary to our hypothesis, in both ages of cell, mTOR was not important for efficient migration as cells continued to migrate when mTOR was inhibited. Both replicatively aged and control myoblasts responded to leucine and HMB supplementation in relation to improved cell migration, although non-passaged control cells were more responsive to supplementation. In addition, it should be remembered that in the presence of supplements, control cells reached migration capacities of aged cells, suggesting a ceiling had been reached. Consequently, the objective was achieved, nevertheless, muscle repair is only the first stage of regeneration. Therefore, the next question to be answered, was whether these replicatively aged myoblast fused efficiently during late stage muscle regeneration and whether there was a benefit of leucine and HMB supplementation compared with control myoblasts.

Although the replicatively aged cells migrated they showed compromised fusion compared to control myoblasts, similar to previous findings from our group (Sharples *et al*., 2011). This was a result of reductions in Akt, mTOR and ERK signalling. This lack of fusion capacity was not rescued with leucine or HMB supplementation, despite Akt and mTOR signalling eliciting beneficial responses. Interestingly, basally in replicatively aged cell migration, when injury via scratch assay was performed, phosphorylation of Akt and ERK was

increased, whereas, without scratch they were reductions in signalling. The differing responses to cell stress require further investigation. In the absence of fusion, myogenin, IGF-I and IGF-II were significantly supressed in replicatively aged cells, regardless of intervention, further underlying the mechanistic impairments resulting in lack of fusion. Conversely, control cells fused over 96 h and fusion capacity was increased further with leucine and HMB supplementation, which is supported by previous literature (Dai *et al*., 2015: Kornasio *et al*., 2009). Thus far, replicatively aged cells migrate efficiently, but do not fuse, even with protein supplementation, despite expressing relevant AA transporters and recognising the AA supplementation through altered signalling profiles, challenging previous theories that aged cells display anabolic resistance per se, given that some of the mechanisms investigated in replicatively aged and control were sensitive to protein supplementation. The lack of fusion was not therefore as a consequence of an inability to mount a signalling response, nor indeed to a reduction in amino acid transporters, at least at the mRNA level, but as a result of a disconnect between the capacity to mount a relevant signal and appropriate upregulation of genes required for fusion. As this becomes a vast question, which could be underpinned by multiple processes, hypothesis driven research was difficult, given the potential for large scale cellular alterations. Therefore, we used proteomic analyses, by measuring proteome abundance and FSR, to begin to identify on a larger scale, which protein groups were altered during myoblast differentiation in replicatively aged vs. control cells. This insight would begin to unravel differences between growing and fusing myoblasts, with potential applications to development and cell fusion.

Dynamic Proteomic Profiling of Replicatively Aged Myoblast Differentiation

In the previous studies (Chapter 3 and 4), we have revealed that replicatively aged cells migrate at an increased rate over 48 h, they do not fuse throughout 96 h of differentiation. This lack of fusion, with reduced levels of gene expression in particular myogenin, IGF-I and IGF-II which are important genes for myoblast differentiation (Stewart *et al*., 1996: Sharples *et al*., 2011), lead to novel investigation of dynamic proteomic profiling on this model of cellular

aging. The first hypothesis was that during the first 24 h of differentiation both replicatively aged and control myoblast have greater FSR compared to myotubes. This hypothesis was accepted, which allowed us to conclude that during early differentiation, there was an increased rate of protein production. By analysing individual protein abundance, we observed a reduction in ribosomal protein abundance in replicatively aged myoblasts and contractile proteins in myotubes. In addition, replicatively aged myoblasts had significantly greater abundance of metabolic enzymes involved in glycolysis compared to control. This suggests that the cells are requiring more ATP for the cell to function, possibly favouring cell survival over myotube formation. The findings in control myoblasts and myotubes were similar to those reported in the literature (Tannu *et al*., 2004: Kislinger *et al*., 2005). Therefore, throughout replicatively aged myoblast differentiation into myotubes, this study has revealed that the reduction of ribosomal proteins could result in decreased production of proteins involved in myoblasts differentiation. In turn, as evidenced in the previous study (chapter 4), there was reduction in both Akt and mTOR activity, which could result in overall impaired FSR and finally the production of essential ribosomal proteins and proteins involved in differentiation. Following these insights into our model of ageing and the surprising differences between the capacity of replicatively aged cells to migrate and then fuse, the next step was to investigate the physiological responses post an acute damaging protocol in humans, with the focus on repair and recovery, and the impact of leucine and HMB supplementation.

Repair and Recovery in Males and Females Following Acute Bout of Exercise: Impact of Leucine and HMB.

So far, we have investigated the cellular responses on C_2C_{12} myoblasts and on our model of replicative ageing. In particular, revealed the effects on cell repair and myotube formation, processes critical for regeneration. After bouts of exercise, skeletal muscle goes through the same regenerative processes. Therefore, we aimed to improve recovery and facilitate repair following acute bout of damaging exercise. Although, due to ethical reasons, the human study was not performed in older participants, investigation into the effects of leucine

and HMB were performed. To this end, healthy young males and females performed 100 drop jumps causing increased lactate accumulation, altered creatine kinase profiles, the sensation of DOMS and altered inflammatory cytokine profiles involved in muscle repair and regeneration. Leucine and HMB did not reduce indirect indicators of DOMS (soreness, CK). These data are in contrast to other published evidence (Kirby *et al.*, 2011: Wilson *et al.*, 2009: Rankin *et al.*, 2015: Van-Someren *et al.*, 2005: Shimomura *et al.*, 2010). However, because the literature is lacking in leucine and HMB supplementation, some comparisons could not be directly made (Rankin *et al.*, 2015: Shimomura *et al.*, 2010). BCAA (Shimomura *et al.*, 2010) and milk (Rankin *et al.*, 2015) supplementation include other contents, including valine and isoleucine in BCAA and carbohydrate and fats in milk, which compared to leucine and HMB may underpin the differences in data. Indeed, both milk and BCAA do contain leucine. This discrepancy ultimately complicates the interpretation of results compared to previous literature. However, in our study, leucine and HMB did reduce cytokine responses (IL-7, IL-8, TNFr1-α) in males vs. females, suggesting that nutritional supplements may impact on satellite cell repair and regeneration, warranting further investigation. The cytokines IL-7, IL-8 and TNFr1-α are reportedly involved in the immune response to muscle damage (Townsend *et al.*, 2013) and are important for cell migration (Bartlett *et al.*, 2016: Engelhardt *et al.*, 1998). The data on the repair and regeneration of skeletal muscle derived from younger cohorts demonstrated potential impact on an immune and therefore potentially cellular level in the absence and presence of supplementation.

7.4 Thesis Strengths and Limitations

7.4.1 Thesis Strengths

The first study was novel as it investigates the effect of eccentric contractions in males and females and the impact of leucine and HMB on muscle repair and recovery, something not previously reported in a single research study. The exercise protocol was designed to apply to sporting settings, as multiple sports/training use repeated jumps, for instance: basketball, volleyball, football and plyometric training. Furthermore, in this study we extended the investigation period to two weeks as the anti-inflammatory phase and myofiber fusion and growth can last beyond 7 days (Dumont *et al.*, 2015). Finally, this is the first study to investigate 10 different cytokines over 7 days in each experimental group.

The second study was the first to investigate migration capacity in our model of replicatively aging with leucine and HMB supplementation. Further, underpinning mechanisms, signalling cascades, were investigated with appropriate inhibitors and measuring the phosphorylation status. In addition, the analysis of migration capacity by measuring individual cell velocity, directionality and distance provides detailed information on cell responses, when compared simply to number of cells which have entered the wound.

The strength of the third study was the novelty of supplementing leucine and HMB in replicatively aged myoblasts and assessing impact on differentiation. Most studies to date suggest the incidence of metabolic resistance with ageing. Whereas the data derived, albeit in cell models, contradicts the dogma, suggesting aged cells are responsive to nutritional supplementation, however, the output may de different to non-aged cells. Briefly, this study reproduced previous findings, indicating that replicatively aged cells do not fuse in contrast to control myoblasts (Sharples *et al.*, 2011). Mechanisms on different levels were investigated to understand a larger snapshot of the lack of fusion in

replicatively aged cells and the increased fusion in control cells with protein supplementation. The mechanisms included: metabolic (CK, LDH), cellular (morphology), intracellular (signalling) and molecular (gene expression), including various genes from amino acid transportation to cell-cell adhesion to genes related to myoblast differentiation. Key is the capacity of the aged cells to respond to amino acids, albeit without fusion as an output measure.

The final study was the first to determine proteome abundance and FSR in control and replicatively aged myoblasts and myotubes. Thus, enabling comparison on protein by protein level. Analysing the proteome allowed for comparisons of hundreds of proteins involved in multiple processes from glycolysis to protein chaperoning. The use of heavy water labelling was fundamental in determining protein synthesis rates in cell culture models.

To conclude, the major strengths of this thesis were the novelty of each study and the use of different models and techniques. Generating experiments on multiple biological levels from whole body physiology to cellular to protein to intracellular and finally molecular and large scale data analyses are unusual. Although in a number of cases our hypotheses were not confirmed, we provide novel data illustrating that although nutritional supplements *in vivo* may not have had a functional benefit, they may impact at an immune cellular level, which would in the long term be beneficial. Further the concept that ageing muscle is suboptimal compared with control is also challenged, through the use of different output measures e.g. migration is enhanced in aged vs. control myoblasts and the capacity to fuse, while compromised in aged cells, does not appear to be as a consequence of reduced amino acid transporters, or a reduced capability to mount a relevant signalling response, but rather to a different need of the cells. This concept is strengthened through the proteomic analyses, which suggest this differing need in replicatively aged cells may be metabolic and that the compromised fusion may be as a result of reduced ribosomal and contractile proteins but increased metabolic function.

7.4.2 Thesis Limitations

One of the limitations to this study was lack of placebo group, instead of control. This would have created a double blinded study scenario controlling for participant bias towards the supplements. However, given the different supplements used, multiple placebo groups would have been required and this was beyond the scope of the study. Further, the difference in participant number between groups altered statistical power. The sample size for some groups was also relatively small (n = 9) which would have likely added variability to results, and possibly impacted statistical outcomes. In addition, the inclusion of maximal voluntary contraction, as an output measure, is common in this literature (Baumert *et al.*, 2018) and would have provided an indication of force loss as a result of our exercise intervention. Controlling diet over two weeks is difficult unless pre-planned food is prepared for the participants which was not feasible for this study. Lastly, measuring cytokine activity within the first 24 h would provide an indication if there was an immediate response in serum concentrations giving a more comprehensive timescale.

In contrast, the limitation of the second study was the relevance of these findings to human cellular responses, as with all murine cell culture experiments. Therefore, the interpretation of results should be considered carefully. The analysis of intracellular phosphorylation of Akt, ERK and mTOR pathways confined findings to conventional pathways and therefore data may be undersold.

The use of the C_2C_{12} cell line, which is strongly compared to primary muscle cells warrants consideration. Ultimately performing these studies in young and aged myoblasts would be a more relevant model set.

The limitation of analysing the proteome was the relatively small total protein identifications and sensitivity of the technique. For instance, running each sample for 90 minutes instead of 60 minutes which would have provided additional protein identifications, however, the data storage in the software was

insufficient to store and process that much data. In addition, the larger proteins with multiple peptides dominate the analytical landscape. Indeed, the mass spectrometer was also not sensitive enough to identify the very small peptides running through the machine. The number of proteins analysed could have been increased by fractionation techniques prior to protein digestion. In addition, only a fraction of the protein that was synthesised was measured instead of absolute synthesis. Other mechanisms that were not measured could influence protein abundance and turnover, such as protein breakdown and post-translation modifications (Vogel & Marcotte 2013).

7.5 Future Directions

7.5.1 Study 1 and 2

In these studies, our group and this thesis has provided some underlying mechanisms of replicatively ageing, but more research is required. For instance, the investigation into the proteins secreted by myoblasts/myotubes (including exosomes), oxidative proteins, alterations in cytoskeleton, extracellular matrix and basal lamina proteins. In addition, interventions such as transfecting cells with myogenin, or supplementing replicatively aged cells with control secretome and vice versa, to ascertain niche vs. milieu adaptations, warrants investigation. Other interventions could include providing a mechanical stimulus, in the form of stretch and compression using Flexcell equipment, for example. Muscle cell lines are easy to use, do not require ethics and a more efficient way to produce results, therefore, generation of important questions can be identified first, and translated to primary cells, once methodologies have been optimised.

One of the main challenges with using non-human cell lines is the translation of the data into human cellular responses. If possible, future research in myoblasts should involve primary human muscle cells, isolated from muscle biopsies. With our replicatively ageing model, the main advantage is the responses are purely intrinsic and not affected by the microenvironment. Therefore, serially passaging young human myoblasts would allow for a model to investigate intrinsic cellular responses. Experiments could also include aged and young myoblasts and comparisons can be made on a number of mechanistic outcomes. For instance, the use of human serum could be used to identify the effect on young and old cells. Indeed, young myoblasts, which have undergone serial passaging could be treated with participant matched young serum to investigate the cellular response. To validate the replicatively aged model, experiments investigating the difference between primary myoblasts and C_2C_{12} myoblasts can be completed. For instance, in study 2, the data demonstrate increased myoblast migration in replicatively aged cells, would this be the same in primary human myoblasts from a 70-year-old participant, vs. a

25-year-old? With that, the differences in gender and training/nutritional status can also be investigated in primary human cells lines. One questions of interest would be how the myogenic potential differs from a trained endurance athlete compared to a body builder, for example. Thus, other comparisons could include a master athlete compared to an aged matched sedentary individual.

7.5.2 Study 3

Repeating the same experimental design for proteomic analyses of young and old primary human myoblasts would provide an insight to the protein abundance and turnover of numerous proteins. Once again, comparisons between gender and training status of participants could be researched. The additional challenge with these experiments is the consideration of additional cell types (fibroblasts) and the ratio between myoblasts and fibroblasts and their impact on adaptation. Cell sorting techniques could be implemented, but then the environment from which primary cells grow has been altered, giving a different perspective.

Over the last decade, the number of studies involving omic techniques have increased. For example, metabolomic studies in both myoblasts and on their serum can be researched, including studies investigating the comparison between replicatively aged and control myoblasts and myotubes or in primary human myoblasts and myotubes. However, the challenge with metabolomics is the demand to control external cues as much as possible, to enable reliable and robust data analysis.

7.5.3 Study 4

Many human studies recruit males as participants, with recommendations from these studies being generalised to both males and females. Therefore, there is a requirement for human intervention studies to be undertaken in females also. The validity of interpreting data from males and applying to females is misleading and the excuse not to include females due to altered hormonal

profiles is not sustainable. In addition, although ethically challenging, future research should focus on different responses as we age in both males and females. Hypothetically thinking, what are differences in recovery and repair after an eccentric bout of exercise from a male or a female aged 25 vs. 45 vs. 65 vs. 75-years? The major challenge would be the protocol implemented, for instance, 100 drop jumps can be completed by a 25-year-old, but possibly not by an untrained 75-year-old. Other protocols such as eccentric contractions using an isokinetic dynamometer of the quadricep muscle that range from 100 - 300 leg extensions (Jimenez-Jimenez *et al*., 2008: Sorensen *et al*., 2018). Also, using the isokinetic dynamometer, damage has been induced on elbow flexors with 50 maximal contractions (Evans *et al*., 2002). Alternatively, eccentric cycling and downhill are other protocols that are reported in muscle damage studies in individuals of all ages, including the elderly (Toft *et al*., 2002: Hameed *et al*., 2008: Hamada *et al*., 2004). However, trained 75-year-old (master athlete) may well be able to complete this protocol due to training continuously over the years, so impact of training status also requires further investigation, especially as we age. Furthermore, the risk of falls, following the pre-meditated induction of damage in older people is of concern and any not gain ethical approval.

Further, for strenuous eccentric protocols, there is a need for research on the severity of different protocols and classifications to be drawn from these. For instance, the protocol utilised in this study increased CK, soreness and stimulated a cytokine response. However, other protocols, routinely reported in the literature e.g. eccentric isokinetic chair-based contractions were more severe and apparently caused greater muscle damage (Baumert *et al*., 2018), although whether these protocols cause Z-line disruption was largely unknown. Research indicates that eccentric exercise activates satellite cell response via varying mechanical cues, including immune cell signalling, ECM protein release and muscle fibre disruption (Hyldahl *et al*., 2014: Hyldahl *et al*., 2014: Mackey *et al*., 2011). Therefore, a universal definition of exercise induced muscle damage needs to be developed and validated. The factors that should be considered are: intensity, volume, mode of exercise, muscle group/s affected, individual variability, immune responses, gender, molecular mechanisms,

genetics (Baumert *et al.*, 2016, 2017, 2018) and validated markers (for example Tenascin C; Mackey *et al.* 2011). Also, most of the mechanisms behind the measures used are poorly understood, for instance, the science behind how muscle soreness is increased is not fully defined. To help with these challenges, the implementation of advanced techniques is required. For example, although invasive, muscle biopsies can provide information of membrane disruption, satellite responses and calcium kinetics. Further details around protocol differences with advantages and disadvantages are reported in appendix 1.

Future investigations should also focus more closely on diet and on nutrient dense foods, for example, greek yoghurt which is high in protein or milk-based products as some research has done (Cockburn *et al.* 2012: Rankin *et al.*, 2015) or meals which contain specific amounts of protein, carbohydrates and fats. This approach focuses on food first, instead of supplements which are accessible but expensive. However, the major challenge is the tracking of nutrient intake during the intervention period, which is underreported in the literature. It is important to consider how the habitual intake effects the interpretation of results.

7.5.4 Contributions to the Literature and Essential Future Work

Using an established model of ageing, we have provided evidence that not all regenerative processes are impaired during ageing, indeed, the ability to migrate appears to be improved. In study 1 and 2, in replicatively aged myoblasts, we reveal evidence that leucine and HMB stimulate pathways related to protein synthesis, which contradicts anabolic resistance per se. The use of novel techniques throughout provides areas for future research in different models. With both *in vivo* and *in vitro* models, we have demonstrated that what occurs on a cellular level might not translate physiologically. Three immediate areas can build from this work and include: 1) Comparison from cell study results to primary human cells to translate, and further validate this model 2) the use of novel proteomic method on different cell types and 3) acute eccentric exercise in older vs. younger men and women with additional protein

intake with a focus on mechanisms (cytokine response and cell signalling) of injury and repair *in vivo* and *in vitro*.

7.6 Thesis Conclusion and Implications

Worldwide the ageing population is increasing rapidly, with detrimental consequences on the socio-economic landscape. Sarcopenia is linked with numerous pathological and functional aetiologies. To alleviate the progression of sarcopenia, exercise and nutrition interventions have been utilised. The capability of muscle to regenerate following muscle injury is integral in ageing, including the capacity for cells to migrate and then fuse. We ascertained whether there was a difference in cellular responses to damage, as a consequence of replicative ageing and whether this was altered with supplementation. Cell migration was more efficient in aged cells compared to young. With leucine and HMB treatment, both ages of cells responded, albeit at a greater relative response in younger cells. However, this ability to migrate did not correspond to efficient myoblast fusion in aged cells, compared to young, despite the fact that the aged cells were capable of sensing the supplements and responding with changes in e.g. Akt activation. Finally, to try and provide a larger insight into the underlying mechanisms underpinning the absence of fusion in the aged cells, myoblast and myotube protein abundance and FSR were measured. There was a distinct lack of ribosomal and contractile proteins, as well as reduced FSR in replicatively aged myoblast and myotubes. By contrast, these cells contained a greater abundance of metabolic enzymes compared with controls. Following, to understand and translate the mechanisms of repair and recovery in humans, we performed eccentric contractions in young individuals supplemented without and with leucine and HMB. We found no functional impact of the supplements, although the exercise bout activated immune cell responses, which were altered with supplementation. Therefore, although in young participants, at a physiological level the supplements did not elicit a beneficial response, on a cellular level there were responses in myoblast function, which was impacted by replicative ageing. This thesis provides some indication, that the aged cells could favour

survival over full regeneration due to lack of fusion and increased energy demand, through glycolysis.

Therefore, the challenge for the future is to further determine whether regular exercise and nutrition throughout lifespan can alleviate sarcopenia, and to identify how important muscle regeneration are to those processes.

Chapter 8: Appendices

8.1 Appendix 1: Eccentric Exercise Markers and Protocol Differences

There are many differences in study designs and protocols that could result in the differences in reported research findings. For example, the population being studied, duration, intensity and types of exercise protocols can all result in different outcomes as a result of, for example, multiple eccentric contractions. Importantly, the use of cells, animal and human studies, the subject population (male or females, trained, untrained or elite individuals) can all influence the findings. Finally, the use of subjective, objective, direct or indirect markers of eccentric exercise can result in variability, with direct measures usually the more expensive but more accurate and indirect, more commonly used but with limitations. All these differences will be evaluated in the following paragraphs, with the focus of being aware of the limitations of varying methods.

Currently, there are only two direct methods of analysing muscle damage, these are electron and/or light microscopy and histological techniques. Through these methods, both disrupted sarcomeres and damage to the excitation-contraction coupling system (Proske and Morgan, 2001) are observed. It is suggested that the observations of sarcomere damage, commonly through damage to the Z-disk (Lauritzen *et al.*, 2009) are observed 5 minute-72 h after eccentric contractions. Furthermore, damage to the excitation-contraction coupling system, through alternations in the T-tubules are suggested to occur 48 h-72 h post damage (Takekura *et al.*, 2001)

In contrast to direct markers, indirect markers often include intramuscular proteins in the serum, muscle function and muscle soreness measures. The most common marker of damage used in studies is CK, as fibres in uninjured conditions would not result in CK leakage, however, once damage occurs, CK is released through the damaged membrane ((Fridén and Lieber, 2001). Indeed, CK is also used to measure the magnitude of damage, even though it

should be used with caution due to the additional CK release through the reticuloendothelial system. It is apparent however, that CK levels fluctuate greatly with different modes, intensity, durations of exercise and between individuals. For instance, exercise including downhill running, squats and eccentric knee extensions produce low CK levels, (<1000 IU) (Eston *et al.*, 1996; Davies *et al.*, 2009) compared to vertical jumps (Skurvydas *et al.*, 2011) where the CK levels reach 1400 IU at 48 h. Other serum proteins include LDH, is found to increase between 6-12 h post exercise. However, LDH analysis is suggested to be used when the muscle cell membrane is irreversibly damaged (Gissel and Clausen, 2001).

In addition, indirect markers also include muscle soreness and function. Following eccentric actions muscle soreness occurs in the form of a dull aching pain (Armstrong, 1984), with soreness increasing and lasting up to 96 h (Twist and Eston, 2005). Muscle function is also commonly used, with MVC, used to measure force, declining as a consequence of damage. There are various methods used to assess MVC, the most common using the isokinetic dynamometry. Researchers have also adopted the use of vertical jumps (squat, countermovement, drop jump) to assess damage, as they allow for the examination of the stretch shortening cycle (Byrne and Eston, 2002).

The differences between the physiology of animal and human studies are not discussed in this review, however, it is important that researchers know the disparities. Indeed, it is the validity of the models that should be noted. For instance, animal studies are commonly used for their strong internal validity, where the environmental conditions can be tightly controlled. Whereas, these models have very little connection to 'real world' as they involve little external validity. For instance, there are multiple physiological differences between mice and humans, in particular the size difference, especially regarding important organs such as the heart and brain, as well as skeletal muscle. Also, humans are exposed to environmental cues daily changing their physiology, which mouse models are not. The strength of using animal studies is for their clinical use and to provide insight to biochemical mechanisms. For example, many drugs for disease use are developed on animals before application to humans

can be considered. In contrast, human studies give researchers the capability to relate their design to 'real world' situations, for example, designing protocols to sporting movements. Indeed, the external validity is difficult to control, through the many environmental factors that could influence the subjects and their physiology. Recently, researchers that have access to the facilities are now combining human protocols with biochemical, molecular and cell culture methodologies. For instance, the collection of blood samples and muscle biopsies are taken at multiple time points for biochemical and molecular analysis. In addition, the use of three dimensional/flexwell stretch cell culture models is used to elicit damage of human tissue, which provides novel understanding of the processes involved, these protocols would be extremely difficult to administer in humans, due to ethical reasons. It is important to consider both animal and human models for developing research, however, the differences and interpretation of findings should be considered and more so with the development of technology used to aid scientific application.

Not only is the control of external validity difficult, the differences in participant gender, level of fitness and protocol varieties are essential to consider. Unfortunately, not many studies have used females with many researchers favouring the male population. In humans, the findings are equivocal, with no differences in force loss between genders (Sayers and Clarkson, 2001). In addition, there also seems to be no differences in the levels of DOMS, CK and myoglobin responses (Eston *et al.*, 2000; Dannecker *et al.*, 2005). However, it is important to note the influence of higher and lower responders to these variables, future research should always integrate individual responses, and not just averages. A unique study with large sample size investigated the differences in response to maximal eccentric exercise (Sewright *et al.*, 2008). This study tested on 42 men and 58 women, with only placebo treatments used. The results showed that females lost significantly greater force immediately post exercise, with males having significantly greater CK response at four days. Importantly, these findings were mainly driven by higher female and male responders. Overall, even though evidence is still lacking, researchers should take into account gender when analysing results.

Furthermore, individuals who complete increased levels of training and/or training and competition (international/elite performers) require damaging protocols that are more strenuous (Armstrong *et al.*, 1991). This is suggested to sufficiently damage the muscle to promote the Ca^{2+} disruption, inflammation and satellite cell activation. Importantly, the definitions regarding the training level of the participants are often misunderstood and sometimes vague, therefore, researchers are advised to complete detailed assessment of their training levels. Alternatively, apply relative pre and post assessments (for example VO_2 max test/1RM etc) to analyse their fitness level.

The most noticeable differences in the literature are the actual intervention protocols and subsequent supplement dosing strategies. For studies details, refer to table 8.1. Firstly, the type of muscle group that is damaged differs in the literature, with studies focusing on the whole body, the quadriceps or biceps (Howatson and van Someren, 2008). These differences can present alternative findings, with bicep and quadriceps damage not reflecting the whole-body response. In addition, focusing on individual muscle groups does give greater internal validity (control), whereas, whole body exercise/sporting movements can give greater external validity, and can be related more to the applied setting. Furthermore, differences in the duration and intensity of protocol shows the inconsistencies in the damage incurred and the data presented in the literature. Regarding different intensities, some eccentric knee damaging protocols include: 10 sets x 10 reps, 15 sets x 10 reps or 20 sets x 10 reps (Buckley *et al.*, 2010; Farup *et al.*, 2014; Gray *et al.*, 2014), the varieties in sets is critical for levels of intensity and also the rest periods (data not shown). In addition, studies that involve downhill running vary in protocol durations, at 30 minutes, and 90 minutes (Sacheck *et al.*, 2003; Close *et al.*, 2006), which once again elicit varying trauma. Further examples include, running test (Mackey *et al.*, 2007) compared to 100 eccentric contractions (Mikkelsen *et al.*, 2009) and 2 x 70 eccentric actions (Paulsen *et al.*, 2010). Therefore, when interpreting data and findings it is important to notice and note the methodological differences, which in turn, can lead to differences in results and interpretation of data.

Table 8.1. Review of the current studies that have supplemented whey, BCAA, leucine and HMB in response to varying eccentric protocols in the young.

Study	Damaging Protocol	Supplementation	Outcome (Compared to control)
Buckley et al. (2010)	10 sets of 10 repetitions of eccentric knee contractions.	Whey protein (25 g) immediately post and 2 h and 22 h post exercise.	Peak isometric torque was attenuated.
De Lisio et al. (2015)	15 sets of 10 repetitions of eccentric knee extensions.	Hydrolysed whey protein (28 g) + carbohydrate (28 g) immediately after, at three-hour intervals, then at 24 h and 48 h at the same time-points (10:00, 13:00, 16:00)	No differences in soreness, CK or TNF-α. No difference in pericyte response. No physiological markers assessed.
Etheridge et al. (2008)	30 minutes of downhill running	Protein meal (100 g: 40 g EAA) immediately after exercise.	No difference in muscle soreness, endurance time, strength measures. Maintained PPO and MVC.
Farup et al. (2014)	15 sets of 10 repetitions of eccentric knee extensions.	Hydrolysed whey protein (28 g) + carbohydrate (28 g) immediately after, at three-hour intervals, then at 24 h and 48h at the same time-points (10:00, 13:00, 16:00)	No difference in soreness and CK. Increased satellite cell number, attenuation in MVC. No difference in CK, soreness.

Foure *et al.* (2016)	40 Neuromuscular electrically stimulated contractions.	BCAA (100 mg/kg) at 30 minutes before, immediately before and after exercise.	No difference in muscle soreness, force, CK concentrations.
Howatson *et al.* (2012)	5 sets of 20 drop jumps.	BCAA (20 g/d) for 7 days prior and 5 days post exercise.	Attenuation of muscle soreness, CK at 24 h, MVC. No difference in vertical jump, thigh circumference, calf circumference.
Jackman *et al.* (2010)	12 set of 10 reps of eccentric knee contractions.	BCAA (29.2 g/d) immediately post and then for four days.	No difference in muscle force loss, IL-6, CK. Attenuated muscle soreness.
Kirby *et al.* (2012)	100 drop jumps, consisting of 6 sets of 10 repetitions.	Leucine (250 mg/kg) was administered 30 mins before exercise during, immediately post, and then for 96h post exercise.	Attenuated decrease in mean, not individual peak force. No difference in CK, Mb, static jump. Significantly higher soreness in leucine group.
Nosaka *et al.* (2006)	Arm curl exercise, 30 minutes, (900 actions).	Amino acid supplementation (4.5 g per timepoint), pre, post, 6 h, 24 h, 48 h, 72 h, 96 h.	Attenuated DOMS. CK, aldolase, myoglobin, muscle soreness significantly lower in amino acid group.
Paddon-Jones *et al.* (2001)	24 maximal isokinetic eccentric contractions of the elbow flexors	HMB (3 g/d) prior to exercise bout and for 10 days post exercise.	No effect on CK, soreness, arm girth, strength.

Ra *et al*. (2013)	6 sets of 5 repetitions of eccentric elbow contractions.	BCAA (9.6 g/d) and taurine (6.0 g/d) for 14 days prior and	Attenuated soreness, arm circumference, LDH and hydroxyguanosine concentration. No difference in CK or serum aldolase activity.
Shimomura *et al*. (2010)	7 sets of 20 squats	BCAA (5.5 g) immediately before, 15 minutes after.	DOMS, MVC and myoglobin concentration was attenuated. No difference in plasma elastase.
Wilson *et al*. (2009)	55 maximum eccentric knee extension/flexions	HMB (3 g/d) 1-day pre and for 72 h post exercise.	No impact on force, soreness or CK. Prevented increases in LDH vs. placebo.
Wilson *et al*., (2013)	3 sets of 12 resistance exercises including squats, deadlifts and pull ups.	HMB (3 g/d) for pre and 48 h post exercise.	HMB decreased CK and perceived pain.
Van-Someren *et al*., 2005	3 sets of 10 bicep curls at 70 % 1RM	HMB (3 g/d) 14 days prior and for 72 h post exercise.	HMB reduced CK, soreness, percent decrement in force and limb

8.2 Appendix 2: Additional Figures Supplementary to Chapter 3

8.2.1 Squat Jumps and Chair Rises in Females with Leucine and HMB Supplementation
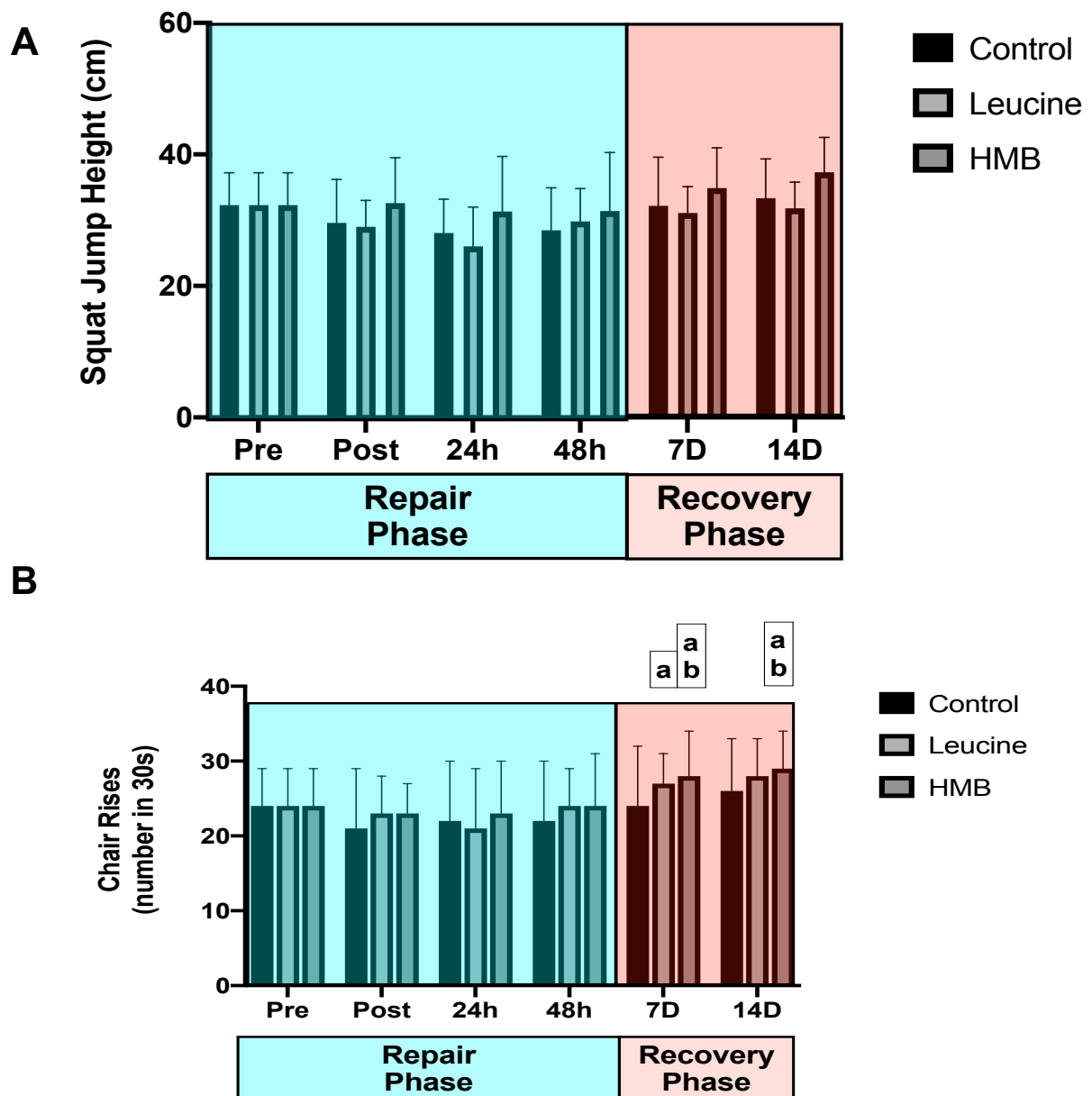
Figure 8.1. Squat Jump (A) and Chair rises (B) over time in females in the absence or presence of leucine and HMB. Data displayed as average ± SD. Significance was set at $P < 0.05$. Significant comparisons: a: pre, b: post vs. other time points.

8.2.3 Squat Jumps Between Male and Females with Leucine and HMB Supplementation
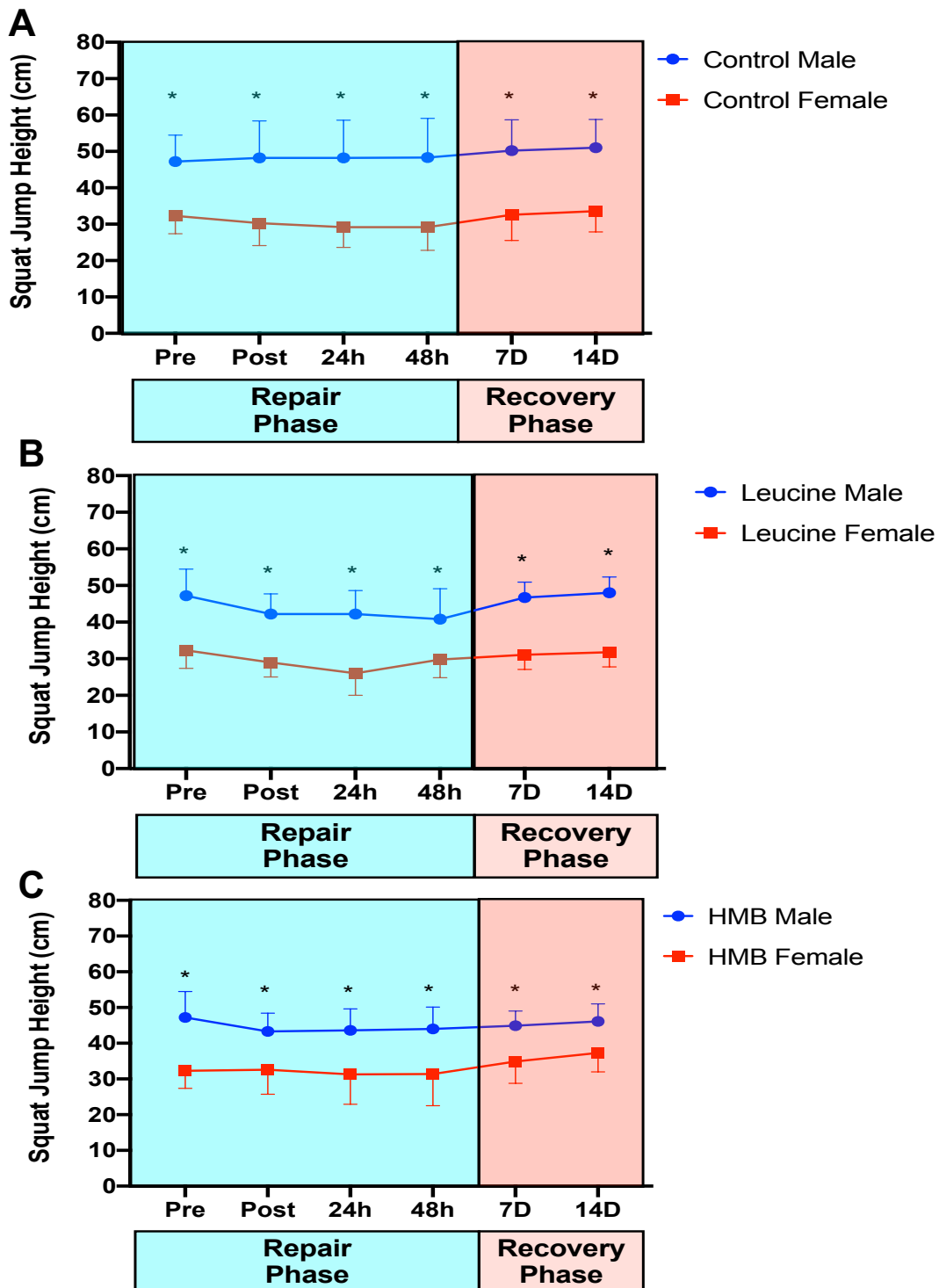
Figure 8.2. Squat jump height in male vs. female in control (A), leucine (B) and HMB (C) groups. Data presented as mean $\pm$ SD. Significance (*) was between male vs. female and set at $P < 0.05$.

8.2.3 Chair Rises Between Male and Females with Leucine and HMB Supplementation
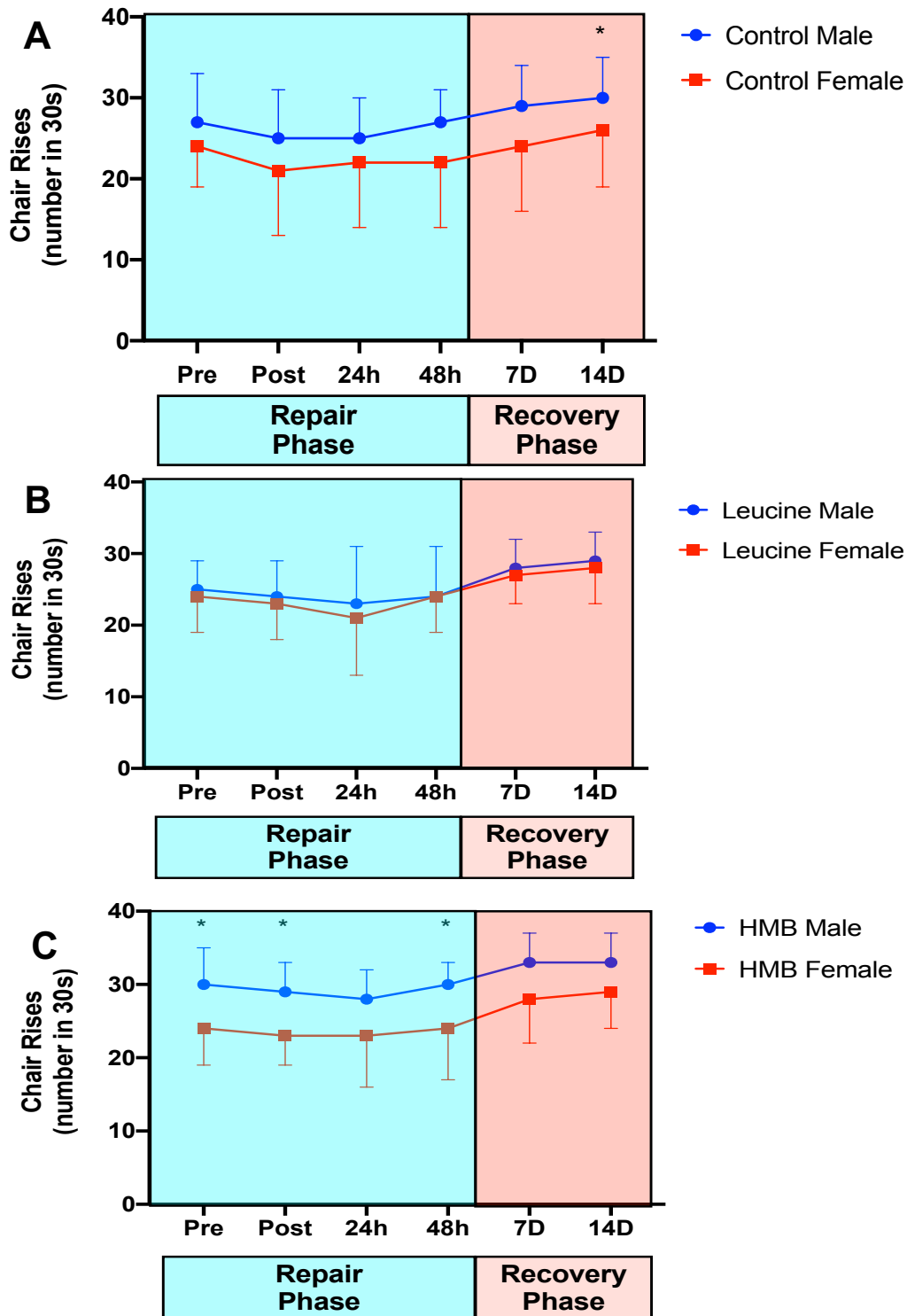
Figure 8.3. Chair rises in male vs. female in control (A), leucine (B) and HMB (C) groups. Data presented as mean ± SD. Significance (*) was between male vs. female and set at P < 0.05.

8.3 Appendix 3: Publication 1: Murine Myoblast Migration: Influence of Replicative Ageing and Nutrition

CrossMark

RESEARCH ARTICLE

Murine myoblast migration: influence of replicative ageing and nutrition

Alexander D. Brown · Graeme L. Close · Adam P. Sharples · Claire E. Stewart

Abstract Cell migration is central to skeletal muscle repair following damage. Leucine and β-Hydroxy β-methylbutyric acid (HMB) are supplements consumed for recovery from muscle damaging exercise in humans, however, their impact on muscle cell migration with age is not yet understood. We hypothesised that replicatively aged ("aged"; P46–P48) myoblasts would be less efficient at basal and supplemented repair versus parental controls ("control"; P12–P16). Aged and control myoblasts were scratch-damaged and migration velocity, directionality and distance assessed over 48 h in the absence and presence of leucine (10 mM) or HMB (10 mM) ± PI3K/Akt (LY294002 10 μM), ERK (PD98059 5 μM) or mTOR (rapamycin 0.5 μM) inhibition. Opposing our hypothesis, aged cells displayed increased velocities, directionality and distance migrated (P < 0.001) versus control. Leucine and HMB significantly increased (P < 0.001) the same parameters in control cells. The supplements were with smaller, albeit significant impact on aged cell velocity (P < 0.001) and in presence of HMB only, distance (P = 0.041). Inhibitor studies revealed that, PI3K and ERK activation were essential for velocity, directionality and migration distance of aged cells in basal conditions, whereas mTOR was important for directionality only. While PI3K activation was critical for all parameters in control cells (P < 0.001), inhibition of ERK or mTOR improved, rather than reduced, control cell migration distance. Enhanced basal velocity, directionality and distance in aged cells required ERK and PI3K activation. By contrast, in control cells, basal migration was underpinned by PI3K activation, and facilitated by leucine or HMB supplementation, to migration levels seen in aged cells. These data suggest that replicatively aged myoblasts are not anabolically resistant per se, but are capable of efficient repair, underpinned by altered signaling pathways, compared with unaged control myoblasts.

Keywords Myoblast · HMB · Leucine · PI3K · ERK · mTOR · Damage · Ageing

Introduction

During the human lifespan, a gradual loss of skeletal muscle mass and strength occurs, referred to as sarcopenia. While muscle mass and strength in young individuals can be preserved through nutritional supplementation, it is reported that muscle in older adults displays a level of anabolic resistance (Breen and Phillips 2011). The capacity of the muscle to

A. D. Brown (✉) · G. L. Close · A. P. Sharples · C. E. Stewart
Stem Cells, Ageing & Molecular Physiology Unit,
Research Institute for Sport and Exercise Sciences
(RISES), School of Sport and Exercise Sciences,
Liverpool John Moores University, Liverpool, UK
e-mail: a.d.brown@2014.ljmu.ac.uk

Springer

255

regenerate following exercise induced muscle damage is reportedly impaired in ageing rodents and humans (Brooks and Faulkner 1988; Faulkner et al. 1991). It is reported that altered satellite cell behaviour may negatively impact not only on muscle mass and strength, but also on the muscle regeneration processes (Welle 2002; Shefer et al. 2006; Day et al. 2010; Bigot et al. 2015).

Recently, interest has arisen relating to the use of nutraceuticals to facilitate muscle growth. Data suggest old muscle may be anabolically resistant and require higher concentrations of protein to elicit a hypertrophic response versus young muscle (Breen and Phillips 2011). Leucine, an essential amino acid, is reportedly a potent anabolic agent (Koopman et al. 2006) and is also consumed following damaging exercise, with the aim to improve muscle regeneration (Farup et al. 2014). Recent studies have investigated the effects of leucine administration on myoblast fusion (Areta et al. 2014; Dai et al. 2015) and demonstrated that increasing leucine in a dose responsive manner (5 and 16.5 mM) stimulated the mTOR signaling pathway and the phosphorylation of P70S6K, resulting in significantly increased myoblast fusion. Furthermore, in young recreationally active males, whey protein, which contains high doses of leucine (8 g per 100 g), increased muscle satellite cell number at 48 h post eccentric damage, compared with control (Farup et al. 2014).

Hydroxy β-methylbutyric acid (HMB), a metabolite of leucine, is increasing in popularity as an ergogenic aid for muscle recovery and regeneration. HMB studies in human myoblasts and rodents demonstrate positive effects on satellite cell proliferation, differentiation and survival, following MAPK/ERK and PI3K/Akt activation (Kornasio et al. 2009; Vallejo et al. 2016). Supplementation of human myoblasts with HMB (0–85 mM) stimulated cell proliferation via the MAPK/ERK pathway and induced differentiation via the PI3K/Akt pathway (Kornasio et al. 2009). Further studies by Vallejo et al. (2016) investigated the impact of HMB on C_2C_{12} myoblasts (25–125 μM) and on the contractile force of ageing murine soleus muscle (514 mg/kg). HMB treatment increased C_2C_{12} myoblast proliferation and myoblast viability. In mice, HMB prolonged force generation and reduced the amount of time for peak muscle contraction following damage (Vallejo et al. 2016). Together, these studies indicated that leucine and HMB could impact positively on muscle differentiation, survival and function.

Adequate skeletal muscle mass and function are essential in supporting human health and well-being [reviewed in (Sharples et al. 2015)]. However, the molecular regulators of skeletal muscle cell migration are relatively understudied, despite the fact that skeletal muscle has a remarkable ability to regenerate. Understanding the signaling pathways that regulate myoblast migration, direction and velocity is therefore important in advancing capacity to promote skeletal muscle regeneration. Evidence exists supporting the role of the Rho family, in regulating satellite cell migration (Raftopoulou and Hall 2004). Upstream of the Rho family is the PI3K/Akt pathway, which we demonstrated, when inhibited, resulted in impaired myoblast migration (Dimchev et al. 2013). Furthermore, the MAPK/ERK pathway is also reportedly involved in efficient myoblast migration, albeit findings are somewhat equivocal (Leloup et al. 2007; Ranzato et al. 2009; Al-Shanti et al. 2011).

Given a global drive to reduce/refine animal research, relevant cell models are required to inform future in vivo studies. To this end, we have developed a myoblast model, with application to ageing muscle cell behavior (Sharples et al. 2011). Using a process of replicative ageing, C_2C_{12} murine skeletal muscle cells were subjected to 58 population doublings versus parental control and were reported to display impaired differentiation both in 2-D and 3-D models (Sharples et al.2011, 2012; Deane et al. 2013). While these cells have been extensively characterised with regards to hypertrophy and atrophy and compare well with replicatively aged human cells (Bigot et al. 2008), human and rodent cells isolated from ageing muscle (Lees et al. 2006; Bigot et al. 2008; Léger et al. 2008; Lees et al. 2009; Pietrangelo et al. 2009) and muscle biopsy tissue derived from older individuals (Welle et al. 2003; Léger et al. 2008), little research has focused on their ability to repair damage. Furthermore, although the potential of nutraceuticals in muscle preservation is being avidly investigated (Phillips et al. 2009), the question remaining to be challenged is whether nutraceuticals elicit a beneficial impact on muscle cell migration and repair and whether this is compromised with ageing.

Therefore, the goal of this study is to investigate the impact of leucine and HMB on control and aged skeletal muscle cell repair. The objectives are: 1. To

determine the migration capacity of replicatively aged (but not senescent) C_2C_{12} skeletal muscle cells versus controls that have not undergone any population doublings relative to aged cells. 2. To investigate the impact of the nutritional supplements leucine and HMB on migration capacity and; 3. To begin to determine relevant signaling pathways (PI3K, ERK and mTOR) that may be important for successful migration and wound closure. We hypothesised that: (1) replicatively aged (P46–P48; 'aged') myoblasts would be less efficient at damage repair versus unaged controls (P12–P16, 'control'); (2) leucine and HMB would increase the migration potential in control but not aged cells and; (3) that the PI3K and ERK, but not mTOR (given its critical role in myoblast fusion) pathways would be required for effective migration in both models.

Methods

Cell culture

All cell culture procedures were conducted using a Kojair Biowizard Silverline class II hood (Kojair, Vippula, Finland). Commercially available C_2C_{12} mouse skeletal myoblasts were purchased from ATCC and passages 12–16 (referred to as 'control') and passages 44–48 (replicative aged and referred to as 'aged'; (130–140 population doublings)) were used in this study. The cells were incubated in a HERAcell 150i incubator (Thermo Scientific, Cheshire, UK) at: 5% CO_2 and 37 °C. Cells were resuscitated from liquid nitrogen storage and seeded onto gelatinised T75 flasks (Nunc, Roskilde, Denmark) at 1×10^6 cells/ml in growth medium (GM) that consisted of: Dulbecco's Modified Eagle Medium (DMEM), 10% heat-inactivated fetal bovine serum, 10% heat-inactivated newborn calf serum, 2 mM L-glutamine, and 1% penicillin–streptomycin.

Damage protocol and cell treatments

Once 80% confluency was attained, cells were trypsinized, counted and seeded at 100,000 cells/ml on gelatinised six or twelve well plates (Nunc, Roskilde, Denmark) and grown to 80% confluence. Cells were washed once with PBS prior to an established in vitro wound/repair model to assess

migration in myoblasts via applying a damaging scratch to monolayer cells as previously reported by our group (Dimchev et al. 2013; Owens et al. 2015). Cells were washed twice with PBS to remove any debris, prior to dosing in differentiation medium (DM containing: DMEM, 2% heat-inactivated horse serum, 2 mM L-glutamine, 1% penicillin–streptomycin), in the absence or presence of leucine (10 mM) or HMB (10 mM). Doses were selected following basal dose response studies (0–10 mM, data not shown). In addition, signaling pathways, in the absence or presence of leucine or HMB, were manipulated with: LY294002 (10 μM), inhibitor of PI3K signalling, PD98059 (5 μm), inhibitor of ERK signalling or rapamycin (0.5 μM) inhibitor of mTOR (Dimchev et al. 2013; Hatfield et al. 2015). For inhibitor studies, cells were allowed to quiesce for 30 min, in DM, prior to addition of respective inhibitors for 30 min, followed by supplements for up to 48 h. All cell experiments were repeated 3 times in duplicate.

Wound healing assay and migration analysis

For the wound/repair healing assays, immediately following treatment, cells were incubated in a controlled live imaging environment (Leica DMB 6000; equipped with PeCon incubation and gas control system) at 37 and 5% CO_2. Microscopic images were obtained from two points within each wound (using track and find), every 30 min for 48 h at ×10 magnification. For the analysis of cell migration dynamics, the directionality, accumulated distance and velocity were determined using TIF image stacks and Image J software (IBIDI, Munich, Germany). The manual tracking and chemotaxis plug-ins were installed which allowed for individual cell trajectory and migration to be analysed. The chemotaxis tool analyses the raw data from the manual tracking plug-in and provides quantitative data on cell directionality (arbitrary units), velocity (μm/min) and accumulated distance (μm).

Cell fixation and preparation for flow cytometry

FLOW cytometry was performed to simultaneously assess multiple phosphoproteins in relevant cell samples (Schubert et al. 2009, Sharples et al. 2011). At ∼ 80% confluence, the cells were washed, damaged and quiesced prior to dosing and harvest as

257

detailed above. This 30 min quiescence timepoint was designated as time 0 h. The cells were either fixed at time 0 h or dosed with 10 mM leucine or HMB for 15, 60 and 120 min post damage. The cells were washed twice in PBS prior to trypsinisation, neutralisation and centrifugation at 775 g for 5 min at 4 °C. The supernatant was removed and the cells were fixed in 2% paraformaldehyde at room temperature for 60 min. The cells were centrifuged as above and re-suspended in 100% methanol. Cells were stored at − 20 °C until further analyses by FLOW. The cells were washed in FLOW buffer (PBS + 0.5% FBS) and centrifuged at 500 g for 5 min at 4 °C and re-suspended in FLOW buffer. The anti-human/mouse phospho-AKT (S473; APC; 675/25; 0.5 ug), anti-human/mouse phospho-ERK1/2 (T202/Y204; Alex-afluor 488; 533/30; 0.03 ug) and anti-human/mouse phospho-mTOR (S2448; PerCP; 670/LP; 0.125 ug) antibodies (Thermo Fisher Scientific inc, Waltham, USA) were added to each sample and incubated at room temperature in the dark for 60 min. The cells were washed a further three times, and re-suspended in 200 μl FLOW buffer. The samples were analysed using flow cytometry on a BD Accuri C6 flow cytometer with BD CFlow® Software, collecting 2000 events per sample. Fluorophores used in flow cytometry can emit photons of multiple energies and wavelengths, compensation of individual fluorescent antibodies in multiple detectors was performed to reduce spectral overlap. Forward scatter and side scatter gating was performed to ensure single populations of cells. Together these processes should reduce data skew and improve accuracy.

Statistical analysis

SPSS Predictive Analytics Software (version 23; IBM) was used for all statistical analyses. Data were assessed and normal distribution confirmed. For the comparison of replicative aging (control vs. aged C_2C_{12} cells) versus supplements (DM alone, leucine, HMB) a two by three-way ANOVA was used, where significant main effects and interactions were present, the Bonferroni post hoc pairwise comparisons test was used. For within test comparisons, either, independent t-tests, or one-way analysis of variance (ANOVA) was used. All data are presented as mean ± SD and significance as ≤ 0.05.

Results

Improved migration in replicatively aged versus unaged control C_2C_{12} skeletal muscle cells

Following scratch damage, aged and control cell migration into the wound site was measured over 48 h (Fig. 1). In contrast to our hypothesis, under basal conditions in replicatively aged versus control cells respectively, there was a 1.27-fold increase in cell velocity (0.28 ± 0.07 μm/min^{-1} vs. 0.22 ± 0.07 μm/min^{-1}; P < 0.001; Fig. 2a), a 1.27-fold increase in directionality (0.71 ± 0.12 vs. 0.61 ± 0.17; P < 0.001; Fig. 2b) and a 1.29-fold increase in overall migration distance (802 ± 202 μm vs. 622 ± 188 μm; P < 0.001; Fig. 2c). This increased migration in the aged cells was associated with altered phosphorylation of Akt, ERK, and mTOR (Fig. 3a, b, c, respectively). In aged cells ERK activation was significantly increased (P = 0.028) versus control cells at 15 min and while still elevated at 60 min, significance was not attained. Akt phosphorylation was not different between the two cell groups at 15 min. However, while Akt phosphorylation decreased in the unaged controls to 60 min where it plateaued to 120 min, it increased over the time course in the aged cells reaching significance (P = 0.047) versus control at 120 min. Finally, mTOR phosphorylation did not significantly change over the time course assessed in aged or control cells and no significant differences were observed between the two models.

Wishing to determine whether the altered signaling profiles evident between the cell models may impact on improved migration in the replicatively aged model, inhibitor studies were performed. Cell velocity was 2.8-fold (0.28 ± 0.07 μm/min^{-1} vs. 0.10 ± 0.04 μm/min^{-1}; P < 0.001), directionality, 1.5-fold (0.71 ± 0.12 vs. 0.49 ± 0.20; P < 0.001) and overall migration distance, 2.4-fold (802 ± 202 μm vs. 332 ± 123 μm; P < 0.001) greater in the absence versus presence of the PI3K inhibitor, LY294002, respectively (Fig. 4). Similarly, when aged cells were incubated with the ERK inhibitor (PD98059), cell velocity was 1.3-fold (0.28 ± 0.07 μm/min^{-1} vs. 0.21 ± 0.08 μm/min^1; P = 0.001), directionality, 1.1-fold (0.71 ± 0.12 vs. 0.64 ± 0.17; P < 0.001) and accumulated distance 1.3-fold (802 ± 202 μm vs. 618 ± 219 μm;
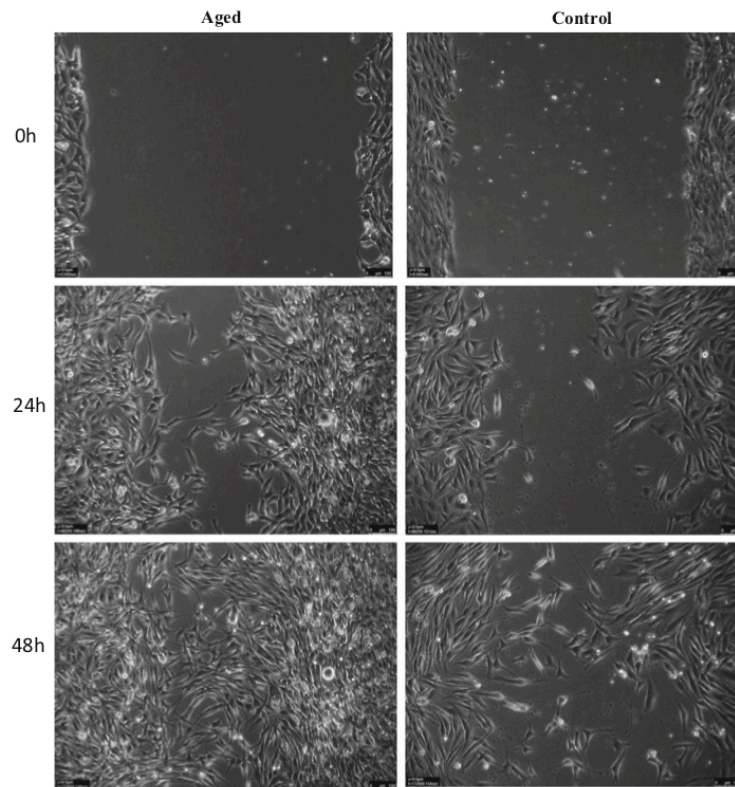
Fig. 1 Images to show the difference between aged and control cells at 0, 24 and 48 h

$P < 0.001$) higher under control versus inhibitor conditions, respectively (Fig. 4). Indeed, in the presence of PD98059, migration potential of the aged cells was reduced to that of control cells, the latter under control conditions. Finally, under aged control versus mTOR inhibition (rapamycin administration), despite a small reduction in velocity versus untreated aged control (Fig. 4), significance was not attained (0.24 ± 0.07 μm/min^{-1} vs. 0.28 ± 0.07 μm/min^{-1}). Compared with untreated aged control cells in the presence of rapamycin, directionality was significantly reduced by 1.15-fold (0.71 ± 0.12 vs. 0.62 ± 0.17; $P < 0.001$), however, this was not sufficient to significantly reduce overall migration distance (802 ± 202 μm vs. 697 ± 213 μm).

Having determined central roles for PI3K/Akt and ERK in all parameters of aged cell migration and

mTOR in directionality, equivalent studies were performed in the control cell model (Fig. 4). Similar to the aged cells, compared with control, when incubated with PI3K/Akt inhibitor (LY294002), cell velocity was 1.6-fold (0.22 ± 0.07 μm/min^{-1} vs. 0.14 ± 0.06 μm/min^{-1}, $P < 0.001$), directionality, 1.6-fold (0.61 ± 0.17 vs. 0.38 ± 0.18, $P < 0.001$) and accumulated migration distance, 1.45-fold (622 ± 188 μm vs. 437 ± 174 μm; $P < 0.001$) higher under control versus inhibitor conditions, respectively. By contrast, compared with control, in the presence of ERK inhibition via PD98059 administration, cell velocity (0.22 ± 0.07 μm/min^{-1} vs. 0.21 ± 0.08 μm/min^{-1}) directionality (0.61 ± 0.17 vs. 0.57 ± 0.15) and overall migration distance (622 ± 188 μm vs. 678 ± 217 μm; $P = 0.013$), were not altered (Fig. 4). Therefore, while ERK inhibition

259
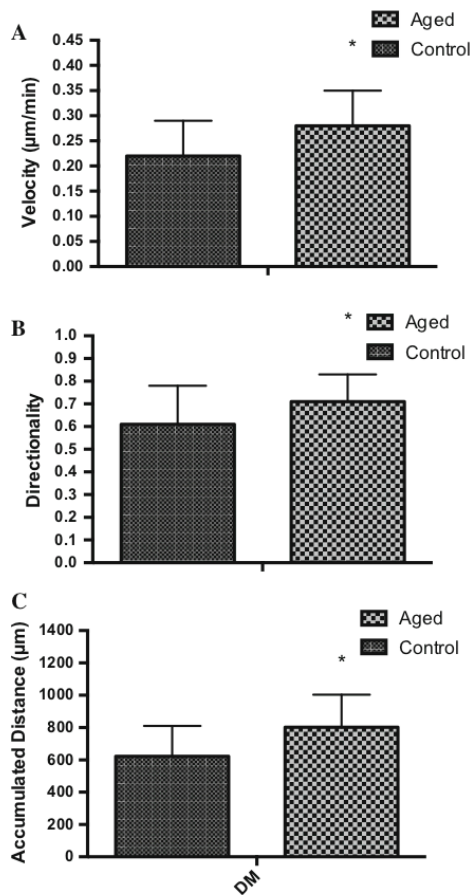
Fig. 2 Bar charts illustrating the differences in cell velocity (**a**), directionality (**b**) and accumulated distance (**c**) between the aged and control over 48 h. The data is shown as mean with SD. Significance is set at P < 0.05, and the significance between aged versus control was indicated using *. The experiment consisted of 3 repeats all in duplicate

reduced the migration potential of aged cells to control capabilities; it was without impact on control cell migration. Finally, in complete contrast to the aged cell model, compared with control, when control cells were incubated with mTOR inhibitor, rapamycin, cell velocity was 1.4-fold ($0.22 \pm 0.07 \mu m/min^{-1}$ vs. $0.31 \pm 0.06 \mu m/min^{-1}$; P < 0.001) higher. Directionality, which was reduced in aged cells, was unaltered (0.61 ± 0.17 vs. 0.62 ± 0.16), however, in
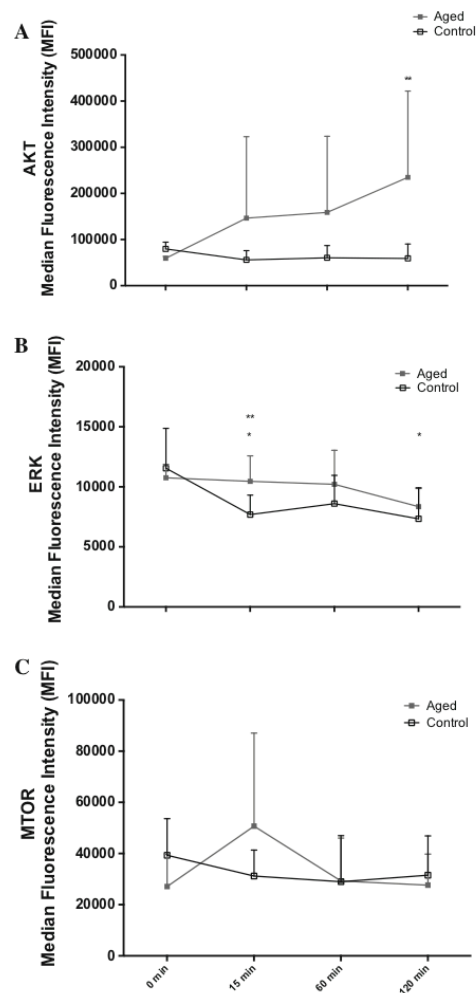
Fig. 3 Line charts illustrating the differences in the phosphorylation of Akt (**a**), ERK (**b**) and mTOR (**c**) molecules between the aged and control over 120 min. The data is shown as mean with SD. Significance is set at P < 0.05. Significance was indicted versus 0 min (*) and versus corresponding time-point (**). The experiment consisted of 3 repeats all in duplicate

line with increased velocity in control cells with rapamycin, overall migration distance was significantly increased by 1.4-fold ($622 \pm 188 \mu m$ vs. $884 \pm 180 \mu m$; P < 0.001) versus control. Indeed, the enhanced migration potential of control cells in the presence of rapamycin now was equivalent to that of
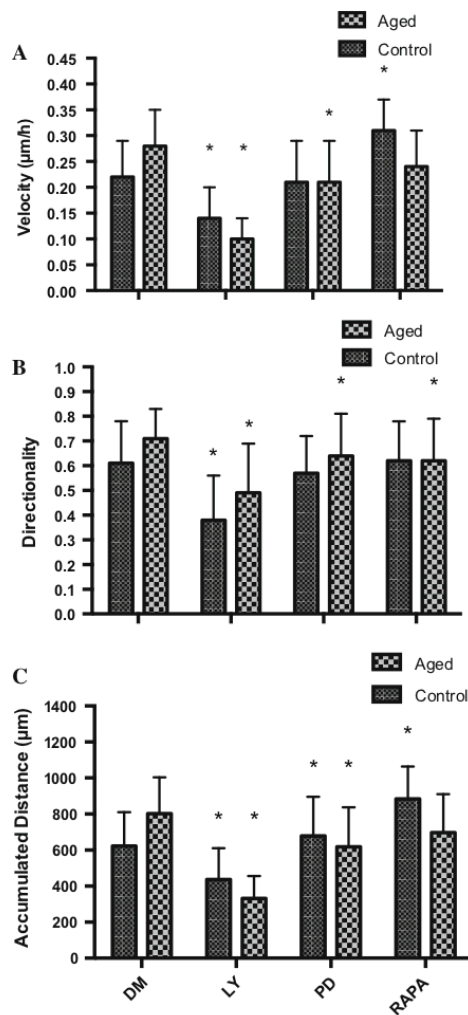
Fig. 4 Bar charts illustrating the differences in cell velocity (**a**), directionality (**b**) and accumulated distance (**c**) in the aged and control versus LY294002, PD98059 and rapamycin. The data is shown as mean with SD. Significance is set at P < 0.05, and the significance between the inhibitors versus basal aged and control cells, was indicated using *. The experiment consisted of 3 repeats all in duplicate

aged cells (velocity and distance) under control conditions (Fig. 4).

Under basal conditions, inhibition of PI3K using LY294002 resulted in a significant reduction in aged

cell migration velocity vs. control cells $(0.10 \pm 0.04 \ \mu m/min^{-1}$ vs. $0.14 \pm 0.06 \ \mu m/min^{-1}$; P < 0.001; Fig. 4a), significantly reduced control cell directionality versus aged $(0.38 \pm 0.18$ vs. 0.49 ± 0.20; P < 0.001; Fig. 4b) and resulted in an overall reduction in migration distance of aged vs. unaged cells $(332 \pm 123 \ \mu m$ vs. $437 \pm 174 \ \mu m$; P < 0.001; Fig. 4c). By contrast, when administration of ERK inhibitor, PD98059, there were no significant differences between control and replicatively aged cell velocity $(0.21 \pm 0.08 \ \mu m/min^{-1}$ vs. $0.21 \pm 0.08 \ \mu m/min^{-1}$; Fig. 4a). However, despite cell directionality being reduced in control versus aged cells basally $(0.57 \pm 0.15$ vs. 0.64 ± 0.17; P = 0.001; Fig. 4b), overall migration distance was significantly lower in aged versus control cells with ERK inhibition $(618 \pm 219 \ \mu m$ vs. $678 \pm 217 \ \mu m$; P < 0.05; Fig. 4c). Finally, the impact of rapamycin on cell velocity was greater in control versus aged cells $(0.31 \pm 0.06 \ \mu m/min^{-1}$ vs. $0.24 \pm 0.07 \ \mu m/min^{-1}$; P < 0.001; Fig. 4a) and despite no differences in cell directionality (Fig. 4b), rapamycin resulted in a significantly increased migration distance in control versus aged cells $(884 \pm 180 \ \mu m$ vs. $697 \pm 213 \ \mu m$; P < 0.001; Fig. 4c).

Effect of leucine and HMB supplementation on rodent C_2C_{12} skeletal muscle cells migration

To determine whether aged cell migration could be enhanced, treatment with leucine (10 mM) and HMB (10 mM) were performed. When supplemented with leucine, there was a small but significant 1.07-fold increase in aged cell velocity $(0.30 \pm 0.07 \ \mu m/min^{-1}$ vs. $0.28 \pm 0.07 \ \mu m/min^{-1}$; P < 0.001) and a small but significant 0.97-fold decrease in directionality $(0.67 \pm 0.13$ vs. control 0.71 ± 0.12; P = 0.001) versus untreated control. Together, these changes were not sufficient to impact on overall migration distance, which was not different from untreated aged control (Fig. 5). In the presence of HMB, there was a small but significant 1.15-fold increase in velocity $(0.32 \pm 0.07$ vs. $0.28 \pm 0.07 \ \mu m/min^{-1}$; P < 0.001), no impact on directionality and an overall 1.15-fold increase in migration distance versus untreated aged control $(921 \pm 215 \ \mu m$ vs. $802 \pm 202 \ \mu m$; P = 0.041).

In contrast, to aged cells, it was hypothesised, that migration of control cells would be increased when

A

B

C
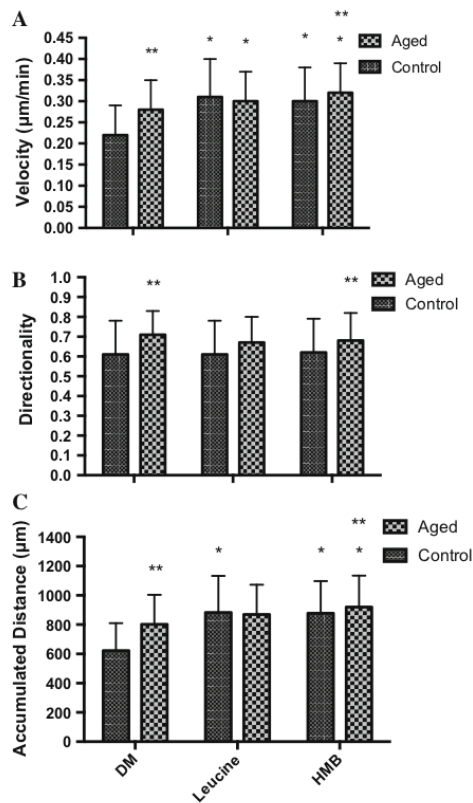
Fig. 5 Bar charts illustrating the differences in cell velocity (**a**), directionality (**b**) and accumulated distance (**c**) in the aged and control versus leucine and HMB. The data is shown as mean with SD. Significance is set at $P < 0.05$, and the significance between the supplements versus basal aged and control cells, was indicated using *. The significance between the aged versus control was indicated using **. The experiment consisted of 3 repeats all in duplicate

supplemented with leucine or HMB. In the presence of leucine, cell velocity was significantly increased by 1.4-fold, (0.31 ± 0.09 μm/min^{-1}; vs. 0.22 ± 0.07 μm/min^{-1}; $P < 0.001$) versus untreated control, directionality was unaltered and overall migration distance increased by 1.4-fold (883 ± 250 μm vs. 622 ± 188 μm; $P < 0.001$). Indeed, in the presence of leucine, the enhanced velocity (0.31 ± 0.09 μm/min^{-1}) and overall migration distance (883 ± 250 μm) of control cells were now not significantly different from velocity

(0.30 ± 0.07 μm/min^{-1}) and migration distance (871 ± 202 μm) of aged cells with leucine (Fig. 5). Similar to leucine, in control cells, HMB supplementation resulted in a 1.36-fold increase in velocity (0.30 ± 0.08 μm/min^{-1} vs. 0.22 ± 0.07 μm/min^{-1}; $P < 0.001$) versus untreated control, no impact on directionality and a 1.41-fold increase in overall migration distance (878 ± 219 μm vs. 622 ± 188 μm; $P < 0.001$). Despite improved migration, in the presence of HMB, aged cells still displayed increased cell velocity (0.32 ± 0.07 μm/min^{-1} vs. 0.30 ± 0.08 μm/min^{-1}; $P < 0.05$), directionality (0.68 ± 0.14 vs. 0.62 ± 0.17; $P < 0.001$) and overall migration distance (920 ± 215 μm vs. 878 ± 219 μm; $P < 0.05$) versus control cells, respectively (Fig. 5).

Proposed signaling pathways that regulate cell migration

Having identified the impact of leucine and HMB on cell migration, the next step was to investigate their impact on relevant signaling molecules. In line with the small impact that these supplements had on aged cell migration, there was little impact on Akt, ERK or mTOR activation versus untreated aged control. Indeed, over a 2 h time course, despite small changes in signaling profiles, no significant differences were evident between untreated aged control versus leucine or versus HMB treatment (Fig. 6).

Given the limited impact of leucine or HMB aged cell migration or on PI3K/Akt, ERK or mTOR activation versus aged cell controls, the hypothesis to be challenged next was that these supplements would not rescue inhibited cell velocity, directionality, overall migration distance in the presence of LY294002, PD98059 or rapamycin (Fig. 7a–c), respectively. Indeed, aged cell velocity was significantly blocked by LY294002 in the absence (0.10 ± 0.04 μm/min^{-1}; $P < 0.001$) or presence of leucine (0.12 ± 0.06 μm/min^{-1}; $P < 0.001$) or HMB (0.12 ± 0.05 μm/min^{-1}; $P < 0.001$) versus untreated aged control (0.30 ± 0.07 μm/min^{-1}). There was no significant difference between LY294002 alone versus LY294002 with leucine or with HMB, indicating that there was no rescue of cell velocity by supplements in the presence of reduced PI3K/Akt activation (Fig. 7a). Similar to these data, when treated with LY294002 directionality was significantly reduced in the absence
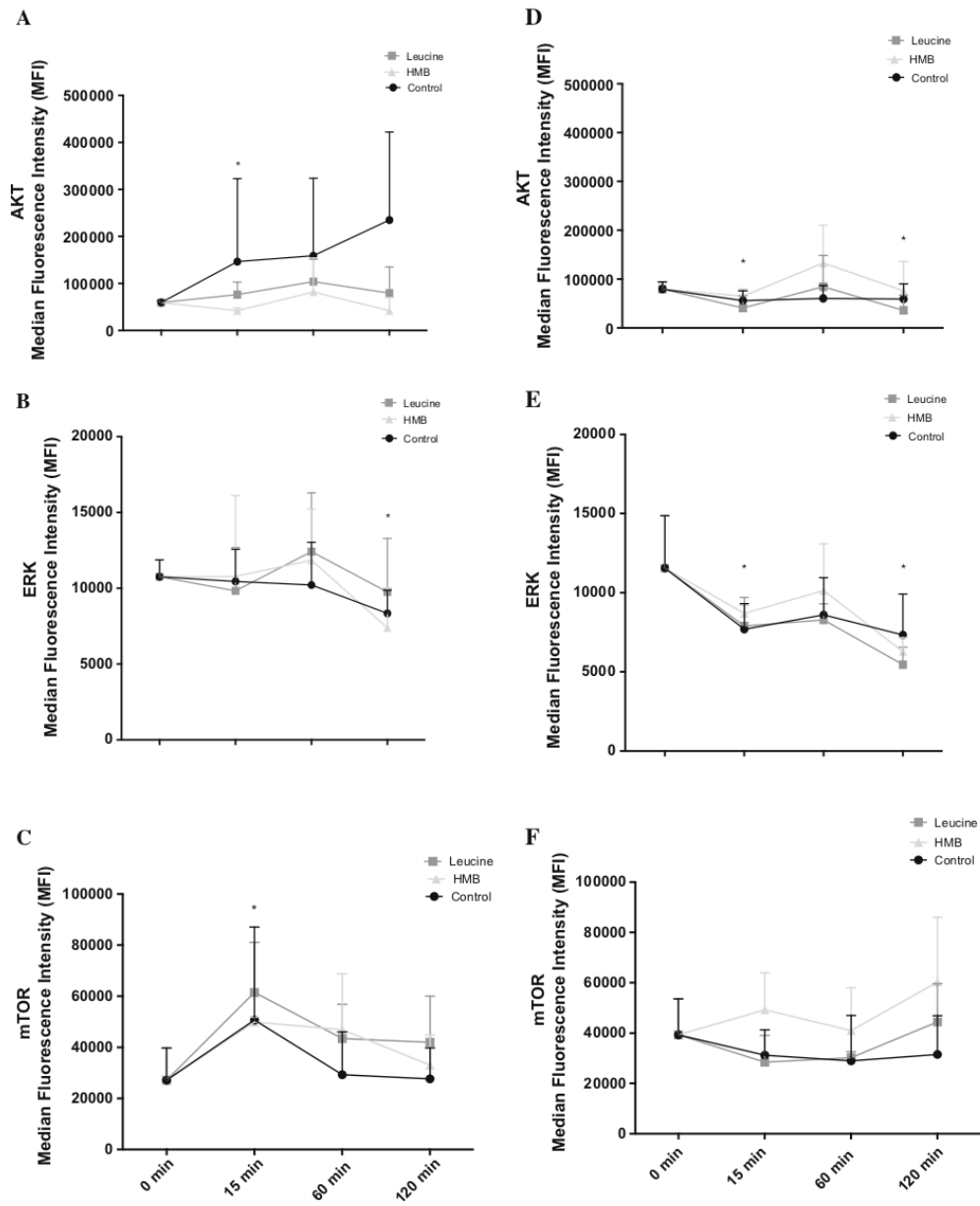
Fig. 6 Line charts illustrating the differences in the phospho-rylation of aged Akt (**a**), ERK (**b**) and mTOR (**c**) and control Akt (**d**), ERK (**e**) and mTOR (**f**) molecules, with cells treated with leucine and HMB over 120 min. The data is shown as mean with SD. Significance is set at $P < 0.05$ and was indicted versus 0 min (*) time-point. The experiment consisted of 3 repeats all in duplicate

Springer

263

Fig. 7 Bar charts illustrating the differences in cell velocity with the inhibition of LY294002 (**a**), PD98059 (**b**), and rapamycin (**c**) in the presence or absence of leucine and HMB over 48 h. The data is shown as mean with SD. Significance is set at P < 0.05. Significance was shown as: aged versus control (^), versus control (*), versus inhibitor (//), leucine versus HMB (/) and inhibitor with supplement versus supplement alone (#). The experiment consisted of 3 repeats all in duplicate

(0.49 ± 0.20; P < 0.001) or presence of leucine (0.52 ± 0.19; P < 0.001) or HMB (0.54 ± 0.22; P < 0.001) versus untreated aged control (0.71 ± 0.12; Fig. 8a). Finally, overall migration distance in the presence of LY294002 was significantly reduced in the absence (332 ± 123 μm; P < 0.001) or presence of leucine (388 ± 157 μm; P < 0.001) or HMB (399 ± 167 μm; P < 0.001) versus untreated aged control (802 ± 202 μm; Fig. 9a). Interestingly and in contrast to our hypothesis, there was a small but significant increase in overall migration distance, compared with LY294002, when co-incubated with either supplement (P = 0.05).

As with PI3K/Akt inhibition, when aged cells were treated with PD98059, velocity was significantly decreased in the absence (0.21 ± 0.08 μm/min^{-1}; P = 0.001) or presence of leucine (0.24 ± 0.06 μm/min^{-1}) or HMB (0.23 ± 0.08 μm/min^{-1}), versus untreated aged control (0.28 ± 0.07 μm/min^{-1}; Fig. 7b). Similarly, directionality was significantly reduced in the absence (0.64 ± 0.17; P < 0.001) or presence of either leucine (0.67 ± 0.15; P < 0.001) or HMB (0.68 ± 0.15; P < 0.001) versus untreated aged control (0.71 ± 0.12; Fig. 8b). Overall migration distance was also significantly blunted when incubated with PD98059 (618 ± 219 μm; P < 0.001) versus untreated aged control (802 ± 202 μm; Fig. 9b). Interestingly there was a small but significant increase in overall migration distance, compared with PD98059 alone, when co-incubated with either supplement (P < 0.01).

Rapamycin conditions were not significantly different (0.24 ± 0.07 μm/min^{-1}) in cell velocity (Fig. 7c) versus untreated aged control (0.28 ± 0.07 μm/min^{-1}) and were not altered by co-incubation with leucine (0.26 ± 0.06 μm/min^{-1}) or HMB (0.29 ± 0.07 μm/min^{-1}). Furthermore, rapamycin in absence (0.62 ± 0.17; P < 0.001) or presence of leucine (0.64 ± 0.16; P < 0.001) or HMB (0.65 ± 0.14; P < 0.001) significantly reduced the
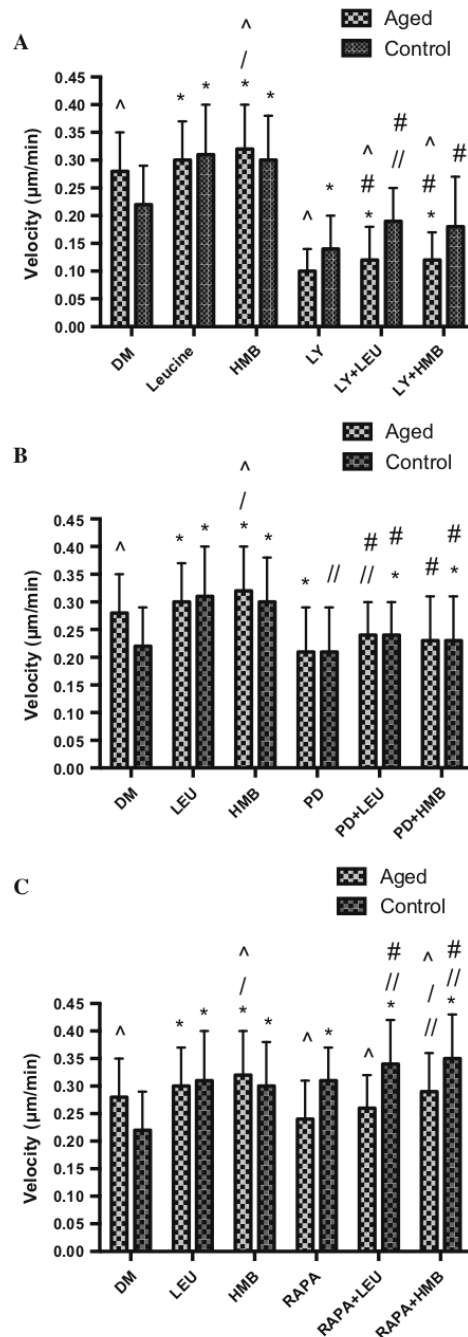
Fig. 8 Bar charts illustrating the differences in cell direction-▶ ality with the inhibition of LY294002 (**a**), PD98059 (**b**), and rapamycin (**c**) in the presence or absence of leucine and HMB over 48 h. The data is shown as mean with SD. Significance is set at P < 0.05. Significance was shown as: aged versus control (^), versus control (*), versus inhibitor (//), leucine vs. HMB (/) and inhibitor with supplement versus supplement alone (#). The experiment consisted of 3 repeats all in duplicate

cell directionality versus untreated aged control (0.71 ± 0.12; Fig. 8c). The overall migrated distance in the presence of rapamycin (697 ± 213 μm; Fig. 9c) was not significantly different to untreated aged control (802 ± 202 μm), this was sustained in the presence of leucine (757 ± 159 μm) or HMB (849 ± 205 μm). Compared to rapamycin alone, the co-incubation of leucine did not significantly increase overall distance, whereas HMB was able to promote increases in overall distance (P < 0.001).

Together these data suggest that indeed the ability of leucine or HMB to rescue aged cell migration in the presence of inhibited PI3K/Akt or ERK signaling is compromised. Given the improved basal migration in control cells supplemented with leucine or HMB and the roles that PI3K/Akt and ERK appear to play in control cell migration, the next hypothesis to be tested was that these supplements may rescue inhibited cell migration in the presence of PI3K/Akt and ERK but not mTOR inhibition.

Control cell velocity was significantly reduced with LY294002 treatment, in the absence (0.14 ± 0.06 μm/min^{-1} P < 0.001) of supplements versus untreated control (0.22 ± 0.07 μm/min^{-1}). In the presence of leucine, but not HMB, cell velocity was increased versus LY294002 (0.19 ± 0.06 μm/min^{-1}; P < 0.001), which was not significantly different from control (Fig. 7a). The directionality of control cells was significantly blocked when inhibited with LY294002 (0.38 ± 0.18; P < 0.001) versus untreated control (0.61 ± 0.17; Fig. 8a). Co-incubation with leucine or HMB, respectively, rescued directionality versus LY294002 alone (0.51 ± 0.16; P < 0.001; 0.46 ± 0.21; P = 0.047). The co-incubation with HMB was rescued back to control, as there was no significant difference. Despite improvements in cell velocity and directionality, through co-incubation with supplements and the small increases in overall migration distance (Fig. 9a), neither leucine (495 ± 205 μm) or HMB (476 ± 206 μm) were able
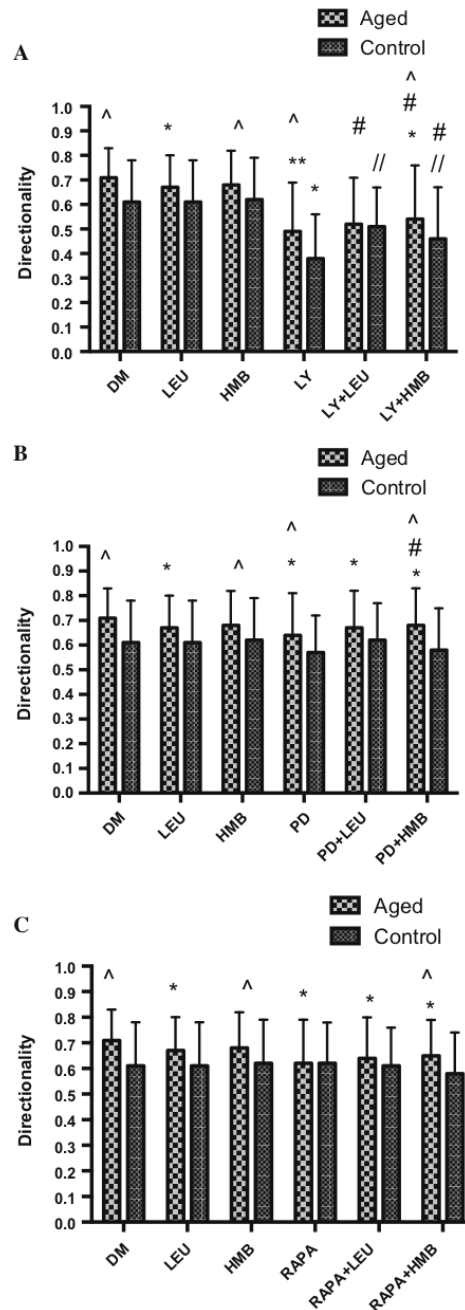
Fig. 9 Bar charts illustrating the differences in cell accumulated distance with the inhibition of LY294002 (**a**), PD98059 (**b**), and rapamycin (**c**) in the presence or absence of leucine and HMB over 48 h. The data is shown as mean with SD. Significance is set at P < 0.05. Significance was shown as: aged versus control (^), versus control (*), versus inhibitor (//), leucine vs. HMB (/) and inhibitor with supplement versus supplement alone (#). The experiment consisted of 3 repeats all in duplicate

to significantly increase overall migration distance versus LY294002 alone (437 ± 174 μm).

Cell velocity did not change when inhibited with PD98059 (0.21 ± 0.08 μm/min^{-1}) versus control (0.22 ± 0.07 μm/min^{-1}); it is not therefore surprising that co-incubation in the presence of either leucine (0.24 ± 0.06 μm/min^{-1}; P = 0.001) or HMB (0.23 ± 0.08 μm/min^{-1}; P = 0.032) resulted in improved cell velocity versus control alone (Fig. 7b). PD98059 in the absence or presence of supplements was without impact on directionality (Fig. 8b), however when compared with control (622 ± 188 μm; Fig. 9b), migration distance was improved with PD98059 (678 ± 217 μm; P = 0.013) in the absence or presence of leucine (756 ± 217 μm; P < 0.001) or HMB (742 ± 256 μm; P < 0.001).

In control cell following rapamycin treatment, there was an increase in cell velocity (0.31 ± 0.06 μm/min^{-1}; P < 0.001) versus control (0.22 ± 0.07 μm/min^{-1}), which was further enhanced in the presence of leucine (0.34 ± 0.08 μm/min^{-1}; P < 0.001) or HMB (0.35 ± 0.08 μm/min^{-1}; P < 0.001) vs. untreated control (Fig. 7c). Indeed, when compared with rapamycin alone, leucine (P = 0.036) or HMB (P < 0.001) co-incubation both also significantly increased cell velocity versus rapamycin alone. Cell directionality was unaltered by rapamycin or by rapamycin plus either supplement (Fig. 8c), however in the presence of rapamycin, the significant increase in migration distance (884 ± 180 μm; P < 0.001) versus control (622 ± 188 μm; Fig. 9c), was further enhanced in the presence of leucine (970 ± 232 μm; P < 0.001) or HMB (1010 ± 227 μm; P < 0.001). Indeed, these increases were significantly higher than rapamycin alone for both co-incubations with leucine (P = 0.036) or HMB (P < 0.001).

Given the unexpected potential of mTOR inhibition, via rapamycin, to improve not reduce cell migration, particularly in control cells and wishing to determine possible compensatory mechanisms,

Springer

266
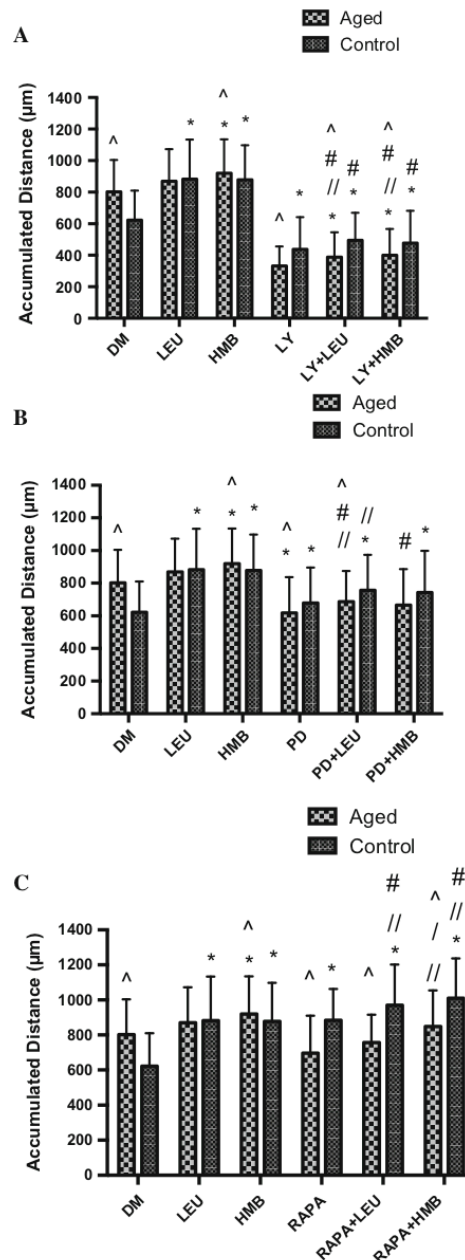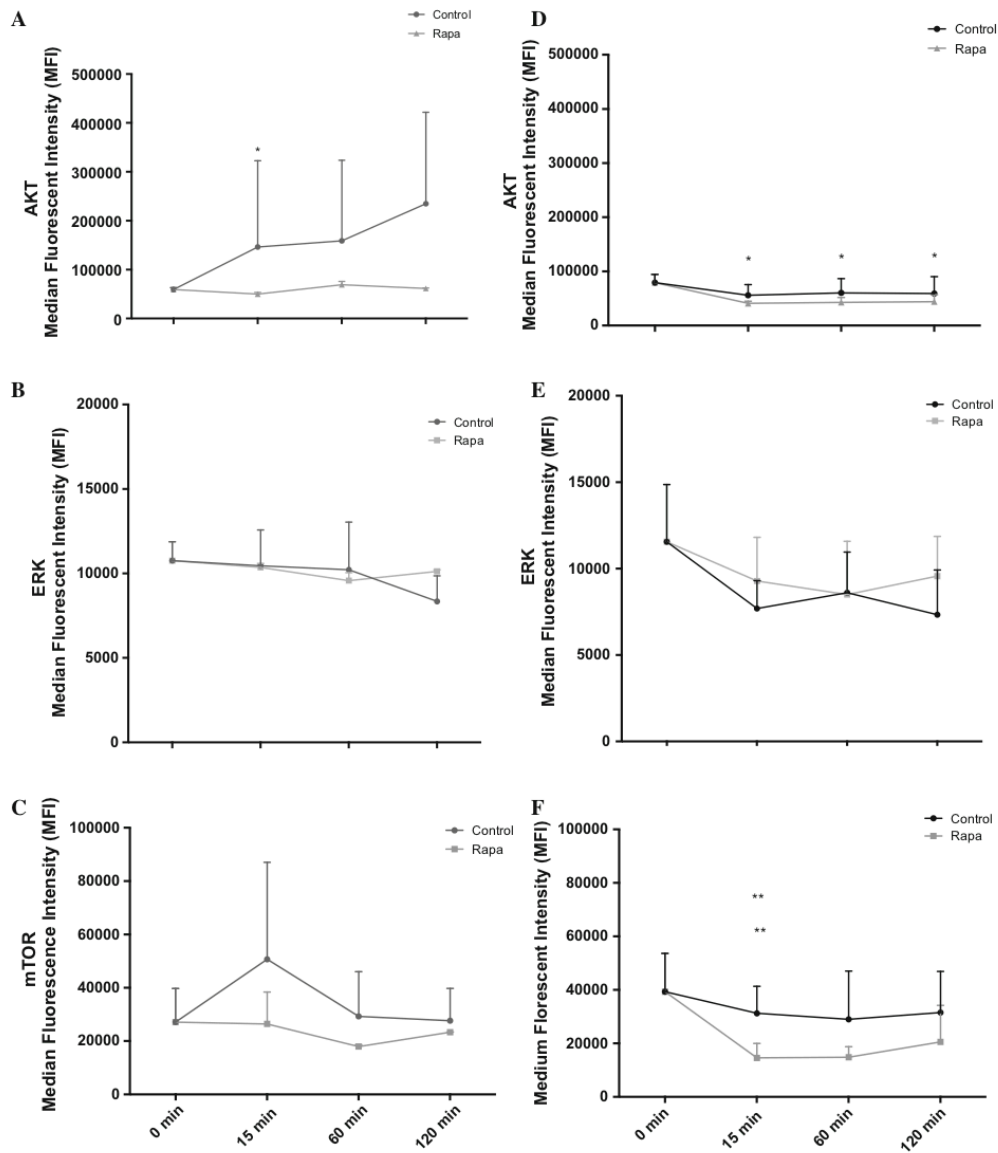
Fig. 10 Line charts illustrating the differences in the phosphorylation of aged Akt (**a**), ERK (**b**) and mTOR (**c**) and control Akt (**d**), ERK (**e**) and mTOR (**f**) molecules, with cells treated with rapamycin over 120 min. The data is shown as mean with SD.

Significance was indicted versus 0 min (*) and versus corresponding time-point (**). The experiment consisted of 3 repeats all in duplicate

267

which may be involved in this adaptation, the cells were incubated with rapamycin and the phosphorylation of Akt, ERK and mTOR were analysed. In both aged and control cells, rapamycin led to a significant decrease in mTOR phosphorylation. Rapamycin treated aged cells had suppressed Akt phosphorylation versus control, there was a significant decrease at 15 min (P = 0.037) versus 0 min, but not at any other time points (Fig. 10a). There was no difference between ERK (Fig. 10b) and mTOR (Fig. 10c) in aged cells until 60 min, where activity decreased in control, and increased with rapamycin. Similar to Akt, mTOR phosphorylation was greatly suppressed with rapamycin treatment versus control over 120 min. In control cells, Akt phosphorylation was also significantly reduced with rapamycin treatment at 15, 60 and 120 min versus 0 min (P = 0.005; P = 0.009; P = 0.014 respectively; Fig. 10d). The activation of ERK was reduced and suppressed until 60 min (Fig. 10e). At 120 min ERK activation spiked, which is contrary to the treatments. Rapamycin treated cells significantly reduced mTOR phosphorylation at 15 min (P = 0.026) and 60 min (P = 0.026) versus 0 min (Fig. 10f). At 120 min, the levels increase back to baseline and at 15 min, there was a significant difference between control versus rapamycin treatment (P = 0.035).

Discussion

The aim of this study was to determine the capacity of replicatively aged versus non-replicated control cells to migrate, the signaling mechanisms underpinning this capacity and whether leucine and/or HMB could impact models of skeletal myoblast repair. We hypothesised that: (1) replicatively aged (P46–P48; "aged") myoblasts would be less efficient at damage repair versus control (P12–P16; "control"); (2) leucine and HMB would increase the migration potential in control but not aged cells and; (3) that the PI3K and ERK but not mTOR pathways would be required for effective basal migration in both models.

The main outcome of this investigation and in contrast to hypothesis 1, was that under basal conditions, the aged passaged cells closed the wound more quickly compared to their control counterparts. This was evident in the overall velocity, directionality and accumulated distance of the cells. However, in

accordance with our hypothesis 2, the supplementation of leucine or HMB enhanced the migration potential of control cells compared to the aged cells. Interestingly, the enhanced migration of control cells, in the presence of supplements, resulted in overall migration distances equivalent to those obtained in aged cells in the absence of supplements, suggesting the control cells were "catching up" with aged cells, following supplementation. Finally, in accordance with hypothesis 3, PI3K and ERK were important for basal migration in both models, but in contrast to predictions, mTOR inhibition, not activation, enabled facilitated wound repair in the absence or presence of supplements and most markedly in control versus aged cell models.

To date, when studying the impact of age and nutrition on muscle adaptation, the majority of published research has focused on sarcopenia (Churchward-Venne et al. 2014), the progressive loss of muscle mass and strength with age and on anabolic resistance in aged individuals (Burd et al. 2013). However, it is also reported that the capability of the muscle to regenerate in the aged individuals is impaired, compared with control counterparts (Jang et al. 2011). In vitro, mechanistic studies to underpin this latter observation are, however, currently sparse. Owens et al. (2015) investigated the impact of vitamin D on muscle regeneration in primary human muscle cells, and reported average control migration rates equivalent to those in this model (666 ± 288 vs. 622 ± 188 µm). Our data challenge our hypothesis of impaired migration with age, with aged cells migrating more efficiently than control ones, perhaps as a result of improved PI3K/Akt and ERK signaling. The improved wound closure is not a result of cellular replication, with previous studies using mitomycin-C to block proliferation in unaged and aged myoblasts reporting migration capabilities which remain intact (Falcone et al. 1984; Dimchev et al. 2013). Replicatively aged C_2C_{12} myoblasts also retain telomeres (Yaffe and Saxel 1977; Holt et al. 1996; O'connor et al. 2009) and express decreased levels of IGF-1 and Akt phosphorylation (Benbassat et al. 1997; Léger et al. 2008), similar to aged primary muscle stem cells. The absence of a response to leucine and HMB supplementation in aged cells may arise as a result of optimised migration under basal conditions—this is supported via the observation that when control cells are supplemented with either leucine or HMB,

migration is significantly improved, but only to levels seen in untreated aged cells.

To substantiate this theory, in both cell models, when the PI3K/Akt pathway was inhibited, the cell velocity, directionality and accumulated distance all decreased, suggesting that this pathway is integral to myoblast migration. The basal enhancement in the aged versus control cells may account for improved migration under control conditions. Neither leucine nor HMB were able to rescue reduced migration in the presence of LY294002, suggesting the fundamental role of this pathway in effective migration of myoblasts. Interestingly, while PD98059 reduced basal velocity and distance migrated in aged cells, it was without impact in control cells extending our observations to suggest that PI3K and ERK function together to facilitate increased migration in aged versus control cells. Under inhibitor conditions and unlike PI3K inhibition, co-incubation with leucine or HMB incurred partial rescue to the aged cell velocity and migration distance. By contrast, while basal velocity and overall migration distance were not negatively impacted by PD98059 in control cells, the facilitated migration velocity and distance in the presence of leucine or HMB was significantly reduced, compared with either supplement alone. Therefore, while partial rescue can be incurred via supplementation in aged cells when ERK is inhibited, the capacity of control cells to respond to supplements is reduced in the absence of ERK activation, despite no impact on basal cell migration potential. These data suggest both shared and divergent pathways underpinning aged versus control myoblast migration.

Dai et al. (2015) recently researched the effects of leucine on rat satellite cell proliferation and differentiation. The authors reported that leucine promoted proliferation and differentiation through the mTOR-MyoD signalling pathway. Research reinforcing these results demonstrated that leucine starvation led to inhibition of myoblast differentiation (Averous et al. 2012). Areta et al. (2014) also demonstrated the benefits on supplementing leucine on C_2C_{12} muscle cell growth. Research by Kornasio et al. (2009) is the only study, to the author's knowledge, to investigate the effects of HMB on aged myoblast activity. This study suggested that HMB stimulated myoblast proliferation, differentiation and survival compared to control, with both the PI3K/Akt and ERK/MAPK signalling pathways involved in these processes. Cell migration was not assessed. Further, studies by Kornasio et al. support the concept that HMB has beneficial effects on the proliferation and differentiation of myoblasts, through the MAPK/ERK and PI3K/Akt pathways (Kornasio et al. 2009; Vallejo et al. 2016). Although migration in the presence of supplements was not investigated in these reports, data from Dimchev et al. suggest that the ability of myoblasts to migrate depends on the PI3K/Akt and ERK/MAPK pathways (Dimchev et al. 2013).

The data from our study support the hypothesis that when inhibiting the PI3K/Akt pathway with LY294002, the cell velocity, directionality and accumulated distance is reduced. Previous studies have supported this finding (Suzuki et al. 2000; Kawamura et al. 2004; Al-Shanti et al. 2011; Dimchev et al. 2013). Raftopoulou and Hall (2004) suggested that the PI3K/Akt pathway is integral in the development of cellular protrusions. Moreover, Kawamura et al. (2004) demonstrated that the PI3K/Akt pathway is essential for cell migration through lamellipodial formation, which is important in cell directionality and velocity (Raftopoulou and Hall 2004). It is apparent therefore, that the PI3K/Akt pathway is integral for myoblast migration, irrespective of the replicative status of the myoblasts. This may not be the case for ERK activation, where ERK activity appears important for improved migration of the aged cells, but not control, in this study. However, the data underpinning a role for ERK in myoblast migration are equivocal. For instance, Leloup et al. (2007) suggested that the ERK/MAPK pathway was responsible for stimulating growth factor mediated stimulation of myoblast migration. Conversely, Ranzato et al. (2009) suggested that it was primarily Akt and p38 MAPK signaling proteins that stimulated myoblast migration not the ERK pathway. Whereas, other research has also supported the notion that the ERK/MAPK pathway was involved in cell migration (Al-Shanti et al. 2011; Dimchev et al. 2013). The differences in studies could be attributed to the dose of inhibitor used as well as the myoblast models, alternatively, this apparent controversy warrants further investigation, as it may have important implications for cellular need, for example, fusion in the control versus migration in the aged models.

Intriguingly, and not reported in the Kornasio study (Kornasio et al. 2009), when rapamycin was added to the wound model detailed in this manuscript, it was with no impact on basal migration of aged cells, but

269

significantly increased, not decreased, cell velocity and basal migration of control cells, which were both further increased with co-incubations of leucine or HMB. The mTOR pathway is largely regarded to be integral for muscle protein synthesis (MPS) and is stimulated by both exercise and protein ingestion, and is further increased when both are combined (Hawley et al. 2011). Further research proposes that leucine is the primary initiator of MPS (Churchward-Venne et al. 2012). The mTOR target is downstream of the PI3K and Akt signaling cascades which then stimulate S6K which leads to MPS (reviewed in: (Sharples et al. 2015). The impact of this pathway on muscular hypertrophy and muscle wasting is well known (reviewed in: Sharples et al. 2015), however, the impact on cell migration has not been studied. These observations would suggest that mTOR activation is detrimental to control cell migration, but integral to myoblast hypertrophy/fusion (Averous et al. 2012; Areta et al. 2014; Dai et al. 2015), again raising the concept of differential drivers of cellular behavior with age. Indeed, the data derived in this study suggest that the PI3K/Akt pathway is an integral pathway, shared in control and aged cell migration, that ERK further enhances aged cell migration, but that mTOR reduces control cell migration. These changing signaling pathways may underpin the adaptation that appears to have occurred as a result of replicative ageing.

Conclusion

Taken together, basally, the aged cells migrate more quickly than control myoblasts, potentially at the expense of efficient fusion (Sharples et al. 2011). However, with the supplementation of leucine and HMB, the capacity of the control cells to migrate is increased to that of the aged cells. This implies that 1, the control cells are more responsive to the supplements or 2, that maximal migration capacity has been attained in aged cells under basal conditions and therefore supplements cannot improve their migration capability. In control myoblasts, it is the PI3K/Akt pathway that appears central for migration, which is in line with previous research. However, our data show that the ERK/MAPK pathway is less important for control myoblast migration, where the results in the literature are still equivocal. Activation of both

pathways are required for replicatively aged myoblast migration. To the author's knowledge, this is the first study to investigate the potential role of the mTOR pathway in myoblast migration. The results are interesting, showing that this pathway, when activated, could reduce control myoblast migration, perhaps to ensure successful protein synthesis and hypertrophy. Differential activation of the PI3K/Akt, ERK/MAPK and mTOR pathways appear to underpin the differences observed in control or supplemented control and aged myoblast migration. Future research is required to establish further the mechanisms underpinning altered migration, including the roles of lamellipod/filapod formation and actin polarisation; cell/matrix interactions should also be determined.

References

Al-Shanti N, Faulkner SH, Saini A, Loram I, Stewart CE (2011) A semi-automated programme for tracking myoblast migration following mechanical damage: manipulation by chemical inhibitors. Cell Physiol Biochem 27:625–636

Areta JL, Hawley JA, Ye J-M, Chan MS, Coffey VG (2014) Increasing leucine concentration stimulates mechanistic target of rapamycin signaling and cell growth in C2C12 skeletal muscle cells. Nutr Res 34:1000–1007

Averous J, Gabillard J-C, Seiliez I, Dardevet D (2012) Leucine limitation regulates myf5 and myoD expression and inhibits myoblast differentiation. Exp Cell Res 318:217–227

Benbassat CA, Maki KC, Unterman TG (1997) Circulating levels of insulin-like growth factor (IGF) binding protein-1 and-3 in aging men: relationships to insulin, glucose, IGF, and dehydroepiandrosterone sulfate levels and anthropometric measures. J Clin Endocrinol Metab 82:1484–1491

Bigot A, Jacquemin V, Debacq-Chainiaux F, Butler-Browne GS, Toussaint O, Furling D, Mouly V (2008) Replicative aging down-regulates the myogenic regulatory factors in human myoblasts. Biol Cell 100:189–199

Bigot A, Duddy WJ, Ouandaogo ZG, Negroni E, Mariot V, Ghimbovschi S et al (2015) Age-associated methylation suppresses SPRY1, leading to a failure of re-quiescence and loss of the reserve stem cell pool in elderly muscle. Cell Rep 13:1172–1182

Breen L, Phillips SM (2011) Skeletal muscle protein metabolism in the elderly: interventions to counteract the anabolic resistance of ageing. Nutr Metab 8:68

270

Brooks SV, Faulkner JA (1988) Contractile properties of skeletal muscles from young, adult and aged mice. J Physiol 404:71–82

Burd NA, Gorissen SH, van Loon LJ (2013) Anabolic resistance of muscle protein synthesis with aging. Exerc Sport Sci Rev 41:169–173

Churchward-Venne TA, Burd NA, Mitchell CJ, West DW, Philp A, Marcotte GR et al (2012) Supplementation of a suboptimal protein dose with leucine or essential amino acids: effects on myofibrillar protein synthesis at rest and following resistance exercise in men. J Physiol 590:2751–2765

Churchward-Venne TA, Breen L, Phillips SM (2014) Alterations in human muscle protein metabolism with aging: protein and exercise as countermeasures to offset sarcopenia. BioFactors 40:199–205

Dai J-M, Yu M-X, Shen Z-Y, Guo C-Y, Zhuang S-Q, Qiu X-S (2015) Leucine promotes proliferation and differentiation of primary preterm rat satellite cells in part through mTORC1 signaling pathway. Nutrients 7:3387–3400

Day K, Shefer G, Shearer A, Yablonka-Reuveni Z (2010) The depletion of skeletal muscle satellite cells with age is concomitant with reduced capacity of single progenitors to produce reserve progeny. Dev Biol 340:330–343

Deane CS, Hughes DC, Sculthorpe N, Lewis MP, Stewart CE, Sharples AP (2013) Impaired hypertrophy in myoblasts is improved with testosterone administration. J Steroid Biochem Mol Biol 138:152–161

Dimchev GA, Al-Shanti N, Stewart CE (2013) Phospho-tyrosine phosphatase inhibitor Bpv (Hopic) enhances C2C12 myoblast migration in vitro. Requirement of PI3K/AKT and MAPK/ERK pathways. J Muscle Res Cell Motil 34:125–136

Falcone G, Boettiger D, Alema S, Tato F (1984) Role of cell division in differentiation of myoblasts infected with a temperature-sensitive mutant of Rous sarcoma virus. EMBO J 3:1327

Farup J, Rahbek SK, Knudsen IS, de Paoli F, Mackey AL, Vissing K (2014) Whey protein supplementation accelerates satellite cell proliferation during recovery from eccentric exercise. Amino Acids 46:2503–2516

Faulkner JA, Brooks SV, Zerba E (1991) Skeletal muscle weakness and fatigue in old age: underlying mechanisms. In: Vincent J (ed) Special focus on the biology of aging. Springer, Berlin, pp 147–166

Hatfield I, Harvey I, Yates ER, Redd JR, Reiter LT, Bridges D (2015) The role of TORC1 in muscle development in Drosophila. Sci Re 5:9676

Hawley JA, Burke LM, Phillips SM, Spriet LL (2011) Nutritional modulation of training-induced skeletal muscle adaptations. J Appl Physiol 110:834–845

Holt SE, Wright WE, Shay JW (1996) Regulation of telomerase activity in immortal cell lines. Mol Cell Biol 16:2932–2939

Jang Y, Sinha M, Cerletti M, Dall'Osso C, Wagers A (2011) Skeletal muscle stem cells: effects of aging and metabolism on muscle regenerative function. Cold Spring Harb Symp Quant Biol 76:101–111

Kawamura K, Takano K, Suetsugu S, Kurisu S, Yamazaki D, Miki H et al (2004) N-WASP and WAVE2 acting downstream of phosphatidylinositol 3-kinase are required for

myogenic cell migration induced by hepatocyte growth factor. J Biol Chem 279:54862–54871

Koopman R, Verdijk L, Manders RJ, Gijsen AP, Gorselink M, Pijpers E et al (2006) Co-ingestion of protein and leucine stimulates muscle protein synthesis rates to the same extent in young and elderly lean men. Am J Clin Nutr 84:623–632

Kornasio R, Riederer I, Butler-Browne G, Mouly V, Uni Z, Halevy O (2009) β-hydroxy-β-methylbutyrate (HMB) stimulates myogenic cell proliferation, differentiation and survival via the MAPK/ERK and PI3K/Akt pathways. Biochim Biophys Acta (BBA)-Mol Cell Res 1793:755–763

Lees SJ, Rathbone CR, Booth FW (2006) Age-associated decrease in muscle precursor cell differentiation. Am J Physiol-Cell Physiol 290:C609–C615

Lees SJ, Zwetsloot KA, Booth FW (2009) Muscle precursor cells isolated from aged rats exhibit an increased tumor necrosis factor-α response. Aging Cell 8:26–35

Léger B, Derave W, De Bock K, Hespel P, Russell AP (2008) Human sarcopenia reveals an increase in SOCS-3 and myostatin and a reduced efficiency of Akt phosphorylation. Rejuvenation Res 11:163–175B

Leloup L, Daury L, Mazères G, Cottin P, Brustis J-J (2007) Involvement of the ERK/MAP kinase signalling pathway in milli-calpain activation and myogenic cell migration. Int J Biochem Cell Biol 39:1177–1189

O'connor MS, Carlson ME, Conboy IM (2009) Differentiation rather than aging of muscle stem cells abolishes their telomerase activity. Biotechnol Prog 25:1130–1137

Owens DJ, Sharples AP, Polydorou I, Alwan N, Donovan T, Tang J et al (2015) A systems-based investigation into vitamin D and skeletal muscle repair, regeneration, and hypertrophy. Am J Physiol-Endocrinol Metab 309:E1019–E1031

Phillips SM, Tang JE, Moore DR (2009) The role of milk-and soy-based protein in support of muscle protein synthesis and muscle protein accretion in young and elderly persons. J Am Coll Nutr 28:343–354

Pietrangelo T, Puglielli C, Mancinelli R, Beccafico S, Fanò G, Fulle S (2009) Molecular basis of the myogenic profile of aged human skeletal muscle satellite cells during differentiation. Exp Gerontol 44:523–531

Raftopoulou M, Hall A (2004) Cell migration: Rho GTPases lead the way. Dev Biol 265:23–32

Ranzato E, Balbo V, Boccafoschi F, Mazzucco L, Burlando B (2009) Scratch wound closure of C2C12 mouse myoblasts is enhanced by human platelet lysate. Cell Biol Int 33:911–917

Schubert R, Geiger H, Zielen S, Baer PC (2009) Simultaneous detection of ERK-, p38-, and JNK-MAPK phosphorylation in human adipose-derived stem cells using the Cytometric Bead Array technology. J Immunol Methods 350:200–204

Sharples AP, Al-Shanti N, Lewis MP, Stewart CE (2011) Reduction of myoblast differentiation following multiple population doublings in mouse C2C12 cells: a model to investigate ageing? J Cell Biochem 112:3773–3785

Sharples AP, Player DJ, Martin NR, Mudera V, Stewart CE, Lewis MP (2012) Modelling in vivo skeletal muscle ageing in vitro using three-dimensional bioengineered constructs. Aging Cell 11:986–995

271

Sharples AP, Hughes DC, Deane CS, Saini A, Selman C, Stewart CE (2015) Longevity and skeletal muscle mass: the role of IGF signalling, the sirtuins, dietary restriction and protein intake. Aging Cell 14:511–523

Shefer G, Van de Mark DP, Richardson JB, Yablonka-Reuveni Z (2006) Satellite-cell pool size does matter: defining the myogenic potency of aging skeletal muscle. Dev Biol 294:50–66

Suzuki J, Yamazaki Y, Guang L, Kaziro Y, Koide H (2000) Involvement of Ras and Ral in chemotactic migration of skeletal myoblasts. Mol Cell Biol 20:4658–4665

Vallejo J, Spence M, Cheng A-L, Brotto L, Edens NK, Garvey SM, Brotto M (2016) Cellular and physiological effects of dietary supplementation with β-hydroxy-β-methylbutyrate (HMB) and β-alanine in late middle-aged mice. PLoS ONE 11:e0150066

Welle S (2002) Cellular and molecular basis of age-related sarcopenia. Can J Appl Physiol 27:19–41

Welle S, Brooks AI, Delehanty JM, Needler N, Thornton CA (2003) Gene expression profile of aging in human muscle. Physiol Genomics 14:149–159

Yaffe D, Saxel O (1977) Serial passaging and differentiation of myogenic cells isolated from dystrophic mouse muscle. Nature 270:725–727

Springer

8.4 Appendix 4: Publication 2: Exercising Bioengineered Skeletal Muscle In Vitro: Biopsy to Bioreactor

Chapter 5

Exercising Bioengineered Skeletal Muscle In Vitro: Biopsy to Bioreactor

Daniel C. Turner, Andreas M. Kasper, Robert A. Seaborne, Alexander D. Brown, Graeme L. Close, Mark Murphy, Claire E. Stewart, Neil R. W. Martin, and Adam P. Sharples ⓘ

Abstract

The bioengineering of skeletal muscle tissue in-vitro has enabled researchers to more closely mimic the in-vivo skeletal muscle niche. The three-dimensional (3-D) structure of the tissue engineered systems employed to date enable the generation of highly aligned and differentiated myofibers within a representative biological matrix. The use of electrical stimulation to model concentric contraction, via innervation of the myofibers, and the use of mechanical loading to model passive lengthening or stretch has begun to provide a manipulable environment to investigate the cellular and molecular responses following exercise mimicking stimuli in-vitro. Currently available bioreactor systems allow either electrical stimulation or mechanical loading to be utilized at any given time. In the present manuscript, we describe in detail the methodological procedures to create 3-D bioengineered skeletal muscle using both cell lines and/or primary human muscle derived cells from a tissue biopsy, through to modeling exercising stimuli using a bioreactor that can provide both electrical stimulation and mechanical loading simultaneously within the same in-vitro system.

Key words Skeletal muscle, Tissue engineering, Bioengineering, Myoblasts, Satellite cells, Exercise, Biological scaffolds

---

1 Introduction

Exercising differentiated multinucleated skeletal muscle cells (myotubes/fibers) in monolayer cultures by means of electrical stimulation [1, 2] and mechanical stretch [3, 4] has partially mimicked responses following resistance [4, 5] and endurance [6, 7] exercise in-vivo. Following pioneering work by Vandenburgh and colleagues three decades ago, culturing in 3-dimensional (3-D) microenvironments may however be considered a more representative

---

model of the in-vivo skeletal muscle niche [8, 9] and with continuing progression, may predominate as an in-vitro tool for investigating the underlying mechanisms of exercise adaptation. Indeed, 3-D tissue engineered skeletal muscle models display highly aligned and differentiated myotubes [10, 11], permitting measures of muscle function [12–16] that are not entirely possible with monolayer cultures where swirling myotube formation results in non-uniaxial force generation. Furthermore, embedding skeletal muscle cells within representative extracellular matrices (e.g. collagen, laminin, fibrin) and allowing their differentiation into myotubes increases the amount of time the myotubes can be kept in culture. Where in monolayer, myotubes may begin to detach, especially following spontaneous contraction due to poorer matrix attachment [10]. The use of self-assembling fibrin "myooids" may also prove advantageous for 3-D skeletal muscle tissue engineering given that the cells can easily proliferate and become confluent prior to differentiation versus the use of a stiffer matrix such as collagen where proliferation maybe inhibited, and therefore fibrin "myooids" usually require lower seeding densities. This is particularly useful if trying to generate bioengineered muscle using limited primary muscle derived cells that eventually senesce. Fibrin myooids also provide superior functionality, such as force production vs. other biological scaffolds and can allow efficient gene transfection [14, 15, 17–20]. Collectively, the advantages of these engineered systems may help delineate the underlying mechanisms of physiological adaptation in response to exercise mimicking stimuli in-vitro. Once fully formed into a cyclindrical-like muscle, constructs undergo electrical [5, 12–15, 17, 21] or mechanical [22, 23] stimulation which can mimic shortening and lengthening contraction of skeletal muscle, respectively. Typically however, only one of these stimulation modes is utilized at once. Therefore, a system that can perform both of these functions simultaneously would be advantageous. Furthermore, delivering an electrical input during the lengthening portion of the movement would also provide a more relevant contraction vs. simply a passive lengthening/stretch, as muscle activity/tension is required to control an eccentric contraction in-vivo. Here, we describe the methodological procedures for creating 3-D bioengineered skeletal muscle constructs, using human skeletal muscle derived cells (SkMDC's) and/or the C2C12 myoblast cell line [24, 25] within a fibrin matrix. We further describe how to undertake stimulatory regimes using a commercially available (with customizations) bioreactor system permitting simultaneous electrical and mechanical stimulation.

274

2 Materials

2.1 Skeletal Muscle Biopsy Procedure

1. Disposable sterile scalpel.

2. Sterile biopsy instrument: Monopty® disposable core biopsy instrument (e.g., CR Bard, Crawley, UK) or a conchotome biopsy tool (e.g., Gebrüder Zepf Medizintechnik, Dürbheim, DEU) (see **Note 1**).

3. 6 × 75 mm steri-strips.

4. 7.5 cm × 5 cm sterile wound dressing plaster with transparent waterproof film.

5. 1.5 ml 0.5% bupivacaine hydrochloride prescribed by a designated physician/medical doctor.

6. Sterile wound cleansing and dressing pack (including swabs, sheet and tray).

7. Fine intramuscular injection needle.

8. Sterile 5 ml syringe.

9. Hydrex surgical scrub (e.g., Ecolab©, UK).

10. Sterile surgical gloves.

11. Disposable hospital razor.

12. 1.5 ml transfer medium: Ham's F-10 medium that includes 1 mM L-glutamine, 0.1% heat inactivated fetal bovine serum (hiFBS) (see **Note 2**), 0.1% heat inactivated new born calf serum (hiNBCS) (see **Note 2)**, 100 U/ml penicillin, 100 μg/ml streptomycin, 2.5 μg/ml amphotericin B. Stored and used at 4 °C.

13. Sterile 2 ml Eppendorf tube containing transfer medium submerged in ice.

2.2 Human Primary Cell Isolation

1. Growth medium: Ham's F-10 medium that includes 1 mM L-glutamine, 10% hiFBS, 10% hiNBCS, supplemented with an additional 2 mM L-glutamine, 100 U/ml penicillin, 100 μg/ml streptomycin, 2.5 μg/ml amphotericin B. Stored at 4 °C.

2. Horse serum (HS) (to neutralize trypsin).

3. 0.5% Trypsin-0.2% EDTA.

4. 0.01 M phosphate buffered saline $(1\times)$ (PBS): PBS dissolved in distilled water $(dH_2 0)$, 100 U/ml penicillin, 100 μg/ml streptomycin, 2.5 μg/ml amphotericin B (see **Note 1**). Stored at room temperature.

5. 2× sterile scalpels: either blades (see **Note 1**) or disposable sterile scalpel.

6. Magnetic stirring bar (6 × 35 mm) with platform (preheated to 37 °C) (see **Note 1**).

7. Disposable sterile petri dish (100 mm diameter).

275

8. Sterile 100 ml specimen container.

9. 2 mg/ml gelatin from porcine skin (Type A; Sigma-Aldrich, G2500) dissolved in distilled water (dH$_2$0) (*see* **Notes 1** and **3**).

2.3   Cryopreservation of Cells

1. Growth medium for primary human cell culture: Ham's F-10 medium that includes 1 mM L-glutamine, 10% hiFBS, 10% hiNBCS, supplemented with an additional 2 mM L-glutamine and 100 U/ml penicillin, 100 μg/ml streptomycin, 2.5 μg/ml amphotericin B. Stored at 4 °C.

2. Growth medium for C2C12 cell culture: Dulbecco's modified Eagle's medium (DMEM) that includes 4 mM L-glutamine, 10% hiFBS, 10% hiNBCS, supplemented with an additional 2 mM L-glutamine, 100 U/ml penicillin, 100 μg/ml streptomycin. Stored at 4 °C.

3. Cell culture grade dimethyl sulfoxide (DMSO).

4. Cryopreservation freezer container (e.g. "Mr. frosty").

5. PBS (*see* **Note 1**). Stored at room temperature.

6. 0.5% Trypsin-0.2% EDTA.

2.4   Resuscitation of Cryopreserved Cells

1. 2 mg/ml gelatin (*see* **Note 3**). Stored at room temperature.

2. Growth medium for primary human cell culture: Ham's F-10 medium that includes 1 mM L-glutamine, 10% hiFBS, 10% hiNBCS, supplemented with an additional 2 mM L-glutamine and 100 U/ml penicillin, 100 μg/ml streptomycin, 2.5 μg/ml amphotericin B. Stored at 4 °C.

3. Growth medium for C2C12 cell culture: DMEM that includes 4 mM L-glutamine, 10% hiFBS, 10% hiNBCS, supplemented with an additional 2 mM L-glutamine and 100 U/ml penicillin, 100 μg/ml streptomycin. Stored at 4 °C.

2.5   3-D Culture Dishes

1. Easy-Grip 35 mm dishes (BD Falcon®).

2. Sylgard® 184 Elastomer kit (Dow Corning, MI, USA) (*see* **Note 4**).

3. 0.15 mm minutien pins (*see* **Note 5**).

4. Silk suture thread (2.0) (*see* **Note 6**).

5. 70% ethanol.

6. 0.01 M PBS (*see* **Note 1**). Stored at room temperature.

2.6   Fibrin Skeletal Muscle Constructs

1. Fibrinogen from Bovine Plasma (Sigma-Aldrich, F8630): Dissolve fibrinogen (stored at −20 °C) at 20 mg/ml in preheated (37 °C) Ham's F12-K medium and incubate at 37 °C for 2–3 h, swirling every 30 min (*see* **Note 7**). Vacuum filter (0.22 μm; *see* **Note 8**), aliquot and store at −20 °C (*see* **Note 9**).

2. Thrombin from Bovine Plasma (Sigma-Aldrich, T4648): Dissolve thrombin at 200 U/ml in 5 ml of high glucose (4.5 g/l) DMEM (*see* **Note 10**). Sterile filter (0.22 μm), aliquot and store at −20 °C (*see* **Note 9**).

3. Aprotinin from Bovine Lung (Sigma-Aldrich, A3428-10MG): Dissolve total 10 mg aprotinin in 1 ml of distilled water (dH$_2$0) to ensure a stock concentration of 10 mg/ml. Sterile filter (0.22 μm), aliquot and store at −20 °C.

4. 6-Aminocaproic Acid (Sigma-Aldrich, A7824): Dissolve 6-aminocaproic acid at 50 mg/ml in distilled water (dH$_2$0). Sterile filter (0.22 μm), aliquot and store at 4 °C (*see* **Note 11**).

5. L-Ascorbic Acid (Sigma-Aldrich, A4403): Dissolve total 100 mg L-ascorbic acid in 11.36 ml of high glucose (4.5 g/l) DMEM to ensure a stock concentration of 50 mM. Sterile filter (0.22 μm), aliquot and store at 4 °C (*see* **Note 12**).

6. L-Proline (Sigma-Aldrich, P8865): Dissolve 100 mg L-proline in 17.37 ml 0.01 M PBS (*see* **Note 1)** to ensure a stock concentration of 50 mM. Sterile filter (0.22 μm), aliquot and store at 4 °C (*see* **Note 12**).

7. Genipin (Sigma-Aldrich, G4796): Dissolve genipin at 10 mg/ml in DMSO (*see* **Note 13)**. Sterile filter (0.22 μm), aliquot and store at −20 °C.

8. Growth medium: High glucose (4.5 g/l) DMEM that includes 4 mM L-glutamine, 10% hiFBS, 10% hiNBCS, supplemented with an additional 2 mM L-glutamine,100 U/ml penicillin, 100 μg/ml streptomycin (*see* **Note 14)**, 0.5 mg/ml 6-aminocaproic acid, 50 μM L-ascorbic acid, 50 μM L-proline (*see* **Note 12**). Stored at 4 °C.

9. Differentiation medium: High glucose (4.5 g/l) DMEM that includes 4 mM L-glutamine, 2% HS, supplemented with an additional 2 mM L-glutamine, 100 U/ml penicillin, 100 μg/ml streptomycin (*see* **Note 14)**, 1 mg/ml 6-aminocaproic acid, 50 μM L-ascorbic acid, 50 μM L-proline (*see* **Note 12**). Stored at 4 °C.

10. Maintenance medium: High glucose (4.5 g/l) DMEM that includes 4 mM L-glutamine, 3.5% hiFB, 3.5% hiNBCS, supplemented with an additional 2 mM L-glutamine, 100 U/ml penicillin, 100 μg/ml streptomycin (*see* **Note 14)**, 1 mg/ml 6-aminocaproic acid, 50 μM L-ascorbic acid, 50 μM L-proline (*see* **Note 12**). Stored at 4 °C.

11. Sylgard coated dishes (*see* **Note 4**).

2.7   TC-3 Bioreactor System (Ebers Medical Technology, ESP) (See Note 15)

1. Control module.

2. 3-D bioreactor cell culture chamber(s) including parts such as clamps and screws (*see* **Note 1).**

3. Laptop/desktop with controlling software.

277

4. Peristaltic pump/perfusion box.

5. Electrical Stimulation: Electrical stimulation module, output box, electrode anode/cathode splitter, platinum/pure iridium or stainless steel electrodes (*see* **Note 1**).

6. Mechanical Stimulation: Mechanical stimulation box.

2.8 From the Culture Dish to the Bioreactor

1. TC-3 Bioreactor chamber(s) (e.g. Ebers Medical Technology, ESP).

2. 2× sets of angled surgical tweezers (*see* **Notes 1** and **16**).

3. Maintenance medium: High glucose (4.5 g/l) DMEM that includes 4 mM L-glutamine, 3.5% hiFB, 3.5% hiNBCS, supplemented with an additional 2 mM L-glutamine, 100 U/ml penicillin, 100 μg/ml streptomycin (*see* **Note 14**), 1 mg/ml 6-aminocaproic acid, 50 μM L-ascorbic acid, 50 μM L-proline (*see* **Note 12**). Stored at 4 °C.

3   Methods

All procedures must be conducted under fully aseptic conditions. Following relevant ethical approval and informed consent of the participants, the skeletal muscle biopsy procedure must be undertaken by fully trained and insured individuals, usually a physician/clinician. A full medical screen by the physician of the participant is also required and the participants GP/family doctor should be informed. When preparing all biopsy equipment/contents, it is essential that direct contact is only made to the exterior packaging. If transported, the muscle tissue must be immersed in chilled (4 °C) transfer medium and transported to a sterile Class 2 cell culture hood/microbiological safety cabinet (BSC) as soon as possible to undergo subsequent cell isolation procedures. Furthermore, the storage and disposal of any tissue and waste should be in accordance to the relevant legislation, (e.g. in the UK, the Human Tissue Act (2004), and Control of Substances Hazardous to Health (2002) regulations, respectively).

3.1 Skeletal Muscle Biopsy Procedure

1. Ensure participant is laying in a supine position before shaving the desired area (in this case, the skin above the belly of the vastus lateralis) with a disposable razor.

2. Empty the wound dressing pack onto a sterile trolley, avoiding contact with the inner dressing. The biopsy instrument, syringe, needle gauge, scalpel, suture pack and plaster can now be opened and placed on the sheet of the sterile dressing pack (Fig. 1).

3. Pour the surgical scrub into the wound dressing tray and unpackage the Marcain and sterile surgical gloves.
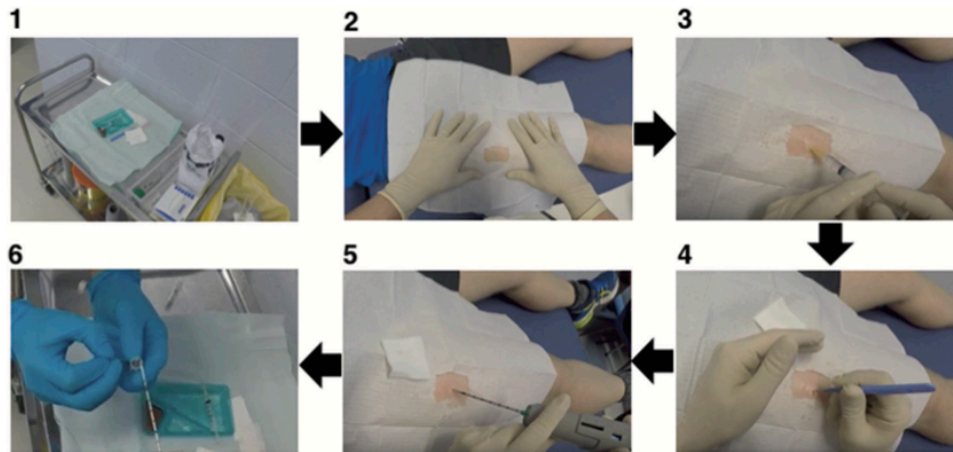
Fig. 1 Depicts (1) removing all packaging of relevant equipment and placing onto a sterile working trolley. (2) Wound dressing sheet placed over the subjects leg with the skin of the biopsy area exposed. (3) Injection of anaesthetic into the deep fascia. (4) Incision of scalpel through the superficial layers and epimysium of the muscle. (5) Insertion of the biopsy needle to obtain muscle tissue which is then (6) transferred to the Eppendorf tube containing transfer medium (4 °C) and submerged in ice

4. Put on the sterile surgical gloves, ensuring the exterior does not make contact with the skin or objects which are non-sterile.

5. Using wound dressing swabs and surgical scrub, wipe the desired biopsy area in order to cleanse the skin. Place the wound dressing sheet/fenestrated drape over the participants leg with the skin of the desired biopsy area exposed (Fig. 1).

6. Assemble the sterile needle and syringe and withdraw the prescribed amount of anesthetic (1.5 ml) ensuring no air bubbles are present. Insert the needle subcutaneously and inject ~50% (~0.75 ml) of until there are signs of peau d'orange (skin resembles orange peel). Insert the needle a little deeper and inject the remaining anesthetic into the deep fascia (Fig. 1) (*see* **Note 17**). To ensure the anesthetic has taken effect (usually ~ 1–2 min post administration), gently apply pressure to the biopsy area with a scalpel (without incision) and ask the participant to verbally confirm a lack of feeling together with numbness.

7. Once anesthetized, using the scalpel, make an incision through the superficial layers and epimysium of the muscle. The tip of the biopsy gun may now be inserted into the wound and muscle tissue may be obtained (Fig. 1). Alternatively, when obtaining muscle tissue using a conchotome instrument, it is important to ensure an incision is made to the fascia to avoid additional pressure and discomfort. You may then insert and rotate (90°) the instrument to cut and extract the muscle tissue [26] (*see* **Note 18**).

279

8. Using a sterile scalpel, scrape the muscle tissue into a sterile tube containing transfer medium (4 °C) and submerge in ice (Fig. 1).

9. Following 2–3 min (needle biopsy instrument) or 5–10 min (conchotome) of applied pressure to stop the bleeding, clean the area using surgical scrub prior to dressing the wound. Once dry, place the steri-strips both horizontally and diagonally across the wound. Finally, cover the wound with a large sterile waterproof dressing. Instruct the participant that he/she should keep the dressing on for 1–2 weeks and should refrain from swimming, especially in open water or in public pools, alongside covering with waterproof film when showering to further reduce risk of infection.

10. The biopsy sample can now be transferred on ice to the class 2 cell culture hood/BSC for subsequent primary cell isolation.

3.2 Human Primary Cell Isolation

1. Using a modified version of methods previously used [27], empty the contents of the sterile tube into an irradiated sterile petri dish and pipette off the transfer medium (*see* **Note 19**). The biopsy sample should then undergo $3 \times$ PBS (preheated to 37 °C) washes and any visible connective and adipose tissue must be removed using a sterile scalpel.

2. Add 5 ml of trypsin-EDTA (preheated to 37 °C) to the sample and mince using two sterile scalpels for at least 1 min.

3. Add the trypsin-EDTA solution and a sterile magnetic stirrer (*see* **Note 1**) to a sterile 100 ml specimen container and place on a heated magnetic stirring platform at 37 °C for 10 min. Alternatively, place the sterile specimen container on a magnetic stirring platform without heating in an oven/incubator set at 37 °C for 10 min.

4. While the sample is digesting, add 1 ml of preheated (37 °C) HS into a separate 15 ml sterile tube. This will neutralize the trypsin in **step 5**.

5. Following 10 mins of heated stirring, remove the trypsin-EDTA solution/supernatant via hand pipetting (*see* **Note 19**) and add to the pre-prepared HS as in **step 4**, leaving the remaining dissected tissue sample in the petri dish. Place the 15 ml tube containing the supernatant and HS into an incubator (37 °C).

6. Add another 5 ml of trypsin-EDTA to the remaining dissected tissue and dissect/mince again for at least 1 min. Place the tissue back on the heated stirrer and repeat as in **step 3.**

7. Once stirred, remove the 5 ml trypsin-EDTA and add to HS/trypsin-EDTA mixture (6 ml) already derived as in **step 5**, yielding approximately 11 ml of solution (1 ml HS and 2×5 ml trypsin-EDTA/supernatant) within the 15 ml tube.

280

8. To isolate the cells from the supernatant, centrifuge the 15 ml tube at $340 \times g$ for 5 min at 24 °C.

9. While in the centrifuge, the remaining tissue in the petri dish should be plated on a pregelatinized T25 flask with 7.5 ml of growth medium to derive any remaining cells using an explant technique from the post enzymatically digested tissue derived above (*see* **Note 20**).

10. Following centrifugation after **step 8** above, a cell pellet should be visible at the bottom of the tube. Carefully remove the top 2.5 ml of supernatant (*see* **Note 19**).

11. Resuspend the next 5 ml of supernatant in 5 ml of fresh growth medium in a separate pregelatinized T25 to enable the culture of the isolated cells (*see* **Note 20**).

12. Finally, resuspend the remaining bottom 2.5 ml of supernatant (including cell pellet) in 7.5 ml of fresh growth medium in a separate pregelatinized T25 to enable the culture of cells derived from the above enzymatic digestion (*see* **Note 20**).

13. Allow cells to culture over the ensuing 5+ days without disturbing or removing from the incubator. Additional growth medium should only be added at 7 days to enable full adherence and maintain any cell secreted factors. Cells should then be monitored frequently to assess cell growth and to avoid cells becoming over-confluent and any unwanted cell fusion. Once 80% confluent, cells can be split into larger T75 flasks to generate enough cells for the creation of fibrin bioengineered skeletal muscle (*see* **Note 21**) dependant on the experimental design and the number of fibrin gels required (*see* Sect. 3.6). Cells can also be cryopreserved for later use (*see* Sect. 3.3 below).

3.3 Cryopreservation of Cells

1. Preheat growth medium (primary or C2C12 culture medium), PBS, and trypsin-EDTA to 37 °C.

2. Once PBS is heated, wash the cells 2–3 times, aspirating/removing PBS after each wash.

3. Add 1 ml of trypsin-EDTA and incubate at 37 °C for 5 min. Gently agitate the cells and visualize down an inverted phase contrast microscope to ensure they have all detached from the plastic culture flask surface.

4. Add 4 ml of growth medium to neutralize the trypsin-EDTA solution. Pool cell solution from all flasks of the same participant (primary) or passage number (C2C12) and add to a sterile tube (e.g., 15 ml or 50 ml). Homogenize cell solution slowly (*see* **Note 22**).

5. Count cells using preferred method (i.e. manually using a hemocytometer or electronically using an automated cell counter) and dilute solution to 1×10^6 cells/ml using fresh growth medium.

6. Pool solution into a sterile 100 ml specimen container or 50 ml tube and add 10% DMSO (*see* **Note 23**) to prevent formation of ice crystals.

7. Once resuspended, pipette 2 ml of cell solution per prelabeled cryovial (name, cell type, passage number, cell density, and date) and place into a cryopreservation freezer container (i.e. "Mr frosty") filled with isopropanol to ensure a gradual (~1 °C/min) decrease in temperature, further reducing the likelihood of ice crystal formation.

8. Place the cells into a −80 °C freezer for 24 h prior to storing cells in liquid nitrogen.

3.4 Resuscitation of Cryopreserved Cells

1. Preheat growth medium to 37 °C and gelatinize a T25 (primary cells) or T75 (C2C12 cells) flask per vial.

2. Remove the cryovial(s) from the liquid nitrogen Dewar and thaw at room temperature (C2C12 cells) or within an incubator at 37 °C (primary cells).

3. For C2C12 cells, seed cell suspension onto the pregelatanized T75 flask(s) and add 10 ml of growth medium per flask. Gently agitate to ensure even distribution across the culture flask surface and place in an incubator (37 °C) to allow cells to grow to 80% confluency over the ensuing days (typically 72 h).

4. For primary cells, transfer cell suspension into a sterile 15 ml tube and centrifuge at $200 \times g$ for 10 min.

5. Remove supernatant and resuspend cell suspension and 6 ml of growth medium onto the pregelatinized T25 flask.

6. Once 80% confluent, resuspend primary cells onto a T75 flask and passage until the desired cell population is attained (*see* **Note 21**).

3.5 Preparation of 3-D Culture Dishes

1. Sylgard coat dishes according to the manufacturer's instructions. Briefly, on a covered surface, add curing agent to elastomer and stir to ensure a consistent silicone solution (*see* **Note 4**). Using a syringe (without needle), add 1.5 ml of silicone to each dish. Allow coated dishes to cure for approximately 24 h. Once cured, replace lids and store for at least 1 week prior to using for muscle cultures (*see* **Note 24**).

2. Prepare 4×0.15 mm minutien pins and 2×6 mm silk sutures per dish (*see* **Notes 5** and **6**).

3. Using a "fine point" sharpie and ruler, mark the 6, 12, 18, 24, 30 mm points across the center of each dish (*see* **Note 25**).
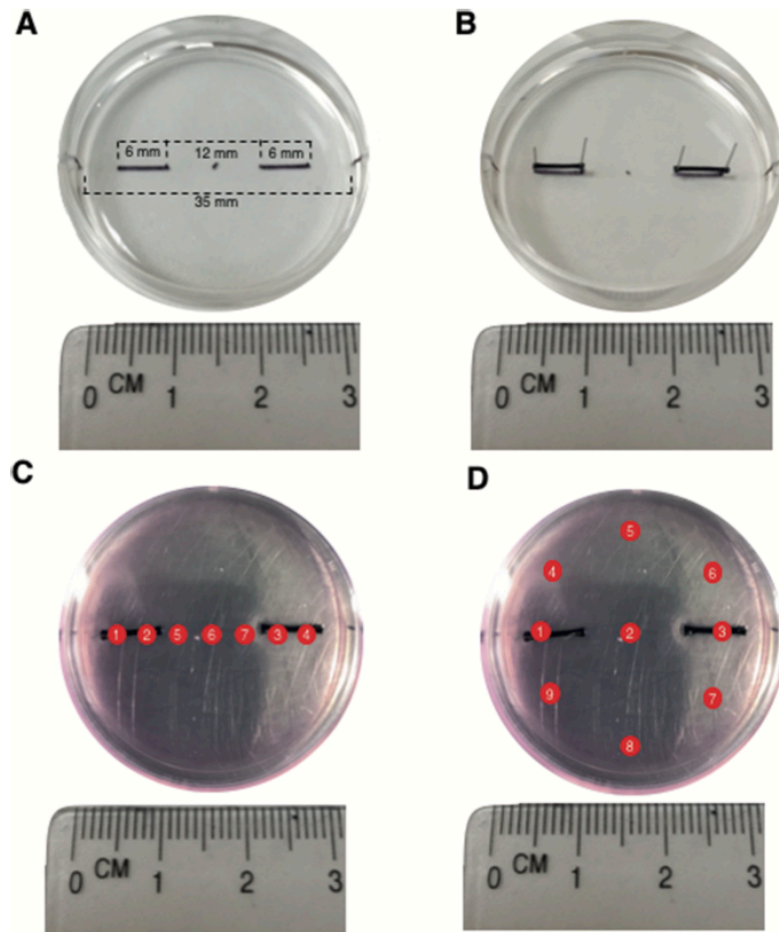
Fig. 2 Depicts (**A**) marked sylgard coated 3-D culture dish with (**B**) silk sutures pinned in place. (**C**) Depicts thrombin solution placement to ensure sutures are saturated and (**D**) indicates pipetting fibrinogen dropwise prior to gentle agitation to ensure even distribution across the cell culture dish surface

Mark a line between the 6–12 and 24–30 mm points to ensure accurate silk suture alignment when pinning in place (Fig. 2).

4. Align silk sutures between 6–12 and 24–30 mm points and pin in place ensuring a 12 mm gap in-between (Fig. 2).

5. Following preparation of 3-D culture dishes, thoroughly spray the inside of the lid and culture dish with 70% immersed methylated spirit (IMS)/ethanol and leave in a Class 2 cell culture hood/BSC under UV to sterilise and air dry overnight (*see* **Note 26**).

283
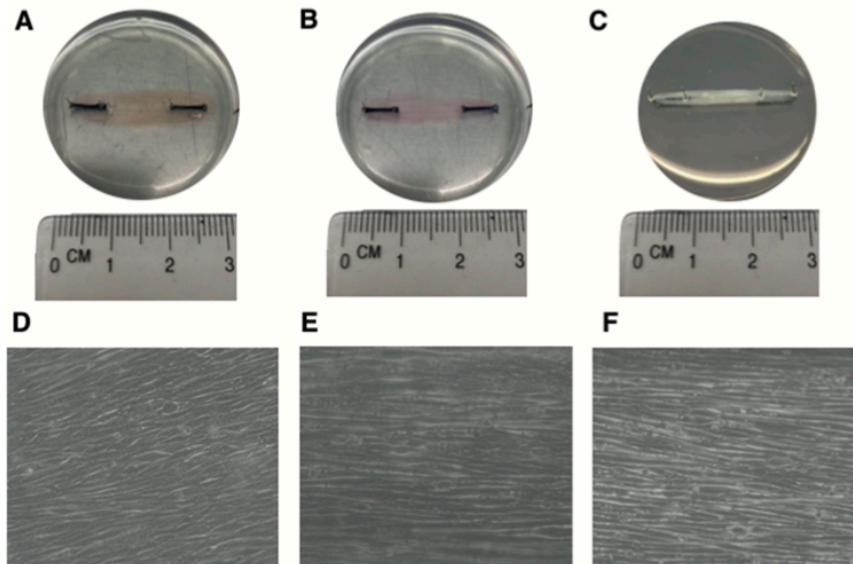
Fig. 3 Macroscopic images of C2C12 3-D fibrin muscle constructs at (**a**) 3 days (**b**) 7 days and (**c**) 14 days in culture. (**d**–**f**) depict microscopic bright field images (10 × magnification) at 3, 7 and 14 days, respectively

3.6 Preparation and Maintenance of Fibrin Skeletal Muscle Constructs

1. Before proceeding, ensure all 3-D culture dishes, relevant reagents, medium and cells are prepared as described above. For each fibrin muscle construct, thaw 50 μl/ml thrombin, 8 μl/ml aprotinin (*see* **Note 27**), 20 μl/ml genipin (*see* **Note 13**) and 200 μl fibrinogen at room temperature while cell suspension is incubating at 37 °C. Growth medium for thrombin solution should also reach room temperature prior to using.

2. Add thrombin, aprotinin and genipin (*see* **Note 13**) to growth medium to ensure 500 μl of solution per gel (*see* **Notes 27** and **28**).

3. Coat dishes with 500 μl of thrombin/aprotinin/genipin gel solution (*see* **Note 29**) (Fig. 2).

4. Add 200 μl of fibrinogen dropwise around the culture dishes and agitate gently to ensure even distribution with the thrombin solution (Fig. 2).

5. Allow the fibrin gel to polymerize at room temperature for 10 mins prior to incubating at 37 °C for 1 h.

6. Following polymerization, seed 2 ml cell suspension per dish consisting of 100,000–200,000 cells/ml (primary [10]) or 50,000–90,000 cells/ml (C2C12) in growth medium (*see* **Note 30**).
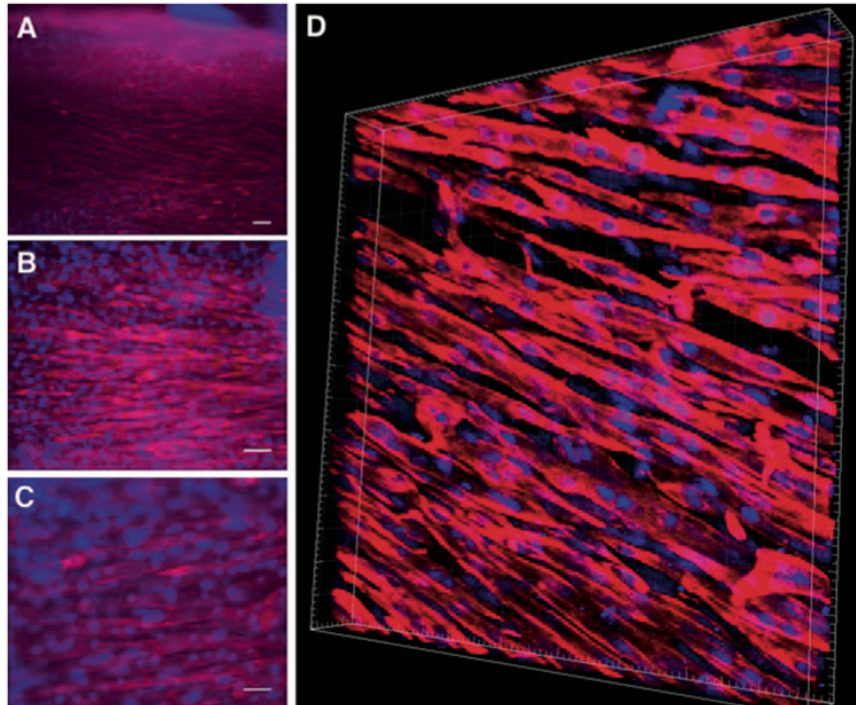
Fig. 4 Immuno-stained microscopic (Nikon, Eclipse Ti-S) images of C2C12 3-D fibrin constructs at (**a**) 10 × (scale bar = 50 µm) (**b**) 20 × (scale bar = 20 µm) and (**c**) 40 × (scale bar = 20 µm) magnification. (**d**) *Z*-stack animated confocal (Olympus, IX83) microscopic image (40 × magnification). Constructs were stained for desmin (red) and nuclei (blue)

7. Gently agitate culture dishes and place in the incubator at 37 °C. Growth medium should be changed every 48 h until cells reach ~90% confluency (Fig. 3).

8. Once approximately 90% confluent, aspirate remaining growth medium and 3× PBS wash (*see* **Note 31**).

9. Transfer to 2 ml of preheated (37 °C) differentiation medium and incubate at 37 °C for 48 h (*see* **Notes 31** and **32**).

10. Remove differentiation media and wash cells as in **step 8** (*see* **Note 31**), transfer to 2 ml of maintenance medium, and incubate at 37 °C (*see* **Note 33**). Be sure to wash cells as in **step 8** (*see* **Note 31**) and top up or change maintenance medium (*see* **Note 34**) for 14 days to allow constructs to mature (Figs. 3 and 4). The gel will contract from the edge of the dish and roll into a cylindrical-like muscle whereby multinucleated myotubes will form in aligned and parallel fashion in line with the direction of the sutures (Figs. 3 and 4).

3.7 From the Culture Dish to the Bioreactor

1. Preheat maintenance medium to 37 °C.

2. Remove bioreactor chamber(s) and parts (screws, clamps, etc.) from the autoclave bag and assemble the bottom the clamps.

3. Manually adjust the distance between the medial edge of each clamp to ensure a 12 mm gap (*see* **Note 35)** and tighten to prevent any unwanted change in resting length.

4. Using sterile angled tweezers (*see* **Note 1**), remove pins from the culture dish and transfer the muscle construct (leaving sutures in if possible) from the cell culture well/dish to the bioreactor chamber(s) (*see* **Notes 16**, **35–37**).

5. Avoiding any stretching or twisting of the muscle construct, clamp the medial end of each suture embedded within either side of the construct (*see* **Notes 36** and **37**).

6. Submerge the clamped construct(s) with 20 ml of maintenance medium by pipetting into the bioreactor chamber(s) (*see* **Notes 31** and **38)**.

7. The muscle construct is now ready to undergo electrical and/or mechanical stimulation.

3.8 Bioreactor Setup

1. Ensure enough free bench space to position all bioreactor equipment (Fig. 5).

2. Connect electrical stimulation and control modules to the mains power supply (ensure the mains is switched off until all other equipment is connected).

3. Connect laptop/desktop, mechanical stimulation box, and electrical stimulation output box to the control module.

4. Connect neutral, anode (+ve), and cathode (−ve) from the electrical stimulation module to the electrical stimulation output box.

5. Connect the anode/cathode splitter to the electrical stimulation output box.

6. Feed electrodes through bioreactor chamber(s) and connect to the anode/cathode splitter (*see* **Notes 39** and **40**) (Fig. 6).

7. Attach bioreactor chamber(s) to mechanical stimulation unit, ensuring the resting length (12 mm) is maintained (*see* **Note 41**).

8. Once assembled, loosen the tension of the chamber (s) mechanical arm to permit movement when initiating the mechanical stretch regime.

3.9 Electrical and Mechanical Stimulation

1. Open the "Ebers TC-3 with Electrical Stimulation" software from the desktop/application menu.

2. From the "port settings" dropdown menu, ensure the control module is connected to the device containing the controlling software in order to proceed ("COM3").
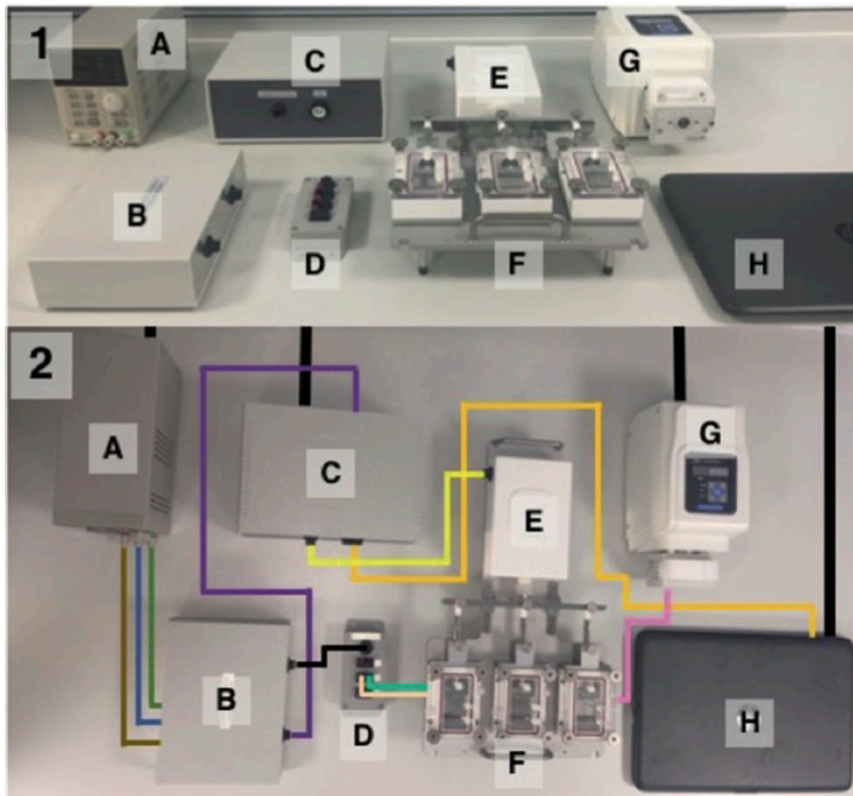
Fig. 5 (**1**) Frontal and (**2**) bird's-eye view of the TC-3 Bioreactor System, (EBERS Medical Technology, ESP) including the (**A**) electrical stimulation module, (**B**) electrical stimulation output box, (**C**) control module, (**D**) electrode anode/cathode splitter, (**E**) bioreactor mechanical stimulation box, (**F**) bioreactor 3-D cell culture chamber, (**G**) peristaltic pump/perfusion box, (**H**) laptop and controlling software. Image and figure legend adapted from [28] with permission from Wiley

3. Click "start" from the "manual mode" panel until the mechanical stretch arm reaches the desired resting length.

4. Click "stop" and "Set to 0" to confirm the starting length. It is at this point you may loosen the tension of the mechanical stretch arm as the chamber should be securely attached to the mechanical stimulation unit (*see* **Note 41**).

5. From the "program mode" panel, select the desired "Run (seconds; s)" and "Pause (seconds; s)" duration, the "ramp mode" and whether you would like the regime to "cycle" (Fig. 7).

6. Navigate to the "record number" to alter "velocity mode" and "frequency mode" settings (Fig. 7).

7. From the "velocity mode" function, the desired stretch limit/ "travel" (millimeters; mm), direction (backward/forward),

287
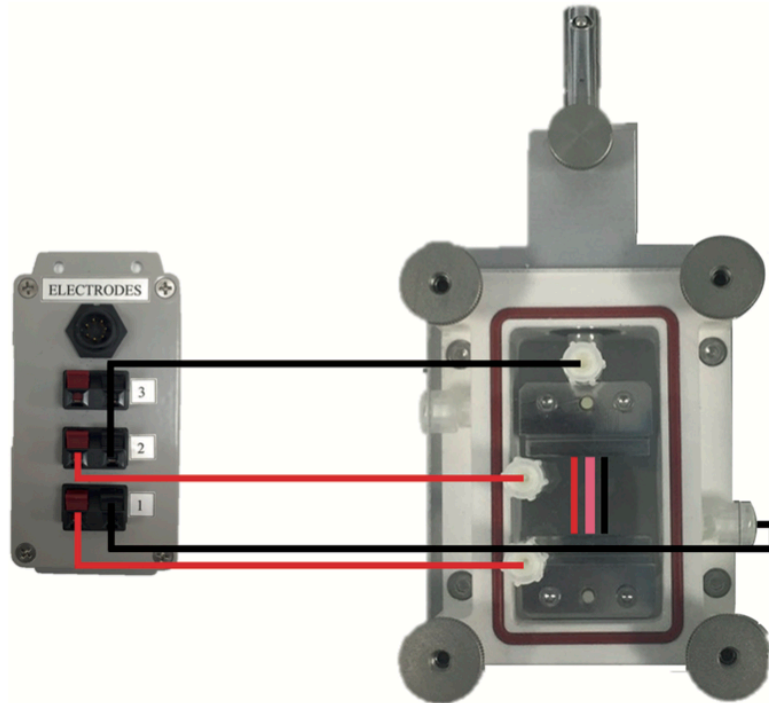
Fig. 6 Electrode placement for electrical stimulation. Anode (red) and cathode (black) pathways to the electrical anode/cathode splitter using platinum or stainless steel wire running parallel to the clamped muscle construct (pink)
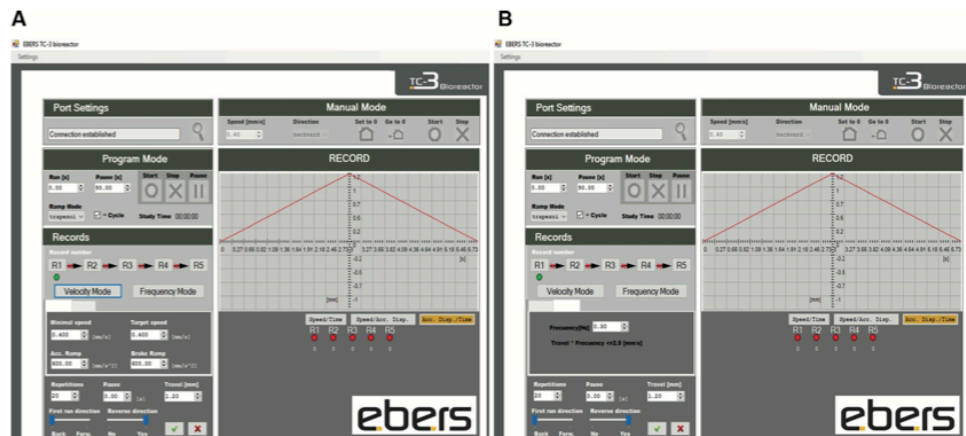
Fig. 7 Ebers TC-3 Software. Mechanical stretch navigation menu for adjusting (**a**) velocity and (**b**) frequency mode settings
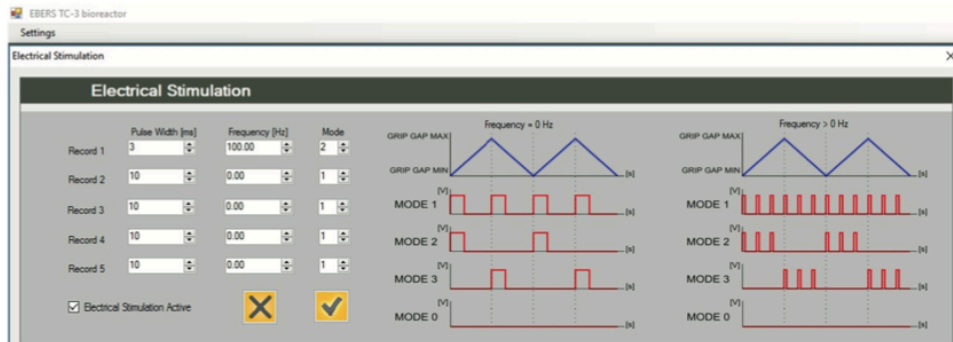
Fig. 8 Ebers TC-3 Software. Electrical stimulation navigation menu for adjusting pulse width (ms), frequency (Hz) and "MODE"

"minimal/target speed" (millimeters per second; mm/s) and "acceleration/brake ramp" (millimeters per second squared; mm/s^2) can be altered (Fig. 7; *see* **Note 42**).

8. From the "frequency mode" function, the stretch frequency (hertz; Hz) can be altered. Click the "green tick" to confirm the desired mechanical stretch regime (*see* **Note 42**).

9. To adjust the electrical stimulation protocol, navigate to the "electrical stimulation" function from the "settings" drop-down menu. Here, single impulses or pulse trains can be applied during the "forward" (when the muscle returns to its' resting length; MODE 3), "backward" (when the muscle is lengthening to reach the desired stretch limit; MODE 2), forward and backward movements combined (MODE 1) or at "rest" (MODE 0) (*see* **Notes 43** and **44**; Fig. 8).

10. Set the desired pulse width (milliseconds; ms), frequency (Hertz; Hz), amplitude (voltage; V), pulse train (seconds; s) and "MODE" number (*see* **Note 44**).

11. Confirm the desired electrical stimulatory parameters via clicking the "Electrical Stimulation Active" option followed by the tick option on screen (Fig. 8).

12. Following cessation of the mechanical and/or electrical stimulatory regime, click "stop" and lock the bioreactor chamber(s) stretch arm.

13. Ensure the electrical stimulation module is switched off at the mains and disconnect the electrodes from the anode/cathode splitter.

14. Place the chamber(s) in the incubator at 37 °C and incubate for the desired postexercise period.

15. Remove chamber(s) from the incubator and place in a sterile Class 2 cell culture hood.

289

16. Remove the clamps using sterile tools (*see* **Note 1**) and transfer the stimulated fibrin muscle using sterile tweezers (*see* **Notes 1 and 16**) for your desired sample preparation. For RNA/DNA/ protein isolation we recommend homogenization in tubes containing MagNA Lyser Green Beads (submerged in the relevant lysis buffer) in a MagNA tissue Lyser for 6,000 rpm × 40 s (with 5 min rest on ice in between each cycle), and repeated 3 times.

17. Ensure all equipment is switched off and all working areas are thoroughly cleaned.

18. Ensure to package bioreactor chamber(s), relevant parts (clamps and screws) and tools and sterilise for future use (*see* **Note 1**).

4 Notes

1. Sterilize via autoclaving (e.g., 122 °C for 30 min).

2. hiFBS and hiNBCS are purchased from South America (EU approved) and New Zealand. It is also important to use serum from the same origin due to disparities in hormonal milieu (hiFBS from US vs. EU origin) which may alter the engineered muscle phenotype [29].

3. Use gelatin from porcine skin A (and not B) given that gelatin B may negatively affect skeletal muscle cell growth.

4. Pour curing agent into Sylgard, mixing thoroughly from side-to-side as well as top-to-bottom to guarantee curing when coating the culture dishes (it is normal for small bubbles to appear when mixing). It is also important to syringe (without a needle) Sylgard onto the culture dishes as soon as possible followed by agitation to ensure even distribution.

5. Cut pins in half to enable replacement of culture dish lids. There is no required length of pins, as long as the lid can be replaced.

6. Cut silk suture thread to 6 mm lengths. Using a disposable scalpel is preferable as using scissors causes greater incidence of fraying.

7. Dissolve 1 g of fibrinogen in 50 ml of Ham's F12-K medium to ensure enough reagent for approximately 250 fibrin gels given 200 μl is required per fibrin muscle construct.

8. It is suggested to filter fibrinogen through a 0.22 μm large vacuum filter as fibrinogen blocks the filter membranes when using 0.22 μm syringe filters.

9. Do not freeze-thaw.

10. Thrombin can be purchased as 1KU containing 27 mg. Therefore, there are approximately 37 units per mg, totalling 999 units. Each 1KU should therefore provide enough reagent for 200 fibrin gels at 10 U/ml when diluted with growth medium given 25 μl is required per fibrin muscle construct.

11. 6-Aminocaproic acid inhibits plasmin activity and subsequent fibrinolysis [30] induced by high levels of plasminogen by C2C12 myoblast cells. Overall use and specific concentration should therefore depend on the occurrence and rate of fibrinolysis since plasminogen is also required for muscle cell differentiation [31, 32]. It is suggested to culture without at first and then add 0.5% (final conc. 0.25 mg/ml) to growth medium, 1% (final conc. 0.5 mg/ml) to differentiation medium and 1% (final conc. 0.5 mg/ml) to maintenance medium if the fibrin matrix is degrading. If these concentrations do not reduce fibrinolysis, attempt to increase the concentrations to those described herein.

12. The amino acid L-proline and cofactor L-ascorbic acid (vitamin C) may encourage the production of ECM proteins in primary cultures, such as collagen and improve engineered musculoskeletal mechanics [33]. Use should therefore depend on the occurrence and rate of fibrin degradation. They are not always required if the gels are not degrading.

13. Genipin slows fibrin matrix degradation rates however at the expense of reduced force production [18]. Genipin also autofluoresces, negatively affecting any fluorescent/confocal microscopy performed and subsequent morphological analysis [18]. Therefore, its use should be determined by the most important dependant variables of interest within individual experiments.

14. Depending on the desired experimental measures, perhaps refrain from using streptomycin given the resultant alterations in force production and muscle phenotype following electrical stimulation [34, 35].

15. The TC-3 bioreactor system (Ebers Medical Technology, ESP) described herein is a commercially available, easy-to-use bioreactor system that permits simultaneous mechanical and electrical stimulation according to software amendments (*see* **Note 41**). Although the protocol described herein is specific to using the TC-3 bioreactor system, the principles remain the same if using customized/other commercially available bioreactor systems that enable similar stimulatory regimes.

16. Holding both sets of angled tweezers in one hand for simultaneous opening and closing permits greater control when transferring the muscle construct from the culture wells into the bioreactor chamber(s).

291

17. Local anesthetic, particularly bupivacaine are considered to induce myotoxic effects [36] which may be attributable to increased intracellular calcium release with simultaneous inhibition of calcium reuptake into the sarcoplasmic reticulum [37]. Inclusion and/or selection of local anesthetic should therefore be determined by the most important dependant variables of interest within individual experiments.

18. A needle biopsy yields 20–30 mg whereas a conchotome biopsy can yield 100–250 mg of skeletal muscle tissue. If conducting a needle biopsy, you may require multiple passes. Therefore, use the sterile wound dressing kit to wipe and clear the biopsy area before proceeding with the next pass of a needle biopsy in order to reduce risk of infection.

19. Hand pipette as opposed to vacuum aspirate to ensure greater control.

20. If the enzymatic digestion technique is successful, there are typically a low number of cells that grow from the remaining explanted tissue over the ensuing days. If so, dispose of the remaining explanted tissue according to the relevant legislations, (e.g. in the UK, the Human Tissue Act, 2004).

21. Primary human skeletal muscle derived cells start to senesce after several passages. Some may senesce even after 5–8 passages in-vitro depending on the age of the donor. This is because their drive in-vivo is to undergo a few rounds of proliferation only before fusing to fibers to repair/regenerate the fiber. Cells will still fuse once senescent but this may affect their initial growth when expansion/proliferation is required for the initial stage of making a self-assembling fibrin bioengineered muscle. Therefore, this should be a consideration when determining participant number, expected cell retrieval and the number of fibrin bioengineered constructs required to suit the experimental design of the study.

22. Homogenize suspension via pipetting up and down prior to resuspending.

23. Pipette DMSO down the side of the specimen container/tube in a dropwise manner while simultaneously swirling/mixing the solution in the tube.

24. It is best to allow sylgard spillages on bench surfaces to completely dry before removing using a gel scraper (or similar) and wiping.

25. Usually, there are lined marks on either side of the dish indicating the center line. Therefore, holding a ruler in line with these points when marking ensures accurate suture alignment when pinning in place.

26. Plates may only require 30 mins of sterilization to remove visible ethanol; however, it is likely that the sutures will still be saturated in ethanol. Therefore, air drying overnight is preferable.

27. Concentration of the protease inhibitor aprotinin should be optimized according to the rate of fibrinolysis (degradation of fibrin). Since the C2C12 myoblast cell line produces high levels of plasminogen and matrix metalloproteinases, we suggest adding 8 μl/ml of aprotinin to the thrombin solution. However, when using human skeletal muscle derived cells that contain a proportion of fibroblasts within the myoblast population that lay down additional matrix, we suggest reducing concentrations to 4 μl/ml.

28. Prepare sufficient excess thrombin gel solution for an additional gel (every 10 fibrin gels) to compensate for any potential minor pipetting error or loss of residual solution from the outside of pipette tips.

29. To ensure consistency between gels, pipette the thrombin solution along the sutures (outside to inside) and then across the center to join both sutures. Next, tilt the dish horizontally along the line of the sutures. Once the solution makes contact with both edges of the dish, rotate the dish in a circular motion so the solution now covers the entire edge of the dish. Resting the base of the dish on the culture hood surface, gently agitate to ensure even distribution across the dish surface (Fig. 2). It is important any bubbles appearing during this process are carefully removed, popping with a sterile syringe needle if required.

30. It is essential that cells are spread evenly across the dish to ensure consistent growth and attachment of the cells in a uniform fashion. We recommend adding 2 ml of cell suspension at 200,000 cells/ml for primary human gels [10] and 90,000 cells/ml for C2C12 gels.

31. Avoid pipetting PBS or media directly onto the fibrin gel in attempt to reduce cell disruption and potential tearing of the gel.

32. Gels are changed to lower serum to enable fusion/differentiation of single cells to form multinucleated myotubes.

33. Cells are switched from low serum (2% HS) differentiation medium to higher serum (7% hiFBS/hiNBCS) maintenance medium to reduce likelihood of gel degradation. Cells will continue to fuse and myotubes mature when under tension within the bioengineered system while in the presence of 7% serum in the medium.

34. Cells must be provided with sufficient nutrients to promote maturation and reduce the risk of gel degradation. Maintenance medium is changed following 2× PBS washes every

48 h. However, 0.5 ml of fresh medium is added on days where medium is not changed to help maintain any secreted factors by the cells that may promote differentiation and myotube hypertrophy.

35. Loosen the tension on the bioreactor chamber(s) arm to enable adjustment. Using a ruler, ensure a 12 mm gap between the medial edges of both clamps and tighten the bioreactor chamber(s) arm to avoid any unwanted changes in resting length.

36. Using the Ebers TC-3 bioreactor (Ebers Medical Technology, ESP), it is possible to mechanically load × 3 muscle constructs per chamber, totalling 9 muscle constructs per single regime (across 3 × chambers). However, the electrical stimulation setup described herein permits stimulation of just one muscle construct per chamber due to the space required for electrode wiring.

37. If the sutures are removed from the muscle construct during the transferring process, it is important to ensure the amount of muscle clamped at either side is the same. Ideally all other constructs in the same experiment would then be treated in this way, or that gel removed from the experiment.

38. If stimulating engineered muscle constructs in the absence or presence of specific nutrients (e.g. amino acids) according to the desired experimental measures, immersing constructs in Krebs Ringer HEPES (KRH) buffer rather than maintenance medium may be preferable. For Krebs-Ringer-HEPES (KRH) buffer at pH 7.4 ($10\times$): 10 mM HEPES, 138 mM NaCl, 4.7 mM KCl, 1.25 mM CaCl$_2$, 1.25 mM MgSO, 5 mM Glucose and 5 mg/ml bovine serum albumin (BSA) diluted in dH$_2$0.

39. Use rounded plyers to bend electrodes and feed through the culture chamber(s) to ensure electrodes run parallel with the muscle construct (Fig. 6).

40. For health and safety reasons, purchase electrode wire surrounded with plastic coating or self-coat with only the portion assembled through the bioreactor chamber(s) being exposed.

41. Attach the bottom of the bioreactor chamber(s) to the mechanical stretch unit, ensuring each chamber is slightly tilted (approximately 45°). Manually adjust the mechanical stretch unit arm onscreen using the "start" function until the mechanical arm attached to the bioreactor chamber(s) clicks in place. Click "stop" and "set to 0" to set the starting position.

42. Example Mechanical Stretch Regimes:
    - Cyclic stretch (1 cycle = 3 sets × 5 reps, each set interspersed with ~30 s rest). Undertake these cycles with 5% strain for 2 days, 10% strain for 2 days, and 15% strain for

4 days in an attempt to model progressive overload that has been demonstrated to evoke myotube hypertrophy [23].

- Static stretch, where the construct is stretched to 10% quickly (e.g., 0.4 mm/s resulting in 1.2 mm stretch of a 1.2 cm fibrin muscle after 3 s) and held at 10% stretch for 1 h to provide a model that would be most similar to synergistic ablation [22, 38].

- Continuous ramp load at 0.35 mm/h, which is the same rate at which stretch stimulates in-vivo bone elongation during development [9].

- 10% intermittent stretch − (1 interval = 4 sets × 10 reps at 0.4 mm/s during stretch and return to resting length, resulting in 1.2 mm stretch of a 1.2 cm fibrin muscle in 3 s and a return to resting length after 3 s, with each set interspersed with 90 s rest). Each interval is separated by 3.5 min rest and repeated, e.g., 3–5 times in an attempt to replicate a similar number of repetitions performed during a typical in-vivo bout of resistance type exercise that evokes hypertrophy (e.g., 4 sets × 10 reps × 3–5 exercises per muscle group).

43. Initially, only mechanical stretch or electrical stimulation could be applied at a given time. Specifically, a single pulse could only be applied when the desired stretch limit was attained or when at the initial resting position. Therefore, we liaised with the manufacturer (Ebers Medical Technology, ESP) regarding potential software (TC-3) modifications that would enable simultaneous electrical and mechanical stimulation to the 3D fibrin muscle constructs Ebers proceeded with the requested amendments, with the TC-3 bioreactor now permitting the application of pulse trains (rather than a single pulse at maximal stretch or at resting length) for continuous synchronized impulses during the whole mechanical cycle (Fig. 8). Furthermore, the bioreactor system now also permits the use of an external electrical stimulator for synchronization of mechanical stretch and electrical stimulation, providing a fail-safe if the internal stimulation box was to stop working but also enabling the use of more powerful or in-house stimulators in the future for higher sustained/repetitive pulse frequencies.

44. Example Electrical Stimulation Regimes:
- Chronic low-frequency stimulation (CLFS) to evoke slow fiber formation (pulse frequency = 10 Hz; contraction duration = 60–600 s, adjusting rest intervals to ensure 60% active time, changing medium every 24 h and continue for a 14 day period) [39].

- Higher frequency stimulatory regime to more closely mimic a more forceful contraction (pulse frequency = 100 Hz;

295

amplitude = 2.5 V/mm; 4 × 0.1 ms pulses delivered in a 400 ms pulse train followed by 3.6 s recovery) and repeated the desired number of times to mimic, e.g., resistance exercise in-vivo [5].

References

1. Brevet A, Pinto E, Peacock J, Stockdale FE (1976) Myosin synthesis increased by electrical stimulation of skeletal muscle cell cultures. Science 193(4258):1152–1154

2. Wehrle U, Dusterhoft S, Pette D (1994) Effects of chronic electrical stimulation on myosin heavy chain expression in satellite cell cultures derived from rat muscles of different fiber-type composition. Differentiation 58 (1):37–46. https://doi.org/10.1046/j.1432-0436.1994.5810037.x

3. Vandenburgh H, Kaufman S (1979) In vitro model for stretch-induced hypertrophy of skeletal muscle. Science 203(4377):265–268

4. Baar K, Torgan CE, Kraus WE, Esser K (2000) Autocrine phosphorylation of p70(S6k) in response to acute stretch in myotubes. Mol Cell Biol Res Commun 4(2):76–80. https://doi.org/10.1006/mcbr.2000.0257

5. Donnelly K, Khodabukus A, Philp A, Deldicque L, Dennis RG, Baar K (2010) A novel bioreactor for stimulating skeletal muscle in vitro. Tissue Eng Part C Methods 16 (4):711–718. https://doi.org/10.1089/ten.TEC.2009.0125

6. Nedachi T, Fujita H, Kanzaki M (2008) Contractile C2C12 myotube model for studying exercise-inducible responses in skeletal muscle. Am J Physiol Endocrinol Metab 295(5): E1191–E1204. https://doi.org/10.1152/ajpendo.90280.2008

7. Nikolic N, Bakke SS, Kase ET, Rudberg I, Flo Halle I, Rustan AC, Thoresen GH, Aas V (2012) Electrical pulse stimulation of cultured human skeletal muscle cells as an in vitro model of exercise. PLoS One 7(3):e33203. https://doi.org/10.1371/journal.pone.0033203

8. Vandenburgh HH (1988) A computerized mechanical cell stimulator for tissue culture: effects on skeletal muscle organogenesis. In Vitro Cell Dev Biol 24(7):609–619

9. Vandenburgh HH, Karlisch P (1989) Longitudinal growth of skeletal myotubes in vitro in a new horizontal mechanical cell stimulator. In Vitro Cell Dev Biol 25(7):607–616

10. Martin NR, Passey SL, Player DJ, Khodabukus A, Ferguson RA, Sharples AP, Mudera V, Baar K, Lewis MP (2013) Factors affecting the structure and maturation of human tissue engineered skeletal muscle. Biomaterials 34(23):5759–5765. https://doi.org/10.1016/j.biomaterials.2013.04.002

11. Sharples AP, Player DJ, Martin NR, Mudera V, Stewart CE, Lewis MP (2012) Modelling in vivo skeletal muscle ageing in vitro using three-dimensional bioengineered constructs. Aging Cell 11(6):986–995. https://doi.org/10.1111/j.1474-9726.2012.00869.x

12. Dennis RG, Kosnik PE 2nd (2000) Excitability and isometric contractile properties of mammalian skeletal muscle constructs engineered in vitro. In Vitro Cell Dev Biol Anim 36 (5):327–335. https://doi.org/10.1290/1071-2690(2000)036<0327:eaicpo>2.0.co;2

13. Dennis RG, Kosnik PE 2nd, Gilbert ME, Faulkner JA (2001) Excitability and contractility of skeletal muscle engineered from primary cultures and cell lines. Am J Physiol Cell Physiol 280(2):C288–C295

14. Huang YC, Dennis RG, Baar K (2006) Cultured slow vs. fast skeletal muscle cells differ in physiology and responsiveness to stimulation. Am J Physiol Cell Physiol 291(1): C11–C17. https://doi.org/10.1152/ajpcell.00366.2005

15. Huang YC, Dennis RG, Larkin L, Baar K (2005) Rapid formation of functional muscle in vitro using fibrin gels. J Appl Physiol 98 (2):706–713. https://doi.org/10.1152/japplphysiol.00273.2004

16. Martin NR, Passey SL, Player DJ, Mudera V, Baar K, Greensmith L, Lewis MP (2015) Neuromuscular junction formation in tissue-engineered skeletal muscle augments contractile function and improves cytoskeletal organization. Tissue Eng Part A 21 (19–20):2595–2604. https://doi.org/10.1089/ten.TEA.2015.0146

17. Khodabukus A, Baar K (2012) Defined electrical stimulation emphasizing excitability for the development and testing of engineered skeletal muscle. Tissue Eng Part C Methods 18 (5):349–357. https://doi.org/10.1089/ten.TEC.2011.0364

18. Khodabukus A, Baar K (2009) Regulating fibrinolysis to engineer skeletal muscle from the C2C12 cell line. Tissue Eng Part C

Methods 15(3):501–511. https://doi.org/10.1089/ten.TEC.2008.0286

19. Cheng CS, Ran L, Bursac N, Kraus WE, Truskey GA (2016) Cell density and joint microRNA-133a and microRNA-696 inhibition enhance differentiation and contractile function of engineered human skeletal muscle tissues. Tissue Eng Part A 22(7–8):573–583. https://doi.org/10.1089/ten.TEA.2015.0359

20. Shahini A, Choudhury D, Asmani M, Zhao R, Lei P, Andreadis ST (2017) NANOG restores the impaired myogenic differentiation potential of skeletal myoblasts after multiple population doublings. Stem Cell Res 26:55–66. https://doi.org/10.1016/j.scr.2017.11.018

21. Khodabukus A, Baar K (2015) Contractile and metabolic properties of engineered skeletal muscle derived from slow and fast phenotype mouse muscle. J Cell Physiol 230 (8):1750–1757. https://doi.org/10.1002/jcp.24848

22. Player DJ, Martin NR, Passey SL, Sharples AP, Mudera V, Lewis MP (2014) Acute mechanical overload increases IGF-I and MMP-9 mRNA in 3D tissue-engineered skeletal muscle. Biotechnol Lett 36(5):1113–1124. https://doi.org/10.1007/s10529-014-1464-y

23. Powell CA, Smiley BL, Mills J, Vandenburgh HH (2002) Mechanical stimulation improves tissue-engineered human skeletal muscle. Am J Physiol Cell Physiol 283(5):C1557–C1565. https://doi.org/10.1152/ajpcell.00595.2001

24. Yaffe D, Saxel O (1977) Serial passaging and differentiation of myogenic cells isolated from dystrophic mouse muscle. Nature 270 (5639):725–727

25. Blau HM, Pavlath GK, Hardeman EC, Chiu CP, Silberstein L, Webster SG, Miller SC, Webster C (1985) Plasticity of the differentiated state. Science 230(4727):758–766

26. Patel HP, Syddall HE, Martin HJ, Stewart CE, Cooper C, Sayer AA (2010) Hertfordshire sarcopenia study: design and methods. BMC Geriatr 10:43. https://doi.org/10.1186/1471-2318-10-43

27. Crown AL, He XL, Holly JM, Lightman SL, Stewart CE (2000) Characterisation of the IGF system in a primary adult human skeletal muscle cell model, and comparison of the effects of insulin and IGF-I on protein metabolism. J Endocrinol 167(3):403–415

28. Kasper AM, Turner DC, Martin NRW, Sharples AP (2018) Mimicking exercise in three-dimensional bioengineered skeletal muscle to investigate cellular and molecular mechanisms of physiological adaptation. J Cell Physiol 233 (3):1985–1998. https://doi.org/10.1002/jcp.25840

29. Khodabukus A, Baar K (2014) The effect of serum origin on tissue engineered skeletal muscle function. J Cell Biochem 115 (12):2198–2207. https://doi.org/10.1002/jcb.24938

30. Adelman B, Rizk A, Hanners E (1988) Plasminogen interactions with platelets in plasma. Blood 72(5):1530–1535

31. Lopez-Alemany R, Suelves M, Munoz-Canoves P (2003) Plasmin generation dependent on alpha-enolase-type plasminogen receptor is required for myogenesis. Thromb Haemost 90(4):724–733. https://doi.org/10.1160/th03-04-0291

32. Suelves M, Lopez-Alemany R, Lluis F, Aniorte G, Serrano E, Parra M, Carmeliet P, Munoz-Canoves P (2002) Plasmin activity is required for myogenesis in vitro and skeletal muscle regeneration in vivo. Blood 99 (8):2835–2844

33. Paxton JZ, Grover LM, Baar K (2010) Engineering an in vitro model of a functional ligament from bone to bone. Tissue Eng Part A 16 (11):3515–3525. https://doi.org/10.1089/ten.TEA.2010.0039

34. Khodabukus A, Baar K (2015) Glucose concentration and streptomycin alter in vitro muscle function and metabolism. J Cell Physiol 230 (6):1226–1234. https://doi.org/10.1002/jcp.24857

35. Khodabukus A, Baar K (2015) Streptomycin decreases the functional shift to a slow phenotype induced by electrical stimulation in engineered muscle. Tissue Eng Part A 21 (5–6):1003–1012. https://doi.org/10.1089/ten.TEA.2014.0462

36. Zink W, Sinner B, Zausig Y, Graf BM (2007) Myotoxicity of local anaesthetics: experimental myth or clinical truth? Anaesthesist 56 (2):118–127. https://doi.org/10.1007/s00101-006-1121-5

37. Zink W, Graf BM, Sinner B, Martin E, Fink RH, Kunst G (2002) Differential effects of bupivacaine on intracellular Ca2+ regulation: potential mechanisms of its myotoxicity. Anesthesiology 97(3):710–716

38. Goldberg AL (1967) Work-induced growth of skeletal muscle in normal and hypophysectomized rats. Am J Phys 213(5):1193–1198. https://doi.org/10.1152/ajplegacy.1967.213.5.1193

39. Khodabukus A, Baehr LM, Bodine SC, Baar K (2015) Role of contraction duration in inducing fast-to-slow contractile and metabolic protein and functional changes in engineered muscle. J Cell Physiol 230(10):2489–2497. https://doi.org/10.1002/jcp.24985

8.5 Appendix 5: Conference Abstract: British Society on Research and Ageing (BSRA) 2016

The Promiscuous Roles of Leucine and HMB Supplementation on Young and Old Satellite Cell Fusion, Migration and Repair

Alexander D Brown[1], *Dr Graeme L Close[1], *Dr Adam P Sharples[2] & *Professor Claire E Stewart[1]

Abstract

Purpose: Skeletal muscle regenerates following damage, however, this is compromised with age. The impact of leucine and betaHydroxy betamethylbutyric acid (HMB) on muscle repair is unknown. We hypothesised that these supplements will enhance muscle regeneration in the young vs. old myoblasts. *Methods:* Following damage or control conditions old and young myoblasts were treated with leucine or HMB (0, 10mM) in the absence or presence of PI3kinase (LY294002; 10µM), mTOR (rapamysin; 0.5µM) or ERK (PD98059; 5µM) inhibitors. Photomicrographs (migration (wound closure, distance, velocity, directionality) and fusion) and supernatant (lactate dehydrogenase (LDH)) were obtained at 0h, 24h, 48h and 144h. *Results:* Old cells migrated significantly more quickly vs. young ($P<0.001$), with 10mM leucine and HMB further increasing migration ($P<0.001$). Basal and supplemented migration were significantly reduced with LY and PD ($P<0.001$), but not rapamyosin. Older cells secreted significantly higher LDH vs. young ($P<0.001$) and at 48h, 10mM leucine significantly attenuated the increase ($P<0.001$). Both supplements increased myotube diameter ($P<0.001$), area ($P<0.001$) and length ($P<0.05$) in young cells only. *Discussion:* Migration in young and old cells requires Akt/Erk signaling, regardless of treatment. Fusion in young cells was facilitated via leucine and HMB while elevated LDH secretion by older cells was attenuated by leucine, suggesting differential responses to supplementation with age.

8.6 Appendix 6: Conference Abstract: British Society on Research and Ageing (BSRA) 2017

Mechanisms underpinning enhanced migration capabilities of replicatively aged C2C12 myoblasts

Alexander D Brown[1], *Dr Graeme L Close[1], *Dr Adam P Sharples[2] & *Professor Claire E Stewart[1]

Abstract

The ability of skeletal muscle to remodel and regenerate following damage is thought to be compromised with age. We hypothesised that replicatively aged (P46–P48; old) myoblasts would be less efficient at damage repair versus control (P12–P16). Old and control myoblasts were damaged and migration velocity, directionality and distance were assessed over 48h. Intracellular signalling mechanisms (ERK, Akt, mTOR), previously shown in our laboratory to modulate myoblast migration, were measured via flow cytometry. To validate findings, myoblasts were treated with inhibitors of PI3kinase (LY294002; 10µM), ERK (PD98059; 5µM) and mTOR (rapamycin; 0.5µM). Surprisingly, old myoblasts migrated more efficiently versus control, with significant (all $P<0.001$) increases in velocity (27%), directionality (16%) and distance (29%). Post damage, this corresponded to increased ERK ($P=0.028$) and Akt ($P=0.047$) phosphorylation at 15min and 2h, respectively. LY294002 revealed PI3Kinase/Akt activation was essential for velocity, directionality and overall migration distance in both old and control cells. PD98059 administration reduced, velocity, directionality and distance migrated in old, but only impaired migration distance in control cells. Finally, mTOR inactivation increased old cell directionality ($P<0.001$), and control myoblast velocity and distance ($P<0.001$). These novel data suggest that improved, not compromised wound closure, underpinned by differential signalling mechanisms occurs in old versus control cells.

8.7 Appendix 7: Conference Abstract: British Society on Research and Ageing (BSRA) 2018

Leucine and β-Hydroxy β-Methylbutyrate Enhance Replicatively Aged C2C12 Myoblasts Migration but Not Fusion

Alexander D Brown[1], *Dr Graeme L Close[1], *Dr Adam P Sharples[2] & *Professor Claire E Stewart[1]

Abstract

Introduction: With ageing the ability to retain skeletal muscle mass and function declines (sarcopenia), with associated "anabolic resistance" being reported. Since, the migration and fusion of resident myoblasts are critical to these processes, we **hypothesised** that these would be compromised with age. Our ultimate **aim** is to implement models of ageing muscle degeneration and regeneration to enable interventions targeting sarcopenia by enhancing repair and maintaining muscle mass. Methods: Confluent control and replicatively aged [1] myoblasts were damaged in the absence or presence of 10mM leucine or HMB. Migration velocity, directionality and distance were assessed (0-48h). Myotube formation was assessed morphologically and biochemically (creatine kinase (CK), lactate dehydrogenase (LDH)) and gene expression all at 0, 24 and 96h. Results: Surprisingly, aged myoblasts migrated more efficiently versus control, with significant (all $P<0.001$) increases in velocity, directionality and distance and near significance in increased expression of ADAMS10 ($P=0.056$). Supplementation significantly impacted on aged cell velocity ($P<0.001$) and in the presence of HMB only, distance ($P=0.041$). Although control cells showed significant fusion with time ($P<0.001$), aged myoblasts did not fuse in the absence or presence of supplementation and displayed significant reductions in CK ($P<0.001$) and myogenin expression ($P<0.001$) and significant increases in LDH ($P<0.001$) and myostatin expression ($P=0.06$), vs control. LDH levels were significantly attenuated with leucine at 48h ($P=0.002$) and 96h ($P=0.007$). Conclusion: These novel data suggest that improved migration (potentially linked to increased ADAMS10 expression), but not fusion (linked to reduced myogenin and elevated myostatin expression) occur in aged vs. control myoblasts with "anabolic resistance" being constrained to hypertrophy only.

Chapter 9: References

Aggarwal, S, and Yadav, AK (2016). False discovery rate estimation in proteomics. In: Methods in Molecular Biology.

Al-Shanti, N, Faulkner, SH, Saini, A, Loram, I, and Stewart, CE (2011). A semi-automated programme for tracking myoblast migration following mechanical damage: Manipulation by chemical inhibitors. Cell Physiol Biochem.

Al-Shanti, N, and Stewart, CE (2008). PD98059 enhances C2 myoblast differentiation through p38 MAPK activation: A novel role for PD98059. J Endocrinol.

Albert, WJ, Wrigley, AT, McLean, RB, and Sleivert, GG (2006). Sex differences in the rate of fatigue development and recovery. Dyn Med.

Allen, DL, Teitelbaum, DH, and Kurachi, K (2003). Growth factor stimulation of matrix metalloproteinase expression and myoblast migration and invasion in vitro. Am J Physiol Physiol.

Allen, RE, Sheehan, SM, Taylor, RG, Kendall, TL, and Rice, GM (1995). Hepatocyte growth factor activates quiescent skeletal muscle satellite cells in vitro. J Cell Physiol.

Alsharidah, M, Lazarus, NR, George, TE, Agley, CC, Velloso, CP, and Harridge, SDR (2013). Primary human muscle precursor cells obtained from young and old donors produce similar proliferative, differentiation and senescent profiles in culture. Aging Cell.

Altman, AM, Gupta, V, Ríos, CN, Alt, EU, and Mathur, AB (2010). Adhesion, migration and mechanics of human adipose-tissue-derived stem cells on silk fibroin-chitosan matrix. Acta Biomater.

Alway, SE, Pereira, SL, Edens, NK, Hao, Y, and Bennett, BT (2013). β-Hydroxy-β-methylbutyrate (HMB) enhances the proliferation of satellite cells in fast muscles of aged rats during recovery from disuse atrophy. Exp Gerontol.

Andersen, JL (2003). Muscle fibre type adaptation in the elderly human muscle. In: Scandinavian Journal of Medicine and Science in Sports.

Areta, JL, Hawley, JA, Ye, JM, Chan, MHS, and Coffey, VG (2014). Increasing leucine concentration stimulates mechanistic target of rapamycin signaling and cell growth in C2C12 skeletal muscle cells. Nutr Res.

Armstrong, RB (1984). Mechanisms of exercise induced delayed onset: a brief review. Med Sci Sport Exerc.

Arnold, L, Henry, A, Poron, F, Baba-Amer, Y, van Rooijen, N, Plonquet, A, Gherardi, RK, and Chazaud, B (2007). Inflammatory monocytes recruited after skeletal muscle injury switch into antiinflammatory macrophages to support myogenesis. J Exp Med.

Arthur, ST, and Cooley, ID (2012). The effect of physiological stimuli on sarcopenia; Impact of Notch and Wnt signaling on impaired aged skeletal muscle repair. Int J Biol Sci.

Asakura, A, Seale, P, Girgis-Gabardo, A, and Rudnicki, MA (2002). Myogenic specification of side population cells in skeletal muscle. J Cell Biol.

Atherton, PJ, Kumar, V, Selby, AL, Rankin, D, Hildebrandt, W, Phillips, BE, Williams, JP, Hiscock, N, and Smith, K (2017). Enriching a protein drink with leucine augments muscle protein synthesis after resistance exercise in young and older men. Clin Nutr.

Auffray, C, Fogg, D, Garfa, M, Elain, G, Join-Lambert, O, Kayal, S, Sarnacki, S, Cumano, A, Lauvau, G, and Geissmann, F (2007). Monitoring of blood vessels and tissues by a population of monocytes with patrolling behavior. Science (80-).

Aurora, AB, and Olson, EN (2014). Immune modulation of stem cells and regeneration. Cell Stem Cell.

Averous, J, Gabillard, JC, Seiliez, I, and Dardevet, D (2012). Leucine limitation regulates myf5 and myoD expression and inhibits myoblast differentiation. Exp Cell Res.

Baier, S, Johannsen, D, Abumrad, N, Rathmacher, JA, Nissen, S, and Flakoll, P (2009). Year-long changes in protein metabolism in elderly men and women supplemented with a nutrition cocktail of β-hydroxy-β-methylbutyrate (HMB), L-arginine, and L-lysine. J Parenter Enter Nutr.

Barbieri, E et al. (2011). Morphofunctional and biochemical approaches for studying mitochondrial changes during myoblasts differentiation. J Aging Res.

Barbour, HG (1937). The Basis of the Pharmacological Action of Heavy Water in Mammals. Yale J Biol Med.

Bartlett, A, Sanders, AJ, Ruge, F, Harding, KG, and Jiang, WG (2016). Potential implications of interleukin-7 in chronic wound healing. Exp Ther Med.

Bauer, J et al. (2013). Evidence-based recommendations for optimal dietary protein intake in older people: A position paper from the prot-age study group. J Am Med Dir Assoc.

Baumert, P, Lake, MJ, Drust, B, Stewart, CE, and Erskine, RM (2017). TRIM63 (MuRF-1) gene polymorphism is associated with biomarkers of exercise-induced muscle damage. Physiol Genomics 50, 142–143.

Baumert, P, Lake, MJ, Stewart, CE, Drust, B, and Erskine, RM (2016). Genetic variation and exercise-induced muscle damage: implications for athletic performance,

injury and ageing. Eur J Appl Physiol.

Baumert, P, Stewart, CE, Lake, MJ, Drust, B, and Erskine, RM (2018). Variations of collagen-encoding genes are associated with exercise-induced muscle damage. Physiol Genomics.

Benbassat, CA, Maki, KC, and Unterman, TG (1997). Circulating levels of insulin-like growth factor (IGF) binding protein- 1 and -3 in aging men: Relationships to insulin, glucose, IGF, and dehydroepiandrosterone sulfate levels and anthropometric measures. J Clin Endocrinol Metab.

Benjamini, Y, and Hochberg, Y (1995). Controlling the False Discovery Rate: A Practical and Powerful Approach to Multiple Testing. J R Stat Soc Ser B.

Bentzinger, CF, von Maltzahn, J, Dumont, NA, Stark, DA, Wang, YX, Nhan, K, Frenette, J, Cornelison, DDW, and Rudnicki, MA (2014). Wnt7a stimulates myogenic stem cell motility and engraftment resulting in improved muscle strength. J Cell Biol.

Bentzinger, CF, Wang, YX, and Rudnicki, MA (2012). Building muscle: molecular regulation of myogenesis. Cold Spring Harb Perspect Biol.

Bernet, JD, Doles, JD, Hall, JK, Kelly Tanaka, K, Carter, TA, and Olwin, BB (2014). P38 MAPK signaling underlies a cell-autonomous loss of stem cell self-renewal in skeletal muscle of aged mice. Nat Med.

Bigot, A et al. (2015). Age-Associated Methylation Suppresses SPRY1, Leading to a Failure of Re-quiescence and Loss of the Reserve Stem Cell Pool in Elderly Muscle. Cell Rep.

Bigot, A, Jacquemin, V, Debacq-Chainiaux, F, Butler-Browne, GS, Toussaint, O, Furling, D, and Mouly, V (2008). Replicative aging down-regulates the myogenic regulatory factors in human myoblasts. Biol Cell.

Bizzarro, V, Fontanella, B, Carratù, A, Belvedere, R, Marfella, R, Parente, L, and Petrella, A (2012). Annexin A1 N-Terminal Derived Peptide Ac2-26 Stimulates Fibroblast Migration in High Glucose Conditions. PLoS One.

Bizzarro, V, Fontanella, B, Franceschelli, S, Pirozzi, M, Christian, H, Parente, L, and Petrella, A (2010). Role of annexin A1 in mouse myoblast cell differentiation. J Cell Physiol.

Blau, HM, Pavlath, GK, Hardeman, EC, Chiu, CP, Silberstein, L, Webster, SG, Miller, SC, and Webster, C (1985). Plasticity of the differentiated state. Science (80-).

Bodine, SC et al. (2001). Akt/mTOR pathway is a crucial regulator of skeletal muscle hypertrophy and can prevent muscle atrophy in vivo. Nat Cell Biol.

Bowen, TS et al. (2017). Small-molecule inhibition of MuRF1 attenuates skeletal muscle atrophy and dysfunction in cardiac cachexia. J Cachexia Sarcopenia Muscle.

Brack, AS, Conboy, IM, Conboy, MJ, Shen, J, and Rando, TA (2008). A Temporal Switch from Notch to Wnt Signaling in Muscle Stem Cells Is Necessary for Normal Adult Myogenesis. Cell Stem Cell.

Brack, AS, and Rando, TA (2007). Intrinsic changes and extrinsic influences of myogenic stem cell function during aging. Stem Cell Rev.

Breen, L, and Churchward-Venne, TA (2012). Leucine: A nutrient "trigger" for muscle anabolism, but what more? J Physiol.

Breen, L, and Phillips, SM (2011). Skeletal muscle protein metabolism in the elderly: Interventions to counteract the "anabolic resistance" of ageing. Nutr Metab.

Brinkmeier, H, and Ohlendieck, K (2014). Chaperoning heat shock proteins: Proteomic analysis and relevance for normal and dystrophin-deficient muscle. Proteomics - Clin Appl.

Brook, MS, Wilkinson, DJ, Mitchell, WK, Lund, JN, Szewczyk, NJ, Greenhaff, PL, Smith, K, and Atherton, PJ (2015). Skeletal muscle hypertrophy adaptations predominate in the early stages of resistance exercise training, matching deuterium oxide-derived measures of muscle protein synthesis and mechanistic target of rapamycin complex 1 signaling. FASEB J.

Buckley, JD, Thomson, RL, Coates, AM, Howe, PRC, DeNichilo, MO, and Rowney, MK (2010). Supplementation with a whey protein hydrolysate enhances recovery of muscle force-generating capacity following eccentric exercise. J Sci Med Sport.

Buono, R, Vantaggiato, C, Pisa, V, Azzoni, E, Bassi, MT, Brunelli, S, Sciorati, C, and Clementi, E (2012). Nitric oxide sustains long-term skeletal muscle regeneration by regulating fate of satellite cells via signaling pathways requiring Vangl2 and cyclic GMP. Stem Cells.

Burd, NA, Gorissen, SH, and Van Loon, LJC (2013). Anabolic resistance of muscle protein synthesis with aging. Exerc Sport Sci Rev.

Burgess, KE, Pearson, SJ, and Onambélé, GL (2009). Menstrual cycle variations in oestradiol and progesterone have no impact on in vivo medial gastrocnemius tendon mechanical properties. Clin Biomech.

Burniston, JG, Connolly, J, Kainulainen, H, Britton, SL, and Koch, LG (2014). Label-free profiling of skeletal muscle using high-definition mass spectrometry. Proteomics.

Burzyn, D et al. (2013). A Special Population of regulatory T Cells Potentiates muscle

repair. Cell.

Busch, R et al. (2006). Measurement of protein turnover rates by heavy water labeling of nonessential amino acids. Biochim Biophys Acta - Gen Subj.

Butler, JT, Hall, LL, Smith, KP, and Lawrence, JB (2009). Changing nuclear landscape and unique PML structures during early epigenetic transitions of human embryonic stem cells. J Cell Biochem.

Byrne, C, and Eston, R (2002). The effect of exercise-induced muscle damage on isometric and dynamic knee extensor strength and vertical jump performance. J Sports Sci.

Cambridge, SB, Gnad, F, Nguyen, C, Bermejo, JL, Krüger, M, and Mann, M (2011). Systems-wide proteomic analysis in mammalian cells reveals conserved, functional protein turnover. J Proteome Res.

Camera, DM, Burniston, JG, Pogson, MA, Smiles, WJ, and Hawley, JA (2017). Dynamic proteome profiling of individual proteins in human skeletal muscle after a high-fat diet and resistance exercise. FASEB J.

Cammas, A et al. (2014). Destabilization of nucleophosmin mRNA by the HuR/KSRP complex is required for muscle fibre formation. Nat Commun.

Campbell, MJ, McComas, AJ, and Petito, F (1973). Physiological changes in ageing muscles. J Neurol Neurosurg Psychiatry.

Cardinalli, B, Castellani, L, Fasanaro, P, Basso, A, Alemà, S, Martelli, F, and Falcone, G (2009). Microrna-221 and microrna-222 modulate differentiation and maturation of skeletal muscle cells. PLoS One.

Carlson, ME, Conboy, MJ, Hsu, M, Barchas, L, Jeong, J, Agrawal, A, Mikels, AJ, Agrawal, S, Schaffer, D V., and Conboy, IM (2009). Relative roles of TGF-β1 and Wnt in the systemic regulation and aging of satellite cell responses. Aging Cell.

Carmeli, E, Coleman, R, and Reznick, AZ (2002). The biochemistry of aging muscle. Exp Gerontol.

Carter, M, Shieh, J, Carter, M, and Shieh, J (2015). Chapter 14 – Cell Culture Techniques. In: Guide to Research Techniques in Neuroscience.

Casciola-Rosen, L, Hall, JC, Mammen, AL, Christopher-Stine, L, and Rosen, A (2012). Isolated elevation of aldolase in the serum of myositis patients: A potential biomarker of damaged early regenerating muscle cells. Clin Exp Rheumatol.

Chakravarthy, M V., Abraha, TW, Schwartz, RJ, Fiorotto, ML, and Booth, FW (2000). Insulin-like growth factor-I extends in vitro replicative life span of skeletal muscle

satellite cells by enhancing G 1 /S cell cycle progression via the activation of phosphatidylinositol 3'-kinase/Akt signaling pathway. J Biol Chem.

Chan, FKM, Moriwaki, K, and De Rosa, MJ (2013). Detection of necrosis by release of lactate dehydrogenase activity. Methods Mol Biol.

Chan, J, O'Donoghue, K, Gavina, M, Torrente, Y, Kennea, N, Mehmet, H, Stewart, H, Watt, DJ, Morgan, JE, and Fisk, NM (2006). Galectin-1 Induces Skeletal Muscle Differentiation in Human Fetal Mesenchymal Stem Cells and Increases Muscle Regeneration. Stem Cells.

Charras, G, and Paluch, E (2008). Blebs lead the way: How to migrate without lamellipodia. Nat Rev Mol Cell Biol.

Charrasse, S, Meriane, M, Comunale, F, Blangy, A, and Gauthier-Rouvière, C (2002). N-cadherin-dependent cell-cell contact regulates Rho GTPases and β-catenin localization in mouse C2C12 myoblasts. J Cell Biol.

Chen, B, and Shan, T (2019). The role of satellite and other functional cell types in muscle repair and regeneration. J Muscle Res Cell Motil.

Chen, BH et al. (2017). Leukocyte telomere length, T cell composition and DNA methylation age. Aging (Albany NY).

Chen, EH, and Olson, EN (2005). Unveiling the mechanisms of cell-cell fusion. Science (80-).

Chodzko-Zajko, WJ, Proctor, DN, Fiatarone Singh, MA, Minson, CT, Nigg, CR, Salem, GJ, and Skinner, JS (2009). Exercise and physical activity for older adults. Med Sci Sports Exerc.

Chung, HY, Cesari, M, Anton, S, Marzetti, E, Giovannini, S, Seo, AY, Carter, C, Yu, BP, and Leeuwenburgh, C (2009). Molecular inflammation: Underpinnings of aging and age-related diseases. Ageing Res Rev.

Churchward-Venne, TA, Breen, L, and Phillips, SM (2014). Alterations in human muscle protein metabolism with aging: Protein and exercise as countermeasures to offset sarcopenia. BioFactors.

Churchward-Venne, TA, Burd, NA, Mitchell, CJ, West, DWD, Philp, A, Marcotte, GR, Baker, SK, Baar, K, and Phillips, SM (2012). Supplementation of a suboptimal protein dose with leucine or essential amino acids: Effects on myofibrillar protein synthesis at rest and following resistance exercise in men. J Physiol.

Churchward-Venne, TA, Tieland, M, Verdijk, LB, Leenders, M, Dirks, ML, de Groot, LCPGM, and van Loon, LJC (2015). There are no nonresponders to resistance-type

exercise training inolder men and women. J Am Med Dir Assoc.

Clark, BC, and Manini, TM (2010). Functional consequences of sarcopenia and dynapenia in the elderly. Curr Opin Clin Nutr Metab Care.

Clarkson, PM, Byrnes, WC, McCormick, KM, Turcotte, LP, and White, JS (1986). Muscle soreness and serum creatine kinase activity following isometric, eccentric, and concentric exercise. Int J Sports Med.

Clevers, H, Loh, KM, and Nusse, R (2014). An integral program for tissue renewal and regeneration: Wnt signaling and stem cell control. Science (80-).

Close, GL, Ashton, T, Cable, T, Doran, D, Holloway, C, McArdle, F, and MacLaren, DPM (2006). Ascorbic acid supplementation does not attenuate post-exercise muscle soreness following muscle-damaging exercise but may delay the recovery process. Br J Nutr.

Conboy, IH, Conboy, MJ, Smythe, GM, and Rando, TA (2003). Notch-Mediated Restoration of Regenerative Potential to Aged Muscle. Science (80-).

Condon, KJ, and Sabatini, DM (2019). Nutrient regulation of mTORC1 at a glance. J Cell Sci.

Coolican, SA, Samuel, DS, Ewton, DZ, McWade, FJ, and Florini, JR (1997). The mitogenic and myogenic actions of insulin-like growth factors utilize distinct signaling pathways. J Biol Chem.

Cooper, ST, Maxwell, AL, Kizana, E, Ghoddusi, M, Hardeman, EC, Alexander, IE, Allen, DG, and North, KN (2004). C2C12 co-culture on a fibroblast substratum enables sustained survival of contractile, highly differentiated myotubes with peripheral nuclei and adult fast myosin expression. Cell Motil Cytoskeleton.

Cornelison, DDW, Olwin, BB, Rudnicki, MA, and Wold, BJ (2000). MyoD(-/-) satellite cells in single-fiber culture are differentiation defective and MRF4 deficient. Dev Biol.

Corrick, KL, Stec, MJ, Merritt, EK, Windham, ST, Thomas, SJ, Cross, JM, and Bamman, MM (2015). Serum from human burn victims impairs myogenesis and protein synthesis in primary myoblasts. Front Physiol.

Cosgrove, BD, Gilbert, PM, Porpiglia, E, Mourkioti, F, Lee, SP, Corbel, SY, Llewellyn, ME, Delp, SL, and Blau, HM (2014). Rejuvenation of the muscle stem cell population restores strength to injured aged muscles. Nat Med.

Costello, JT, Bieuzen, F, and Bleakley, CM (2014). Where are all the female participants in Sports and Exercise Medicine research? Eur J Sport Sci.

Cram (2002). Flow cytometry, an overview. Methods Cell Sci 24, 1–9.

Cuthbertson, D, Smith, K, Babraj, J, Leese, G, Waddell, T, Atherton, P, Wackerhage, H, Taylor, PM, and Rennie, MJ (2005). Anabolic signaling deficits underlie amino acid resistance of wasting, aging muscle. FASEB J.

Cuthbertson, DJ, Babraj, J, Smith, K, Wilkes, E, Fedele, MJ, Esser, K, and Rennie, M (2006). Anabolic signaling and protein synthesis in human skeletal muscle after dynamic shortening or lengthening exercise. Am J Physiol - Endocrinol Metab.

Dai, JM, Yu, MX, Shen, ZY, Guo, CY, Zhuang, SQ, and Qiu, XS (2015). Leucine promotes proliferation and differentiation of primary preterm rat satellite cells in part through mTORC1 signaling pathway. Nutrients.

Daimon, E, Shibukawa, Y, and Wada, Y (2013). Calponin 3 regulates stress fiber formation in dermal fibroblasts during wound healing. Arch Dermatol Res.

Dalkilic, I, Schienda, J, Thompson, TG, and Kunkel, LM (2006). Loss of FilaminC (FLNc) Results in Severe Defects in Myogenesis and Myotube Structure. Mol Cell Biol.

Dannecker, EA, Hausenblas, HA, Kaminski, TW, and Robinson, ME (2005). Sex differences in delayed onset muscle pain. Clin J Pain.

Davies, RC, Rowlands, A V., and Eston, RG (2009). Effect of exercise-induced muscle damage on ventilatory and perceived exertion responses to moderate and severe intensity cycle exercise. Eur J Appl Physiol.

Davis, RL, Weintraub, H, and Lassar, AB (1987). Expression of a single transfected cDNA converts fibroblasts to myoblasts. Cell.

Day, K, Shefer, G, Shearer, A, and Yablonka-Reuveni, Z (2010). The depletion of skeletal muscle satellite cells with age is concomitant with reduced capacity of single progenitors to produce reserve progeny. Dev Biol.

Deane, CS, Hughes, DC, Sculthorpe, N, Lewis, MP, Stewart, CE, and Sharples, AP (2013). Impaired hypertrophy in myoblasts is improved with testosterone administration. J Steroid Biochem Mol Biol.

Decker, T, and Lohmann-Matthes, ML (1988). A quick and simple method for the quantitation of lactate dehydrogenase release in measurements of cellular cytotoxicity and tumor necrosis factor (TNF) activity. J Immunol Methods.

Dedieu, S, Poussard, S, Mazères, G, Grise, F, Dargelos, E, Cottin, P, and Brustis, JJ (2004). Myoblast migration is regulated by calpain through its involvement in cell attachment and cytoskeletal organization. Exp Cell Res.

Delgado, I, Huang, X, Jones, S, Zhang, L, Hatcher, R, Gao, B, and Zhang, P (2003). Dynamic gene expression during the onset of myoblast differentiation in vitro.

Genomics.

Deng, J, Erdjument-Bromage, H, and Neubert, TA (2019). Quantitative Comparison of Proteomes Using SILAC. Curr Protoc Protein Sci.

Deschenes, MR (2004). Effects of aging on muscle fibre type and size. Sport Med.

Deutz, NEP et al. (2014). Protein intake and exercise for optimal muscle function with aging: Recommendations from the ESPEN Expert Group. Clin Nutr.

Devlin, RB, and Emerson, CP (1978). Coordinate regulation of contractile protein synthesis during myoblast differentiation. Cell.

Dickinson, JM, and Rasmussen, BB (2011). Essential amino acid sensing, signaling, and transport in the regulation of human muscle protein metabolism. Curr Opin Clin Nutr Metab Care.

Dickinson, JM, and Rasmussen, BB (2013). Amino acid transporters in the regulation of human skeletal muscle protein metabolism. Curr Opin Clin Nutr Metab Care.

Dimchev, GA, Al-Shanti, N, and Stewart, CE (2013). Phospho-tyrosine phosphatase inhibitor Bpv(Hopic) enhances C2C12 myoblast migration in vitro. Requirement of PI3K/AKT and MAPK/ERK pathways. J Muscle Res Cell Motil.

Doherty, KR (2005). Normal myoblast fusion requires myoferlin. Development.

Domingues-Faria, C, Vasson, MP, Goncalves-Mendes, N, Boirie, Y, and Walrand, S (2016). Skeletal muscle regeneration and impact of aging and nutrition. Ageing Res Rev.

Drummond, MJ, Fry, CS, Glynn, EL, Timmerman, KL, Dickinson, JM, Walker, DK, Gundermann, DM, Volpi, E, and Rasmussen, BB (2011). Skeletal muscle amino acid transporter expression is increased in young and older adults following resistance exercise. J Appl Physiol.

Duan, R et al. (2018). Spectrin is a mechanoresponsive protein shaping fusogenic synapse architecture during myoblast fusion. Nat Cell Biol.

Dumont, N, Lepage, K, Côté, CH, and Frenette, J (2007). Mast cells can modulate leukocyte accumulation and skeletal muscle function following hindlimb unloading. J Appl Physiol.

Dumont, NA, Bentzinger, CF, Sincennes, MC, and Rudnicki, MA (2015). Satellite cells and skeletal muscle regeneration. Compr Physiol.

Durcan, PJ, Al-Shanti, N, and Stewart, CE (2013). Identification and characterization of novel Kirrel isoform during myogenesis. Physiol Rep.

Durcan, PJ, Conradie, JD, Van Devyver, M, and Myburgh, KH (2014). Identification of

novel Kirrel3 gene splice variants in adult human skeletal muscle. BMC Physiol.

Duval, D, Trouillas, M, Thibault, C, Dembelé, D, Diemunsch, F, Reinhardt, B, Mertz, AL, Dierich, A, and Bœuf, H (2006). Apoptosis and differentiation commitment: Novel insights revealed by gene profiling studies in mouse embryonic stem cells. Cell Death Differ.

Eiling, E, Bryant, AL, Petersen, W, Murphy, A, and Hohmann, E (2007). Effects of menstrual-cycle hormone fluctuations on musculotendinous stiffness and knee joint laxity. Knee Surgery, Sport Traumatol Arthrosc.

Eliazer, S, Muncie, JM, Christensen, J, Sun, X, D'Urso, RS, Weaver, VM, and Brack, AS (2019). Wnt4 from the Niche Controls the Mechano-Properties and Quiescent State of Muscle Stem Cells. Cell Stem Cell.

Engelhardt, E, Toksoy, A, Goebeler, M, Debus, S, Bröcker, EB, and Gillitzer, R (1998). Chemokines IL-8, GROα, MCP-1, IP-10, and mig are sequentially and differentially expressed during phase-specific infiltration of leukocyte subsets in human wound healing. Am J Pathol.

Epstein, JA, Shapiro, DN, Cheng, J, Lam, PY, and Maas, RL (1996). Pax3 modulates expression of the c-Met receptor during limb muscle development. Proc Natl Acad Sci.

Erbay, E, and Chen, J (2001). The Mammalian Target of Rapamycin Regulates C2C12 Myogenesis via a Kinase-independent Mechanism. J Biol Chem.

Ervasti, JM, and Campbell, KP (1993). A role for the dystrophin-glycoprotein complex as a transmembrane linker between laminin and actin. J Cell Biol.

Eston, RG, Finney, S, Baker, S, and Baltzopoulos, V (1996). Muscle tenderness and peak torque changes after downhill running following a prior bout of isokinetic eccentric exercise. J Sports Sci.

Eston, RG, Lemmey, AB, McHugh, P, Byrne, C, and Walsh, SE (2000). Effect of stride length on symptoms of exercise-induced muscle damage during a repeated bout of downhill running. Scand J Med Sci Sport.

Etheridge, T, Philp, A, and Watt, PW (2008). A single protein meal increases recovery of muscle function following an acute eccentric exercise bout. Appl Physiol Nutr Metab.

Falcone, G, Boettiger, D, Alemà, S, and Tatò, F (1984). Role of cell division in differentiation of myoblasts infected with a temperature-sensitive mutant of Rous sarcoma virus. EMBO J.

Farup, J, De Lisio, M, Rahbek, SK, Bjerre, J, Vendelbo, MH, Boppart, MD, and Vissing, K (2015). Pericyte response to contraction mode-specific resistance exercise training

in human skeletal muscle. J Appl Physiol.

Farup, J, Rahbek, SK, Knudsen, IS, De Paoli, F, Mackey, AL, and Vissing, K (2014). Whey protein supplementation accelerates satellite cell proliferation during recovery from eccentric exercise. Amino Acids.

Fayard, E, Tintignac, LA, Baudry, A, and Hemmings, BA (2005). Protein kinase B/Akt at a glance. J Cell Sci.

Fleming, KK, and Hubel, A (2006). Cryopreservation of hematopoietic and non-hematopoietic stem cells. Transfus Apher Sci.

Flores, DF, Gentil, P, Brown, LE, Pinto, RS, Carregaro, RL, and Bottar, M (2011). Dissociated time course of recovery between genders after resistance exercise. J Strength Cond Res.

Foletta, VC, Palmieri, M, Kloehn, J, Mason, S, Previs, SF, McConville, MJ, Sieber, OM, Bruce, CR, and Kowalski, GM (2016). Analysis of mammalian cell proliferation and macromolecule synthesis using deuteratedwater and gas chromatography-mass spectrometry. Metabolites.

Foulstone, EJ, Huser, C, Crown, AL, Holly, JMP, and Stewart, CEH (2004). Differential signalling mechanisms predisposing primary human skeletal muscle cells to altered proliferation and differentiation: Roles of IGF-I and TNFα. Exp Cell Res.

Foulstone, EJ, Meadows, KA, Holly, JMP, and Stewart, CEH (2001). Insulin-like growth factors (IGF-I and IGF-II) inhibit C2 skeletal myoblast differentiation and enhance TNFα-induced apoptosis. J Cell Physiol.

Foulstone, EJ, Savage, PB, Crown, AL, Holly, JMP, and Stewart, CEH (2003). Role of insulin-like growth factor binding protein-3 (IGFBP-3) in the differentiation of primary human adult skeletal myoblasts. J Cell Physiol.

Fouré, A, Nosaka, K, Gastaldi, M, Mattei, JP, Boudinet, H, Guye, M, Vilmen, C, Le Fur, Y, Bendahan, D, and Gondin, J (2016). Effects of branched-chain amino acids supplementation on both plasma amino acids concentration and muscle energetics changes resulting from muscle damage: A randomized placebo controlled trial. Clin Nutr.

Frantz, C, Stewart, KM, and Weaver, VM (2010). The extracellular matrix at a glance. J Cell Sci.

Fridén, J, and Lieber, RL (2001). Eccentric exercise-induced injuries to contractile and cytoskeletal muscle fibre components. In: Acta Physiologica Scandinavica.

Frock, RL, Kudlow, BA, Evans, AM, Jameson, SA, Hauschka, SD, and Kennedy, BK

312

(2006). Lamin A/C and emerin are critical for skeletal muscle satellite cell differentiation. Genes Dev.

Fujita, H, Nedachi, T, and Kanzaki, M (2007a). Accelerated de novo sarcomere assembly by electric pulse stimulation in C2C12 myotubes. Exp Cell Res.

Fujita, S, Dreyer, HC, Drummond, MJ, Glynn, EL, Cadenas, JG, Yoshizawa, F, Volpi, E, and Rasmussen, BB (2007b). Nutrient signalling in the regulation of human muscle protein synthesis. J Physiol.

Gandevia, SC (2001). Spinal and Supraspinal Factors in Human Muscle Fatigue. Physiol Rev.

Garcia, AJ, Vega, MD, and Boettiger, D (1999). Modulation of Cell Proliferation and Differentiation through Substrate-dependent Changes in Fibronectin Conformation. Mol Biol Cell.

Gard, DL, and Lazarides, E (1980). The synthesis and distribution of desmin and vimentin during myogenesis in vitro. Cell.

Gault, M (2013). Aging, Functional Capacity and Eccentric Exercise Training. Aging Dis.

Georgiadis, V, Stewart, HJS, Pollard, HJ, Tavsanoglu, Y, Prasad, R, Horwood, J, Deltour, L, Goldring, K, Poirier, F, and Lawrence-Watt, DJ (2007). Lack of galectin-1 results in defects in myoblast fusion and muscle regeneration. Dev Dyn.

Germani, A, Di Carlo, A, Mangoni, A, Straino, S, Giacinti, C, Turrini, P, Biglioli, P, and Capogrossi, MC (2003). Vascular endothelial growth factor modulates skeletal myoblast function. Am J Pathol.

Giancotti, FG (1997). Integrin signaling: Specificity and control of cell survival and cell cycle progression. Curr Opin Cell Biol.

Gillespie, MA, Le Grand, F, Scimè, A, Kuang, S, Von Maltzahn, J, Seale, V, Cuenda, A, Ranish, JA, and Rudnicki, MA (2009). p38-γ-dependent gene silencing restricts entry into the myogenic differentiation program. J Cell Biol.

Girven, M, Dugdale, HF, Owens, DJ, Hughes, DC, Stewart, CE, and Sharples, AP (2016). l-glutamine Improves Skeletal Muscle Cell Differentiation and Prevents Myotube Atrophy After Cytokine (TNF-α) Stress Via Reduced p38 MAPK Signal Transduction. J Cell Physiol.

Gissel, H, and Clausen, T (2001). Excitation-induced Ca2+ influx and skeletal muscle cell damage. In: Acta Physiologica Scandinavica.

Glading, A, Lauffenburger, DA, and Wells, A (2002). Cutting to the chase: Calpain

proteases in cell motility. Trends Cell Biol.

Goldring, K, Jones, GE, Thiagarajah, R, and Watt, DJ (2002). The effect of galectin-1 on the differentiation of fibroblasts and myoblasts in vitro. J Cell Sci.

Gong, Z, and Muzumdar, RH (2012). Pancreatic function, type 2 diabetes, and metabolism in aging. Int J Endocrinol.

Goodpaster, BH, Thaete, FL, and Kelley, DE (2000). Thigh adipose tissue distribution is associated with insulin resistance in obesity and in type 2 diabetes mellitus. Am J Clin Nutr.

Gopinath, SD, Webb, AE, Brunet, A, and Rando, TA (2014). FOXO3 promotes quiescence in adult muscle stem cells during the process of self-renewal. Stem Cell Reports.

Gordon, S, and Martinez, FO (2010). Alternative activation of macrophages: Mechanism and functions. Immunity.

Le Grand, F, Jones, AE, Seale, V, Scimè, A, and Rudnicki, MA (2009). Wnt7a Activates the Planar Cell Polarity Pathway to Drive the Symmetric Expansion of Satellite Stem Cells. Cell Stem Cell.

Gray, P, Chappell, A, Jenkinson, AME, Thies, F, and Gray, SR (2014). Fish oil supplementation reduces markers of oxidative stress but not muscle soreness after eccentric exercise. Int J Sport Nutr Exerc Metab.

Grossi, A, Lametsch, R, Karlsson, AH, and Lawson, MA (2011). Mechanical stimuli on C2C12 myoblasts affect myoblast differentiation, focal adhesion kinase phosphorylation and galectin-1 expression: a proteomic approach. Cell Biol Int.

Gu, X, Orozco, JM, Saxton, RA, Condon, KJ, Liu, GY, Krawczyk, PA, Scaria, SM, Wade Harper, J, Gygi, SP, and Sabatini, DM (2017). SAMTOR is an S-adenosylmethionine sensor for the mTORC1 pathway. Science (80-).

Hameed, M, Harridge, SDR, and Goldspink, G (2002). Sarcopenia and hypertrophy: A role for insulin-like growth factor-1 in aged muscle? Exerc Sport Sci Rev.

Hameed, M, Lange, KHW, Andersen, JL, Schjerling, P, Kjaer, M, Harridge, SDR, and Goldspink, G (2004). The effect of recombinant human growth hormone and resistance training on IGF-I mRNA expression in the muscles of elderly men. J Physiol.

Han, B, Tong, J, Zhu, MJ, Ma, C, and Du, M (2008). Insulin-like growth factor-1 (IGF-1) and leucine activate pig myogenic satellite cells through mammalian target of rapamycin (mTOR) pathway. Mol Reprod Dev.

Hanson, J, and Huxley, HE (1953). Structural basis of the cross-striations in muscle.

Nature.

Hasty, P, Bradley, A, Morris, JH, Edmondson, DG, Venuti, JM, Olson, EN, and Klein, WH (1993). Muscle deficiency and neonatal death in mice with a targeted mutation in the myogenin gene. Nature.

Hatfield, I, Harvey, I, Yates, ER, Redd, JR, Reiter, LT, and Bridges, D (2015). The role of TORC1 in muscle development in Drosophila. Sci Rep.

Haugen, F, Norheim, F, Lian, H, Wensaas, AJ, Dueland, S, Berg, O, Funderud, A, Skålhegg, BS, Raastad, T, and Drevon, CA (2010). IL-7 is expressed and secreted by human skeletal muscle cells. Am J Physiol Physiol.

Hauschka, SD, and Konigsberg, IR (1966). The influence of collagen on the development of muscle clones. Proc Natl Acad Sci.

Hawke, TJ, and Garry, DJ (2001). 筋肥大における筋衛星細胞の重要性Myogenic satellite cells Physiology to molecular biology. J Appl Physiol.

Hawkins, SA, Wiswell, RA, and Marcell, TJ (2003). Exercise and the Master Athlete-- A Model of Successful Aging? Journals Gerontol Ser A Biol Sci Med Sci.

Hawley, JA, Burke, LM, Phillips, SM, and Spriet, LL (2011). Nutritional modulation of training-induced skeletal muscle adaptations. J Appl Physiol.

Hawley, JA, Tipton, KD, and Millard-Stafford, ML (2006). Promoting training adaptations through nutritional interventions. In: Nutrition and Football: The FIFA/FMARC Consensus on Sports Nutrition.

Heredia, JE, Mukundan, L, Chen, FM, Mueller, AA, Deo, RC, Locksley, RM, Rando, TA, and Chawla, A (2013). Type 2 innate signals stimulate fibro/adipogenic progenitors to facilitate muscle regeneration. Cell.

Hesketh, S, Srisawat, K, Sutherland, H, Jarvis, J, and Burniston, J (2016). On the Rate of Synthesis of Individual Proteins within and between Different Striated Muscles of the Rat. Proteomes.

Hicks, AL, Kent-Braun, J, and Ditor, DS (2001). Sex differences in human skeletal muscle fatigue. Exerc Sport Sci Rev.

Hill, DW, and Smith, JC (1993). Gender difference in anaerobic capacity: Role of aerobic contribution. Br J Sports Med.

Hill, M, Wernig, A, and Goldspink, G (2003). Muscle satellite (stem) cell activation during local tissue injury and repair. J Anat.

Holt, SE, Wright, WE, and Shay, JW (1996). Regulation of telomerase activity in

immortal cell lines. Mol Cell Biol.

Horsley, V, Jansen, KM, Mills, ST, and Pavlath, GK (2003). IL-4 acts as a myoblast recruitment factor during mammalian muscle growth. Cell.

Hoshino, S et al. (2013). The CHC22 clathrin-GLUT4 transport pathway contributes to skeletal muscle regeneration. PLoS One.

Howatson, G, Hoad, M, Goodall, S, Tallent, J, Bell, PG, and French, DN (2012). Exercise-induced muscle damage is reduced in resistance-trained males by branched chain amino acids: A randomized, double-blind, placebo controlled study. J Int Soc Sports Nutr.

Howatson, G, and Van Someren, KA (2008). The prevention and treatment of exercise-induced muscle damage. Sport Med.

Hubal, MJ, Rubinstein, SR, and Clarkson, PM (2008). Muscle function in men and women during maximal eccentric exercise. J Strength Cond Res.

Hughes, DC, Stewart, CE, Sculthorpe, N, Dugdale, HF, Yousefian, F, Lewis, MP, and Sharples, AP (2016). Testosterone enables growth and hypertrophy in fusion impaired myoblasts that display myotube atrophy: deciphering the role of androgen and IGF-I receptors. Biogerontology.

Hughes, VA, Frontera, WR, Roubenoff, R, Evans, WJ, and Fiatarone Singh, MA (2002). Longitudinal changes in body composition in older men and women: Role of body weight change and physical activity. Am J Clin Nutr.

Husmann, I, Soulet, L, Gautron, J, Martelly, I, and Barritault, D (1996). Growth factors in skeletal muscle regeneration. Cytokine Growth Factor Rev.

Huxley, HE (2004). Fifty years of muscle and the sliding filament hypothesis. Eur J Biochem.

Hyldahl, RD, Olson, T, Welling, T, Groscost, L, and Parcell, AC (2014). Satellite cell activity is differentially affected by contraction mode in human muscle following a work-matched bout of exercise. Front Physiol.

Ishikawa, H, Bischoff, R, and Holtzer, H (1968). Mitosis and intermediate-sized filaments in developing skeletal muscle. J Cell Biol.

Isobe, M, Lee, S, Waguri, S, and Kametaka, S (2018). Clathrin adaptor GGA1 modulates myogenesis of C2C12 myoblasts. PLoS One.

Ivaska, J, Pallari, HM, Nevo, J, and Eriksson, JE (2007). Novel functions of vimentin in cell adhesion, migration, and signaling. Exp Cell Res.

Jackman, SR, Witard, OC, Jeukendrup, AE, and Tipton, KD (2010). Branched-chain

amino acid ingestion can ameliorate soreness from eccentric exercise. Med Sci Sports Exerc.

Jang, YC, Sinha, M, Cerletti, M, Dall'osso, C, and Wagers, AJ (2011). Skeletal muscle stem cells: Effects of aging and metabolism on muscle regenerative function. Cold Spring Harb Symp Quant Biol.

Janssen, I, Heymsfield, SB, and Ross, R (2002). Low relative skeletal muscle mass (sarcopenia) in older persons is associated with functional impairment and physical disability. J Am Geriatr Soc.

Jones, NC, Tyner, KJ, Nibarger, L, Stanley, HM, Cornelison, DDW, Fedorov, Y V., and Olwin, BB (2005). The p38α/β MAPK functions as a molecular switch to activate the quiescent satellite cell. J Cell Biol.

Jones, NL, McCartney, N, Graham, T, Spriet, LL, Kowalchuk, JM, Heigenhauser, GJ, and Sutton, JR (2017). Muscle performance and metabolism in maximal isokinetic cycling at slow and fast speeds. J Appl Physiol.

Kachinsky, AM, Dominov, JA, and Miller, JB (1994). Myogenesis and the intermediate filament protein, nestin. Dev Biol.

Kastner, S, Elias, MC, Rivera, AJ, and Yablonka-Reuveni, Z (2000). Gene expression patterns of the fibroblast growth factors and their receptors during myogenesis of rat satellite cells. J Histochem Cytochem.

Kasumov, T, Dabkowski, ER, Shekar, KC, Li, L, Ribeiro, RF, Walsh, K, Previs, SF, Sadygov, RG, Willard, B, and Stanley, WC (2013). Assessment of cardiac proteome dynamics with heavy water: slower protein synthesis rates in interfibrillar than subsarcolemmal mitochondria. Am J Physiol Circ Physiol.

Kaur, G, and Dufour, JM (2012). Cell lines: Valuable tools or useless artifacts. Spermatogenesis.

Kawamura, K, Takano, K, Suetsugu, S, Kurisu, S, Yamazaki, D, Miki, H, Takenawa, T, and Endo, T (2004). N-WASP and WAVE2 acting downstream of phosphatidylinositol 3-kinase are required for myogenic cell migration induced by hepatocyte growth factor. J Biol Chem.

Keller, A, Peltzer, J, Carpentier, G, Horváth, I, Oláh, J, Duchesnay, A, Orosz, F, and Ovádi, J (2007). Interactions of enolase isoforms with tubulin and microtubules during myogenesis. Biochim Biophys Acta - Gen Subj.

Kent-Braun, JA, Ng, A V., and Young, K (2000). Skeletal muscle contractile and noncontractile components in young and older women and men. J Appl Physiol.

Khalek, WA, Cortade, F, Ollendorff, V, Lapasset, L, Tintignac, L, Chabi, B, and Wrutniak-Cabello, C (2014). SIRT3, a mitochondrial NAD+-dependent deacetylase, is involved in the regulation of myoblast differentiation. PLoS One.

Kim, J, Won, KJ, Lee, HM, Hwang, BY, Bae, YM, Choi, WS, Song, H, Lim, KW, Lee, CK, and Kim, B (2009). p38 MAPK participates in muscle-specific RING finger 1-mediated atrophy in cast-immobilized rat gastrocnemius muscle. Korean J Physiol Pharmacol.

Kim, JS, Wilson, JM, and Lee, SR (2010). Dietary implications on mechanisms of sarcopenia: roles of protein, amino acids and antioxidants. J Nutr Biochem.

Kirby, TJ, Triplett, NT, Haines, TL, Skinner, JW, Fairbrother, KR, and McBride, JM (2012). Effect of leucine supplementation on indices of muscle damage following drop jumps and resistance exercise. Amino Acids.

Kislinger, T, Gramolini, AO, Pan, Y, Rahman, K, MacLennan, DH, and Emili, A (2005). Proteome Dynamics during C2C12 Myoblast Differentiation. Mol Cell Proteomics.

Komar, B, Schwingshackl, L, and Hoffmann, G (2015). Effects of leucine-rich protein supplements on anthropometric parameter and muscle strength in the elderly: A systematic review and meta-analysis. J Nutr Heal Aging.

Komiya, Y, and Habas, R (2008). Wnt signal transduction pathways. Organogenesis.

Konopka, AR, and Sreekumaran Nair, K (2013). Mitochondrial and skeletal muscle health with advancing age. Mol Cell Endocrinol.

Koopman, R, Verdijk, L, Manders, RJF, Gijsen, AP, Gorselink, M, Pijpers, E, Wagenmakers, AJM, and Van Loon, LJC (2006). Co-ingestion of protein and leucine stimulates muscle protein synthesis rates to the same extent in young and elderly lean men. Am J Clin Nutr.

Kornasio, R, Riederer, I, Butler-Browne, G, Mouly, V, Uni, Z, and Halevy, O (2009). β-hydroxy-β-methylbutyrate (HMB) stimulates myogenic cell proliferation, differentiation and survival via the MAPK/ERK and PI3K/Akt pathways. Biochim Biophys Acta - Mol Cell Res.

Krajnak, K, Waugh, S, Miller, R, Baker, B, Geronilla, K, Alway, SE, and Cutlip, RG (2006). Proapoptotic factor Bax is increased in satellite cells in the tibialis anterior muscles of old rats. Muscle and Nerve.

Kuang, S, Kuroda, K, Le Grand, F, and Rudnicki, MA (2007). Asymmetric Self-Renewal and Commitment of Satellite Stem Cells in Muscle. Cell.

Kubo, K, Miyamoto, M, Tanaka, S, Maki, A, Tsunoda, N, and Kanehisa, H (2009).

Muscle and tendon properties during menstrual cycle. Int J Sports Med.

Lacour, F et al. (2017). R-spondin1 Controls Muscle Cell Fusion through Dual Regulation of Antagonistic Wnt Signaling Pathways. Cell Rep.

Larsson, L, and Karlsson, J (1978). Isometric and dynamic endurance as a function of age and skeletal muscle characteristics. Acta Physiol Scand.

Lassar, AB (2009). The p38 MAPK family, a pushmi-pullyu of skeletal muscle differentiation. J Cell Biol.

Lauritzen, F, Paulsen, G, Raastad, T, Bergersen, LH, and Owe, SG (2009). Gross ultrastructural changes and necrotic fiber segments in elbow flexor muscles after maximal voluntary eccentric action in humans. J Appl Physiol.

Lavender, AP, and Nosaka, K (2006). Comparison between old and young men for changes in makers of muscle damage following voluntary eccentric exercise of the elbow flexors. Appl Physiol Nutr Metab.

Lazarus, NR, and Harridge, SDR (2017). Declining performance of master athletes: silhouettes of the trajectory of healthy human ageing? J Physiol.

Leavy, O (2014). Inflammation: Regulating ROS. Nat Rev Immunol.

Lees, SJ, Rathbone, CR, and Booth, FW (2006). Age-associated decrease in muscle precursor cell differentiation. Am J Physiol Physiol.

Lees, SJ, Zwetsloot, KA, and Booth, FW (2009). Muscle precursor cells isolated from aged rats exhibit an increased tumor necrosis factor-α response. Aging Cell.

Léger, B, Derave, W, De Bock, K, Hespel, P, and Russell, AP (2008). Human Sarcopenia Reveals an Increase in SOCS-3 and Myostatin and a Reduced Efficiency of Akt Phosphorylation. Rejuvenation Res.

Leikina, E, Defour, A, Melikov, K, Van Der Meulen, JH, Nagaraju, K, Bhuvanendran, S, Gebert, C, Pfeifer, K, Chernomordik, L V., and Jaiswal, JK (2015). Annexin A1 deficiency does not affect myofiber repair but delays regeneration of injured muscles. Sci Rep.

Leikina, E, Melikov, K, Sanyal, S, Verma, SK, Eun, B, Gebert, C, Pfeifer, K, Lizunov, VA, Kozlov, MM, and Chernomordik, L V. (2013). Extracellular annexins and dynamin are important for sequential steps in myoblast fusion. J Cell Biol.

Leloup, L, Daury, L, Mazères, G, Cottin, P, and Brustis, JJ (2007). Involvement of the ERK/MAP kinase signalling pathway in milli-calpain activation and myogenic cell migration. Int J Biochem Cell Biol.

Leloup, L, Mazères, G, Daury, L, Cottin, P, and Brustis, JJ (2006). Involvement of

calpains in growth factor-mediated migration. Int J Biochem Cell Biol.

Lewis, SA, and Cowan, NJ (1988). Complex regulation and functional versatility of mammalian α- and β-tubulin isotypes during the differentiation of testis and muscle cells. J Cell Biol.

Li, C, Gao, HL, Shimokawa, T, Nabeka, H, Hamada, F, Araki, H, Cao, YM, Kobayashi, N, and Matsuda, S (2013). Prosaposin expression in the regenerated muscles of mdx and cardiotoxin-treated mice. Histol Histopathol.

Li, H, Choudhary, SK, Milner, DJ, Munir, MI, Kuisk, IR, and Capetanaki, Y (1994). Inhibition of desmin expression blocks myoblast fusion and interferes with the myogenic regulators myoD and myogenin. J Cell Biol.

Li, Y, Jiang, BH, Ensign, WY, Vogt, PK, and Han, J (2000). Myogenic differentiation requires signalling through both phosphatidylinositol 3-kinase and p38 MAP kinase. Cell Signal.

Lieber, RL (2002). Skeletal muscle structure, function, and plasticity, Lippincott Williams & Wilkins.

Lin, JJC, and Lin, JLC (1986). Assembly of different isoforms of actin and tropomyosin into the skeletal tropomyosin-enriched microfilaments during differentiation of muscle cells in vitro. J Cell Biol.

De Lisio, M, Jensen, T, Sukiennik, RA, Huntsman, HD, and Boppart, MD (2014). Substrate and strain alter the muscle-derived mesenchymal stem cell secretome to promote myogenesis. Stem Cell Res Ther.

Liu, CJ, and Latham, NK (2009). Progressive resistance strength training for improving physical function in older adults. Cochrane Database Syst Rev.

Liu, N, Nelson, BR, Bezprozvannaya, S, Shelton, JM, Richardson, JA, Bassel-Duby, R, and Olson, EN (2014). Requirement of MEF2A, C, and D for skeletal muscle regeneration. Proc Natl Acad Sci.

Liu, TY, Chen, YC, Jong, YJ, Tsai, HJ, Lee, CC, Chang, YS, Chang, JG, and Chang, YF (2017). Muscle developmental defects in heterogeneous nuclear Ribonucleoprotein A1 knockout mice. Open Biol.

Liu, Y, and Schneider, MF (2014). FGF2 activates TRPC and Ca2+ signaling leading to satellite cell activation. Front Physiol.

Livak, KJ, and Schmittgen, TD (2001). Analysis of relative gene expression data using real-time quantitative PCR and the 2-ΔΔCT method. Methods.

Lombardi, D, Sacchi, A, D'agostino, G, and Tibursi, G (1995). The association of the

Nm23-M1 protein and β-tubulin correlates with cell differentiation. Exp Cell Res.

Lowery, RP, Joy, JM, Rathmacher, JA, Baier, SM, Fuller, JC, Shelley, MC, Jäger, R, Purpura, M, Wilson, SMC, and Wilson, JM (2016). Interaction of beta-hydroxy-beta-methylbutyrate free acid and adenosine triphosphate on muscle mass, strength, and power in resistance trained individuals. J Strength Cond Res.

Machida, S, Spangenburg, EE, and Booth, FW (2003). Forkhead transcription factor FoxO1 transduces insulin-like growth factor's signal to p27Kip1 in primary skeletal muscle satellite cells. J Cell Physiol.

Mackey, AL et al. (2007). The influence of anti-inflammatory medication on exercise-induced myogenic precursor cell responses in humans. J Appl Physiol.

Mackey, AL, Brandstetter, S, Schjerling, P, Bojsen-Moller, J, Qvortrup, K, Pedersen, MM, Doessing, S, Kjaer, M, Magnusson, SP, and Langberg, H (2011). Sequenced response of extracellular matrix deadhesion and fibrotic regulators after muscle damage is involved in protection against future injury in human skeletal muscle. FASEB J.

MacLaren & Morton (2011). Biochemistry for sport and exercise metabolism, John Wiley & Sons.

Maley, MAL, Fan, Y, Beilharz, MW, and Grounds, MD (1994). Intrinsic differences in myod and myogenin expression between primary cultures of sjl/j and balb/c skeletal muscle. Exp Cell Res.

Von Maltzahn, J, Bentzinger, CF, and Rudnicki, MA (2012). Wnt7a-Fzd7 signalling directly activates the Akt/mTOR anabolic growth pathway in skeletal muscle. Nat Cell Biol.

Maretzky, T, Reiss, K, Ludwig, A, Buchholz, J, Scholz, F, Proksch, E, de Strooper, B, Hartmann, D, and Saftig, P (2005). ADAM10 mediates E-cadherin shedding and regulates epithelial cell-cell adhesion, migration, and -catenin translocation. Proc Natl Acad Sci.

Matsumoto, K, Koba, T, Hamada, K, Sakurai, M, Higuchi, T, and Miyata, H (2009). Branched-chain amino acid supplementation attenuates muscle soreness, muscle damage and inflammation during an intensive training program. J Sports Med Phys Fitness.

Mauro, A (1961). SATELLITE CELL OF SKELETAL MUSCLE FIBERS. J Cell Biol.

Mayer, U (2003). Integrins: redundant or important players in skeletal muscle? J Biol Chem 278, 14587–14590.

McCully, KK, and Faulkner, JA (2017). Injury to skeletal muscle fibers of mice following lengthening contractions. J Appl Physiol.

McGlory, C, and Phillips, SM (2015). Exercise and the Regulation of Skeletal Muscle Hypertrophy. In: Progress in Molecular Biology and Translational Science.

McKay, BR, Ogborn, DI, Bellamy, LM, Tarnopolsky, MA, and Parise, G (2012). Myostatin is associated with age-related human muscle stem cell dysfunction. FASEB J.

McLennan, IS, and Koishi, K (2002). The transforming growth factor-betas: Multifaceted regulators of the development and maintenance of skeletal muscles, motoneurons and Schwann cells. Int J Dev Biol.

Melnikova, IN, Bounpheng, M, Schatteman, GC, Gilliam, D, and Christy, BA (1999). Differential biological activities of mammalian Id proteins in muscle cells. Exp Cell Res.

Mikkelsen, UR, Langberg, H, Helmark, IC, Skovgaard, D, Andersen, LL, Kjær, M, and Mackey, AL (2009). Local NSAID infusion inhibits satellite cell proliferation in human skeletal muscle after eccentric exercise. J Appl Physiol.

Miles, MP, and Schneider, CM (1993). Creatine kinase isoenzyme MB may be elevated in healthy young women after submaximal eccentric exercise. J Lab Clin Med.

Millay, DP, O'Rourke, JR, Sutherland, LB, Bezprozvannaya, S, Shelton, JM, Bassel-Duby, R, and Olson, EN (2013). Myomaker is a membrane activator of myoblast fusion and muscle formation. Nature.

Miller, BF, Wolff, CA, Peelor, FF, Shipman, PD, and Hamilton, KL (2015). Modeling the contribution of individual proteins to mixed skeletal muscle protein synthetic rates over increasing periods of label incorporation. J Appl Physiol.

Molkentin, JD, Black, BL, Martin, JF, and Olson, EN (1995). Cooperative activation of muscle gene expression by MEF2 and myogenic bHLH proteins. Cell.

Montero-Fernández, N, and Serra-Rexach, JA (2013). Role of exercise on sarcopenia in the elderly. Eur J Phys Rehabil Med.

Moore, DR, Churchward-Venne, TA, Witard, O, Breen, L, Burd, NA, Tipton, KD, and Phillips, SM (2015). Protein ingestion to stimulate myofibrillar protein synthesis requires greater relative protein intakes in healthy older versus younger men. Journals Gerontol - Ser A Biol Sci Med Sci.

Mounier, R et al. (2013). AMPKα1 regulates macrophage skewing at the time of resolution of inflammation during skeletal muscle regeneration. Cell Metab.

Mourkioti, F, and Rosenthal, N (2005). IGF-1, inflammation and stem cells: Interactions during muscle regeneration. Trends Immunol.

Moyes, CD, Mathieu-Costello, OA, Tsuchiya, N, Filburn, C, and Hansford, RG (2017). Mitochondrial biogenesis during cellular differentiation. Am J Physiol Physiol.

Murphy, MM, Lawson, JA, Mathew, SJ, Hutcheson, DA, and Kardon, G (2011). Satellite cells, connective tissue fibroblasts and their interactions are crucial for muscle regeneration. J Cell Sci.

Musarò, A, McCullagh, K, Paul, A, Houghton, L, Dobrowolny, G, Molinaro, M, Barton, ER, L Sweeney, H, and Rosenthal, N (2001). Localized Igf-1 transgene expression sustains hypertrophy and regeneration in senescent skeletal muscle. Nat Genet.

Narici, M V., and Maffulli, N (2010). Sarcopenia: Characteristics, mechanisms and functional significance. Br Med Bull.

Navarro, M, Valentinis, B, Belletti, B, Romano, G, Reiss, K, and Baserga, R (2001). Regulation of Id2 gene expression by the type 1 IGF receptor and the insulin receptor substrate-1. Endocrinology.

Neels, JG, and Olefsky, JM (2006). Inflamed fat: What starts the fire? J Clin Invest.

Neufer, PD et al. (2015). Understanding the Cellular and Molecular Mechanisms of Physical Activity-Induced Health Benefits. Cell Metab.

Neuhaus, P, Oustanina, S, Loch, T, Kruger, M, Bober, E, Dono, R, Zeller, R, and Braun, T (2003). Reduced Mobility of Fibroblast Growth Factor (FGF)-Deficient Myoblasts Might Contribute to Dystrophic Changes in the Musculature of FGF2/FGF6/mdx Triple-Mutant Mice. Mol Cell Biol.

Nishimura, T, Nakamura, K, Kishioka, Y, Kato-Mori, Y, Wakamatsu, JI, and Hattori, A (2008). Inhibition of matrix metalloproteinases suppresses the migration of skeletal muscle cells. J Muscle Res Cell Motil.

Nobes, CD, and Hall, A (1999). Rho GTPases control polarity, protrusion, and adhesion during cell movement. J Cell Biol.

Nosaka, K, Sacco, P, and Mawatari, K (2006). Effects of amino acid supplementation on muscle soreness and damage. Int J Sport Nutr Exerc Metab.

Nowak, SJ, Nahirney, PC, Hadjantonakis, A-K, and Baylies, MK (2009). Nap1-mediated actin remodeling is essential for mammalian myoblast fusion. J Cell Sci.

O'Connor, MS, Carlson, ME, and Conboy, IM (2009). Differentiation rather than aging of muscle stem cells abolishes their telomerase activity. In: Biotechnology Progress.

Ohno, Y, Ando, K, Ito, T, Suda, Y, Matsui, Y, Oyama, A, Kaneko, H, Yokoyama, S,

Egawa, T, and Goto, K (2019). Lactate stimulates a potential for hypertrophy and regeneration of mouse skeletal muscle. Nutrients.

Ohno, Y, Oyama, A, Kaneko, H, Egawa, T, Yokoyama, S, Sugiura, T, Ohira, Y, Yoshioka, T, and Goto, K (2018). Lactate increases myotube diameter via activation of MEK/ERK pathway in C2C12 cells. Acta Physiol.

Ong, S-E, Blagoev, B, Kratchmarova, I, Kristensen, DB, Steen, H, Pandey, A, and Mann, M (2002). Stable Isotope Labeling by Amino Acids in Cell Culture, SILAC, as a Simple and Accurate Approach to Expression Proteomics. Mol Cell Proteomics.

Ong, SE, and Mann, M (2007). A practical recipe for stable isotope labeling by amino acids in cell culture (SILAC). Nat Protoc.

Otis, JS, Niccoli, S, Hawdon, N, Sarvas, JL, Frye, MA, Chicco, AJ, and Lees, SJ (2014). Pro-inflammatory mediation of myoblast proliferation. PLoS One.

Owens, DJ et al. (2015). A systems-based investigation into vitamin D and skeletal muscle repair, regeneration, and hypertrophy. Am J Physiol Metab.

Pajcini, K V., Corbel, SY, Sage, J, Pomerantz, JH, and Blau, HM (2010). Transient inactivation of Rb and ARF yields regenerative cells from postmitotic mammalian muscle. Cell Stem Cell.

Palecek, SP, Schmidt, CE, Lauffenburger, DA, and Horwitz, AF (1996). Integrin dynamics on the tail region of migrating fibroblasts. J Cell Sci.

Park, IH, and Chen, J (2005). Mammalian target of rapamycin (mTOR) signaling is required for a late-stage fusion process during skeletal myotube maturation. J Biol Chem.

Paulsen, G, Egner, IM, Drange, M, Langberg, H, Benestad, HB, Fjeld, JG, Hallén, J, and Raastad, T (2010). A COX-2 inhibitor reduces muscle soreness, but does not influence recovery and adaptation after eccentric exercise. Scand J Med Sci Sport.

Perdiguero, E et al. (2007). Genetic analysis of p38 MAP kinases in myogenesis: Fundamental role of p38α in abrogating myoblast proliferation. EMBO J.

Pereira, MG, Baptista, IL, Carlassara, EOC, Moriscot, AS, Aoki, MS, and Miyabara, EH (2014). Leucine supplementation improves skeletal muscle regeneration after cryolesion in rats. PLoS One.

Periasamy, M, and Kalyanasundaram, A (2007). SERCA pump isoforms: Their role in calcium transport and disease. Muscle and Nerve.

Phillips, SM (2015). Nutritional Supplements in Support of Resistance Exercise to Counter Age-Related Sarcopenia. Adv Nutr.

Phillips, SM, Chevalier, S, and Leidy, HJ (2016). Protein "requirements" beyond the RDA: implications for optimizing health. Appl Physiol Nutr Metab.

Phillips, SM, and Martinson, W (2019). Nutrient-rich, high-quality, protein-containing dairy foods in combination with exercise in aging persons to mitigate sarcopenia. Nutr Rev.

Phillips, SM, Tang, JE, and Moore, DR (2009). The role of milk- and soy-based protein in support of muscle protein synthesis and muscle protein accretion in young and elderly persons. J Am Coll Nutr.

Pietrangelo, T, Puglielli, C, Mancinelli, R, Beccafico, S, Fanò, G, and Fulle, S (2009). Molecular basis of the myogenic profile of aged human skeletal muscle satellite cells during differentiation. Exp Gerontol.

Pisconti, A, Cornelison, DDW, Olguín, HC, Antwine, TL, and Olwin, BB (2010). Syndecan-3 and Notch cooperate in regulating adult myogenesis. J Cell Biol.

Pizza, FX, Peterson, JM, Baas, JH, and Koh, TJ (2005). Neutrophils contribute to muscle injury and impair its resolution after lengthening contractions in mice. J Physiol.

Price, FD, Von Maltzahn, J, Bentzinger, CF, Dumont, NA, Yin, H, Chang, NC, Wilson, DH, Frenette, J, and Rudnicki, MA (2014). Inhibition of JAK-STAT signaling stimulates adult satellite cell function. Nat Med.

Proske, U, and Allen, TJ (2005). Damage to skeletal muscle from eccentric exercise. Exerc Sport Sci Rev.

Proske, U, and Morgan, DL (2001). Muscle damage from eccentric exercise: Mechanism, mechanical signs, adaptation and clinical applications. J Physiol.

Przewoźniak, M, Czaplicka, I, Czerwińska, AM, Markowska-Zagrajek, A, Moraczewski, J, Stremińska, W, Jańczyk-Ilach, K, Ciemerych, MA, and Brzoska, E (2013). Adhesion Proteins - An Impact on Skeletal Myoblast Differentiation. PLoS One.

Przybyla, B, Gurley, C, Harvey, JF, Bearden, E, Kortebein, P, Evans, WJ, Sullivan, DH, Peterson, CA, and Dennis, RA (2006). Aging alters macrophage properties in human skeletal muscle both at rest and in response to acute resistance exercise. Exp Gerontol.

Ra, SG, Miyazaki, T, Ishikura, K, Nagayama, H, Komine, S, Nakata, Y, Maeda, S, Matsuzaki, Y, and Ohmori, H (2013). Combined effect of branched-chain amino acids and taurine supplementation on delayed onset muscle soreness and muscle damage in high-intensity eccentric exercise. J Int Soc Sports Nutr.

Raftopoulou, M, and Hall, A (2004). Cell migration: Rho GTPases lead the way. Dev Biol.

Rankin, P, Stevenson, E, and Cockburn, E (2015). The effect of milk on the attenuation of exercise-induced muscle damage in males and females. Eur J Appl Physiol.

Ranzato, E, Balbo, V, Boccafoschi, F, Mazzucco, L, and Burlando, B (2009). Scratch wound closure of C2C12 mouse myoblasts is enhanced by human platelet lysate. Cell Biol Int.

Rawls, A, Valdez, MR, Olson, EN, Richardson, J, Zhang, W, and Klein, WH (1998). Overlapping functions of the myogenic bHLH genes MRF4 and MyoD revealed in double mutant mice. Development.

Ren, K, Crouzier, T, Roy, C, and Picart, C (2008). Polyelectrolyte multilayer films of controlled stiffness modulate myoblast cell differentiation. Adv Funct Mater.

Ríos, R, Carneiro, I, Arce, VM, and Devesa, J (2013). Myostatin is an inhibitor of myogenic differentiation. Am J Physiol Physiol.

Robinson, PA, Brown, S, McGrath, MJ, Coghill, ID, Gurung, R, and Mitchell, CA (2003). Skeletal muscle LIM protein 1 regulates integrin-mediated myoblast adhesion, spreading, and migration. Am J Physiol Physiol.

Romeo, Y, Zhang, X, and Roux, PP (2012). Regulation and function of the RSK family of protein kinases. Biochem J.

Rosenberg, IH (2011). Sarcopenia: Origins and clinical relevance. Clin Geriatr Med.

Rudnicki, MA, Schnegelsberg, PNJ, Stead, RH, Braun, T, Arnold, HH, and Jaenisch, R (1993). MyoD or Myf-5 is required for the formation of skeletal muscle. Cell.

Ruest, LB, Marcotte, R, and Wang, E (2002). Peptide elongation factor eEF1A-2/S1 expression in cultured differentiated myotubes and its protective effect against caspase-3-mediated apoptosis. J Biol Chem.

Sabourin, LA, Girgis-Gabardo, A, Scale, P, Asakura, A, and Rudnicki, MA (1999). Reduced differentiation potential of primary MyoD-/- myogenic cells derived from adult skeletal muscle. J Cell Biol.

Sacheck, JM, Milbury, PE, Cannon, JG, Roubenoff, R, and Blumberg, JB (2003). Effect of vitamin E and eccentric exercise on selected biomarkers of oxidative stress in young and elderly men. Free Radic Biol Med.

Saini, A, Nasser, AS, and Stewart, CEH (2006). Waste management-Cytokines, growth factors and cachexia. Cytokine Growth Factor Rev.

Salmerón-Sánchez, M, Rico, P, Moratal, D, Lee, TT, Schwarzbauer, JE, and García,

AJ (2011). Role of material-driven fibronectin fibrillogenesis in cell differentiation. Biomaterials.

Sanchez, AMJ, Csibi, A, Raibon, A, Cornille, K, Gay, S, Bernardi, H, and Candau, R (2012). AMPK promotes skeletal muscle autophagy through activation of forkhead FoxO3a and interaction with Ulk1. J Cell Biochem.

Sandri, M et al. (2013). Signalling pathways regulating muscle mass in ageing skeletal muscle. the role of the IGF1-Akt-mTOR-FoxO pathway. Biogerontology.

Sanes, J. R., & Lichtman, JW (1992). Development of the vertebrate neuromuscular junction. Annu Rev Neurosci 22, 389–442.

Saxton, RA, and Sabatini, DM (2017). mTOR Signaling in Growth, Metabolism, and Disease. Cell.

Sayers, SP, and Clarkson, PM (2001). Force recovery after eccentric exercise in males and females. Eur J Appl Physiol.

Schaap, LA et al. (2009). Higher inflammatory marker levels in older persons: Associations with 5-year change in muscle mass and muscle strength. Journals Gerontol - Ser A Biol Sci Med Sci.

Schlessinger, K, Hall, A, and Tolwinski, N (2009). Wnt signaling pathways meet Rho GTPases. Genes Dev.

Scholz, A, and Hinssen, H (1995). Biphasic pattern of gelsolin expression and variations in gelsolin-actin interactions during myogenesis. Exp Cell Res.

Schubert, R, Geiger, H, Zielen, S, and Baer, PC (2009). Simultaneous detection of ERK-, p38-, and JNK-MAPK phosphorylation in human adipose-derived stem cells using the Cytometric Bead Array technology. J Immunol Methods.

Schultz, E, Jaryszak, DL, and Valliere, CR (1985). Response of satellite cells to focal skeletal muscle injury. Muscle Nerve.

Schwander, M, Leu, M, Stumm, M, Dorchies, OM, Ruegg, UT, Schittny, J, and Müller, U (2003). β1 integrins regulate myoblast fusion and sarcomere assembly. Dev Cell.

Seaborne, RA et al. (2018). Human Skeletal Muscle Possesses an Epigenetic Memory of Hypertrophy. Sci Rep.

Seaborne, RA et al. (2019). UBR5 is a novel E3 ubiquitin ligase involved in skeletal muscle hypertrophy and recovery from atrophy. J Physiol.

Seals, DF, and Courtneidge, SA (2003). The ADAMs family of metalloproteases: Multidomain proteins with multiple functions. Genes Dev.

Seals, DR, Justice, JN, and Larocca, TJ (2016). Physiological geroscience: Targeting

function to increase healthspan and achieve optimal longevity. J Physiol.

Selman, C et al. (2009). Ribosomal protein S6 kinase 1 signaling regulates mammalian life span. Science (80-).

Serhan, CN, and Petasis, NA (2011). Resolvins and protectins in inflammation resolution. Chem Rev.

Serrano, AL, Baeza-Raja, B, Perdiguero, E, Jardí, M, and Muñoz-Cánoves, P (2008). Interleukin-6 Is an Essential Regulator of Satellite Cell-Mediated Skeletal Muscle Hypertrophy. Cell Metab.

Sewright, KA, Hubal, MJ, Kearns, A, Holbrook, MT, and Clarkson, PM (2008). Sex differences in response to maximal eccentric exercise. Med Sci Sports Exerc.

Sharples, AP, Al-Shanti, N, Hughes, DC, Lewis, MP, and Stewart, CE (2013). The role of insulin-like-growth factor binding protein 2 (IGFBP2) and phosphatase and tensin homologue (PTEN) in the regulation of myoblast differentiation and hypertrophy. Growth Horm IGF Res.

Sharples, AP, Al-Shanti, N, Lewis, MP, and Stewart, CE (2011). Reduction of myoblast differentiation following multiple population doublings in mouse C 2C 12 cells: A model to investigate ageing? J Cell Biochem.

Sharples, AP, Hughes, DC, Deane, CS, Saini, A, Selman, C, and Stewart, CE (2015). Longevity and skeletal muscle mass: The role of IGF signalling, the sirtuins, dietary restriction and protein intake. Aging Cell.

Sharples, AP, Player, DJ, Martin, NRW, Mudera, V, Stewart, CE, and Lewis, MP (2012). Modelling in vivo skeletal muscle ageing in vitro using three-dimensional bioengineered constructs. Aging Cell.

Sharples, AP, and Stewart, CE (2011). Myoblast models of skeletal muscle hypertrophy and atrophy. Curr Opin Clin Nutr Metab Care.

Shefer, G, Van de Mark, DP, Richardson, JB, and Yablonka-Reuveni, Z (2006). Satellite-cell pool size does matter: Defining the myogenic potency of aging skeletal muscle. Dev Biol.

Shen, K et al. (2018). Architecture of the human GATOR1 and GATOR1-Rag GTPases complexes. Nature.

Shi, X, and Garry, DJ (2006). Muscle stem cells in development, regeneration, and disease. Genes Dev.

Shibukawa, Y, Yamazaki, N, Daimon, E, and Wada, Y (2013). Rock-dependent calponin 3 phosphorylation regulates myoblast fusion. Exp Cell Res.

Shibukawa, Y, Yamazaki, N, Kumasawa, K, Daimon, E, Tajiri, M, Okada, Y, Ikawa, M, and Wada, Y (2010). Calponin 3 Regulates Actin Cytoskeleton Rearrangement in Trophoblastic Cell Fusion. Mol Biol Cell.

Shimomura, Y, Inaguma, A, Watanabe, S, Yamamoto, Y, Muramatsu, Y, Bajotto, G, Sato, J, Shimomura, N, Kobayashi, H, and Mawatari, K (2010). Branched-chain amino acid supplementation before squat exercise and delayed-onset muscle soreness. Int J Sport Nutr Exerc Metab.

Shirato, M, Tsuchiya, Y, Sato, T, Hamano, S, Gushiken, T, Kimura, N, and Ochi, E (2016). Effects of combined β-hydroxy-β-methylbutyrate (HMB) and whey protein ingestion on symptoms of eccentric exercise-induced muscle damage. J Int Soc Sports Nutr.

Siegel, AL, Atchison, K, Fisher, KE, Davis, GE, and Cornelison, DDW (2009). 3D timelapse analysis of muscle satellite cell motility. Stem Cells.

Silva-Barbosa, SD, Butler-Browne, GS, De Mello, W, Riederer, I, Di Santo, JP, Savino, W, and Mouly, V (2008). Human myoblast engraftment is improved in laminin-enriched microenvironment. Transplantation.

Sin, J, Andres, AM, Taylo R, DJR, Weston, T, Hiraumi, Y, Stotland, A, Kim, BJ, Huang, C, Doran, KS, and Gottlieb, RA (2016). Mitophagy is required for mitochondrial biogenesis and myogenic differentiation of C2C12 myoblasts. Autophagy.

Skurvydas, A, Brazaitis, M, Venckūnas, T, and Kamandulis, S (2011). Predictive value of strength loss as an indicator of muscle damage across multiple drop jumps. Appl Physiol Nutr Metab.

Smith, HJ, Mukerji, P, and Tisdale, MJ (2005). Attenuation of proteasome-induced proteolysis in skeletal muscle by β-hydroxy-β-methylbutyrate in cancer-induced muscle loss. Cancer Res.

Smith, PK, Krohn, RI, Hermanson, GT, Mallia, AK, Gartner, FH, Provenzano, MD, Fujimoto, EK, Goeke, NM, Olson, BJ, and Klenk, DC (1985). Measurement of protein using bicinchoninic acid. Anal Biochem.

Van Someren, KA, Edwards, AJ, and Howatson, G (2005). Supplementation with β-hydroxy- β-methylbutyrate (hmb) and α-ketoisocaproic acid (KIC) reduces signs and symptoms of exercise-induced muscle damage in man. Int J Sport Nutr Exerc Metab.

Sonnet, C (2006). Human macrophages rescue myoblasts and myotubes from apoptosis through a set of adhesion molecular systems. J Cell Sci.

Sorichter, S, Mair, J, Koller, A, Calzolari, C, Huonker, M, Pau, B, and Puschendorf, B

(2001). Release of muscle proteins after downhill running in male and female subjects. Scand J Med Sci Sport.

Spangenburg, EE, Bowles, DK, and Booth, FW (2004). Insulin-like growth factor-induced transcriptional activity of the skeletal α-actin gene is regulated by signaling mechanisms linked to voltage-gated calcium channels during myoblast differentiation. Endocrinology.

Srikanthan, P, and Karlamangla, AS (2014). Muscle mass index as a predictor of longevity in older adults. Am J Med.

Stewart, CEH, James, PL, Fant, ME, and Rotwein, P (1996). Overexpression of insulin-like growth factor-II induces accelerated myoblast differentiation. J Cell Physiol.

Storey, JD, and Tibshirani, R (2003). SAM Thresholding and False Discovery Rates for Detecting Differential Gene Expression in DNA Microarrays.

Suzuki, S, Yamanouchi, K, Soeta, C, Katakai, Y, Harada, R, Naito, K, and Tojo, H (2002). Skeletal muscle injury induces hepatocyte growth factor expression in spleen. Biochem Biophys Res Commun.

Swailes, NT, Knight, PJ, and Peckham, M (2004). Actin filament organization in aligned prefusion myoblasts. J Anat.

Taaffe, D, Henwood, T, Nails, M, Walker, D, Lang, T, and Harris, T (2009). Alterations in muscle attenuation following detraining and retraining in resistance trained older adults. J Sci Med Sport.

Takekura, H, Flucher, BE, and Franzini-Armstrong, C (2001). Sequential docking, molecular differentiation, and positioning of T-tubule/SR junctions in developing mouse skeletal muscle. Dev Biol.

Talvas, J, Obled, A, Fafournoux, P, and Mordier, S (2006). Regulation of Protein Synthesis by Leucine Starvation Involves Distinct Mechanisms in Mouse C2C12 Myoblasts and Myotubes. J Nutr.

Tannu, NS, Rao, VK, Chaudhary, RM, Giorgianni, F, Saeed, AE, Gao, Y, and Raghow, R (2004). Comparative Proteomes of the Proliferating C 2 C 12 Myoblasts and Fully Differentiated Myotubes Reveal the Complexity of the Skeletal Muscle Differentiation Program . Mol Cell Proteomics.

Tay, CY, Gu, H, Leong, WS, Yu, H, Li, HQ, Heng, BC, Tantang, H, Loo, SCJ, Li, LJ, and Tan, LP (2010). Cellular behavior of human mesenchymal stem cells cultured on single-walled carbon nanotube film. Carbon N Y.

Teixeira, F, Matias, CN, Monteiro, CP, Valamatos, MJ, Reis, JF, Morton, RW, Alves,

F, Sardinha, LB, and Phillips, SM (2019). Leucine metabolites do not attenuate training-induced inflammation in young resistance trained men. J Sports Sci.

Teixeira, FJ, Matias, CN, Monteiro, CP, Valamatos, MJ, Reis, JF, Batista, A, Oliveira, AC, Alves, F, Sardinha, LB, and Phillips, SM (2018). No effect of HMB or α-HICA supplementation on training-induced changes in body composition. Eur J Sport Sci.

Terrente, Y, El Fahime, E, Caron, NJ, Del Bo, R, Belicchi, M, Pisati, F, Tremblay, JP, and Bresolin, N (2003). Tumor necrosis factor-α (TNF-α) stimulates chemotactic response in mouse myogenic cells. Cell Transplant.

Tidball, JG (2011). Mechanisms of muscle injury, repair, and regeneration. Compr Physiol.

Tidball, JG, and Villalta, SA (2010). Regulatory interactions between muscle and the immune system during muscle regeneration. Am J Physiol Integr Comp Physiol.

Tierney, MT, Aydogdu, T, Sala, D, Malecova, B, Gatto, S, Puri, PL, Latella, L, and Sacco, A (2014). STAT3 signaling controls satellite cell expansion and skeletal muscle repair. Nat Med.

Towler, MC (2004). Clathrin Isoform CHC22, a Component of Neuromuscular and Myotendinous Junctions, Binds Sorting Nexin 5 and Has Increased Expression during Myogenesis and Muscle Regeneration. Mol Biol Cell.

Townsend, JR et al. (2013). β-Hydroxy-β-methylbutyrate (HMB)-free acid attenuates circulating TNF-α and TNFR1 expression postresistance exercise. J Appl Physiol.

Troy, A, Cadwallader, AB, Fedorov, Y, Tyner, K, Tanaka, KK, and Olwin, BB (2012). Coordination of satellite cell activation and self-renewal by par-complex-dependent asymmetric activation of p38α/β MAPK. Cell Stem Cell.

Twist, C, and Eston, R (2005). The effects of exercise-induced muscle damage on maximal intensity intermittent exercise performance. Eur J Appl Physiol.

U.N. (2017). World Population Ageing 2017. World Popul Ageing 2017.

Vaittinen, S, Lukka, R, Sahlgren, C, Hurme, T, Rantanen, J, Lendahl, U, Eriksson, JE, and Kalimo, H (2001). The expression of intermediate filament protein nestin as related to vimentin and desmin in regenerating skeletal muscle. J Neuropathol Exp Neurol.

Vallejo, J, Spence, M, Cheng, AL, Brotto, L, Edens, NK, Garvey, SM, and Brotto, M (2016). Cellular and physiological effects of dietary supplementation with β-hydroxy-β- methylbutyrate (hmb) and β-alanine in late middle-aged mice. PLoS One.

Varga, T, Mounier, R, Horvath, A, Cuvellier, S, Dumont, F, Poliska, S, Ardjoune, H,

Juban, G, Nagy, L, and Chazaud, B (2016). Highly Dynamic Transcriptional Signature of Distinct Macrophage Subsets during Sterile Inflammation, Resolution, and Tissue Repair. J Immunol.

Vaz, R, Martins, GG, Thorsteinsdóttir, S, and Rodrigues, G (2012). Fibronectin promotes migration, alignment and fusion in an in vitro myoblast cell model. Cell Tissue Res.

Visser, M, Pahor, M, Taaffe, DR, Goodpaster, BH, Simonsick, EM, Newman, AB, Nevitt, M, and Harris, TB (2002). Relationship of interleukin-6 and tumor necrosis factor-α with muscle mass and muscle strength in elderly men and women: The health ABC study. Journals Gerontol - Ser A Biol Sci Med Sci.

Vogel, C, and Marcotte, EM (2012). Insights into the regulation of protein abundance from proteomic and transcriptomic analyses. Nat Rev Genet.

Volpi, E, Sheffield-Moore, M, Rasmussen, BB, and Wolfe, RR (2001). Basal muscle amino acid kinetics and protein synthesis in healthy young and older men. J Am Med Assoc.

Wagatsuma, A, Shiozuka, M, Kotake, N, Takayuki, K, Yusuke, H, Mabuchi, K, Matsuda, R, and Yamada, S (2011). Pharmacological inhibition of HSP90 activity negatively modulates myogenic differentiation and cell survival in C2C12 cells. Mol Cell Biochem.

Wahl, SM, Hunt, DA, Wakefield, LM, McCartney-Francis, N, Wahl, LM, Roberts, AB, and Sporn, MB (1987). Transforming growth factor type beta induces monocyte chemotaxis and growth factor production. Proc Natl Acad Sci.

Wang, H, Xu, Q, Xiao, F, Jiang, Y, and Wu, Z (2008). Involvement of the p38 Mitogen-activated Protein Kinase , , and Isoforms in Myogenic Differentiation. Mol Biol Cell.

Wang, X, Hu, Z, Hu, J, Du, J, and Mitch, WE (2006). Insulin resistance accelerates muscle protein degradation: Activation of the ubiquitin-proteasome pathway by defects in muscle cell signaling. Endocrinology.

Weaver, JL (2000). Introduction to flow cytometry: A Learning Guide.

Webster, KA, Gunning, P, Hardeman, E, Wallace, DC, and Kedes, L (1990). Coordinate reciprocal trends in glycolytic and mitochondrial transcript accumulations during the in vitro differentiation of human myoblasts. J Cell Physiol.

Wei, L, Zhou, W, Croissant, JD, Johansen, FE, Prywes, R, Balasubramanyam, A, and Schwartz, RJ (1998). RhoA signaling via serum response factor plays an obligatory role in myogenic differentiation. J Biol Chem.

Weitzer, G, Milner, DJ, Kim, JU, Bradley, A, and Capetanaki, Y (1995). Cytoskeletal control of myogenesis: A desmin null mutation blocks the myogenic pathway during embryonic stem cell differentiation. Dev Biol.

Welle, S (2009). Cellular and Molecular Basis of Age-Related Sarcopenia. Can J Appl Physiol.

Welle, S, Brooks, AI, Delehanty, JM, Needler, N, and Thornton, CA (2003). Gene expression profile of aging in human muscle. Physiol Genomics.

Wen, Y, Bi, P, Liu, W, Asakura, A, Keller, C, and Kuang, S (2012). Constitutive Notch Activation Upregulates Pax7 and Promotes the Self-Renewal of Skeletal Muscle Satellite Cells. Mol Cell Biol.

Wiles, B, Miao, M, Coyne, E, Larose, L, Cybulsky, A V., and Wing, SS (2015). USP19 deubiquitinating enzyme inhibits muscle cell differentiation by suppressing unfolded-protein response signaling. Mol Biol Cell.

Wilkes, EA, Selby, AL, Atherton, PJ, Patel, R, Rankin, D, Smith, K, and Rennie, MJ (2009). Blunting of insulin inhibition of proteolysis in legs of older subjects may contribute to age-related sarcopenia. Am J Clin Nutr.

Wilkinson, AW et al. (2019). SETD3 is an actin histidine methyltransferase that prevents primary dystocia. Nature.

Williams, BA, and Ordahl, CP (1994). Pax-3 expression in segmental mesoderm marks early stages in myogenic cell specification. Development.

Willkomm, L, Schubert, S, Jung, R, Elsen, M, Borde, J, Gehlert, S, Suhr, F, and Bloch, W (2014). Lactate regulates myogenesis in C2C12 myoblasts in vitro. Stem Cell Res.

Wilson, JM et al. (2013). β-Hydroxy-β-methylbutyrate free acid reduces markers of exercise-induced muscle damage and improves recovery in resistance-trained men. Br J Nutr.

Wilson, JM et al. (2014). The effects of 12 weeks of beta-hydroxy-beta-methylbutyrate free acid supplementation on muscle mass, strength, and power in resistance-trained individuals: A randomized, double-blind, placebo-controlled study. Eur J Appl Physiol.

Wilson, JM, Kim, JS, Lee, SR, Rathmacher, JA, Dalmau, B, Kingsley, JD, Koch, H, Manninen, AH, Saadat, R, and Panton, LB (2009). Acute and timing effects of beta-hydroxy-beta-methylbutyrate (HMB) on indirect markers of skeletal muscle damage. Nutr Metab.

Wiśniewski, JR, Zougman, A, Nagaraj, N, and Mann, M (2009). Universal sample preparation method for proteome analysis. Nat Methods.

Wolfe, RR, Miller, SL, and Miller, KB (2008). Optimal protein intake in the elderly. Clin Nutr.

Wu, Y, Zhang, X, Salmon, M, Lin, X, and Zehner, ZE (2007). TGFβ1 regulation of vimentin gene expression during differentiation of the C2C12 skeletal myogenic cell line requires Smads, AP-1 and Sp1 family members. Biochim Biophys Acta - Mol Cell Res.

Xiao, GG, Garg, M, Lim, S, Wong, D, Go, VL, and Lee, W-NP (2008). Determination of protein synthesis in vivo using labeling from deuterated water and analysis of MALDI-TOF spectrum. J Appl Physiol.

Yaffe, D, and Saxel, O (1977). Serial passaging and differentiation of myogenic cells isolated from dystrophic mouse muscle. Nature.

Yahiaoui, L, Gvozdic, D, Danialou, G, Mack, M, and Petrof, BJ (2008). CC family chemokines directly regulate myoblast responses to skeletal muscle injury. J Physiol.

Yamada, T, Matsumoto, K, Wang, W, Li, Q, Nishioka, Y, Sekido, Y, Sone, S, and Yano, S (2010). Hepatocyte growth factor reduces susceptibility to an irreversible epidermal growth factor receptor inhibitor in EGFR-T790M mutant lung cancer. Clin Cancer Res.

Yarasheski, KE, Zachwieja, JJ, Campbell, JA, and Bier, DM (2017). Effect of growth hormone and resistance exercise on muscle growth and strength in older men. Am J Physiol Metab.

Yun, BG, and Matts, RL (2005a). Differential effects of Hsp90 inhibition on protein kinases regulating signal transduction pathways required for myoblast differentiation. Exp Cell Res.

Yun, BG, and Matts, RL (2005b). Hsp90 functions to balance the phosphorylation state of Akt during C2C12 myoblast differentiation. Cell Signal.

Zanchi, NE, Gerlinger-Romero, F, Guimarães-Ferreira, L, De Siqueira Filho, MA, Felitti, V, Lira, FS, Seelaender, M, and Lancha, AH (2011). HMB supplementation: Clinical and athletic performance-related effects and mechanisms of action. Amino Acids.

Zehorai, E, Yao, Z, Plotnikov, A, and Seger, R (2010). The subcellular localization of MEK and ERK-A novel nuclear translocation signal (NTS) paves a way to the nucleus. Mol Cell Endocrinol.

Zhang, H, Menzies, KJ, and Auwerx, J (2018). The role of mitochondria in stem cell fate and aging. Development.

Zhao, MJ, Xie, J, Shu, WJ, Wang, HY, Bi, J, Jiang, W, and Du, HN (2019). MiR-15b and miR-322 inhibit SETD3 expression to repress muscle cell differentiation. Cell Death Dis.

Zhong, H, Jin, Z, Chen, Y, Zhang, T, Bian, W, Cui, X, and Jing, N (2008). First intron of nestin gene regulates its expression during C2C12 myoblast differentiation. Acta Biochim Biophys Sin (Shanghai).

Zhou, X, and Platt, JL (2011). Molecular and cellular mechanisms of mammalian cell fusion. Adv Exp Med Biol.

Zhu, H, Pan, S, Gu, S, Morton Bradbury, E, and Chen, X (2002). Amino acid residue specific stable isotope labeling for quantitative proteomics. Rapid Commun Mass Spectrom.